UNIVERSIDADE NOVA DE LISBOA
INSTITUTO DE HIGIENE E MEDICINA TROPICAL
UNIDADE DE BIOLOGIA MOLECULAR

ANALYSIS OF CHANGES IN THE HOST CELL PROTEOME DURING HEPATITIS D VIRUS INFECTION

MARTA MARIA LAVOURAS MENDES

Dissertation to obtain the PhD degree in Molecular and Cellular Biology

SUPERVISOR: PROFESSOR CELSO CUNHA

CO-SUPERVISOR: PROFESSOR ANA COELHO

2011

ACKNOWLEDGEMENTS

This thesis is a result of many efforts. If not for the help of so many people this work would not have been possible. To all of you, my eternal gratitude.

In particular to Professor Celso Cunha, who always stood by me despite everything. Thank you for the support, for the guidance, for the advices and for the availability, but above all thank you for your friendship over the last eight years.

To Professor Ana Coelho, without whom this work would not have been possible. Thank you for the support and the opportunity to work abroad.

To Professor Jesús Vazquéz, for having me in his lab. Thank you for the wonderful experience of working with you, for the availability, for the support, the friendship and for making me feel at home.

To Professor Pedro Cravo, for the availability and orientation in qPCR.

To all the former and present members of the Molecular Biology Lab, Natália Freitas, Sérgio Mota, Ana Casaca, Carolina Alves, Sofia Borges, Louise Rodrigues, Gisela Henriques, Joana Cavaco Silva, Cristina Branco and D. Fernanda Costa my many thanks for all the good moments, scientific or not, and above all to put up with me! A special thanks to Ana Casaca for her help, among other things, with the confocal.

To the members of the Mass Spectrometry lab from ITQB, especially to Elisabete Pires, Catarina Franco and Renata Soares thank you for all your support.

To the members of the Protein Chemistry and Proteomics lab from CBMSO, in Madrid, Horacio Serrano, Pablo Martínez, Pedro Navarro, Daniel Pérez, Elena Bonzon-Kulichenko, Estefania Nuñez and Inma Jorge, a special thanks. This work would not have been possible without you. Thank you for all the good moments, for making me feel at home and for showing me the “secrets” of proteomics!

To the Fundação para a Ciência e Tecnologia who supported this work with a four year grant (SFRH/BD/27630/2006).

To all my friends, thank you for being there.

In particular to Ana Casaca, Carolina Alves and Sérgio Mota. Thank you for everything, in and out of the lab. I know I will never have a team like you.

To all the dancers of AAP, and especially to Orlindo, who always cheered me up with the dancing, the music and the laughters.

To Teresa, because I know you are there.

And finally to my family who means the world to me.

To my brother for all the support, the friendship and for always being present. Thank you for everything and especially for bearing my bad mood. You're a part of me.

To Angela, for taking care of my brother making me feel less guilty when I wasn't there.

To my father and my mother, who always made my dreams come true, including this one. Thank you for the love, the friendship, the advices and the unconditional support. Thank you for always being there.

To Dani, who showed me that fairy tales exist. Thank you for always being there even when we were apart and even when I was being Hulk. This thesis is as much as mine as it is yours. Thank you for giving me the world.

AGRADECIMENTOS

Esta tese foi o resultado de muitos esforços e não teria sido possível sem a ajuda de muitas pessoas. A todas elas o meu mais sincero obrigado.

Em particular ao Professor Celso Cunha, que sempre me apoiou apesar de tudo. Obrigada pelo apoio, pela orientação, pelos conselhos e pela disponibilidade, mas acima de tudo, obrigada pela amizade durante os últimos oito anos.

À Professora Ana Coelho, sem a qual a realização deste trabalho não teria sido possível. Obrigada pelo apoio e pela oportunidade de trabalhar no estrangeiro.

Ao Professor Jesús Vazquéz, por me acolher no seu laboratório. Obrigada pela maravilhosa experiência de trabalhar consigo, pela disponibilidade, pelo apoio, pela amizade e por me fazer sentir em casa.

Ao Professor Pedro Cravo, pela disponibilidade e orientação com o qPCR.

A todos os membros da Biologia Molecular, antigos e actuais, Natália Freitas, Sérgio Mota, Ana Casaca, Carolina Alves, Sofia Borges, Louise Rodrigues, Gisela Henriques, Joana Cavaco Silva, Cristina Branco e D. Fernanda Costa obrigada por todos os bons momentos, científicos ou não, e acima de tudo obrigada por me aguentarem! Um agradecimento especial à Ana Casaca pela sua ajuda com o confocal, para além de outras coisas.

Um agradecimento também ao laboratório de espectrometria de massa do ITQB, especialmente à Elisabete Pires, à Catarina Franco e à Renata Soares. Obrigada pelo vosso apoio.

E aos membros do laboratório de Química de Proteínas e Proteómica do CBMSO, em Madrid, Horacio Serrano, Pablo Martínez, Pedro Navarro, Daniel Pérez, Elena Bónzon-Kulichenko, Estefania Nuñez and Inma Jorge, um agradecimento muito especial. Este trabalho não teria sido possível sem vocês. Obrigada por todos os bons momentos por me fazerem sentir em casa e por me ensinarem todos os "segredos" da proteómica.

À Fundação para a Ciência e Tecnologia que apoiou este trabalho com uma bolsa de doutoramento por quarto anos (SFRH/BD/27630/2006).

A todos os meus amigos, obrigada por existirem.

Em particular à Ana Casaca, à Carolina Alves e ao Sérgio Mota. Obrigada por tudo, dentro e for a do lab. Sei que nunca vou ter outra equipa como vocês!

Aos bailarinos dos AAP, especialmente ao Orlindo, que sempre me animaram com a dança, a música e as gargalhadas.

À Teresa, porque sei que estás aí.

E finalmente à minha família que significa tudo para mim.

Ao meu irmão por todo o apoio, amizade e por estar sempre presente. Obrigada por tudo, especialmente por aguentares o meu mau humor. És uma parte de mim.

À Angela, por cuidar do meu irmão e não fazer-me sentir tão mal quando eu não estava presente.

Ao meu pai e à minha mãe que sempre tornaram os meus sonhos realidade, incluindo este. Obrigada pelo amor, pela amizade, pelo conselhos e pelo apoio incondicional. Obrigada por estarem sempre aí.

Ao Dani, que me mostrou que os contos de fadas existem. Obrigada por estares sempre presente, mesmo quando estávamos separados e mesmo quando eu me transformo em Hulk. Esta tese é tanto minha como tua. Obrigada por me ofereceres o mundo.

ABSTRACT

Hepatitis delta virus is a very simple virus with a 1.7 kb, circular, ssRNA genome which codes for only one protein – the delta antigen (HDAg/δAg). Replication occurs in the nucleus of host cells by a rolling circle mechanism and using host RNA polymerase II giving rise to genomic and antigenomic RNA and a 5'-capped, polyadenylated RNA that acts as mRNA. During replication an editing mechanism occurs in the antigenomic RNA extending the reading frame and a second form of the delta antigen is produced. Despite its simplicity, little is known about which host factors and/or mechanism are involved in, or used by HDV during replication and pathogenesis, mainly due to the lack of an appropriate cell culture system to study it. In a previous work, two proteins, HSP105 and hnRNP H were found to be differentially expressed during HDV replication. In order to determine if and how these proteins may be involved in HDV replication, several assays were performed. Furthermore, using a new model for HDV replication based on a tetracycline inducible cell line, alterations in the proteome of those cells resultant from HDV replication were also determined. This model devises a tetracycline inducible cell line, 293-δAg, in which δAg expression is under the control of tetracycline and cells 293-HDV, in which 293-δAg cell line is transiently transfected with HDV RNAs allowing HDV replication. Using an MS-based quantitative proteomics approach consisting in $^{16}O/^{18}O$ enzymatic labeling together with systems biology, an attempt was made to clarify HDV replication and pathogenesis mechanisms by determining changes in the host cell proteome during hepatitis D infection.

Results showed that HSP105 and hnRNP H affect HDV replication. HSP105 knockdown induced a decrease in LHDAg expression levels and an increase of HDV mRNA levels. Furthermore, HSP105 was also shown to interact with both delta antigens. HSP105 seems to be involved in the ribonucleoprotein (RNP) transport or anchoring in the ER, or even in viral particle assembly. As for hnRNP H, a knockdown of the proteins led to an increase of HDV mRNA levels and a decrease in the expression of the delta antigens. It was also shown that hnRNP H binds to SHDAg. hnRNP H may be recruited by HDV in order to induce alternative splicing of pre-mRNAs that will originate key proteins essential to viral replication.

In order to determine alterations in the host cell proteome during HDV replication, five proteome comparisons, between controls and experiments, were performed. Approximately, 1000 proteins per experiment were identified and from those about 600 proteins were quantified. Finally, 88 proteins were found differentially expressed during HDV replication. From those, most proteins were found to be involved in protein metabolism and energy pathways. It was also possible, using GOTM and IPA, to perform a deeper analysis of the results, by determining interactions between differentially expressed proteins and determine which canonical pathways were most affected by HDV replication. Results showed that several metabolic pathways and key proteins were shown to be associated with HDV replication. Anaerobic glycolysis, HIF1α signaling and G2/M checkpoint regulation were three of the most affected pathways being the last pathway a key pathway in HDV replication leading to uncontrolled cell division.

RESUMO

O virus da hepatite delta (HDV) é um vírus muito simples que apresenta um genoma circular de RNA de cadeia simples com 1.7 Kb, codificando apenas para uma proteina – o antigénio delta (HDAg/δAg). A replicação ocorre no núcleo por um mecanismo de círculo rolante usando a RNA polimerase II do hospedeiro, originando RNA genómico e antigenómico e um RNA 5'-*capped* e poliadenilado que funciona como RNA mensageiro. Durante a replicação a ocorrência de um mecanismo de editing leva à extensão da grelha de leitura e consequentemente à produção de uma segunda forma do antigénio delta. Apesar da sua simplicidade, pouco se sabe sobre que factores e/ou mecanismos do hospedeiro são usados pelo virus durante a sua replicação e patogénese, devido à falta de modelos de estudo adequados. Num trabalho anterior, verificou-se que as proteínas HSP105 e hnRNP H se econtravam diferencialmente expressas durante a replicação do HDV. Vários ensaios foram então efectuados para determinar se e como poderão essas proteínas estar envolvidas na replicação do HDV. Mais ainda, usando un novo modelo de replicação para o HDV baseado numa linha celular induzida por tetraciclina, determinaram-se as alterações causadas pela replicação do HDV no proteoma destas células. Nesta linha celular o δAg foi colocado sobre o controlo do promotor da tetraciclina originando a linha celular 293-δAg. Esta linha foi posteriormente transitoriamente transfectada com os RNAs do HDV dando origem ás células 293-HDV, que permitem a replicação do virus. Usando esta linha celular e as células 293-HDV e uma aproximação de proteómica quantitativa baseada em espectrometria de massa consistindo na marcação enzimática com $^{16}O/^{18}O$ juntamente com biologia de sistemas, determinaram-se as alterações nos proteomas das células durante a replicação do HDV de forma a clarificar os mecanismos de replicação e patogénese do virus.

Os resultados mostraram que de facto as proteínas HSP105 e hnRNP H afectam a replicação do HDV. O silenciamento da proteína HSP105 parece induzir uma diminuição da expressão da proteína LHDAg e um aumento dos níveis de mRNA do HDV. Verificou-se ainda que a proteína HSP105 se liga à proteína LHDAg. A proteína HSP105 parece estar envolvida no transporte ou ligação da ribonucleoproteina (RNP) viral ao retículo endoplasmático ou mesmo na formação das patículas virais. Quanto à proteína hnRNP H, o seu silenciamento parece induzir um aumento dos níveis de

mRNA do HDV e uma diminuição da expressão dos antigénios delta. Verificou-se ainda que a proteína hnRNP H se liga à SHDAg. A proteína hnRNP H parece ser recrutada pelo HDV induzindo *splicing* alternativo de pre-mRNAs que posteriormente irão originar proteínas chave, essenciais para a replicação viral.

Para determinar quais as alterações no proteoma das células do hospedeiro durante a replicação do HDV, cinco comparações de proteomas, entre controlos e ensaios, foram efectuadas. Aproximadamente 1000 proteínas por ensaio foram identificadas, das quais cerca de 600 foram quantificadas. Finalmente, 88 proteínas foram encontradas diferencialmente expressas durante a replicação do HDV. Uma análise mais superficial mostrou que a maioria das proteínas diferencialmente expressas estavam envolvidas no metabolismo de proteínas e nas vias energéticas. Uma análise mais profunda foi posteriormente efectuada usando o GOTM e o IPA permitindo determinar as interacções entre as proteínas diferencialmente expressas e quais as vias canónicas mais alteradas durante a replicação do HDV. Os resultados mostraram que várias vias metabólicas e proteínas chave estão envolvidas na replicação do HDV. Três das vias mais afectadas são a respiração anaeróbica, a via de simalização HIF1*a* e a regulação do *checkpoint* na fase G2/M. Esta última via é de extrema importância uma vez que leva a uma divisão celular descontrolada.

PUBLICATIONS

PUBLISHED PAPERS

Ana P. Batista, Catarina Franco, Marta Mendes, Ana V. Coelho, Manuela M. Pereira. *Subunit composition of Rhodothermus marinus respiratory complex I*, Analytical Biochemistry. 2010 July, 407:104–110.

Mota S, Mendes M, Penque D, Freitas N, Coelho AV, Cunha C., *Proteome analysis of the human liver carcinoma cell line stably expressing Hepatitis Delta virus ribonucleoproteins*. J Proteomics. 2009 May 2;72(4):616-27

Mota S, Mendes M, Penque D, Coelho AV, Cunha C., *Changes in the proteome of Huh7 cells induced by transient expression of hepatitis D virus RNA and antigens*, J Proteomics. 2008 Apr 30;71(1):71-9.

Santos SC, Vala I, Miguel C, Barata JT, Garção P, Agostinho P, Mendes M, Coelho AV, Calado A, Oliveira CR, e Silva JM, Saldanha C., *Expression and subcellular localization of a novel nuclear acetylcholinesterase protein*, J Biol Chem. 2007 Aug 31;282(35):25597-603

MANUSCRIPTS

Marta Mendes, Daniel Pérez, Jesús Vázquez, Ana Coelho, Celso Cunha, *Analysis of changes in the host cell proteome during Hepatitis D infection*. Manuscript.

ABBREVIATIONS

293-δAg	tetracycline inducible cell line expressing the delta antigen
293-HDV	293-δAg transiently transfected with HDV RNA, thus replicating HDV genome
β2MG	β-2-microglobulin
δAg	delta antigen
2DE	Two-dimensional elecrophoresis
a.a	amino acid
AB	Ammonium bicarbonate
APS	Ammonium persulfate
ARM	Arginine rich motif
BLAST	Basic Local Alignment Search Tool
bp	base pair
CCD	Coiled coil domain
cDNA	complementary DNA
DEPC	Diethylpyrocarbonate
DNA	Deoxyribonucleic acid
dNTP	nucleotides (dTTP, dCTP, dATP, dGTP)
dsRNA	double stranded RNA
DTT	Dithiothreitol
EBV	Epstein Barr virus
ECM	Extracellular matrix
ER	Endoplasmic reticulum
FBS	fetal bovine serum
FDR	False discovery rate
FDRs	False discovery rate at the scan level
FDRp	False discovery rate at the peptide level
FDRq	False discovery rate at the protein level
FITC	Fluorescein isothiocyanate
GO	Gene ontology
GOTM	Gene ontology tree machine
GSH	Glutathione

GST	Glutathione-s-transferase
HBV	Hepatitis B virus
HCC	Hepatocellular carcinoma
HCMV	Human cytomegalovirus
HCV	Hepatitis C virus
HDAg	Delta antigens
HDV	Hepatitis delta virus
HEK	Human embryonic kidney cells
HIF	Hypoxia inducible factor
His	Histidine
HIV	Human immunodeficiency virus
HLH	Helix-loop-helix
HSP	Heat shock protein
Huh7	Human hepatoma cell line
Huh7-D12	Human hepatoma cell line stably transfected with HDV cDNA.
IEF	Isoelectric focusing
IFN	Interferon
IOA	Iodoacetamide
IPA	Ingenuity pathway analysis
IPG	immobilized pH gradient
KSHV	Kaposi’s sarcoma-associated herpesvirus
LC	Liquid chromatography
L-HBsAg	Large hepatitis B surface antigen
LHDAg	Large delta antigen
LTQ	linear ion trap mass spectrometer
M-HBsAg	Middle hepatitis B surface antigen
mRNA	messenger RNA
MS	Mass spectrometry
MW	Molecular weight
NBD	Nucleotide binding domain
NES	Nuclear export signal
NLS	Nuclear localization signal
nt	nucleotide
NTR	non translated region

ON	over night
ORF	open reading frame
PAGE	polyacrylamide gel electrophoresis
PBS	Phosphate saline buffer
PCR	Polymerase chain reaction
PDB	Peptide binding domain
PFA	paraformaldehyde
PTM	Posttranslational modification
qPCR	quantitative PCR
RBM	RNA binding domain
RGD	Arginine-Glycine-Aspartic acid
RNA	Ribonucleic acid
RNAi	RNA interference
RNA Pol	RNA Polimerase
RNP	Ribonucleoprotein
RT	room temperature
RT-qPCR	Reverse transcription-quantitative PCR
SDS	Sodium dodecyl sulphate
S-HBsAg	Small hepatitis B surface antigen
SHDAg	Small delta antigen
shRNA	short hairpin RNA
ssRNA	single-stranded RNA
TEMED	N, N, N', N' - Tetramethylethylenediamide
TET	tetracycline
TFA	trifluoroacetic acid
TLCK	N_{α}-Tosyl-L-lysine chloromethyl ketone hydrochloride
UTR	untranslated region
VEGF	vascular endothelial growth factor
Zq	standardized

INDEX

ACKNOWLEDGEMENTS i
AGRADECIMENTOS iii
ABSTRACT v
RESUMO vii
PUBLICATIONS ix
ABBREVIATIONS xi
INDEX xv
INDEX OF FIGURES xix
INDEX OF TABLES xxii
CHAPTER I: HEPATITIS DELTA VIRUS 1
I.1. EPIDEMIOLOGY, PATHOGENESIS AND TREATMENT OF HEPATITIS D VIRUS 2
I.2. HDV AND ITS ORIGINS 4
I.3. THE BIOLOGY OF HDV 5
I.3.1. VIRAL STRUCTURE AND ASSEMBLY 5
I.3.2. HDV GENOME AND RNAS 6
I.3.3. THE DELTA ANTIGENS 7
I.3.4. HDV LIFE CYCLE 11
CHAPTER II: GENERAL OBJECTIVES 15
CHAPTER III: HSP105: A NEW HDV INTERACTING PARTNER 17
III.1. INTRODUCTION 18
III.2. OBJECTIVES 21
III.3. MATERIALS AND METHODS 22
III.3.1. RNA INTERFERENCE INDUCING SYSTEM 22
III.3.2. TARGET SEQUENCE IDENTIFICATION AND SHRNA OLIGONUCLEOTIDE DESIGN 23
III.3.3. VECTOR CLONING AND RECOMBINANT VECTORS SELECTION 24
III.3.4. CELL CULTURE AND TRANSFECTION 25
III.3.5. MRNA ISOLATION AND RT-QPCR 26
III.3.6. SDS-PAGE AND WESTERN BLOT ANALYSIS 27
III.3.7. IMMUNOFLUORESCENCE ASSAYS 28
III.3.8. IMMUNOPRECIPITATION ASSAYS 29
III.4. RESULTS 31

III.4.1. SILENCING OF HSP105 AND ITS INFLUENCE IN THE EXPRESSION OF DELTA ANTIGENS 31
III.4.2. HSP105 CO-LOCALIZES WITH SMALL DELTA ANTIGEN 34
III.4.3. HSP105 INTERACTS WITH THE DELTA ANTIGENS *IN VIVO* 35
III.5. DISCUSSION 37
CHAPTER IV: HNRNP H INTERACTS *IN VIVO* WITH THE DELTA ANTIGENS AFFECTING HDV REPLICATION 39
IV.1. INTRODUCTION 40
IV.2. OBJECTIVES 45
IV.3. MATERIALS AND METHODS 46
IV.3.1. RNA INTERFERENCE INDUCING SYSTEM 46
IV.3.2. TARGET SEQUENCE IDENTIFICATION AND SHRNA OLIGONUCLEOTIDE DESIGN 46
IV.3.3. VECTOR CLONING AND RECOMBINANT VECTORS SELECTION 47
IV.3.4. CELL CULTURE AND TRANSFECTION 47
IV.3.5. MRNA ISOLATION AND RT-QPCR 47
IV.3.6. WESTERN BLOT ANALYSIS 48
IV.3.7. IMMUNOFLUORESCENCE ASSAYS 48
IV.3.8. PULL DOWN ASSAYS 49
IV.3.9. IMMUNOPRECIPITATION ASSAYS 50
IV.4. RESULTS 51
IV.4.1. SILENCING OF HNRNP H AND ITS INFLUENCE IN THE EXPRESSION OF DELTA ANTIGENS 51
III.4.2. HNRNP H CO-LOCALIZES WITH SMALL DELTA ANTIGEN 54
IV.4.3. HNRNP H INTERACTS WITH THE DELTA ANTIGENS *IN VITRO* AND *IN VIVO* 55
IV. 5. DISCUSSION 57
CHAPTER V: ANALYSIS OF CHANGES IN THE HOST CELL PROTEOME DURING HEPATITIS D VIRUS INFECTION 59
V.1. INTRODUCTION 60
V.1.1. MASS SPECTROMETRY-BASED PROTEOMICS 60
V.1.1.1. QUANTITATIVE PROTEOMICS 60
Metabolic labeling 61
Chemical labeling 62
Enzymatic labeling 64
Label-free quantification 65

V.1.1.2 MASS SPECTROMETRY OF PEPTIDES 66
Ionization Methods 66
Mass analyzers 67
V.1.1.3. DATA ANALYSIS 68
V.1.2. THE PROTEOMES OF HEPATITIS B VIRUS AND HEPATITIS C VIRUS INFECTED CELLS AND THE WAY TO HEPATOCELLULAR CARCINOMA 69
Hepatitis B virus 69
Hepatitis C virus 71
Hepatocellular Carcinoma 72
V.1.3. HDV AND HOST CELLULAR PROTEINS 73
V.1.4. STUDY MODELS FOR HDV REPLICATION 77
V.2. OBJECTIVES 79
V.3. MATERIALS AND METHODS 80
V.3.1. CELL LINE AND PROTEIN EXTRACTION 80
V.3.2. SDS PAGE 80
V.3.3. *IN GEL* DIGESTION OF PROTEINS 81
V.3.4. ^{18}O LABELING OF PEPTIDES 82
V.3.5. ISOELECTRIC FOCUSING OF PEPTIDES 83
V.3.6. LC-MS/MS ANALYSIS 84
V.3.7. PROTEIN IDENTIFICATION 84
V.3.8. PEPTIDE QUANTIFICATION AND STATISTICAL ANALYSIS 85
V.3.9. SYSTEMS BIOLOGY 86
V.3.10. WESTERN BLOT ANALYSIS 87
V.4. RESULTS 88
V.4.1. HIGH THROUGHPUT IDENTIFICATION OF PROTEINS IN 293, 293-δAG AND 293- 88
HDV CELLS BY LC-MS/MS ANALYSIS 88
V.4.2. HIGH THROUGHPUT QUANTIFICATION OF PROTEINS DIFFERENTIALLY EXPRESSED DURING HDV REPLICATION 92
V.4.3. VALIDATION OF PROTEOMICS RESULTS 102
p53 103
Transportin-1 104
ELAV-like protein 1 105
V.4.4. SYSTEMS BIOLOGY 106

V.4.5. CELL CYCLE: G2/M DNA DAMAGE CHECKPOINT REGULATION PATHWAY .. 119
V.5. DISCUSSION 121
CHAPTER VI: FINAL CONCLUSIONS AND FUTURE PERSPECTIVES 141
SUPPLEMENTARY INFORMATION I: DIFFERENTIALLY EXPRESSED PROTEINS FOR EXPERIMENTS 1, 2, 3, 4 AND 5 AND SIGNIFICANT DATA ASSOCIATED..... 143
SI.1. DIFFERENTIALLY EXPRESSED PROTEINS IN EXPERIMENTS 1, 2, 3, 4 AND 5. 144
SI.2. DIFFERENTIALLY EXPRESSED PROTEINS IN EXPERIMENTS 1, 2, 3, 4 AND 5 AND RELEVANT STATISTICAL PARAMETERS FOR QUANTIFICATION 148
SUPPLEMENTARY INFORMATION II: SIGNALING PATHWAYS AFFECTED BY SHDAG AND HDV RNA REPLICATION 177
GLYCOLYSIS/GLUCONEOGENESIS PATHWAY 178
HIF1α SIGNALING 179
PROPANOATE METABOLISM PATHWAY 180
PROTEIN UBIQUITINATION PATHWAY 181
VEGF SIGNALING PATHWAY 182
INTEGRIN SIGNALING PATHWAY 183
REFERENCES..... 187

INDEX OF FIGURES

Figure I.1.1. – Global epidemiology of HDV infection according to viral genotype…...3
Figure I.3.1. – Schematic representation of HDV viral particles…….....6
Figure I.3.2. – Representation of the three HDV RNAs……...7
Figure I.3.3. – HDV delta antigens……...9
Figure I.3.4. – Double rolling-circle mechanism for HDV replication.....12
Figure I.3.5. – HDV life cycle……14
Figure III.3.1. – Restriction map and cloning site of the RNAi-Ready pSiren-RetroQ vector……...22
Figure III.3.2. – Oligonucleotide DNA sequence inserted in the RNAi-Ready pSiren-RetroQ vector used to generate small hairpin RNAs……..23
Figure III.3.3. – Synthesized shRNA oligonucleotides targeting proteins HSP105……24
Figure III.4.1. – Restriction analysis of the vector pSiren-RetroQ-HSP105……....31
Figure III.4.2. – Validation of the ΔΔCt method……..…….…..32
Figure III.4.3. – Alterations in mRNA levels of HSP105 due to the presence of a shRNA targeting HSP105 mRNA and consequent alteration of the levels of the HDV Mrna…….33
Figure III.4.4. – Western blot analysis of cellular extracts resulting from the transfection of Huh7-D12 cells with pSiren-RetroQ-HSP105 and from the transfection of Huh7-D12 cells with pSiren-RetroQ-Luciferase…….....34
Figure III.4.5. – Knock down of the protein HSP105 and consequent knock down of the large delta antigen……..……34
Figure III.4.6. – Co-localization of HSP105 and SHDAg……...35
Figure III.4.7. – Co-immunoprecipitation of HDP105 and the delta antigens……36
Figure IV.3.1. – Synthesized shRNA oligonucleotides targeting proteins hnRNP H….46
Figure IV.4.1. – Restriction analysis of the vector pSiren-RetroQ-hnRNP H……51
Figure IV.4.2. – Validation of the ΔΔCt method…….52
Figure IV.4.3. – Alterations in mRNA levels of hnRNP H due to the presence of a shRNA targeting hnRNP H mRNA and consequent alteration of the levels of the HDV mRNA……..53
Figure IV.4.4. – Western blot analysis of cellular extracts resulting from the transfection of Huh7-D12 cells with pSiren-RetroQ-hnRNP H and from the transfection of Huh7-D12 cells with pSiren-RetroQ-Luciferase……...……53

Figure IV.4.5. – Knock down of the protein hnRNP H and consequent knock down of the small delta antigens and of LHDAg……..54
Figure IV.4.6. – Co-localization of hnRNP H and SHDAg……55
Figure IV.4.7. – Pull down of complexes formed with the recombinant protein SHDAg-6xHis……56
Figure IV.4.8. – Co-immunoprecipitation of hnRNP H and the delta antigens……..56
Figure V.1.1. – ICAT labeling reagents…..……63
Figure V.1.2. – iTRAQ labeling reagent ……....64
Figure V.1.3. – Post-digestion ^{18}O labeling…….65
Figure V.4.1. – Experiment design ……89
Figure V.4.2. – SDS-PAGE……..…..89
Figure V.4.3. – Distribution pattern of OFFGEL fractionation……91
Figure V.4.4. – Number of total identifications……..92
Figure V.4.5. – Distribution of labeling efficiencies as function of log2 rations……..93
Figure V.4.6. – Outliers at the scan level……....94
Figure V.4.7. – Outliers at the peptide level……95
Figure V.4.8. – Differentially expressed proteins……...96
Figure V.4.9. – Correlation between assays 2 and 4 and 3 and 5……97
Figure V.4.10. – Quantifications at the scan, peptide and protein levels……....97
Figure V.4.11. – Differentially expressed proteins per experiment……....98
Figure V.4.12. – Significant expression changes……..102
Figure V.4.13. – Biological functions of differentially expressed proteins……..102
Figure V.4.14. – Western blot analysis of p53 and clathrin……..104
Figure V.4.15. – Western blot analysis of transportin-1 and clathrin……...105
Figure V.4.16. – Western blot analysis of ELAV-like protein 1 and clathrin……...106
Figure V.4.17. – Variation of the number of enriched categories accordingly to FDRq…...……..107
Figure V.4.18. – Enriched categories for experiments 4 and 5……108
Figure V.4.19. – Significant affected canonical pathways by the expression of the delta antigen……...111
Figure V.4.20. – Interactions among differentially expressed proteins resulting from cells expressing the small delta antigen……112

Figure V.4.21. – Relevant interactions between differentially expressed proteins resulting from the expression of the small delta antigen……...113
Figure V.4.22. – Significant affected canonical pathways by the accumulation of HDV RNA……..114
Figure V.4.23. – Intercations among differentially expressed proteins resulting from HDV replication……115
Figure V.4.24. – Relevant interactions between differentially expressed proteins resulting from the accumulation of HDV RNA and proteins in IPA database…….116
Figure V.4.25. – Significal canonical pathways affected by HDV replication…….117
Figure V.4.26. – Interactions among differentially expressed proteins resulting from the expression of the delta antigen and HDV replication……118
Figure V.4.27. – Relevant interactions between differentially expressed proteins resulting from experiments 4 and 5 altogether and proteins in IPA database……...119
Figure V.4.28. – Cell cycle:G2/M DNA damage checkpoint regulation pathway…...120
Figure V.4.29. – Western blot analysis of 14-3-3 σ and clathrin……..120
Figure SII.1. – Glycolysis/Gluconeogenesis pathway……...178
Figure SII.2. – HIF1a signaling pathway……..179
Figure SII.3. – Propanoate metabolism pathway……...180
Figure SII.4. – Protein ubiquitination pathway…….181
Figure SII.5. – VEGF pathway……..182
Figure SII.6. – Integrin signaling pathway……183

INDEX OF TABLES

Table III.3.1. – Target sequence from HSP105 mRNA used to design shRNA oligonucleotides……...24
Table III.3.2. – Primers for cDNA amplification of HSP105, β-2-microglobulin and HDV…….27
Table IV.3.1. – Target sequence from hnRNP H mRNA used to design shRNA oligonucleotides……..46
Table IV.3.2. – Primers for cDNA amplification of hnRNP H……...47
Table V.4.1. – Differentially expressed proteins in the presence of the delat antigen and during HDV replication……...98
Table V.4.2. – FDRq at which there is a reliable number of enriched categories that seem to follow a tendency to up or down regulate……108
Table V.4.3. – Differentially expressed proteins associated to the most affected canonical pathways for experiment 4……111
Table V.4.4. – Differentially expressed proteins associated to the most affected canonical pathways for experiment 5……114
Table V.4.5. – Differentially expressed proteins associated to the most affected canonical pathways for experiment 4 and 5 altogether…….117
Table SI.1. – Differentially expressed proteins for experiments 1, 2, 3, 4 and 5……..144
Table SI.2.1. – Differentially expressed proteins for experiments 1, 2, 3, 4 and 5 and respective access numbers, peptide sequence, pI and A and B concentrations……...…….149
Table SI.2.2. – Differentially expressed proteins for experiments 1, 2, 3, 4 and 5 and respective labeling efficiencies and statistical parameters relevant for quantification..159
Table SI.2.3. – Differentially expressed proteins for experiments 1, 2, 3, 4 and 5 and respective statistical parameters relevant for quantification, scans per peptide quantified, peptides per protein quantified and fold……168

CHAPTER I: HEPATITIS DELTA VIRUS

I.1. EPIDEMIOLOGY, PATHOGENESIS AND TREATMENT OF HEPATITIS D VIRUS

In 1977, Mario Rizzetto and co-workers, found what they thought to be a new antigen of Hepatitis B virus (HBV) while studying liver biopsies of patients infected with HBV, with a particular severe course of the disease (Rizzetto *et al.* 1977). In 1980, however, experiments revealed that the "delta antigen" was not an HBV antigen, but rather an antigen belonging to a novel infectious agent that required the helper function of HBV – the Hepatitis D virus (HDV) (Rizzetto *et al.* 1980). HDV thus can only occur in patients infected with HBV. The infection may be a superinfection, where patients with chronic HBV are infected with HDV or a co-infection where patients are infected with both viruses simultaneously. In the first case, HDV infection leads to more severe liver disease than HBV mono-infection and is associated with accelerated fibrosis progression, early hepatic decompensation and increased risk for the development of hepatocellular carcinoma making it one of the most severe forms of viral hepatitis in humans. In the second case, although most cases lead to complete viral clearance, many others may end up in severe acute hepatitis with the potential for fulminant hepatitis (Wedemeyer and Manns 2010). Worldwide, more than 350 million people are considered to have chronic HBV infection, from which 15-20 million are thought to be co-infected with HDV (World Health Organization data from 2008).

HDV, just like HBV, is a blood-bourne disease that may also be transmitted sexually, percutaneoulsy (injection drug use), permucosally (sexual) and also perinatally. HDV is spread all over the world being highly endemic in Mediterranean countries, the Middle East, Central Africa and northern parts of South America (Radjef *et al.* 2004). In southern Europe, however, with better public health standards, HBV vaccination and the effect of measures taken to control Human immunodeficiency virus (HIV), a decrease in HDV infection was achieved leading some investigators to believe that an eradication of HDV in southern Europe was possible (Gaeta *et al.* 2000). Despite the optimistic perspective, recent results show that HDV has not been eradicated and has been maintained stable for the last years, being a major health burden in Central Europe. This prevalence of the HDV in Europe is a result of the immigration of individuals to Europe from highly endemic regions and without health control may lead to a secondary spread of HDV (Wedemeyer *et al.* 2007). Until now, eight HDV genotypes were identified. Genotype I is associated with both severe and mild disease and is distributed by Europe, Middle East, North America and North Africa. Genotype

II is associated with mild disease and is only seen in the Far East. Genotype III is only observed in the north part of South America. Genotype IV is seen in the Far East and finally genotypes V to VIII were only identified in African patients. Figure I.1.1. shows the global prevalence of HDV infection according to viral genotype.

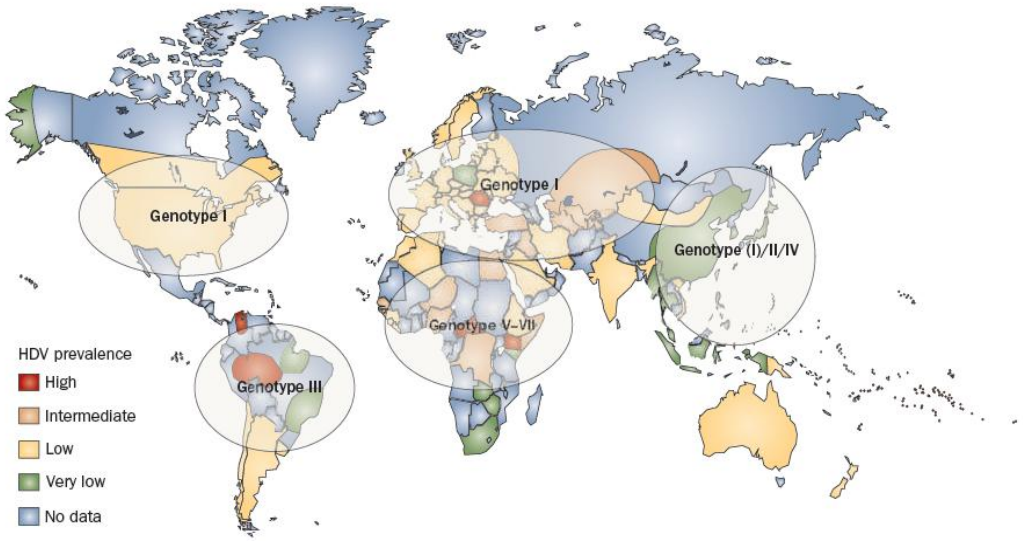

Figure I.1.1.: Global epidemiology of HDV infection according to viral genotype. HDV genotype I is the most frequent genotype and is distributed throughout the world, especially in Middle East, North America and North Africa. By contrast, HDV genotype II is observed in the Far East, and HDV genotype III is seen exclusively in the northern part of South America (Wedemeyer and Manns 2010).

Pathogenesis of HDV is still poorly understood. For several years cytotoxicity of HDV has been studied originating controversial results with some authors stating that HDV is cytotoxic and others stating otherwise. In 2001, Wang *et al*, performed an extensive study showing that HDV was not cytotoxic (Wang *et al.* 2001). Cellular immune responses against HDV also have been reported by a few investigators, suggesting that the quantity and quality of host T-cell responses may be associated with the degree of control of infection (Nisini *et al.* 1997; Huang *et al.* 2004; Zachou *et al.* 2010). These data suggest that HDV is mainly an immune-mediated disease. Another interesting feature of HDV is that in co-infection with HBV, HDV seems to suppress HBV replication and in a triple infection, HDV not only suppresses HBV replication but also suppresses HCV replication (Jardi *et al.* 2001).

HBV vaccine has been of great help preventing the spreading of HDV. However, for super-infected patients, there is no established treatment for HDV. Nucleoside and nucleotide analogs have been used in HDV treatment. Famciclovir, Lamivudine and Ribavirin, all used in HBV treatment, were ineffective in the treatment of HDV (Wedemeyer and Manns 2010)). As for tenofovir, a long term treatment of 6 years showed more promising results leading to the reduction of HDV RNA levels and 3 out of 16 patients became HDV RNA negative (Sheldon *et al.* 2008). Clevudine, a nucleoside analogue also developed to treat HBV, was seen to inhibit HDV viremia in woodchucks, however, no data is still available in humans (Casey *et al.* 2005). Interferon α (IFN-α) has been used to treat HDV since the 1980s (Rizzetto *et al.* 1986). However, optimal doses of IFN-α and the duration of treatments are still not established. Some authors state that high doses of IFN-α are important for long-term beneficial outcome (Farci *et al.* 2004). Others state that long-term treatment (2 years) with IFN-α is more positive in terms of HDV RNA clearance (Niro *et al.* 2005). The National Institute of Health (NIH) reported a case of a patient submitted to a 12 year treatment with IFN-α which resulted in its cure with no HDV infection and HBsAg (Hepatitis B surface antigen) clearance (Lau *et al.* 1999). However, the majority of patients cannot tolerate high doses of IFN-α for such long periods of time (Manns *et al.* 2006). In cases of patients who developed cirrhosis resultant from HDV, liver transplantation is the only treatment.

A vaccine for HDV would be important to prevent patients from an HDV superinfection. Several strategies have been followed to induce protective immune response against HDV superinfection: synthetic peptides, incomplete or complete HDAg expressed in *E. coli*, yeast or baculovirus, vaccinia virus expressing the small delta antigen (SHDAg) or the large delta antigen (LHDAg), the only proteins expressed by HDV, and DNA immunization. However, none of these protocols has been successful in preventing HDV superinfection in animals (Casey 2006).

I.2. HDV AND ITS ORIGINS

Origins of HDV are still unknown. One theory of the origins of HDV is based on its similarity with plant viroids, which are small, circular RNA pathogens that infect several crop plants. HDV and viroids seem to share similarities like genome structure and mechanisms of replication. Other authors support the theory that HDV arose from

an host RNA that might have been used as a template for replication to generate an HDV like species. It was seen that β-globin in humans has a ribozyme domain that is conserved in other primate globin genes and functionally, it resembles self-cleaving ribozymes described for the protein-encoding genes from the myxomycetes *Didymium iridis* and *Physarum polycephalum* (Teixeira *et al.* 2004). These results show an evolutionary conservation of ribozymes that are present in HDV antigenomic RNA. Many HDV-like ribozymes were also detected in diverse eukaryotic species, supporting the theory that HDV may have arose from a host mRNA precursor. The origin of the delta antigens is also still unknown. It was proposed that, because the delta antigen binds to the protein DIPA (delta-interacting protein A) found in animal cells, and based on size and possible sequence homology, a form of viroid RNA might have created the HDV genome by transduction of DIPA-RNA coding sequence. However, homology between the delta antigens and DIPA is low giving some controversial interpretation to this theory (Brazas and Ganem 1996; Long *et al.* 1997). Finally, and because HDV depends on HBV, some authors recently proposed that HDV is a result of an infection of the liver of an HBV infected primate, not necessarily human, by a viroid-like genome assembled by HBV surface proteins. Finally, another possibility is that HDV-like RNAs origin occurred by a chance event during HBV replication (Taylor and Pelchat 2010).

I.3. THE BIOLOGY OF HDV

I.3.1. VIRAL STRUCTURE AND ASSEMBLY

To form infectious viral particles, HDV requires the envelope proteins of HBV. The HDV virion is thus a 36 nm diameter chimerical structure composed by an outer lipid membrane in which the HBV envelope proteins are anchored and an inner ribonucleoprotein (RNP). Apparently, although the proportions of HBV surface proteins in HDV and HBV outer membrane may differ, both viruses have an identical envelope consisting in the outer lipid membrane and the three HBV envelope proteins. These proteins have a common carboxyl-terminus and are designated by their sizes in small (S-HBsAg), middle (M-HBsAg) and large (L-HBsAg). The RNP is a spherical, core-like structure with no apparent icosahedral symmetry with 19 nm diameter and is composed by the virus genome and both viral proteins, the small and the delta antigens.

It includes, per copy of HDV genomic RNAs, about 70 molecules of the SHDAg (Casey 2006). A schematic representation of HDV virion is presented in figure I.3.1.

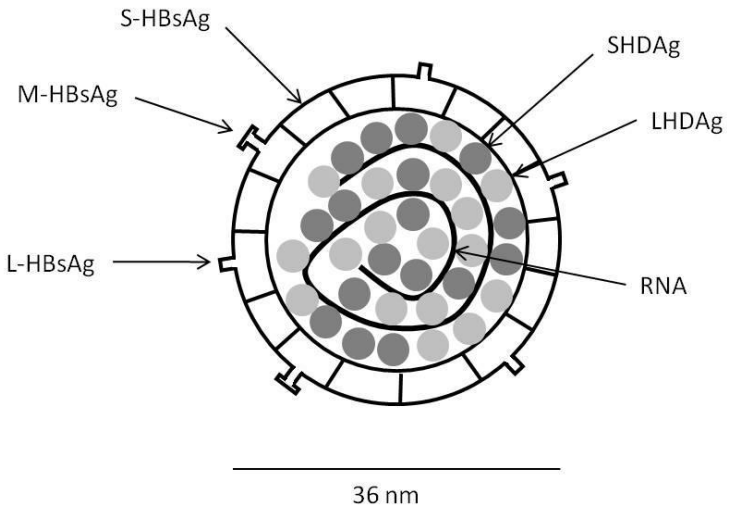

Figure I.3.1.: Schematic representation of HDV viral particle.

The formation of the RNPs and of the viral envelope of HDV, are directed by HDV and HBV, respectively occurring at different locations in cells. While RNPs are formed in the nucleus by HDV, the viral envelope is assembled at the endoplasmic reticulum (ER) by HBV. So that the formation of viral particles can take place, the RNP must encounter the HBV budding system. The RNP, which is formed by HDV RNAs and the delta antigens, shuttles between the nucleus and the cytoplasm due to the nuclear export signal (NES) present in LHDAg allowing the encounter with HBV budding system (Lee *et al.* 2001; Tavanez *et al.* 2002). The farnesyl group at the LHDAg will then probably serve to anchor the RNP to the ER membrane, allowing the formation of viral particles (Otto and Casey 1996).

I.3.2. HDV GENOME AND RNAS

HDV is a very simple virus with a single-stranded RNA genome of 1679 nucleotides (nt) and circular conformation. The genome has a 74% intramolecular base paring due to which it can fold on itself forming an unbranched rod-like structure (figure I.3.2.). During replication a second circular RNA, complementary to the genome, is synthesized. This so-called antigenome contains the open reading frame

(ORF) for the only protein encoded by the virus, the small delta antigen (SHDAg). However, SHDAg is not translated from the circular antigenomic RNA but from a third synthesized linear RNA, with the same polarity as the antigenome, with approximately 800 nt, with a 5'-cap structure and a 3'-poly(A) consistent with a role of mRNA (figure I.3.2.) (Gudima *et al.* 2000). During HDV replication up to 300 000 copies of the HDV genomic RNA, 30 000 copies of HDV antigenomic RNA and approximately 600 copies of HDV mRNA are synthesized.

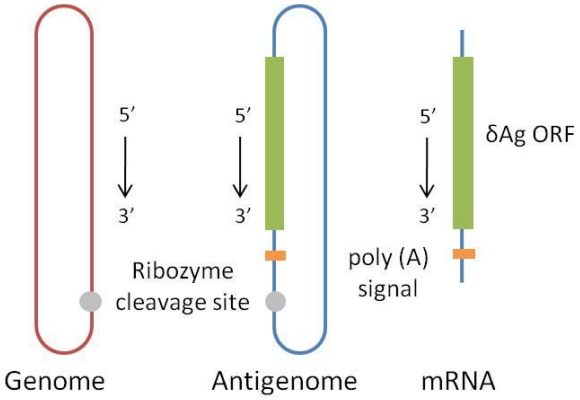

Figure I.3.2.: Representation of the three HDV RNAs. The antigenome is an exact complement of the genome. Both HDV genomic and antigenomic RNA, as a result from base pairing, form unbranched rod-like structures and both present a ribozyme cleavage site. The mRNA is the same polarity as the antigenome and contains delta antigen ORF. Adapted from (Taylor 2009).

Both the genome and the antigenome contain a 85 nt domain that will act as a ribozyme being essential for HDV replication (Sharmeen *et al.* 1988; Ferre-D'Amare *et al.* 1998). HDV replication has been proposed to occur by a rolling circle mechanism, much like viroids, releasing multimeric transcripts. These transcripts are then self-cleaved by their own ribozyme domain originating unit length fragments of the HDV genome and antigenome that will then re-circularize.

I.3.3. THE DELTA ANTIGENS

The small delta antigen (SHDAg), with 195 a.a. and 24 KDa, is essential for initiation of HDV genome replication and accumulation of HDV RNA-directed RNA transcripts (Chao *et al.* 1990). Furthermore, several specific roles for SHDAg in HDV life cycle have been proposed. Among them, Yamaguchi *et al*, proposed that SHDAg acts as a facilitator of processivity during RNA-directed RNA transcription (Yamaguchi

et al. 2001); Cheng *et al* proposed that SHDAg forms an RNP that protects HDV RNAs against adenosine deaminase editing (Cheng *et al.* 2003); and Xia et al, that SHDAg forms an RNP that facilitates transport of the HDV genome to the nucleus (Xia *et al.* 1992). However, the eternal question seems to be if SHDAg contributes directly to the HDV RNA-directed RNA transcription process. During HDV replication in the nucleus, an editing mechanism catalyzed by adenosine deaminase I (ADARI) occurs in HDV antigenome, converting an amber STOP codon UAG into a tryptophan codon UGG by changing the adenosine to inosine (Wong and Lazinski 2002). As a result the reading frame is extended by 19 a.a. and a 214 a.a protein of about 27 KDa, the large delta antigen, is synthesized. LHDAg does not support genome replication and is essential for viral packaging (Chao *et al.* 1990).

SHDAg and LHDAg share many biochemical properties since they are identical in sequence, except for the 19 a.a. extension on the C-terminal of LHDAg. However, during HDV infection these proteins play very different roles. As already described, SHDAg is essential for the initiation of HDV replication *in vivo*. As for LHDAg, synthesized late in the infection, is essential for viral packaging and was described to acts as a dominant negative inhibitor suppressing HDV replication (Chao *et al.* 1990). However, more recent studies have shown that LHDAg mediated suppression only happened when LHDAg was abnormally expressed early in HDV replication cycle (Macnaughton and Lai 2002). Furthermore, when such happened, only synthesis of HDV genomic RNA from HDV antigenomic RNA was suppressed (Modahl and Lai 2000). Sato *et al* confirmed those results, also observing that earlier expression of LHDAg in fact inhibits HDV replication (Sato *et al.* 2004). SHDAg and LHDAg, also share many functions due to its sequence similarity which include stabilization of HDV RNA (Lazinski and Taylor 1994), enhancement of ribozyme activity (Jeng *et al.* 1996) and RNA chaperone activity (Huang and Wu 1998). Several functional domains have been identified in the delta antigens. Three of these domains are shared by the two proteins (figure I.3.3.).

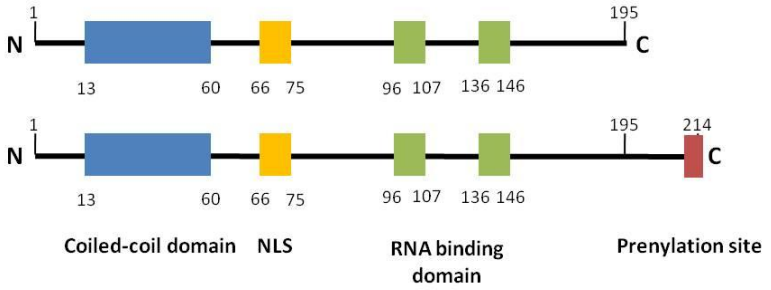

Figure I.3.3.: HDV delta antigens. Both the small form and the large form of HDV present a coiled-coil domain, a NLS and an RNA binding domain. The large form contains an isoprenylation site which is essential for viral particle assembly.

The first domain, located at aminoacids 12 to 60, is a coiled coil domain (CCD), which acts as a dimerization or even multimerization domain promoting protein-protein interactions. It has been proposed that the ability of LHDAg to act as a dominant negative inhibitor of replication occurs via protein-protein interaction with SHDAg. Furthermore LHDAg, seems to interact with SHDAg through the CCD, to bind the HDV RNP and move it to the cytoplasm (Lazinski and Taylor 1993). Another shared domain, adjacent to the CCD, is a nuclear localization signal (NLS). This NLS was considered to be composed by two separated parts (Xia *et al.* 1992), however, a more recent study by Alves *et al*, showed that the sequence located at a.a. 66 to 75, rich in basic a.a., is sufficient to promote nuclear localization (Alves *et al.* 2008). Adjacent to the NLS, is the RNA binding domain, localized at a.a. 97 to 146, which confers the delta antigens the RNA binding capacity. This RNA binding domain is composed of two stretches of arginine-rich motifs (ARMs), which are separated by a spacer region that includes a helix-loop-helix (HLH) motif (Chang *et al.* 1993; Lee *et al.* 1993). Both ARMs and spacer are required for RNA binding (Lee *et al.* 1993). RNA binding of HDAgs appear to be specific for HDV RNA. Furthermore, they bind to several regions of both HDV genomic and antigenomic RNA (Lin *et al.* 1990) and both HDAg bind with equal affinity (Hwang *et al.* 1992). The C-terminal of SHDAg, and the correspondent part of LHDAg, is characterized by a stretch of a.a. rich in proline and glycine residues, but the function of this stretch is still unknown. Finally, the C-terminal 19 a.a. extension of LHDAg is unique for this protein. This 19 a.a. extension contains a four a.a. sequence motif – CXXX – conserved across HDV isolates, that serves as a substrate for prenylation, with the modification occurring at the cysteine residue of this

quartet (Glenn *et al.* 1992). Prenylation alters LHDAg conformation, masking the c-terminal epitope present in SHDAg (Hwang and Lai 1994). This modification promotes membrane binding and is essential for the interaction between LHDAg and HBsAg, critical for HDV particle assembly (Hwang and Lai 1993).

SHDAg and LHDAg both undergo several post-translational modifications. So far HDAgs have shown to be phosphorylated (Chang *et al.* 1988; Mu *et al.* 1999), methylated (Li *et al.* 2004), acetylated (Mu *et al.* 2004) and more recently sumoylated (Tseng *et al.* 2010). Two dimensional phosphoaminoacid analysis revealed that SHDAg is phosphorylated at both serine and threonine residues, while LHDAg is phosphorylated only at the serine residues (Mu *et al.* 1999). Interestingly, although LHDAg is only phosphorylated at serine residues, its phosphorylation levels are approximately sixfold higher than that of SHDAg (Hwang *et al.* 1992; Choi *et al.* 2002). The actual phosphorylation sites of HDAgs have not been completely identified, so putative phosphorylation residues were predicted. SHDAg contains only three conserved serine residues, serine 3 (S3), 123 (S123) and 177 (S177), from which S177 is the only one that has been identified, *in vivo*, by mass spectrometry (Chen *et al.* 2002). Furthermore, by replacing S3 and S123 by alanine, SHDAg phosphorylation was not abolished, suggesting that more phosphorylation sites in SHDAg exist (Mu *et al.* 1999). As for LHDAg, and despite the phosphorylation sites already described above, two more candidate serine residues for phosphorylation exist at the C-terminal 19 a.a. extension, however, experimental assays revealed that phosphorylation of that residues does not occur (Bichko *et al.* 1997). It is still not known why LHDAg is more heavily phosphorylated than SHDAg. Both SHDAg and LHDAg are acetylated, and lysine 72 (K72) of SHDAg was identified as one of the acetylation sites (Mu *et al.* 2004). The authors also suggested that acetylation on K72 of SHDAg may modulate the subcellular localization of SHDAg and participate in viral RNA nucleocytoplamic shuttling and replication. SHDAg was shown to be methylated in vivo and in vitro (Li *et al.* 2004). The major methylation site is at arginine 13 (R13) in the RGGR motif of SHDAg. Methylation of SHDAg is crucial for HDV RNA replication, especially for the replication of the genomic RNA from the antigenomic RNA. More recently, Tseng *et al*, showed that SHDAg is a small ubiquitin-like modifier 1 (SUMO1) target protein. The authors showed that multiple lysine residues are SUMO1 acceptors within SHDAg and conjugation of SUMO1 to SHDAg enhanced HDV genomic RNA and mRNA synthesis but not antigenomic RNA synthesis (Tseng *et al.* 2010).

I.3.4. HDV LIFE CYCLE

HDV attachment and entry into cells is likely to occur by a similar way of that of HBV since HDV shares HBV envelope proteins. There is evidence that sequences within the pre-S1 domain, specific for L-HBsAg, are essential for attachment and entry of both HDV and HBV in susceptible cells (Neurath *et al.* 1986; Sureau *et al.* 1992; Barrera *et al.* 2005). However a study by Sureau *et al*, also showed that by removing the N-linked carbohydrate modification of L-HBsAg, M-HBsAg and S-HBsAg, HBV became non-infectious while HDV remained infectious (Sureau *et al.* 2003). After entry into the cells HDV replication is totally independent of HBV. Mechanisms by which HDV reaches the nucleus for replication are still unknown. Does HDV entry requires an endocytic pathway? How are RNPs uncoated and transported into the nucleus? Is it by microtubules or RNA-binding and NLS abilities of SHDAg? All of these questions still have no answer. When the RNP does reach the nucleus, the next step in HDV life cycle is genome replication. HDV replication is thought to occur by a rolling circle mechanism similar to the proposed for viroids (Branch and Robertson 1984). Briefly, input circular genomic RNA serves as template for the synthesis of the complementary antigenome strand. The growing transcript is then cleaved by the ribozyme activity intrinsic to both HDV genomic and antigenomic RNAs, originating antigenome monomers which then re-circularize. Initially it was though that HDV genome and antigenome had self-ligation capacity (Sharmeen *et al.* 1988) however, more recently, it was shown that this ligation may be carried out by cellular RNA ligase (Reid and Lazinski 2000). The circularized HDV antigenome then serves as a template to synthesize HDV genomic RNA. Again, multimers formed will then be cleaved by the ribozyme activity and monomers will be circularized (figure I.3.4.). During HDV antigenome synthesis, another RNA species, with the same 5' end as the antigenome (Gudima *et al.* 2000) and with 800 nt in size, is also synthesized. This 800-nt RNA then undergoes 5'-capping and 3'-poly(A) processing originating HDV mRNA. Later during replication, RNA editing occurs at the antigenome leading to the production of LHDAg. Because SHDAg is essential to initiate replication it is likely that the first event in the HDV replication cycle is the transcription of SHDAg mRNA.

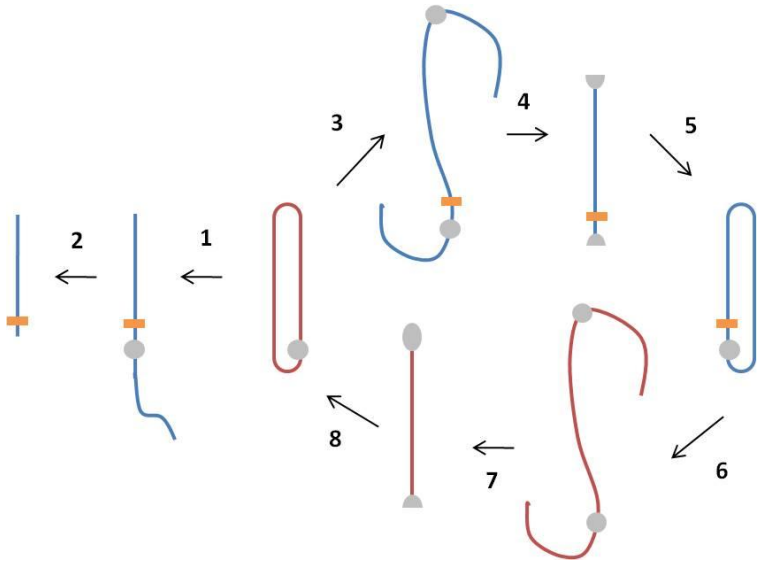

Figure I.3.4.: Double rolling-circle mechanism for HDV replication. HDV genomic RNA serves as template to synthesize antigenomic RNAs, that either are processed to became mRNAs (1, 2) or are cleaved and re-circularized originating new HDV antigenomic RNAs (3-5). These new antigenome strands then serve as templates to produce new genomic RNAs (6-8). Adapted from Taylor 2006.

During HDV replication genomic and antigenomic RNAs are localized in the nucleus of cells (Taylor *et al.* 1987; Tavanez *et al.* 2002). As for SHDAg, during replication it is found in the nucleoplasm of cells (Bichko and Taylor 1996; Chang *et al.* 2008; Han *et al.* 2009), but in the absence of HDV RNAs, this protein is preferentially localized in the nucleolus (Chang *et al.* 2008; Han *et al.* 2009).

HDV replicates through an RNA-directed RNA transcription process using a host RNA polymerase. To the date, several studies have been made to determine which RNA polymerase is actually involved in HDV replication. Most of them seem to indicate that RNA Pol II is necessary for HDV replication. Gudima *et al* and Nie *et al*, showed that the HDV mRNA possessed a 5'-cap structure and a 3'-poly(A), consistent with RNA Pol II transcription (Gudima *et al.* 1999; Nie *et al.* 2004). In cells replicating HDV, low concentration of α-amanitin inhibited HDV replication, showing the involvement of RNA Pol II in HDV replication (Moraleda and Taylor 2001; Chang *et al.* 2006). Furthermore, during HDV replication, SHDAg locates in the nucleoplasm of cells, consistent with the location of RNA Pol II. Finally, Greco-Stewart *et al*, showed an interaction between HDV RNA and RNA Pol II (Greco-Stewart *et al.* 2009). However, if on one hand most studies support RNA Pol II involvement in HDV replication, on the other hand, some authors state that RNA Pol I is also involved in

HDV replication. Some authors showed that, when in presence of α-amanitin, replication of genomic and antigenomic HDV RNAs had different sensitivities to the drug. While replication of HDV genomic RNA was inhibited with low concentrations of α-amanitin, replication of HDV antigenomic RNA was resistant to the drug. Furthermore HDV genomic and antigenomic RNAs seem to be associated to different nuclear bodies, while the former was distributed to the nucleoplasm, the later was localized to the nucleolus, suggesting that HDV genomic and antigenomic RNAs are synthesized by two different transcription machineries (Modahl and Lai 2000; Macnaughton and Lai 2002; Li *et al.* 2006; Tseng *et al.* 2008). More recently, Greco-Stewart *et al*, showed that not only RNA Pol I interacted with both forms of HDV RNA, but also RNA Pol III could interact with both structures (Greco-Stewart *et al.* 2009).

During HDV replication *in vitro*, template switching was observed. HDV replication was seen to be initiated from HDV RNA linear templates (Gudima *et al.* 2004). The same author also saw that when transfecting cells with two RNAs, smaller than the unit length RNA, that together provided fully representation of HDV genome, replication was detected, consistent with the reconstitution of the genome (Gudima *et al.* 2005). Template switching was also reported *in vitro* when cells were transfected with two different HDV RNAs from different genotypes (Wang and Chao 2005) and during natural infections in patient infected with two HDV genotypes (Wu *et al.* 1999).

After replication and translation of both HDV proteins, RNPs are formed in the nucleus of cells. The RNP is then exported to the cytoplasm, due to the nuclear export signal (NES) present in LHDAg, allowing the RNP to reach the ER where the viral particles will be assembled with the envelope proteins of HBV. The farnesyl group at the LHDAg serves as an anchor so that the RNP binds to the ER membrane, allowing the formation of viral particles which will then be released. HDV viral cycle is represented in figure I.3.5.

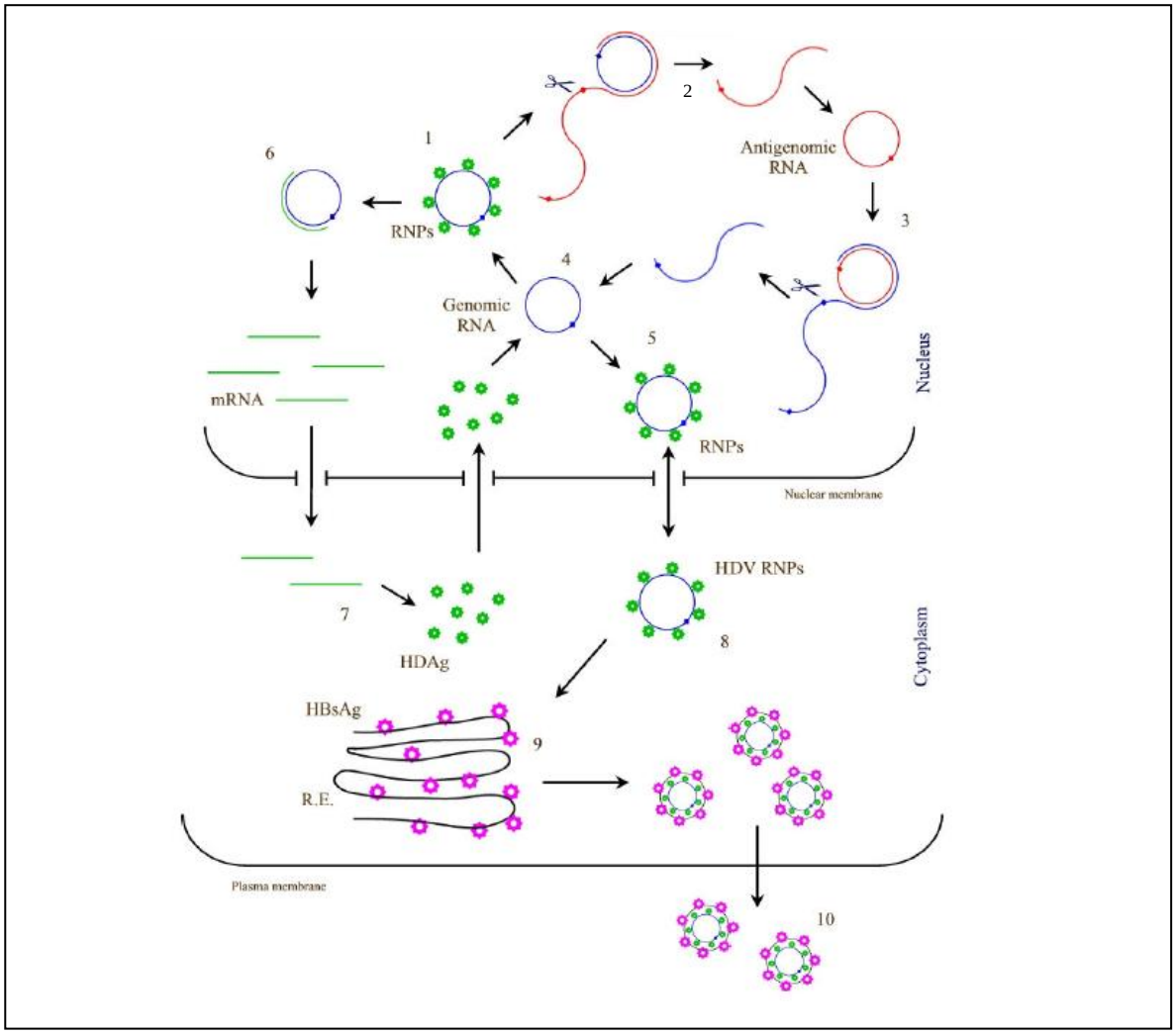

Figure I.3.5.: HDV life cycle. When HDV enters the cell, through still unknown mechanisms, the viral particle is uncoated and the RNP heads to the nucleus of cells where replication takes place. HDV genomic RNA serves as template to synthesize antigenomic RNAs that are cleaved and re-circularized originating new HDV antigenomic RNAs (2). During antigenome synthesis another RNA species of about 800 nt is synthesized, 5' –capped and poly adenylated originating HDV mRNA (6). The new antigenome strands then serve as templates to produce new genomic RNAs (3). HDV mRNA is then translated in the cytoplasm of cells (7) and newly synthesized proteins, which contain an NLS, are directed to the nucleus to form new RNPs (4, 5). RNPs then leave the nucleus to the cytoplasm (8) and reach the ER (9) where viral particle assembly is performed using HBV envelope proteins. Viral particles are finally released (10). Adapted from (Cunha *et al.* 2003).

CHAPTER II: GENERAL OBJECTIVES

The objectives in this work are:

1. To determine if and how HSP105 and hnRNP H, two proteins found differentially expressed during HDV replication, affect HDV replication.

2. To determine alterations in the proteome of a tetracycline inducible cell line expressing the small delta antigen, 293-dAg, and in cells 293-dAg-HDV, transfected with HDV RNA and in which HDV replication occurs, in an attempt to clarify HDV replication and pathogenesis mechanisms.

CHAPTER III: HSP105: A NEW HDV INTERACTING PARTNER

III.1. INTRODUCTION

When cells are exposed to a variety of stress factors, such as heat shock, heavy metals, oxidative stress, etc, they respond by increasing the synthesis of a set of highly conserved proteins named heat shock proteins (HSP), protecting themselves against cytotoxic effects. Under normal physiological conditions HSPs are also expressed in cells, at a normal level, playing important roles in normal cellular functions. Mammalian HSPs are classified accordingly to their molecular weight and several families of HSPs like HSP90, HSP70, HSP60, HSP40 and HSP27 exist (Hendrick and Hartl 1993; Craig *et al.* 1994).

HSP70 family is one of the major and well-characterized groups of HSPs. Several proteins belonging to the HSP70 family are found in different compartments of eukaryotic cells and play central roles in protein synthesis, translocation, folding and assembly/disassembly of multimeric protein complexes as molecular chaperones. Under normal conditions HSP70 is expressed in the cytoplasm however, during heat shock conditions it accumulates in the nucleus and nucleolus of cells thus being associated with the repair of heat-induced nucleolar damage (Welch and Mizzen 1988; Abe *et al.* 1995; Bukau and Horwich 1998). HSP70 family proteins are very similar in sequence and structure. They possess an highly conserved bipartide domain structure composed of a N-terminal ATPase (nucleotide binding domain (NBD)) and a C-terminal substrate or peptide binding domain (PBD) (Bukau *et al.* 2006). The chaperone activity of HSP70 relies on cycles of substrate binding and release driven by conformational changes of HSP70. The ATP bound form of HSP70 binds and releases peptide rapidly, resulting in a low affinity for substrate whereas the ADP-bound form can bind the substrate slowly but more stably, resulting in a higher affinity for substrate. The conformational changes of HSP70 are a result of its intrinsic ATPase activity, which is facilitated by proteins of the HSP40 family (Shaner and Morano 2007).

HSP105α and HSP105β mammalian proteins are members of the HSP105/110 family, a diverged subgroup of the HSP70 family. They are a result of alternative splicing in the *hsp105* gene transcript and although both proteins have an amino-terminal ATP binding domain, a β sheet, a loop and a carboxyl-terminal α helical domain, similar to those of HSP70 family proteins, HSP105β lacks 44 aminoacids (Ishihara *et al.* 1999). HSP105α is expressed constitutively and produced in response to

various forms of stress while HSP105β is specifically produced as a response to heat shock at 42ºC (Hatayama *et al.* 1986; Honda *et al.* 1988). Both proteins exist as complexes associated with HSP70 and HSC70 in mammalian cells and just as HSP70 and HSC70 they suppress the aggregation of denatured proteins caused by heat shock and regulate the HSC70 chaperone system (Hatayama and Yasuda 1998; Wakatsuki and Hatayama 1998; Yamagishi *et al.* 2000). Furthermore, HSP105α and HSP105β are phosphorylated by casein kinase 2 (CK2) which modulates the inhibitory effect of HSP105α on HSP70/HSC70 chaperone activity (Ishihara *et al.* 2003). Yamagishi *et al*, also showed that both forms of HSP105, but not HSP70, play important roles in proteins disaggegation in cells in which the cellular ATP levels decrease markedly under conditions of stress (Yamagishi *et al.* 2003).

Under normal and stress conditions, HSP105α is expressed in the cytoplasm of cells whereas HSP105β localizes in the nucleus. Interestingly, Saito *et al*, showed that both HSP105α and HSP105β contained an NLS sequence and an NES sequence. By treating cells with leptomycin B, which inhibits NES-dependent nuclear export, the authors saw that HSP105α accumulated in the nucleus of cells. And by silencing importin β, an important component for NLS-dependent nuclear transport, inhibited nuclear localization of HSP105β. Furthermore they also showed that the extra 44 amino acids present in HSP105α suppressed its NLS activity, thus explaining its cytoplasmic localization (Saito *et al.* 2007).

HSP105 seems to be over expressed in several human tumors. Over the last five years some studies have shown that HSP105 is involved in malignant transformation by protecting tumor cells from apoptosis. Hosaka *et al*, showed that HSP105 has an anti-apoptotic function and that the over expression of HSP105 is essential for cancer cells to survive (Hosaka *et al.* 2006). Yamagishi *et al*, also showed that over expression of HSP105 suppressed the activation of caspase-3 and caspase-9 by preventing the release of cytochrome c from mithocondria thus preventing apoptosis (Yamagishi *et al.* 2006).

Few works describe the association of HSP150 with viruses. Until very recently, HSP105 was never seen associated with viruses with the exception of the HPV16, whose E7 oncoprotein seemed to induce overexpression of HSP105 (Morozov *et al.* 1995). In a previous work by our laboratory, HSP105 was found to be down-regulated in the presence of the large delta antigen (Mota *et al.* 2008). And during hepatitis C

virus replication, HSP105 was also seen to be differentially expressed (Blais *et al.* 2010).

III.2. OBJECTIVES

In this chapter the objective is to determine if and how HSP105 may be involved with the delta antigens and how that may affect HDV replication.

III.3. MATERIALS AND METHODS

III.3.1. RNA INTERFERENCE INDUCING SYSTEM

RNAi has been used to effectively silence gene expression in mammalian cells by the introduction of small interfering RNAs (siRNAs) in those cells. In this work, a system from Clontech – Knockout™ RNAi Systems – (Clontech) was used to induce RNAi in an human hepatoma cell line. The Knockout™ RNAi System is based in an engineered vector – RNAi-Ready pSiren-RetroQ – which may express small-hairpin RNAs (shRNAs) which are then processed *in vivo* into siRNA-like molecules capable of carrying out gene specific silencing (figure III.3.1.) (Brummelkamp *et al.* 2002; Paddison *et al.* 2002; Paul *et al.* 2002; Yu *et al.* 2002). These vectors may be delivered by viral infection or transfection which may be transient or stable. RNAi-Ready pSiren-RetroQ vector contains a bacterial origin of replication, ColE1 ori, and an ampicilin resistance gene, Amp^r, allowing *E. coli* propagation and an eukaryotic origin of replication, SV40 ori, and a puromycin resistance gene allowing selection of transfectants.

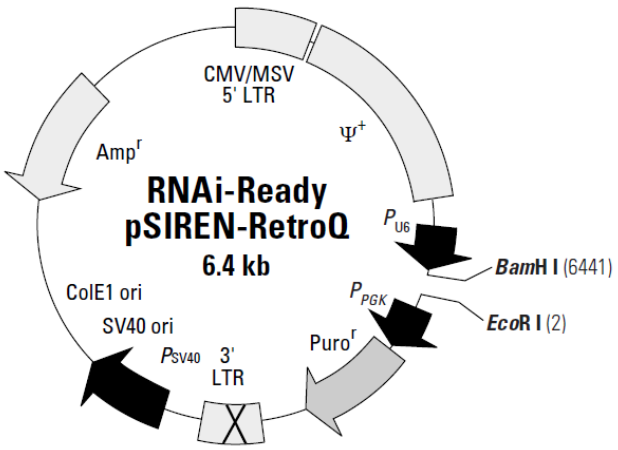

Figure III.3.1.: Restriction map and cloning site of the RNAi-Ready pSiren-RetroQ vector. Adapted from Clontech.

The vector is provided as a linearized vector digested with *Bam*HI and *Eco*RI, ready for ligation with a dsDNA oligonucleotide encoding a shRNA which will be cloned downstream of a Pol III promoter. This dsDNA oligonucleotide contains a

hairpin loop sequence to allow the generation of the shRNA which is located between the sense and antisense target sequences on each complementary strand, a termination site signaled with a poly(T) tract, *Bam*HI and *Eco*RI overhangs to allow insertion in the vector and a unique restriction site to confirm cloning (figure III.3.2.).

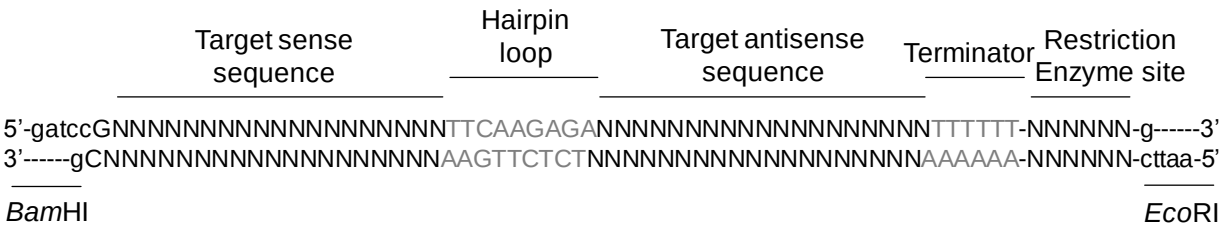

Figure III.3.2.: Oligonucleotide DNA sequence inserted in the RNAi-Ready pSiren-RetroQ vector used to generate small hairpin RNAs.

After insertion of the synthesized oligonucleotide into the RNAi-Ready pSiren-RetroQ vector, the final construction was transfected into cells to express shRNAs.

III.3.2. TARGET SEQUENCE IDENTIFICATION AND SHRNA OLIGONUCLEOTIDE DESIGN

Target sequence identification and shRNA oligonucleotide design were performed with the help of an online tool from Clontech – *RNAi design tool and sequence selection* – available at the company website (http://www.clontech.com/support/tools.asp). Briefly, by inserting the mRNA sequence of interest, this tool identifies possible siRNA target sequences within the mRNA taking into account the following criteria: only sequences of 19 nucleotides were chosen; hairpin maximum temperature of melting was established to 45ºC (Bloomfield 2000); only sequences with GC content ranging from 30%-50% were allowed; sequences with stretches of the same base longer than 4 and sequences with alternated nucleotides (e.g. ACACACA or AACCAACC) were both discarded; only sequences following 'AA' dinucleotides were taken into consideration (Elbashir *et al.* 2001); finally only sequences with one A at position 6 and at least one A or T at the two last positions were selected (Amarzguioui and Prydz 2004). Sequences provided by Clontech online tools were submitted to BLAST (Basic Local Alignment Search Tool) (www.ncbi.nlm.nih.gov) in order to determine homologies among these sequences of interest and sequences in NCBI database. Sequences presenting higher scores and with

no homology with other proteins were selected and used to design shRNA oligonucleotides using once again the Clontech online tools – *shRNA Sequence Designer*. For each target sequence two complementary oligonucleotides were synthesized to allow the formation of the double stranded oligonucleotides described above. These oligonucleotides will then be cloned in the RNAi-Ready pSiren-RetroQ vector and delivered into cells to express shRNAs. A ds oligonucleotide was designed aiming the knockdown of the expression of HSP105 (table III.3.1. and figure III.3.3.).

Target mRNA	Accession	siRNA sequence (5'-3')	GC%	Position	Vector
HSP105	NM_006644	CCATGATTCAGAAGATACT	36	1618	pSiren-RetroQ-HSP105

Table III.3.1.: Target sequence from HSP105 mRNA used to design shRNA oligonucleotides.

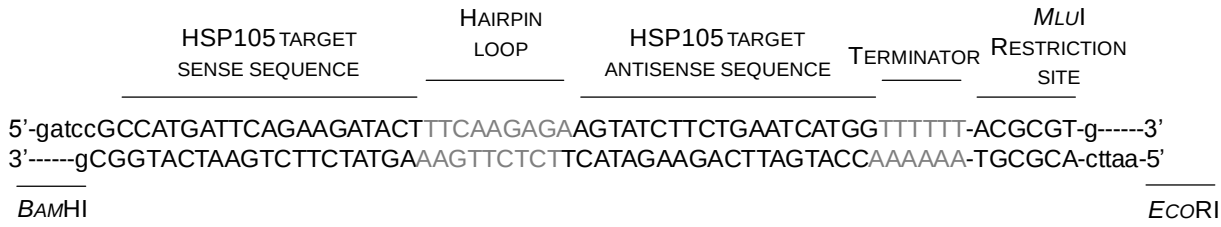

Figure III.3.3.: Synthesized shRNA oligonucleotides targeting proteins HSP105. Top strand and bottom strand were synthesized separately and subsequently annealed.

Besides the vector RNAi-Ready-pSiren-RetroQ, another vector, pSiren-RetroQ-Luciferase, which contains a ds oligonucleotide that targets Luciferase was provided by the manufacturer. This vector was used as a control.

III.3.3. VECTOR CLONING AND RECOMBINANT VECTORS SELECTION

As described before a target sequence from HSP105 mRNA was used to design a ds oligonucleotide which after cloning in the RNAi-Ready pSiren-RetroQ vector and transfection into cells will express shRNA. For that purpose two complementary oligonucleotides were synthesized separately (figure III.3.3) (Metabion International AG). Purified oligonucleotides were resuspended in TE buffer to a concentration of 100 μM and top strand and bottom strand were mixed at a 1:1 ratio which ultimately will

give 50 μM of ds oligo (assuming 100% theoretical annealing). The mixture was heated to 95ºC to remove secondary structures and annealing was performed according to the manufacturers' instructions – 72ºC for 2 minutes, 37ºC for 2 minutes and 25ºC for 2 minutes. Annealed oligonucleotides were stored on ice until insertion in the pSiren-RetroQ vector.

Insertion of the ds oligonucleotide into the pSiren-RetroQ vector was accomplished using T4 DNA Ligase (Fermentas) according to the manufacturers' instructions. Briefly, the ligation mixture was prepared by adding 50 ng of linearized pSiren-RetroQ vector, 0.5 μM annealed oligonucleotides, 10x T4 DNA Ligase buffer, 5% (v/v) PEG 4000 and 5 U of T4 DNA Ligase and the mixture was incubated for 3 h at room temperature (RT). After ligation, the mixture was used to transform competent *E. coli* DH5α cells by the calcium chloride method described elsewhere (Sambrook *et al.* 1989). After incubation, small scale liquid cultures using well isolated colonies were prepared. The transformed colonies were inoculated in LB medium [1% tryptone (w/v), 0.5% yeast extract (w/v) 85,6 mM NaCl, 1 mM NaOH] and incubated O/N at 37ºC, with shaking at 250 rpm. Recombinant vectors were extracted using the commercial kit QIAprep Spin Miniprep Kit (Qiagen) and restriction analysis was performed to confirm ds oligonucleotide insertion. After cloning of the ds oligonucleotides, a new vector was obtained, pSiren-RetroQ-HSP105, encoding for shRNAs targeting HSP105. Restriction analysis of the vector was performed using *Mlu*I and *Hind*III. *Mlu*I has a unique restriction site located in the ds oligonucleotides. As for HindIII there are two restriction sites in the vector pSiren-RetroQ. Restriction analysis of the vector pSiren-RetroQ-HSP105 with both enzymes should thus give a restriction pattern containing three fragments allowing confirmation of oligonucleotide insertion. Sequence analysis was finally performed.

III.3.4. CELL CULTURE AND TRANSFECTION

Two hepatoma cell lines, Huh7 cell line and Huh7-D12 cell line which results from a stable transfection of Huh7 cells with HDV cDNA and thus constitutively expresses HDV ribonucleoproteins, were used in this work. Huh7 cell line was seeded in 25 cm^2 flasks in RPMI 1640 culture medium (Sigma) supplemented with 10% fetal bovine serum (FBS; Gibco) and Huh7-D12 cell line was seeded both in 25 cm^2 flasks

and in coverslips in 35 mm dishes in RPMI 1640 culture medium (Sigma) supplemented with 10% FBS (Gibco) and 200 μg/ml of geneticin (Gibco). Both cell lines were incubated at 37ºC in a humidified atmosphere containing 5% CO_2. Transfection assays were performed using the transfection reagent FuGENE6 (Roche Applied Sciences) following the manufacturer's instructions. Briefly, Huh7-D12 cells were cultured in monolayers until they reach a 50-80% confluence, and transfected using a 3:1 ratio of FuGENE6:DNA (v/w). 24 hours post-transfection culture medium was supplemented with 1 μg/mg of puromycin (Clontech), which allowed the selection of transfected cells. Cells were then harvested after 2-5 days of antibiotic exposure.

III.3.5. mRNA ISOLATION AND RT-qPCR

RNA extraction was performed using the commercial kit Oligotex Direct mRNAMini kit (Qiagen) according to the manufacturer instructions and the extracted mRNA was treated with DNase I (Ambion) according to the manufacturer instructions. cDNA was then synthesized using RevertAid™ Reverse Transcriptase (Fermentas). Briefly, 10 μg of total mRNA were mixed with 0.5 μg of Oligo$(dT)_{18}$ (Fermentas) and diethylpyrocarbonate (DEPC) treated water to a final volume of 12.5 μl and incubated for 5 min at 70ºC allowing to remove secondary structures. After incubation the following reagents were added to the mixture to a final volume of 20 μl: 5x reaction buffer, 20 U of RiboLock™ RNase inhibitor, 10 mM each dNTP mix and 200 U of RevertAid™ Reverse Transcriptase. The reaction mixture was incubated for 1 h at 42ºC and stopped by incubation at 70ºC for 10 min.

Quantitative PCR was performed using the qPCR Core Kit for SYBR® Green I (Eurogentec, Belgium) following the manufacturer specifications. Each reaction mixture, performed in triplicate, was prepared to a final volume of 20 μl and contained 1x reaction buffer, 3.5 mM $MgCl_2$, 200 μM each dNTP, 300 nM of each primer, 0.025/μl of HotGoldStar enzyme and 0.6 μl of diluted SYBR® Green I. Primers for HSP105 cDNA amplification and β-2-microglobulin cDNA amplifictaion, used as housekeeping gene, were design using the software Primer Express™ 1.5 and submitted to the online tool *OligoCalc: Oligonucleotide Properties Calculator* (www.basic.northwestern.edu/biotools/oligocalc.html) to search for the presence of possible secondary structures, complementarity and primers self-annealing. Primers for

cDNA amplification of HSP105, β-2-microglobulin and HDV are displayed in table III.3.2.

Target	Forward Primer (5'-3')	Reverse Primer (5'-3')	Access Code (NCBI database)
HSP105	ATCGAGACCATCGCCAATG	GAATGCTCGGCCATGAAATC	NM_006644
β-2-microglobulin	GGCTATCCAGCGTACTCCAA	TCACACGGCAGGCATACTC	NM_004048
Delta	GAGGCCTCTCAGGGGAGGA	GCCGGCTACTCTTCTTTCCC	M21012

Table III.3.2.: Primers for cDNA amplification of HSP105, β-2-microglobulin and HDV.

qPCR reactions were analyzed in the GeneAmp® 5700 Sequence Detector System (Applied Biosystems) in 96 well plates and the PCR program started with the activation of the HotGoldStar enzyme for 10 min at 95ºC followed by 40 cycles each including a denaturation step of 15 sec at 95ºC, an annealing step of 20 sec at 60ºC and an extension step of 40 sec at 72ºC. Results were analyzed by the ΔΔCt method (Livak and Schmittgen 2001) using the GeneAmp® 5700 SDS (v1.1) software and Microsoft Excel. The ΔΔCt method allows analysis of relative changes in gene expression by using one or more housekeeping genes which are assumed to be uniformly and constantly expressed in all samples. The expression of the gene of interest is then compared with the expression of the housekeeping gene in all samples. For the method to be valid several assumptions have to be made, mainly, that the amplification efficiencies of the target and reference (housekeeping gene) must be approximately equal. Amplification efficiencies for both primers were thus determined by performing amplification of a cDNA sample diluted over a 10000-range with both primers. The logarithms of cDNA dilutions were plotted against Ct (threshold cycle) values and efficiency of the amplification was determined by the formula $E=10^{(-1/m)}-1$, where *m* is the slope of the obtained curve. If efficiencies are approximately equal then the N-Fold=$2^{-\Delta\Delta Ct}$.

III.3.6. SDS-PAGE AND WESTERN BLOT ANALYSIS

Relative quantification by western blot analysis was performed to evaluate the efficiency of the siRNA in silencing the protein HSP105 and the consequences of that silencing in the expression of the delta antigens. After transfection cells were rinsed with Phosphate Buffer Saline (PBS) [1.4 M NaCl, 27 mM KCl, 18 mM Ka_2PO_4, 100 mM $Na2HPO_4$], incubated with trypsin (Trypsin EDTA 10x, Sigma) to allow cell

detachment and recollected with RPMI medium. Cells were centrifuged and washed with PBS and cell pellets were then resuspended in Laemmli buffer [0.0625 M Tris.HCl pH 6.8, 5% SDS, 12.5 mM DTT, 10% glycerol, 0.01% Bromophenol Blue] (Laemmli 1970). 384 U of Benzonase® nuclease (Sigma) were also added to the samples to shear DNA. Finally, protein extracts were separated by SDS-PAGE and proteins were transferred to a nitrocellulose membrane (PROTRAN® Nitrocellulose Transfer Membrane, WHATMAN®, Whatman GmbH, Germany), blocked with 5% low fat milk powder in PBS and incubated ON, at 4ºC, with primary antibodies. Membranes were then washed with 2% low fat milk powder in PBS, supplemented with 0.05% Tween 20 and incubated 1 h with appropriate secondary antibodies conjugated with horseradish peroxidase (BioRad). Membranes were then washed with 2% low fat milk powder in PBS supplemented with 0.05% Tween 20 for three times followed by three time washes with PBS. Membrane development was performed using ECL™ Western Blotting Detection Reagents (GE Healthcare). Finally, images were digitalized and analyzed using ImageJ (http://rsbweb.nih.gov/ij/).

Primary antibodies used in this work were as follows: Rabbit polyclonal antibody against Clathrin HC (Santa Cruz Biotechnology), rabbit polyclonal antibody against HSP105 (Santa Cruz Biotechnology) and rabbit polyclonal antibody against the delta antigens (Saldanha *et al.* 1990).

III.3.7. IMMUNOFLUORESCENCE ASSAYS

Immunofluorescence assays were performed to determine if proteins HSP105 co-localized with the delta antigens. Huh7-D12 cells were cultured, as described before, in coverslips to a 50%-80% confluence. Cells were rinsed 2x with PBS and were then fixed and permeabilized simultaneously with methanol for 10 min at -20ºC and. Cells were washed 3x with 0.05% Tween 20 in PBS (v/v), for 5 min at RT and incubated with rabbit polyclonal antibody against HSP105 (Santa Cruz Biotechnology) in a dark, humidified atmosphere for 1 h. Cells were washed 3x with 0.05% Tween 20 in PBS, for 5 min at RT and were incubated with rabbit polyclonal antibody against the delta antigen for 1 h, in a dark, humidified atmosphere. Cells were washed 3x with 0.05% Tween 20 in PBS, for 5 min at RT and finally incubated with the correspondent secondary antibodies for 1 h, in a dark, humidified atmosphere. Rabbit polyclonal antibody against HSP105 was detected with an anti-rabbit IgG antibody labeled with

Texas Red (Jackson Immunoresearch Laboratories) and rabbit polyclonal antibody against the delta antigens was detected with an anti-rabbit IgG antibody labeled with FITC (Roche). Fluorescent labeled samples were analyzed using the Zeiss LSM 510 META (Carl Zeiss) laser scanning microscope. The microscope is equipped with an argon laser (488 nm) to excite FITC and an helium-neon laser (594 nm) to excite Texas Red. Images were acquired separately in both channels and subsequently merged. Equipment calibration was performed using fluorescent microspheres (Molecular Probes, USA) and a double band filter which allows simultaneous observation of red and green fluorescence.

III.3.8. IMMUNOPRECIPITATION ASSAYS

Immunoprecipitation assays were performed to determine a possible interaction among both HSP105 and the delta antigens *in vivo*.

As described before, Huh7-D12 cells were washed with PBS, trypsinized and recollected with RPMI medium. Cells were centrifuged and washed with PBS for 3 times. Cell pellets were resuspended in lysis buffer [50 mM Tris, pH7.5, 150 mM NaCl, 10% Glycerol, 1% NP-40 and protease inhibitor cocktail (Complete, Mini, EDTA-free kit, Roche)] and incubated for 30 min on ice. Samples were then centrifuged for 30 min, at 20000xg and 4ºC and protein concentration was determined by the Bradford Assay (Bradford 1976).

Immunoprecipitation assays were made with the help of Dynabeads® Protein G (Invitrogen). In order to avoid unspecific binding a pre clearing step was first performed. Protein extracts were incubated with Dynabeads® Protein G and incubated 1 h, at 4ºC with shaking. After incubation, protein extracts were on one hand incubated with antibodies against HSP105 (rabbit polyclonal antibody against HSP105; Santa Cruz Biotechnology) and, on the other hand, with the delta proteins (rabbit polyclonal antibody against the delta antigen), ON, at 4ºC with shaking. Meanwhile, Dynabeads® Protein G were washed with citrate-phosphate buffer, pH 5 [24.5 mM Citric Acid, 52 mM Dibasic sodium phosphate dehydrate], accordingly to the manufacturer instructions. After washing the beads were incubated for 1h, at RT with shaking, with the Huh7-D12 protein extracts previously incubated with antibodies. Samples were washed for 3 times with citrate-phosphate buffer and possible immunocomplexes formed during the assay were eluted in laemmli buffer [0.0625 M Tris.HCl pH 6.8, 5%

SDS, 12.5 mM DTT, 10% glycerol, 0.01% Bromophenol Blue] (Laemmli 1970). The presence of HSP105 in complexes formed with delta antigens and the presence of the delta antigens in complexes formed with HSP105 were detected by Western Blot analysis as described previously.

III.4. RESULTS

III.4.1. SILENCING OF HSP105 AND ITS INFLUENCE IN THE EXPRESSION OF DELTA ANTIGENS

HSP105 was found to be differentially expressed in cells expressing the large delta antigen (Mota *et al.* 2008). In an attempt to understand how HSP105 might interfere with HDV life cycle, an RNAi approach was used to silence HSP105 and determine which were the effects of such silencing. For that purpose, a vector expressing a shRNA targeting HSP105 mRNA, was design. Briefly, a ds oligonucleotide targeting HSP105 mRNA was design with the help of Clontech online tools, commercially synthesized and cloned into the commercial vector pSiren-RetroQ (Clontech) originating the vector pSiren-RetroQ-HSP105. In order to confirm the insertion of the ds oligonucleotides in the vector, restriction analysis was performed using *Hind*III which recognizes 2 restriction sites in the vector pSiren-RetroQ and *Mlu*I which only recognizes one site in the ds oligonucleotide, thus originating three fragments of approximately 500 bp, 1800 bp and 4140 bp. Results showed that the ds oligonucleotide was correctly inserted into the pSiren-RetroQ vector originating the vector pSiren-RetroQ-HSP105 (figure III.4.1.). To confirm this results vector sequencing was performed.

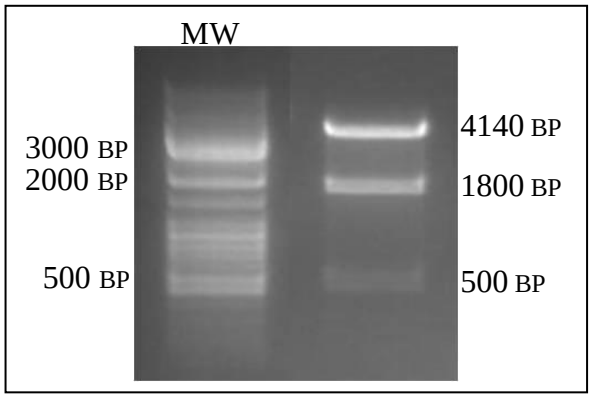

Figure III.4.1.: Restriction analysis of the vector pSiren-RetroQ-HSP105. Two enzymes, *Hind*III and *Mlu*I, which have 2 and 1 restriction sites, respectively, in the vector pSiren-RetroQ-HSP105 were used. Three fragments of approximately 500 bp, 1800 bp and 4140 bp were expected confirming the insertion of the ds oligonucleotide.

Huh7-D12 cells were then either transfected with pSiren-RetroQ-HSP105, to promote silencing of HS105 or with pSiren-RetroQ-Luciferase which will be used as a negative control. Transfected cells were then selected using puromycin and finally harvested. In order to determine if the shRNA targeting of HSP105 mRNA was

successful, silencing HSP105, RT-qPCR was performed to determine HSP105 mRNA levels after transfection with the shRNA. Simultaneously, HDV mRNA levels were also determined in order to see if by interfering with HSP105 mRNA, HDV mRNA levels would also suffer any alterations. Data resultant from qPCR was analyzed by the ΔΔCt method which makes the assumption that the amplification efficiencies of the target and reference (housekeeping gene) must be approximately equal. Amplification efficiencies for the primers HSP105 and β-2-microglobulin were thus determined by performing cDNA amplification of the same sample diluted over a 10000-range and plotting the logarithms of cDNA dilutions against Ct (threshold cycle) values. Amplification efficiencies were of 95.5% for β-2-microglobulin, 97.9% for HSP105 and 100% for HDV (figure III.4.2.).

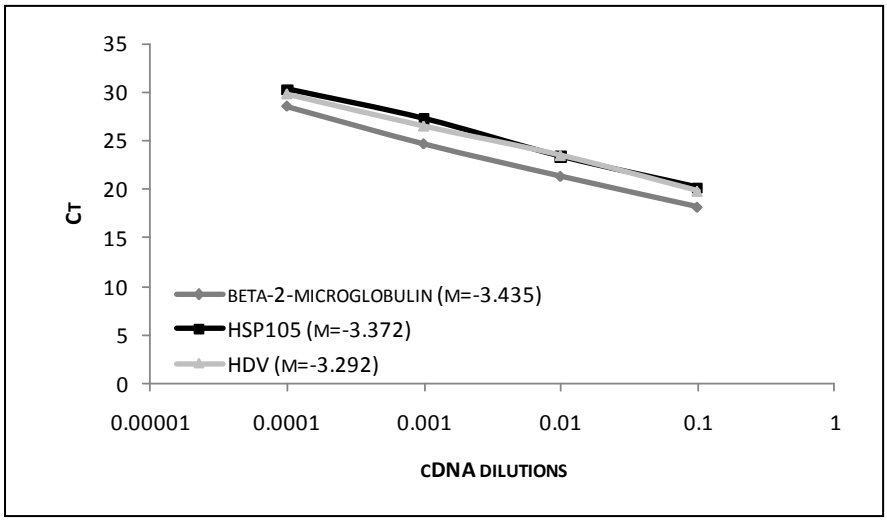

Figure III.4.2.: Validation of the ΔΔCt method. cDNA amplification of the same sample diluted over a 10000-range was performed using primers for β-2-microglobulin, HSP105 and HDV. For each amplification the logarithms of cDNA dilutions were plotted against Ct (threshold cycle) values and efficiency of the primer was determined by $E=10^{(-1/m)}-1$, where m is the slope of the obtained curve.

Applying the ΔΔCt method, results showed that although the shRNA targeting HSP105 was not completely successful in silencing HSP105 mRNA levels, a relative reduction of 1.4 times was achieved. As for HDV mRNA levels they showed a relative increase of 2.3 times (figure III.4.3.).

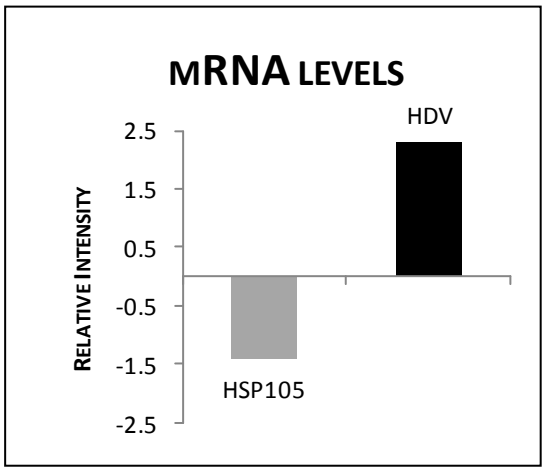

Figure III.4.3.: Alterations in mRNA levels of HSP105 due to the presence of a shRNA targeting HSP105 mRNA and consequent alteration of the levels of the HDV mRNA.

Using Western blot analysis followed by relative quantification using Image J, and knowing that there is in fact interference with HSP105 mRNA, possible alterations in the expression levels of the protein HSP105 and in the delta antigens were looked for.

Huh7-D12 cells transfected with the pSiren-RetroQ-HSP105 vector and Huh7-D12 cells transfected with the pSiren-RetroQ-Luciferase, used as a control, were harvested and protein extracts were prepared. Proteins were separated by SDS-PAGE and transferred to a nitrocellulose membrane. Using specific antibodies, detection for clathrin, used as housekeeping, HSP105 and the delta antigens was performed. All experiments were reproduced at least three times. Figure III.4.4. shows the results obtained by Western blot analysis.

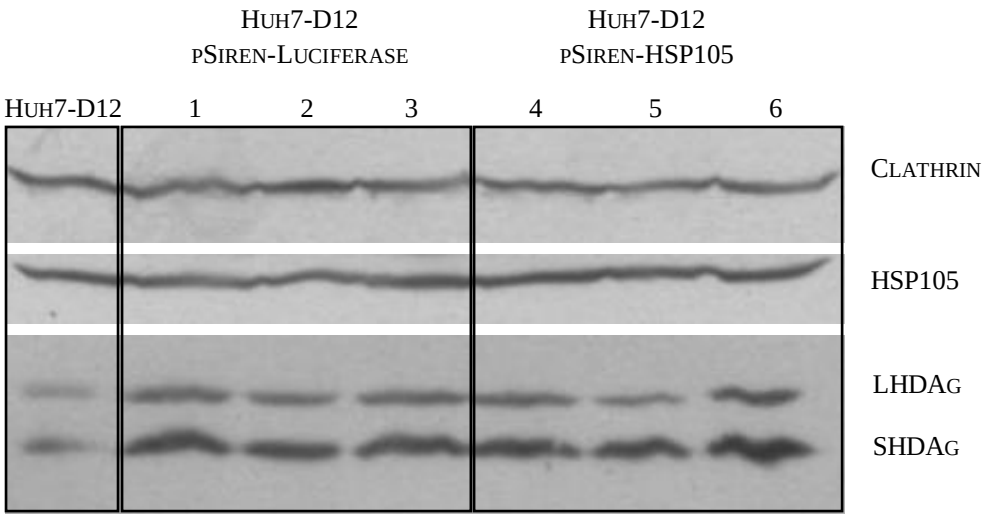

Figure III.4.4.: Western blot analysis of cellular extracts resulting from the transfection of Huh7-D12 cells with pSiren-RetroQ-HSP105 (lanes 4, 5 and 6) and western blot analysis of cellular extracts resulting from the transfection of Huh7-D12 cells with pSiren-RetroQ-Luciferase (lanes 1, 2 and 3). Samples were analyzed by western blot analysis allowing for the detection of Clathrin, used as housekeeping, HSP105 and the delta antigens.

After Western Blot analysis, Image J was used to determine the area of the bands. By dividing the area of the bands of HSP105 and the delta antigens by the area of the bands corresponding to clathrin, used as housekeeping control, in the same sample, the relative quantification of HSP105 and the delta antigens was determined. Results show that, although the vector pSiren-RetroQ-HSP105 was not successful in silencing the protein HSP105, it induced a knock down in its expression of approximately 30% which in turn induced a reduction in the expression of the large delta antigen in approximately 25% (figure III.4.5.). No alterations in the expression of the small delta antigen were detected.

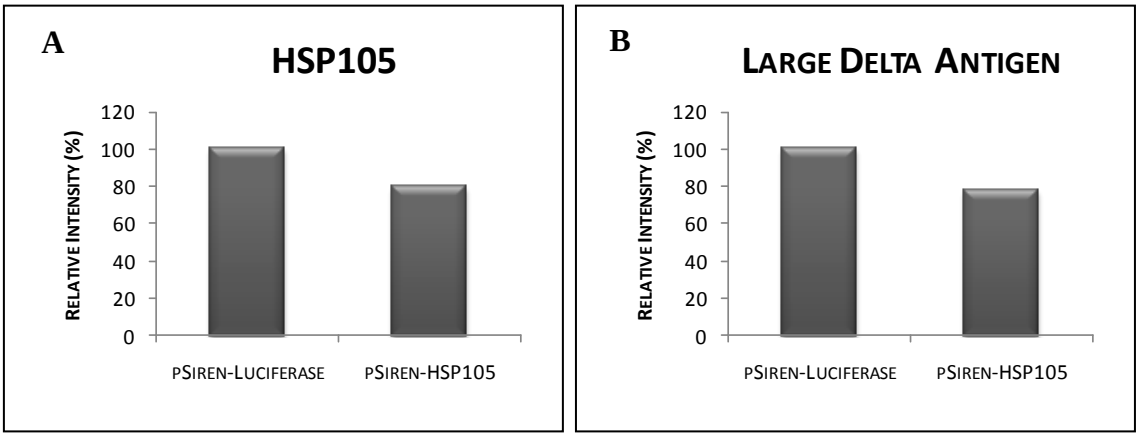

Figure III.4.5.: Knock down of 30% of the protein HSP105 (A) and consequent knock down of 25% of the large delta antigen (B). Using Image J the areas of the bands corresponding to HSP105, the delta antigens and clathrin were determined. By dividing the areas of the bands corresponding to HSP105 and the areas of the bands corresponding to the delta antigens by the areas of the bands corresponding to clathrin in the same samples, the relative quantification of the proteins was determined.

III.4.2. HSP105 CO-LOCALIZES WITH SMALL DELTA ANTIGEN

As described before, HSP105 was found to be differentially expressed in cells expressing the large delta antigen (Mota *et al.* 2008). It was also seen in this work that the knock down of HSP105 induces an increase in HDV mRNA expression levels and an increase of the large form of the delta protein. So it seems that HSP105 interferes, in some way, with the HDV life cycle. In order to understand a little better how HSP105 and HDV life cycle are connected, immunofluorescence assays were performed in order to determine if HSP105 and the SHDAg co-localize in Huh7-D12 cells allowing a physical interaction between proteins.

Immunofluorescence assays were thus performed by labeling both HSP105, in red, and the delta antigen, in green, in Huh7-D12. Results showed that although HSP105 is mainly cytoplasmatic, it is also present in the nucleus of cells thus co-localizing with the delta antigen which is mainly nuclear. In figure III.4.6. it can be seen the localization of SHDAg (in green) in Huh7-D12 cells (figure III.4.6.A) as well as the localization of the HSP105 (in red) in Huh7-D12 cells (figure III.4.6.B). In figure III.4.6.C, images showing localization of HSP105 and SHDAg were merged showing that both proteins co-localize.

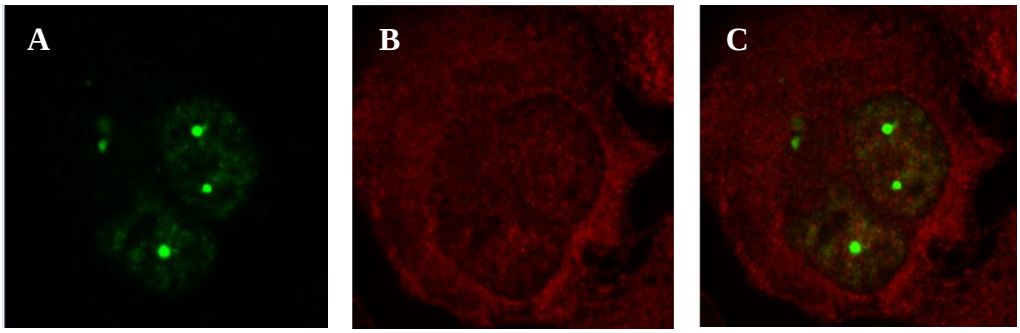

Figure III.4.6.: Co-localization of HSP105 and SHDAg. A shows the nuclear localization of SHDAg in Huh7-D12 cells and B shows the localization of HSP105 in Huh7-D12 cells which is mostly cytoplasmatic. C shows the merge of both figures A and B showing the co-localization of HSP105 and SHDAg.

III.4.3. HSP105 INTERACTS WITH THE DELTA ANTIGENS *IN VIVO*

If HSP105 and SHDAg co-localize in the cell, even if at low levels, it is possible that the two proteins may interact with each other. In order to clarify that hypothesis, immunoprecipitation assays were performed. As described previously, antibodies either for the delta antigens or for HSP105 were incubated with Huh7-D12 cellular extracts and the immunocomplexes formed were than trapped using Protein G, eluted and analyzed by western blot analysis. Results showed that in fact HSP105 seems to interact with both delta antigens although that interaction seems to be more effective with the large delta antigen (figure III.4.7.).

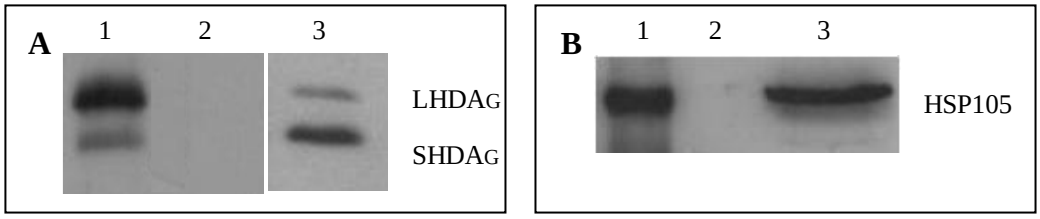

Figure III.4.7.: Co-immunoprecipitation of HSP105 and the delta antigens. As described before, Huh7-D12 protein extracts were incubated either with an antibody against HSP105, α-HSP105, or with an antibody against the delta antigens, B3 to form immunocomplexes which were then trapped using Protein G. Immunocomplexes were eluted and delta antigens were detected by Western blot (A1) in immunoprecipitation with HSP105 and HSP105 was detected by Western blot (B1) in immunoprecipitation with the delta antigens. Lane 2 in figures A and B show the negative control in which Protein G was incubated with Huh7-D12 total protein extracts. Lane 3 in figures A and B show the delta antigens and HSP105 in Huh7-D12 total protein extracts, respectively.

III.5. DISCUSSION

In Huh7 cells transiently expressing LHDAg, and using a proteomic approach, HSP105 was found to be down regulated (Mota *et al.* 2008). Several assays were then performed in order to determine the possible role of the protein in HDV life cycle. Knockdown of HSP105 led to a decrease in LHDAg protein levels and an increase of HDV mRNA levels. As already described before, LHDAg is essential in viral particle assembly and acts as a dominant negative inhibitor suppressing HDV replication. Being so, it is not surprisingly that if knockdown of HSP105 induces a decrease in LHDAg then, an increase of HDV mRNA would occur showing the consistency of the results. Furthermore, by immunofluorescence, it was also observed that although HSP105 is mainly cytoplasmatic, low levels of the protein were seen in the nucleus. These results show that HSP105, by co-localizing with both delta antigens, may interact with these proteins, which was confirmed by immunoprecipitation assays. Immunoprecipitations showed that in fact HSP105 interacts with both delta antigens, with higher affinity to LHDAg wich seems to immunoprecipitate in higher concentrations with HSP105. Interestingly in Huh7-D12 cells, which constitutively express HDV RNPs, LHDAg is seen in lower quantities than SHDAg. This results seem to show that although there is a lightly interaction with SHDAg, it is LHDAg that recruits HSP105 during HDV replication.

During HDV life cycle, when LHDAg is produced, it shuttles into the nucleus to form RNPs. These RNPs then leave the nucleus in order to form viral particles. In this work, a down regulation of HSP105 using siRNAs induced a down-regulation of LHDAg showing that both proteins seem to be regulated in the same direction. This result seems to be consistent with the result of immunoprecipitations that showed that LHDAg recruits, preferentially HSP105. It was also seen that HSP105 is mainly citoplasmatic. These results altogether suggest that HSP105 binds LHDAg and the RNPs facilitating the transport or anchoring of the RNP to the ER, or even that HSP105 may be involved in viral particle assembly.

These results differ from the ones obtained by Mota *el at*, in which HSP105 was seen down-regulated in the presence of LHDAg. However in that case, only LHDAg was present in cells, while all the other viral components were not which may alter the expression of HSP105 in cells.

Although these results are preliminary, they give a good lead on HSP105 as an HDV binding partner that may be involved in HDV RNP transport to the ER or even in viral particle assembly.

Furthermore, HSP105 was also shown to be an anti-apoptotic protein. HDV may recruit HSP105 enabling HDV replication.

Further experiments have to be performed in order to clarify the role of HSP105 in HDV replication. *In situ hybridization* and UV-crosslinking experiments may show if HSP105 interacts with HDV RNAs. Pull down assays with subcellular fractions may give a good idea if HSP105 binds LHDAg in the nucleus, in the cytoplasm or even in the ER. Mass spectrometry could also be useful in this case to identify all the proteins obtained in the pull downs, confirming the interaction of LHDAg and HSP105 and showing more LHDAg interacting partners.

CHAPTER IV: HNRNP H INTERACTS *IN VIVO* WITH THE DELTA ANTIGENS AFFECTING HDV REPLICATION

IV.1. INTRODUCTION

Heterogeneous nuclear ribonucleoproteins (hnRNPs) are a family of highly conserved nuclear proteins that bind to nascent transcripts produced by RNA Pol II. This family is composed by over than 20 proteins, designated with letters from A to U, and all hnRNPs have several functions within the cell. They participate in pre-mRNA processing such as splicing and are important determinants of mRNA export, localization, translation and stability (Dreyfuss *et al.* 1993; Dreyfuss *et al.* 2002). During mRNA biogenesis, hnRNPs are always present. From the moment pre-mRNAs are formed until their maturation into mRNAs, several hnRNPs form large complexes with mRNAs. Throughout the mRNA export pathway, through the nuclear pores to the ribosome, hnRNPs that harbor nuclear-retention signals detach from mRNAs staying in the nucleus, whereas others are released in the cytoplasm of cells undergoing constant nuclear-cytoplasmic shuttling (Dreyfuss *et al.* 2002). While most hnRNPs are expressed in the nucleus having a nucleoplasmic distribution, which is excluded from the nucleolus, others are expressed in the cytoplasm. Examples are hnRNP M, which is a membrane bound receptor, and hnRNP Q which is predominantly cytoplasmic (Mizutani *et al.* 2000; Bajenova *et al.* 2003).

Structurally, these proteins present a modular structure consisting of multiple domains connected by linker regions of varying length. Main domains are RNA-binding motifs (RBMs), that have the capacity to participate both in general and specific interactions with nucleic acids, and at least one auxiliary domain that regulates protein-protein interactions and subcellular localization (Dreyfuss *et al.* 2002). Not all hnRNPs share the same type of RBMs. While most hnRNPs contain a RNP-CS-RBD (ribonicleoprotein-coding sequence-RBD) motif, also called RRM (RNA recognition motif), hnRNP K/E contains K-homology (KH) domains, hnRNP F/H contain a quasi-RMM domains, which induces specific binding to poly(G) tracts, and hnRNP U contains RGG (Arg-Gly-Gly) boxes. As for auxiliary domains they differ from protein to protein being the most well characterized auxiliary domains the glycine-rich domains (Chaudhury *et al.* 2010)). While some hnRNPs have as auxiliary domains classical nuclear localization signals (NLS), hnRNP A1 has a glycine-rich domain called M9 which is a nucleo-cytoplasmic shuttling (NS) domain that is both necessary and sufficient to confer nuclear localization (Siomi and Dreyfuss 1995). hnRNP K contains both classical and NS domains and hnRNP E3 and E4 are exclusively cytosolic lacking

NLS or NS (Michael *et al.* 1997; Chkheidze and Liebhaber 2003). Regarding post-translational modifications, phosphorylation, sumoylation, ubiquitination and methylation were detected in hnRNPs. hnRNP A, B, C, G, K and U are phosphorylated *in vivo*, hnRNP A1 has found to be ubiquitinated and methylated and hnRNPA1, A3, F, H and K have been shown to suffer sumoylation. These modifications also regulate subcellular localization of these proteins (Chaudhury *et al.* 2010).

Several hnRNPs were found to be involved in viral replication. hnRNP A1 is a multifunctional protein involved in RNA processing, alternative splicing, chromosome maintenance and in the nucleocytolplasmic transport of mRNAs (Mayeda and Krainer 1992; Pinol-Roma and Dreyfuss 1992; Matter *et al.* 2000; Ford *et al.* 2002) that was also found to be involved in replication of several viruses. hnRNP A1, was shown to play an essential role in the replication of the Sindbis virus (SV). This protein interacts with the SV 5'-UTR (untranslated region) facilitating translation of viral RNA (Gui *et al.* 2010). In murine hepatitis virus (MHV), hnRNP A1, seems to be involved, directly or indirectly, in MHV RNA synthesis in the cytoplasm (Shi *et al.* 2000). hnRNP A1 also seems to have an important role in HCV replication through RNA-protein and protein-protein interactions. It was shown by Kim *et al*, that hnRNP A1 co-immunoprecipitates with HCV-NS5b (non-structure 5 b) protein and also interacts with the 5'-NTR (non translated region) and the 3'-NTR of HCV RNA containing the *cis*-acting elements required for replication (Kim *et al.* 2007). In human papillomavirus (HPV) 16, hnRNP A1 also seems to have an important role. On one hand, hnRNP H seems to regulate HPV-16 L1 coding sequence, a splicing silencer sequence shown to prevent premature expression of the late L1 gene (Zhao *et al.* 2004). On the other hand, hnRNP A1 also binds to the late regulatory element (LRE) of the HPV-16, facilitating alternative splicing necessary for production of virus late transcripts (Cheunim *et al.* 2008).

As for hnRNP C1/C2, it binds RNA Pol II transcripts in the nucleus, along with other proteins of the core hnRNP complex, and plays an important role in mRNA biogenesis and transport (Dreyfuss *et al.* 1993). hnRNP C was seen to interact with Dengue virus NS1-interacting protein being probably involved in virus replication and/or in cellular responses that allow virus survival in host cells (Noisakran *et al.* 2008). Furthermore, Brunner *at al*, also shown that hnRNP C interacts with poliovirus RNA and proteins increasing the efficiency of viral genomic RNA synthesis (Brunner *et al.* 2010).

hnRNP D is also a multifunctional proteins involved in mRNA decay, telomere maintenance, translation initiation and in major coding-region determinant of instability (mCRD) - mediated mRNA turnover (Brewer 1991; Laroia *et al.* 1999; Eversole and Maizels 2000; Grosset *et al.* 2000; Lu *et al.* 2006). hnRNP D binds HCV internal ribosome entry site (IRES) and promotes translation of the viral protein. It interacts with the stem loop II of HCV 5'-NTR (non-translated region) and its over expression enhances HCV IRES-dependent translation. Furthermore, knockdown of hnRNP D increases HCV replication in cells indicating that the protein represses HCV replication. hnRNP D also functions in modulating HCV proliferation by balancing replication and translation of RNA (Paek *et al.* 2008).

hnRNP F is involved in splicing regulation of numerous pre-mRNAs (Garneau *et al.* 2005). hnRNP F interacts with the influenza A virus NS1 and both proteins seem to directly interact through the GY-rich region of hnRNP F and the RBD of NS1. It seems that by modulating normal cellular mRNA processes through direct interaction with the cellular hnRNP F proteins, the NS1 protein enhances influenza A virus replication (Lee *et al.* 2010).

hnRNP K has been implicated in transcription, mRNA splicing and stability (Michelotti *et al.* 1996; Expert-Bezancon *et al.* 2002; Wei *et al.* 2006; Chen *et al.* 2009). It was seen to interact with ASFV (African Swine Fever Virus) p30 during ASFV infection. p30 modifies hnRNP K subcellular distribution and could contribute to modulate hnRNP K functions related to processing and export of mRNAs during ASFV infection (Hernaez *et al.* 2008).

HDV has been seen to interact with several proteins from the hnRNP family. Sikora et al, showed that HDV genomic RNA co-immunoprecipitaded with hnRNP L (Sikora *et al.* 2009). In our lab, hnRNP L was found down regulated during HDV infection, hnRNP D was found down regulated as a response to the expression of both SHDAg and LHDAg and finally, hnRNP H was found up-regulated as a response to the expression of SHDAg.

hnRNP H, one of the lesser investigated members of the hnRNP family, is a member of the hnRNPF/H family which includes hnRNPsF, H(H1), H'(H2) and 2H9(H3). This family has seen to be implicated in splicing, polyadenylation, capping, export and translation of cellular and viral mRNAs. As for hnRNP H, which is mainly localized in the nucleus, it has been shown be involved in several processes and to

interact with both splicing enhancers and silencers. As already described above, hnRNP H recognizes poly G sequences, or G-tracts. These structures are located mainly in telomeres and also in some promoter regions in DNA. In RNA, G-tracts are frequent splicing recognition elements found both in introns and exons and are crucial for 5'-splice site recognition (Swanson and Dreyfuss 1988; McCullough and Berget 1997; Wang *et al.* 2004). The G-tracts are also abundant downstream of the mammalian polyadenylation signals (Zarudnaya *et al.* 2003). Through binding to the G-tracts, hnRNP H is responsible for the regulation of polyadenylation (Arhin *et al.* 2002; Zarudnaya *et al.* 2003) and the splicing and regulation of numerous pre-mRNAs such as Bcl-x, the rat β-tropomyosin, the Rous sarcoma virus NRS the HIV type I tat and tev and the c-src.

Bcl-x is a member of the Bcl-2 family of proteins that are regulators of apoptosis. The Bcl-x pre-mRNA is alternatively spliced and its splicing is modulated by hnRNP H (Garneau *et al.* 2005). Using rat β-tropomyosin (β-TM) pre-mRNA, to study regulation of alternative splicing, Chen *et al* showed that hnRNP H is involved in splicing. The rat β-TM gene consists of eleven exons and two exon pairs are alternatively spliced. Exons seven and ten are used to form β-TM mRNA in skeletal muscles and fetal cardiac muscle cells. The authors showed that the 5' end of exon 7 functions as an exon splicing silencer (ESS) and that hnRNP H binds to the ESS silencing splicing. hnRNP H thus participate in negative regulation of alternative splicing and is a trans-acting factor involved in ESS activity in vertebrates (Chen *et al.* 1999).

Incomplete RNA splicing is a key feature of the retroviral life cycle in contrast to the processing of most cellular mRNAs which are usually spliced to completion. In Rous sarcoma virus, splicing control is achieved in part through a *cis*-acting element termed negative regulator of splicing (NRS). Fogel *et al*, isolated a p55 protein that binds NRS identified later as hnRNP H. In Rous sarcoma virus, hnRNP H is likely to be involved in NRS-mediated splicing inhibition and/or polyadenylation of viral RNAs (Fogel and McNally 2000).

hnRNP H was also seen to associate to a second exonic splicing silencer (ESS2p) in the 5' extremity of HIV *tat* exon 2, possibly acting as a mediator of its inhibitory property (Jacquenet *et al.* 2001). Furthermore, hnRNP H regulates the splicing of HIV-1 *tev*-specific exon 6 and is required for efficient splicing of an HIV-1

splicing substrate (Caputi and Zahler 2002; Schaub *et al.* 2007). hnRNP H also binds to intronic sequences and activating neural-specific splicing of the c-src mRNA (Chou *et al.* 1999).

IV.2. OBJECTIVES

In this chapter the objective is to determine if hnRNP H interacts with the delta antigens and how it may affect HDV replication.

IV.3. MATERIALS AND METHODS

IV.3.1. RNA INTERFERENCE INDUCING SYSTEM

The RNA interference inducing system used to silence hnRNP H was the Clontech – Knockout™ RNAi System. This system is based on the RNAi- Ready pSiren-RetroQ vector (Clontech), which is an engineered vector that may express shRNAs which are then processed *in vivo* into siRNA-like molecules capable of carrying out gene specific silencing. These system was used as already described in chapter III.3.1.

IV.3.2. TARGET SEQUENCE IDENTIFICATION AND SHRNA OLIGONUCLEOTIDE DESIGN

Target sequence identification and shRNA oligonucleotide design were performed with the help of an online tool from Clontech – *RNAi design tool and sequence selection* – available at the company website (http://www.clontech.com/support/tools.asp) as described in chapter III.3.2.. Table IV.3.1. and figure IV.3.1., show the target sequence used to design the ds oligonucleotide to be cloned in the pSiren-RetroQ vector and the ds oligonucleotide respectively.

Target mRNA	Accession	siRNA sequence (5'-3')	GC%	Position	Vector
hnRNP H	NM_005520	GACAAAGCAAATATGCAAC	36	1113	pSiren-RetroQ-hnRNP H

Table IV.3.1.: Target sequence from hnRNP H mRNA used to design shRNA oligonucleotides.

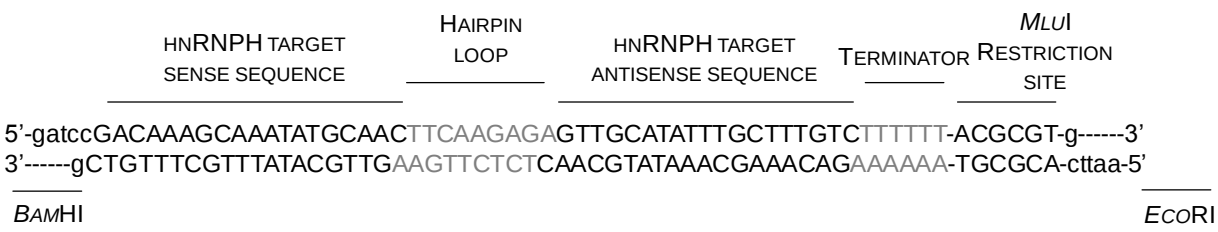

Figure IV.3.1.: Synthesized shRNA oligonucleotides targeting proteins hnRNP H. Top strand and bottom strand were synthesized separately and subsequently annealed.

IV.3.3. VECTOR CLONING AND RECOMBINANT VECTORS SELECTION

As described before a target sequence from hnRNP H mRNA was used to design a ds oligonucleotide which after cloned in the RNAi-Ready pSiren-RetroQ vector and transfected into cells will express shRNA. For that purpose two complementary oligonucleotides (figure IV.3.1.) were synthesized separately (Metabion International AG) and annealed as described in chapter III.3.3. Vector cloning was performed as described in chapter II.3.3. originating the vector pSiren-RetroQ-hnRNP H. The obtained vectors were submitted to restriction analysis to confirm the insertion of the ds oligonucleotide as described in chapter III.3.5.

IV.3.4. CELL CULTURE AND TRANSFECTION

In this work two cell lines were used. Huh7 cell line and Huh7-D12 cell line that results from the stable transfection of Huh7 cells with HDV cDNA. Huh7-D12 constitutively express HDV ribonucleoproteins. Cell culture and transfection was performed as described in chapter III.3.4.

IV.3.5. MRNA ISOLATION AND RT-QPCR

mRNA isolation was performed using the Oligotex Direct mRNAMini kit (Qiagen) as described in chapter III.3.5.. RT-qPCR was performed in two steps as described before in chapter III.3.5. Reverse Transcription was performed using the RevertAid™ Reverse Transcriptase (Fermentas) as described in chapter III.3.5. and qPCR was performed using qPCR Core Kit for SYBR® Green I (Eurogentec, Belgium) and the same conditions described in chapter III.3.5.

Primers used for hnRNP H cDNA amplification were obtained through PrimerBank database (http://pga.mgh.harvard.edu/primerbank) and are displayed in table IV.3.2.

Target	Forward Primer (5'-3')	Reverse Primer (5'-3')	Access Code (NCBI database)
hnRNP H	ATCGAGACCATCGCCAATG	GAATGCTCGGCCATGAAATC	NM_005520

Table IV.3.2.: Primers for cDNA amplification of hnRNP H

β-2-microglobulin was used as housekeeping as described in chapter III.3. Primers for both β-2-microglobulin and HDV mRNA were the same used in chapter III.3.

IV.3.6. WESTERN BLOT ANALYSIS

Relative quantification by western blot analysis was performed to evaluate the efficiency of the siRNA in silencing the protein hnRNP H and consequently if the silencing of hnRNP H affected the expression of the delta antigens. After transfection cells were harvested and cell extracts were prepared as described in chapter III.3. Protein were separated by SDS-PAGE, transferred to a nitrocellulose membrane and incubated first with primary antibodies, washed and incubated finally with appropriate secondary antibodies conjugated with horseradish peroxidase (BioRad) as described in chapter III.3. Images were digitalized and analyzed using ImageJ (http://rsbweb.nih.gov/ij/).

Primary antibodies used in this work were as follows: Rabbit polyclonal antibody against Clathrin HC (Santa Cruz Biotechnology), goat polyclonal antibody against hnRNP H (Santa Cruz Biotechnology) and rabbit polyclonal antibody against the delta antigens (Saldanha *et al.* 1990).

IV.3.7. IMMUNOFLUORESCENCE ASSAYS

Immunofluorescence assays were performed to determine a possible co-localization of hnRNP H and the delta antigens. Huh7-D12 cells were cultured, as described before, in coverslips to a 50%-80% confluence (see chapter III.3.7.). Cells were rinsed 2x with PBS and were then fixed and permeabilized. Cells were fixed in 3.7% paraformaldehyde (PFA, v/v) for 10 min at RT and then permeabilized in a 0.5% Triton-X100 in PBS solution (v/v) for 10 min at RT. Cells were washed and incubated firstly with goat polyclonal antibody against hnRNP H (Santa Cruz Biotechnology), washed again, and incubated with rabbit polyclonal antibody against the delta antigen, washed again and finally incubated with the correspondent secondary antibodies as described in chapter II.3. Goat polyclonal antibody against hnRNP H was detected with an anti-goat IgG antibody labeled with Texas Red (Jackson Immunoresearch Laboratories) and rabbit polyclonal antibody against the delta antigens was detected

with an anti-rabbit IgG antibody labeled with FITC (Roche). Fluorescent labeled samples were analyzed using the Zeiss LSM 510 META (Carl Zeiss) laser scanning microscope. The microscope is equipped with an argon laser (488 nm) to excite FITC and an helium-neon laser (594 nm) to excite Texas Red. Images were acquired separately in both channels and subsequently merged. Equipment calibration was performed using fluorescent microspheres (Molecular Probes, USA) and a double band filter which allows simultaneous observation of red and green fluorescence.

IV.3.8. PULL DOWN ASSAYS

In order to determine the existence of a possible interaction between hnRNP H and the small delta antigen a pull down assay was performed using a recombinant small delta antigen with an histidine tag (6xHis) (Mendes 2003) and TALON® Magnetic beads (Clontech) which are based in IMAC (Immobilized Metal Affinity Chromatography) technology. IMAC is based on the reversible interaction between various aminoacid side chains and metal ions. Depending on the immobilized metal ion, different side chains can be involved in the adsorption process. TALON® Magnetic beads are precharged with Co^{2+} thus having higher specificity for polyhistidine-tagged proteins. Co^{2+} is bound to the beads using a TALON's tetradentate metal chelator, which in turn binds to cobalt at four sites, virtually eliminating metal leakage during purification.

Huh7 cells were washed with PBS, trypsinized and recollected with RPMI medium. Cells were centrifuged and washed with PBS for 3 times. Cell pellets were resuspended in lysis buffer [50 mM Tris, pH7.5, 150 mM NaCl, 10% Glycerol, 1% NP-40 and protease inhibitor cocktail (Complete, Mini, EDTA-free kit, Roche)] and incubated for 30 min on ice. Samples were then centrifuged for 30 min, at 20000xg and 4ºC and protein concentration was determined by the Bradford Assay (Bradford 1976).

Meanwhile, TALON® Magnetic beads were washed with Milli-Q water accordingly to the manufacturer instructions and equilibrated in equilibration buffer [50 mM sodium phosphate, 300 mM NaCl, pH7]. After the equilibration step, 20 μg of a recombinant small delta protein with an histidine tag (SHDAg-6xHis), in equilibration buffer, were added to the beads which were incubated for 1 h at 4 ºC with shaking. Supernatant was removed and 100 μg of total protein extracts, previously prepared, were added to the beads already containing the delta protein in interaction buffer [50

mM sodium phosphate, 300 mM NaCl, 0.005% Tween 20, pH7], and incubated for 1 h at 4º C with shaking. Beads were washed with interaction buffer and finally, protein complexes formed with SHDAg-6xHis were eluted in Laemmli buffer. The presence of hnRNP H in the pull down assay was detected by Western Blot analysis as described previously.

IV.3.9. IMMUNOPRECIPITATION ASSAYS

Immunoprecipitation assays were performed to determine a possible interaction between both hnRNP H and the delta antigens *in vivo*. Immunoprecipitation assays were performed as described in III.3.8. and the presence of hnRNP H in complexes formed with delta antigens and the presence of the delta antigens in complexes formed with hnRNP H were detected by Western Blot analysis as described in capter IV.3.6.

IV.4. RESULTS

IV.4.1. SILENCING OF HNRNP H AND ITS INFLUENCE IN THE EXPRESSION OF DELTA ANTIGENS

hnRNP H was found to be differentially expressed in cells expressing the small delta antigen (Mota *et al.* 2009). In an attempt to determine if hnRNP H is involved in HDV life cycle, silencing by RNAi was performed followed by measure of the expression levels of HDV mRNA and the delta antigens. For RNAi interference, a vector expressing a shRNA targeting hnRNP H mRNA was built. A ds oligonucleotide targeting hnRNP H was designed with the help of Clontech online tools, commercially synthesized and cloned into the commercial vector pSiren-RetroQ (Clontech) originating the vector pSiren-RetroQ-hnRNP H. The correct insertion of the ds oligonucleotide in the vector was verified by restriction analysis using enzymes *Hind*III, which has 2 restriction sites in the vector pSiren-RetroQ, and *Mlu*I which has unique restriction site in the ds oligonucleotide, thus originating three fragments of approximately 500 bp, 1800 bp and 4140 bp. Results showed that the ds oligonucleotide was correctly inserted into the pSiren-RetroQ vector originating the vector pSiren-RetroQ-hnRNP H (figure IV.4.1.). In order to confirm this results the vector pSiren-RetroQ-hnRNP H was sequenced.

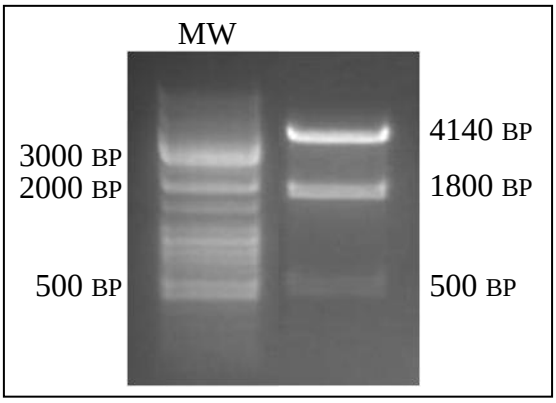

Figure IV.4.1.: Restriction analysis of the vector pSiren-RetroQ-hnRNP H. Two enzymes, *Hind*III and *Mlu*I, which have 2 and 1 restriction sites, respectively, in the vector pSiren-RetroQ-hnRNP H were used. Three fragments of approximately 500 bp, 1800 bp and 4140 bp were expected confirming the insertion of the ds oligonucleotide.

Huh7-D12 cells were then transfected with pSiren-RetroQ-hnRNP H to promote silencing of hnRNP H or with pSiren-RetroQ-Luciferase which will be used as a control. Transfected cells were selected using puromycin and finally harvested. mRNA extraction was performed and RT-qPCR was used to measure the levels of hnRNP H mRNA in cells transfected with the pSiren-RetroQ-hnRNP H allowing to confirm

hnRNP H mRNA interference. Simultaneously, HDV mRNA levels were also measured to determine if interference with hnRNP H mRNA would lead to any alterations in HDV mRNA levels. Data resultant from qPCR was analyzed by the ΔΔCt method. This method makes the assumption that the amplification efficiencies of the target and reference (housekeeping gene) must be approximately equal. Amplification efficiencies for the primers hnRNP H and β-2-microglobulin were determined by performing cDNA amplification of the same sample diluted over a 10000-range and plotting the logarithms of cDNA dilutions against Ct (threshold cycle) values. Amplification efficiencies were of 95.5% for β-2-microglobulin, 93.4% hnRNP H and 100% for HDV (figure IV.4.2.).

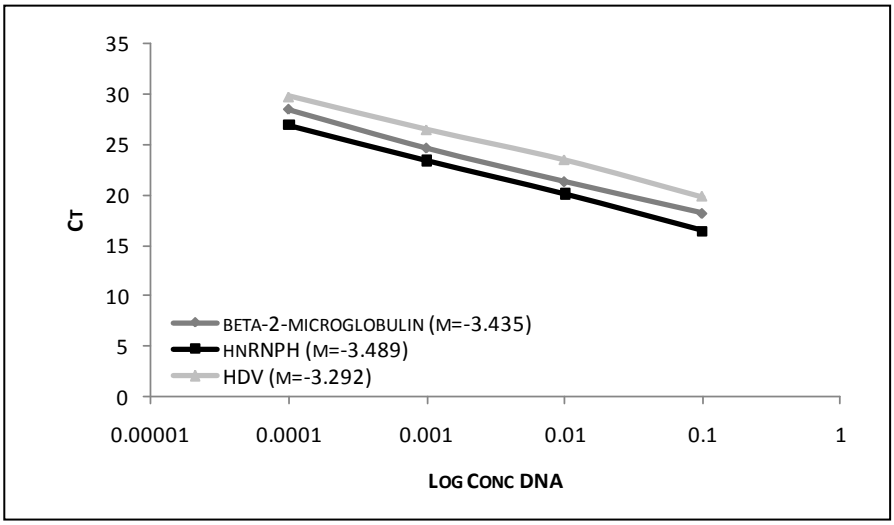

Figure IV.4.2.: Validation of the ΔΔCt method. cDNA amplification of the same sample diluted over a 10000-range was performed using primers for β-2-microglobulin and hnRNP H. For each amplification the logarithms of cDNA dilutions were plotted against Ct (threshold cycle) values and efficiency of the primer was determined by $E=10^{(-1/m)}-1$, where m is the slope of the obtained curve.

Applying the ΔΔCt method, results showed that although silencing of hnRNP H mRNA by the shRNA was not completely successful, the levels of hnRNP H mRNA showed a relative reduction of 1.5 times while HDV mRNA levels showed a relative increase of 1.4 times (figure IV.4.3.).

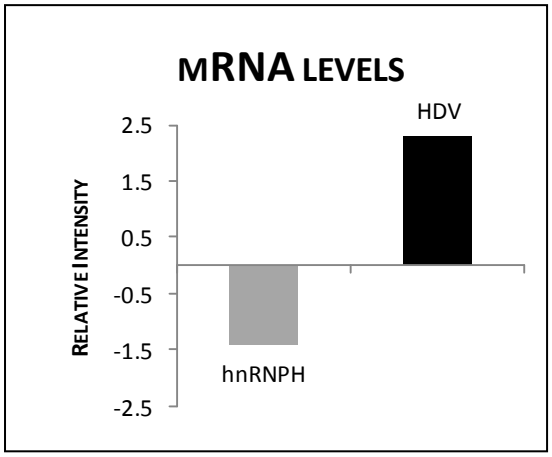

Figure IV.4.3.: Alterations in mRNA levels of hnRNP H due to the presence of a shRNA targeting hnRNP H mRNA and consequent alteration of the levels of the HDV mRNA.

Western blot analysis followed by relative quantification using Image J was then used to determine possible alterations in the expression levels of hnRNP H and consequently in the delta antigens. Huh7-D12 cells transfected with the pSiren-RetroQ-hnRNP H vector and Huh7-D12 cells transfected with the pSiren-RetroQ-Luciferase, used as a control, were harvested and protein extracts were prepared. Proteins were separated by SDS-PAGE and transferred to a nitrocellulose membrane. Using specific antibodies, detection for clathrin, used as housekeeping, hnRNP H and the delta antigens was performed. Figure IV.4.4. shows the results obtained by Western blot analysis.

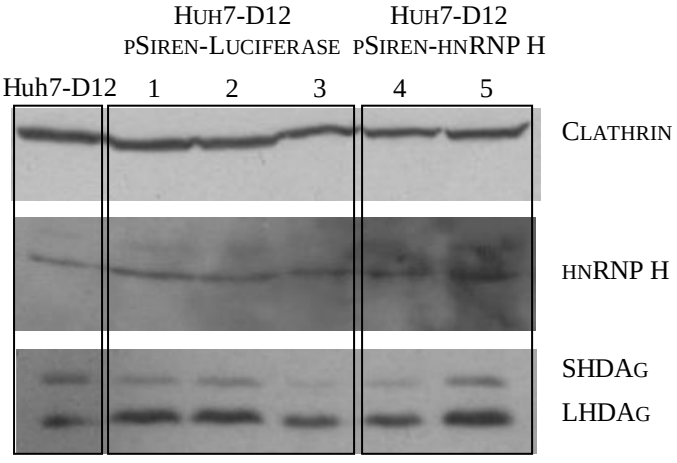

Figure IV.4.4.: Western blot analysis of cellular extracts resulting from the transfection of Huh7-D12 cells with pSiren-RetroQ-hnRNP H (lanes 4 and 5) and western blot analysis of cellular extracts resulting from the transfection of Huh7-D12 cells with pSiren-RetroQ-Luciferase (lanes 1, 2 and 3). Samples were analyzed by western blot analysis allowing for the detection of Clathrin, used as housekeeping, hnRNP H and the delta antigens.

Image J was used to determine the areas of all the bands and relative quantification was performed by dividing the areas of the bands corresponding to hnRNP H and the delta antigens by the areas of the bands corresponding to clathrin in the same sample. Results showed that although silencing of the protein hnRNP H was not completely successful, a knock down of the protein by 70% was achieved. The knock down of hnRNP H induced a decrease in the expression of SHDAg and LHDAg (figure IV.4.5.).

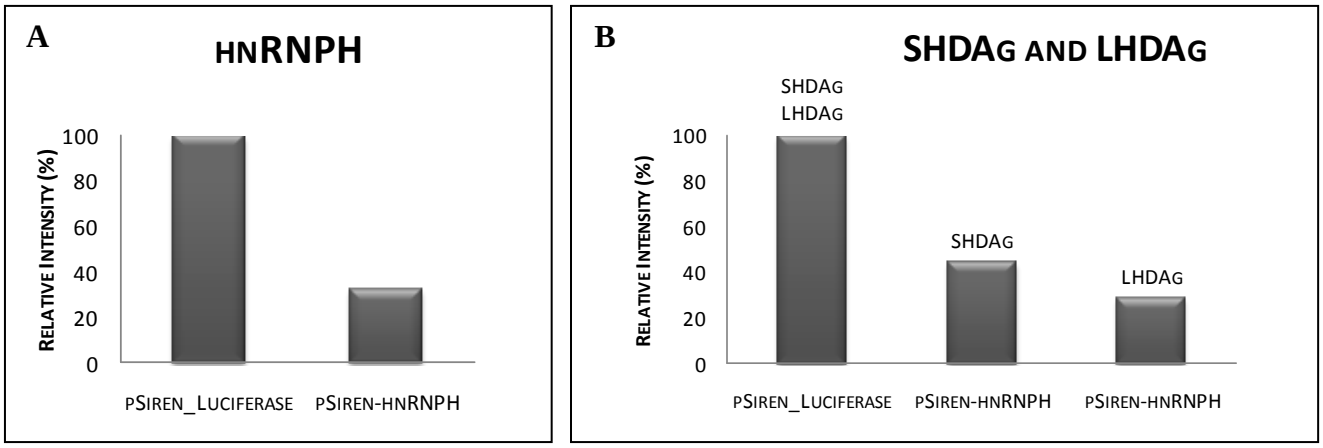

Figure IV.4.5.: Knock down of 70% of the protein hnRNP H (A) and consequent knock down of 60% of the small delta antigens (B) and 70% of LHDAg. Using Image J the areas of the bands corresponding to hnRNP H, the delta antigens and clathrin were determined. By dividing the areas of the bands corresponding to hnRNP H and the areas of the bands corresponding to the delta antigens by the areas of the bands corresponding to clathrin in the same samples, the relative quantification of the proteins was determined.

III.4.2. HNRNP H CO-LOCALIZES WITH SMALL DELTA ANTIGEN

In a previous work by Mota et al, in cell expressing the small delta antigen, hnRNP H was found to be differentially expressed (Mota *et al.* 2008). In this work, it was also shown that by using RNAi it was possible to decrease the levels of hnRNP H mRNA and the protein itself. Furthermore, the silencing of this protein led to an increase of HDV mRNA levels and a decrease in the expression of the delta antigens. These results indicate that hnRNP H affects HDV replication. Immunofluorescence assays were thus performed to determine if hnRNP H and the delta antigens co-localize in Huh7-D12 cells, allowing a physical interaction between both proteins. hnRNP H was labeled in red and the delta antigens were labeled in green.

In figure IV.4.6., results show that SHDAg, in green, is mainly in the nucleus (figure IV.4.6A) while hnRNP H, in red, seems to be present both in the nucleus and in the cytoplasm (figure IV.4.6.B). By merging both images (figure IV.4.6.C), it was observed that a co-localization between both proteins seems to exists, showing that both proteins may interact.

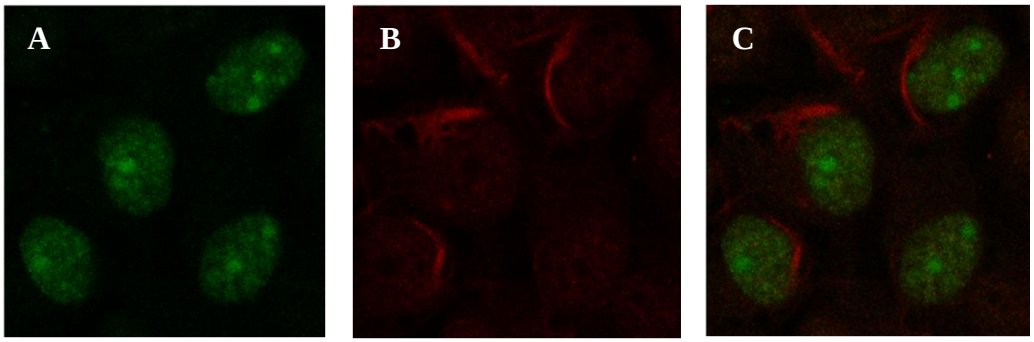

Figure IV.4.6.: Co-localization of hnRNP H and SHDAg. Figure A shows the nuclear localization of SHDAg in Huh7-D12 cells and figure 6B shows the distribution of hnRNP H, in Huh7-D12 cells, in the nucleus and in the cytoplasm of cells. Figure C shows the merge of both figures A and B showing the co-localization of hnRNP H and SHDAg.

IV.4.3. HNRNP H INTERACTS WITH THE DELTA ANTIGENS *IN VITRO* AND *IN VIVO*

If hnRNP H and SHDAg co-localize, an interaction between these proteins is possible. In order to determine if hnRNP H and the delta antigens physically interact with each other pull down assays and immunoprecipitation assays were performed.

By using a recombinant SHDAg protein with an histidine tag (SHDAg-6xHis), produced in the laboratory (Mendes 2003) and TALON® Magnetic beads as described in chapter IV.3., pull down assays were performed in order to determine if hnRNP H and SHDAg would interact *in vitro*. The recombinant SHDAg-6xHis was first bound to the magnetic beads and incubated with Huh7 cellular extracts allowing the interaction between the recombinant protein and the proteins in the cellular extracts. Possible formed complexes were then eluted and analyzed by western blot where detection for both the recombinant SHDAg-6xHis and hnRNP H was performed. Results show that, in vitro, the recombinant SHDAg does interact with hnRNP H (figure IV.4.7.).

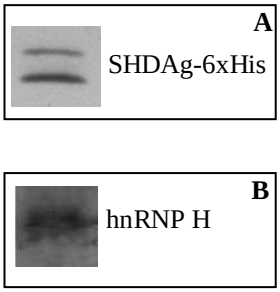

Figure IV.4.7.: Pull down of complexes formed with the recombinant protein SHDAg-6xHis. SHDAg-6xHis was captured using histidine affinity beads (A) and incubated with Huh7 cellular extracts protein complexes formation with the SHDAg-6xHis. Complexes were eluted and analyzed by western blot in order to detect the presence of hnRNP H in such complexes (B).

Immunoprecipitation assays were then performed to confirm this interaction *in vivo*. Antibodies either for the delta antigens or for hnRNP H were incubated with Huh7-D12 cellular extracts and immunocomplexes formed were then trapped using Protein G. Immunocomplexes were finally eluted and analyzed by western blot analysis. Results showed that, in vivo, LHDAg, interacts with hnRNP H (figure IV.4.8.).

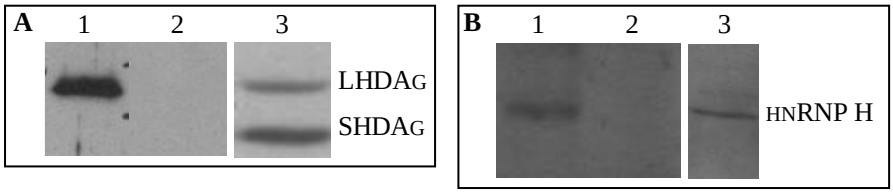

Figure IV.4.8.: Co-immunoprecipitation of hnRNP H and the delta antigens. As described before, Huh7-D12 protein extracts were incubated either with an antibody against hnRNP H, α- hnRNP H, or with an antibody against the delta antigens, B3 to form immunocomplexes which were then trapped using Protein G. Immunocomplexes were eluted and delta antigens were detected by Western blot (A1) in immunoprecipitation with hnRNP H and hnRNP H was detected by Western blot (B1) in immunoprecipitation with the delta antigens. Lane 2 in figures A and B show the negative control in which Protein G was incubated with Huh7-D12 total protein extracts. Lane 3 in figures A and B show the delta antigens and hnRNP H in Huh7-D12 total protein extracts, respectively.

IV. 5. DISCUSSION

Human hepatitis delta virus recruits host cellular proteins in order to replicate. Until now several proteins were already described as interacting partners of HDV (Huang *et al.* 2001; Huang *et al.* 2008; Sikora *et al.* 2009; Tseng *et al.* 2010). In a previous work by Mota *et al*, hnRNP H was found to be up-regulated in cells expressing the small delta antigen (Mota *et al.* 2008). In an attempt to determine in which way hnRNP H could be involved in viral replication and/or pathogenesis, several assays were performed. Knock-down of hnRNP H resulted in the increase of HDV mRNA levels and a decrease in the expression of the SHDAg and LHDAg. Although at first sight these results seem contradictory, it is obvious that hnRNP H affects HDV replication. As already mentioned hnRNP H is mainly involved in pre-mRNA splicing and polyadenylation. Being so, these results seem to suggest that HDV recruits hnRNP H to regulate HDV mRNA translation, directly or indirectly by inducing alternative splicing of key proteins involved in translation. A down regulation of hnRNP H will retain SHDAg and LHDAg mRNAs in the nucleus increasing HDV mRNA levels. Alternatively, down regulation of hnRNP H may also induce SHDAg and LHDAg degradation. It is also possible that HDV recruits hnRNP H to induce alternative splicing of protein of the protein ubiquitination pathway allowing viral replication.

In vitro, but not *in vivo*, hnRNP H interacted with recombinant SHDAg. Recombinant SHDAg used in this work was produced in insect cells and is expected to present all the PTMs present in SHDAg produced in mammals, however, this proteins forms dimers and its conformation may not be the same as the *wild type* (wt) SHDAg, which may induce the interaction with hnRNP H.

In vivo, hnRNP H was found to interact with LHDAg. As already mentioned, hnRNP H is mainly localized in the nucleus, which was visually confirmed by immunofluorescence assays, and a possible interaction between LHDAg and hnRNP H was surprising. Although LHDAg has an NLS and shuttles between the nucleus and the cytoplasm to form RNPs, it is also involved in viral particle assembly and supposedly, one could be lead to think that it acts more in the cytoplasm then in the nucleus. These results, however, seem to show that LHDAg may have other functions then simply be involved in viral particle assembly. Without further analysis it is almost impossible to determine in which way this interaction affects HDV life cycle. However it is possible to speculate that hnRNP H interacts directly with LHDAg facilitating export of the

RNPs to the cytoplasm or even to induce alternative splicing of pre-mRNAs that will produce key proteins for HDV replication and/or viral particle assembly.

Furthermore, it is also possible that hnRNP H may be involved in polyadenylation of HDV RNAs. Because HDV RNA as a poly G tract, between nt 33 and 36 (GGGA), it is possible that hnRNP H binds to the genomic RNA. *In situ* hybridization assays or UV-crosslinking would be of great help in determining if HDV RNA binds hnRNP H.

In conclusion, hnRNP H affects HDV replication. It is likely that HDV recruits hnRNP H to induce splicing of pre-mRNAS involved in translation of the delta antigens. Furthermore, hnRNPH may be involved in the exportation of the RNP to the cytoplasm or by binding to LHDAg may induce splicing of pre-mRNAs that will produce key proteins essential for viral replication and/or assembly.

CHAPTER V: ANALYSIS OF CHANGES IN THE HOST CELL PROTEOME DURING HEPATITIS D VIRUS INFECTION

V.1. INTRODUCTION

V.1.1. MASS SPECTROMETRY-BASED PROTEOMICS

Proteomics – "The study of proteins, how they're modified, when and where they're expressed, how they're involved in metabolic pathways and how they interact with one another."

Marc Wilkins, 1994

The term ***proteomics*** was first defined by Marc Wilkins, in 1994, in the symposium: "2D Electrophoresis: from protein maps to genomes" in Siena, Italy. From that date until now, because of the importance of proteins in cell biology, several progresses have been made in the field mainly with the help of Mass Spectrometry (MS) to perform protein identification. MS-based proteomics has thus become such an attractive methodology because it can determine protein composition, protein modifications, protein expression and more recently decoding signaling networks (Choudhary and Mann 2010) and also lead to some good insights into protein dynamics with the help of systems biology.

V.1.1.1. QUANTITATIVE PROTEOMICS

After genome sequencing and quantification of gene expression, the next step seemed to be the determination of the proteome of cells, tissues and organisms. Due to the advance in methodology, mainly in sample preparation, MS and bioinformatics, not only the determination of proteomes was possible, but also quantification of proteins was made possible. Quantitative proteomics became one of the major areas of interest to molecular and cellular biologists allowing them to determine changes in protein expression in response to all kind of internal and external factors.

Protein quantification may be absolute or relative. Absolute quantification is performed using known standards and gives the amount of protein in terms of concentration. One of the most used methods uses isotope-labeled synthetic standards known as AQUA (Absolute Quantification of proteins) (Gerber *et al.* 2003).

Relative quantification is generally used to determine protein expression changes in biological systems submitted to different conditions. In this case what is measured is the fold of the protein in the sample, relatively to a reference condition. If the fold of a protein is positive the protein is up-regulated and if the fold of a protein is negative, the protein is down-regulated.

Prior to 2000, the major tool for proteomic analysis was Two Dimensional Electrophoresis (2DE) followed by MS. However some limitations of the technique, namely problems regarding reproducibility, the fact that only the more abundant proteins are detected and problems with the detection of proteins with high hydrophobicity and those of extreme basic or acidic pI or extreme molecular masses, led to the search for new approaches for proteomics studies. Differential stable isotope labeling emerged as an alternative technique in which a mass tag is created that will be recognized by the mass spectrometer allowing comparison between two or more samples. In other words, when comparing two identical samples of different stable-isotope composition a mass shift is created allowing to differentiate samples in a mass spectrometer. The ratio of signal intensities from the two samples accurately indicates their abundance ratio. Until now several differential isotopic labels have been used and may be incorporated into samples metabolically, chemically or enzymatically and at the protein level or at the peptide level.

Metabolic labeling

Metabolic labeling consists in the incorporation of stable isotopes during protein synthesis in cell growth. For that purpose, during cell culture, cell culture media is supplemented with the stable isotopes which during cell growth are incorporated into the proteome of the cell.

One type of metabolic labeling is ^{15}N labeling. This type of labeling was first used by Chait and co-workers in 1999 (Oda *et al.* 1999) which used ^{15}N labeled growth medium to perform metabolic labeling of yeast. Later on, this strategy was used for quantitative proteomics in other organisms like *Caenorhabditis elegans* and *melanogaster* (Krijgsveld *et al.* 2003) and *Arabidopsis thaliana* (Nelson *et al.* 2007). Although ^{15}N labeling may be a good choice for plants and bacteria, for mammalian cells ^{15}N-substituted media are difficult and expensive to prepare. Additionally, incorporation may not achieve 100% and quantification is complicated because the

number of replaced nitrogen atoms may vary from peptide to peptide making the exact mass shift unpredictable (Elliott *et al.* 2009).

An alternative for ^{15}N labeling was described by Mann and co-workers in 2002. In this approach, named SILAC (stable isotope labeling by aminoacids in cell culture), aminoacid deficient cell culture media is supplemented with isotopically labeled aminoacids which are then incorporated by cells and consequently by the proteome during protein synthesis. Due to the methodology followed, in which proteins are digested with trypsin, the most commonly used labeled aminoacids in this approach are lysine ($^{13}C_6$-lysine) and arginine ($^{13}C_6$-arginine). After digestion with trypsin, which cuts in lysines and arginines, all tryptic peptides will thus have at least one labeled aminoacid. When comparing the labeled sample with the non-labeled sample, peptide pairs will be recognized by having an exact mass difference corresponding to the difference between heavy and normal aminoacids. The relative intensity of the peaks reflects the abundance of the proteins in the mixture (Ong *et al.* 2002). One of the advantages for SILAC is that more than two comparisons may be performed for the same sample due to the availability of several labels and with a labeling efficiency of, theoretically, 100%. However, SILAC cannot be used with all cell lines being more effective in mammalian cells due to their inability to synthesize all of the aminoacids. In plants, due to their autotrophic nature, SILAC does not work well.

Metabolic labeling has one great advantage: the fact that because labeling is performed at such an early stage, combination of non-labeled sample and labeled sample is performed before almost any sample handling converting this method in one of the most accurate for quantitative MS. With this kind of accuracy metabolic labeling is particularly suitable to determine small changes in protein levels and also for post-translational modifications (Bantscheff *et al.* 2007).

Chemical labeling

Chemical labeling consists on the chemical modification of peptides by stable isotopes-containing tags and to date, several approaches have being used to perform such labeling. ICAT and iTRAQ are two of the most important techniques used for chemical labeling.

ICAT, also known as Isotope-Coded Affinity Tags, was one of the first chemical labeling techniques used in quantitative proteomics and was introduced by Gygi and

Aebersold in 1999. The ICAT reagent exists in two forms – heavy and light – and consists of three elements: a reactive group that has specificity towards thiol and thus cysteines, an isotopically coded linker that can incorporate labeled isotopes that will be differentiated by mass spectrometry and the third is an affinity tag, biotin, which is used to isolate ICAT-labeled peptides (figure V.1.1).

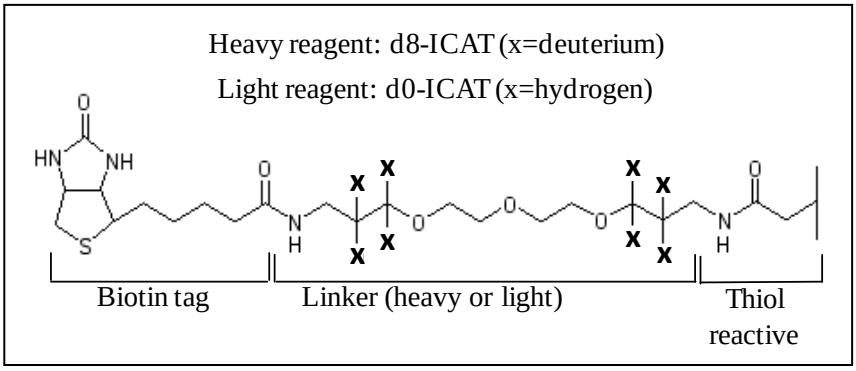

Figure V.1.1: ICAT labeling reagents.

So briefly, proteins from two samples to be compared are labeled with either heavy or light ICAT reagents. Because the reagent has specificity towards thiol groups it will bind to cysteines. Proteins from both samples are mixed and digested with a protease generating peptides. The labeled peptides will have a biotin tag and will be isolated by avidin affinity chromatography. MS analysis is performed and the relative abundance of peptides is determined by the ratio of the signal intensities from the heavy and light forms of each peptide (Gygi *et al.* 1999). The major advantage of the technique is that because there is an enrichment of labeled peptides it favors the detection of low abundance proteins. However, because ICAT can only tags proteins containing cysteine residues, some important proteins may be missed by the technique. Also this technique is restricted to two comparisons per assay.

iTRAQ (isobaric tags for relative and quantification) uses amino-specific isobaric reagents to label N-termini and lysine side chains of peptides in a digest mixture. The iTRAQ reagent consists of a reporter group (based on N-methylpiperazine with a variable mass of 114-117 Da or 113-121 Da), a mass balance group (carbonyl) and a peptide-reactive group (NHS ester) (figure V.1.2) and due to the mass variability of the reporter group up to eight different biological samples can be compared.

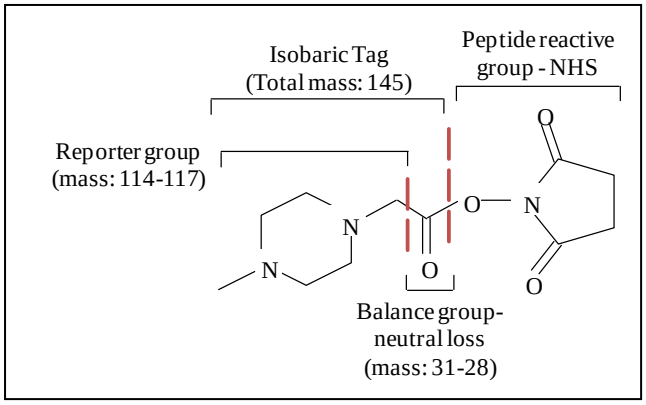

Figure V.1.2: iTRAQ labeling reagent.

As described before, labeling is performed at the peptide level, post-digestion and samples are then mixed and analyzed by mass spectrometry where quantification is made in MS/MS mode. Along with peptide fragmentation, the isobaric amine groups are also fragmented releasing reporter ions with distinct *m/z* ratios. The intensity of each reporter ion is then used to determine relative peptide abundances between samples (Ross *et al.* 2004). Because labeling is performed post-digestion an advantage should be that, in theory, all tryptic peptides should be labeled and multiple peptides can be detected for the same protein, giving multiple quantitation measurements per protein and thus a greater confidence in peptide identification. However, variability in labeling efficiencies and the possible variability due to sample handling, since labeling is performed post-digestion, may be a problem at the time of quantification. Also iTRAQ reagents are considerably expensive.

Enzymatic labeling

Enzymatic labeling consists on the incorporation of ^{18}O water molecules into peptides during or after proteolytic cleavage. When proteins are digested with trypsin, peptide backbones are cleaved at the carboxyl side of lysines and arginines (except when their followed by a proline). In the presence of $H_2{}^{18}O$, ^{18}O exchange can occur at the C-terminal hydroxyl position introducing a mass shift of 2 Da and at the carbonyl group introducing another 2 Da of mass shift leading to a total of 4 Da mass shift in the cleaved peptide (Yao *et al.* 2001) (figure V.1.3).

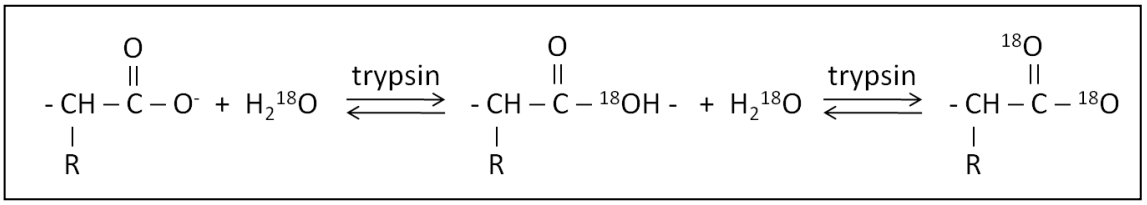

Figure V.1.3: Post-digestion ^{18}O labeling.

As described before, ^{18}O labeling may be performed either during or after proteolytic cleavage with some clear advantages for the latter because when performing post-digestion labeling, digestion and labeling steps may be optimized separately and with a low volume of $H_2{}^{18}O$ (Yao *et al.* 2003). This technique is clearly one of the cheaper stable isotope labeling techniques since the only reagents required to perform labeling are $H_2{}^{18}O$. Like other approaches, ^{18}O labeling has disadvantages. Because labeling is performed during or post-digestion and labeled and non-labeled samples are joined after that, sample handling may be a problem leading to protein losses. ^{18}O labeling reaction is a reversible reaction and in the presence of H_2O trypsin mediated back-exchange can occur. By completely drying samples and using water free reagents this problem may be avoided. Also the use of immobilized trypsin may be an advantage since it becomes easier to remove it after labeling.

Although 100% labeling is rare using this approach, good labeling efficiencies may be achieved and with the appearance of new bioinformatic tools to analyze ^{18}O labeling data, this technique has become a very powerful technique to quantitative proteomics (Bonzon-Kulichenko *et al.* 2010).

Label-free quantification

So far, isotope labeling approaches have been the most used to perform quantitative proteomics. However, as described before all these approaches present limitations such as the complexity of sample preparation which makes these techniques time consuming ones, the high amount of sample required to perform the assays, the high cost of the reagents, the labeling efficiencies which rarely achieve 100% and the requirement for specific software regarding data interpretation. Label-free quantification has thus emerged as a very appealing approach to perform quantitative proteomics. Sample preparation includes protein extraction, reduction, alkylation and digestion; peptide separation by liquid chromatography; and analysis by MS/MS, but the great

advantages are the elimination of the labeling steps thus avoiding possible losses of target peptides and the elimination of the high costs regarding labeling reagents. Each sample is prepared separately and analyzed by LC/MS-MS. Finally, protein quantification is performed using one of two methods: by measuring peak intensity or by spectral counting. Protein quantification by measuring peak intensity is based on the fact that the chromatographic peaks areas correlate linearly with the amount of injected sample (Chelius and Bondarenko 2002). Relative quantification is then achieved by comparing the peak area of a certain ion in multiple LC-MS datasets. Regarding spectral counting, Liu et al demonstrated that spectral count correlates linearly with relative protein abundance and thus relative quantification is achieved by comparing the number of identified MS/MS spectra from the same protein in each of the multiple LC-MS/MS datasets (Liu *et al.* 2004). Normalization and statistical analysis are required but several online bioinformatic tools are already available to help in the analysis (Zhu *et al.* 2010).

V.1.1.2 MASS SPECTROMETRY OF PEPTIDES

Quantitative proteomics was made possible due to MS. While quantitative proteomics grew, MS grew as well trying to address all the issues rose by biologists. Nowadays, several equipments are available to make possible and easier the analysis of entire proteomes.

Mass spectrometry measures the mass to charge ratio (*m/z*) of an ion in the gas phase, which means that peptides, prior to be analyzed for their *m/z*, must be ionized and transferred to the gas phase. The mass spectrometer is thus composed by three parts: the ion source, where analytes are ionized and transferred into the gas phase; the mass analyzer, where ions are separated by their m/z; and finally the detector which monitors the ion current, amplifies it and the signal is transmitted to the system where is recorded in the form of a mass spectra.

Ionization Methods

Two of the most used methods for peptide ionization are Matrix Assisted Laser Desorption/Ionization (MALDI) and electrospray ionization (ESI). For MALDI, peptides are first co-crystallized with a UV-light absorbing organic molecule, the matrix, and then transferred to the ion source, into the vacuum. A UV laser pulse is then

irradiated leading to sublimation of the solid matrix along with peptide ions into the gas phase. The energy absorbed by the matrix leads to its ionization and by proton transfer reactions ionizes the peptide molecules (Mallick and Kuster 2010). In ESI, the peptide mixture is first dissolved in a liquid solvent system. The sample is then passed through a thin needle subjected to an electrostatic potential. At the tip of the needle, the resulting field charges the surface of the emerging liquid, dispersing it by Coulomb forces into a fine spray of droplets. Once the droplets are airborne, and due to the presence of a gas and appropriate temperatures, the solvent evaporates decreasing the size of the droplets and increasing the charge density on its surface. Charge density increases until reaching the point at which Coulomb repulsion becomes of the same order as the surface tension thus tearing droplets apart and producing charged daughter droplets that also evaporate. These events are repeated until the radius of curvature of a daughter droplet becomes small enough that the field due to the surface charge density is strong enough to desorb ions from the droplet into the ambient gas (Fenn *et al.* 1989).

Mass analyzers

Ions can be manipulated by electrostatic and/or magnetic fields and the motion of ions in such a field is often a function of their *m/z* ratio. Several mass analyzers are used in proteomics. Among them, are included the time of flight (TOF), the quadupole, the family of ion traps mass analyzers, the Fourier transform ion cyclotron resonance (FT-ICR) and more recently, the Orbitrap. In TOF, the *m/z* ratio is determined by measuring the time that an ion takes to travel a constant distance inside the mass analyzer. Peptides of low *m/z* travel faster and peptides with high *m/z* travel slower. The flight times of each ion can be converted to *m/z* values using a calibration function built on the time of flight of standards of known *m/z*. In reflectron mode, TOF analyzers have a mass resolution of > 30000, mass accuracy of < 5 ppm and femtomol sensitivity for ions with a mass lower than 4000 Da.

Quadrupoles are other type of mass analyzers which function as a mass filter. In a quadrupole, by applying an oscillating electrostatic field to two pairs of parallel rods, a quadrupolar field is created. Due to this field, ions are forced into a spiraling trajectory through the quadrupole rods. Since ions of different m/z have different oscillations in the quadrupolar field, only ions of a single m/z values can travel through the device at a certain field frequency and amplitude. By scanning the amplitudes of the applied fields,

each m/z value can be focused on the detector allowing to create a full mass spectrum. Resolution and mass accuracy are not very high in quadrupoles, however they are very sensitive.

Ion traps use a quadrupolar field to catch ions. In the trap, the stability of the ions is a function of the applied electrostatic field parameters thud by varying the field parameters ions of different m/z values can be ejected from the trap and focused onto the detector. Ion traps are very sensitive, however mass accuracy and resolution are not very high (~0.1-0.5 amu and 500-2000 respectively) (Mallick and Kuster 2010).

Orbitraps also function as a trap, employing orbital trapping in an electrostatic field. When ions enter the orbitrap their trajectory involves both an orbiting motion around the central electrode, which keeps ions trapped and in simultaneous oscillation along a central spindle. Although all ions have the same amplitude, their frequency changes with the m/z values, therefore ions with the same m/z values oscillate along the spindle altogether, remaining in-phase and assuming the shape of a ring. By moving along the spindle the ring will induce opposite currents creating a signal that is detected by differential amplification (Hu *et al.* 2005). In FT-ICR, ions of different m/z values display different 3D motions in a strong homogeneous magnetic field and their in-phase oscillation frequencies are recorded by an induced current. Both Orbitraps and FT-ICR offer superior mass resolution (>100000) and mass accuracy (<1 ppm) (Mallick and Kuster 2010).

Since ionization and mass analysis are two different steps in a mass spectrometer, it is theoretically possible to combine any ionization technique with any type of mass analyzer. The most used combinations for proteomics so far are MALDI-TOF combined with 2DE or ESI-ion trap combined with liquid chromatography.

V.1.1.3. DATA ANALYSIS

High-throughput quantitative proteomics generates a huge amount of data that may become very difficult to interpret and organize bringing in some cases more confusion than enlightenment. The development of bioinformatic tools for the analysis of proteomic data using statistical principals is thus a very important factor. Several algorithms already exist to perform peptide identification based on searching tandem-MS-spectra against protein sequence databases. PeptideSearch (www.mann.embl-heidelberg.de/GroupPages/PageLink/peptidesearchpage.html), Sequest (Thermo

Finnigan), Mascot (http://www.matrixscience.com/search_form_select.html), Sonar ms/ms http://hs2.proteome.ca/prowl/sonar/sonar_cntrl.html) and ProteinProspector (http://prospector.ucsf.edu/prospector/mshome.htm) are some of the most used algorithms. These tools all operate in a similar manner by taking an experimental MS/MS spectrum as input and compare it against a theoretical fragmentation pattern constructed for peptides from the searched database to find a match. Sequest algorithm, for instance, is a signal-processing technique called autocorrelation that is used to mathematically determine the overlap between a theoretical spectrum that has been derived from every sequence in the database and the experimental spectrum in question. The overlap is given in a form of a score.

As for high-throughput protein quantification, bioinformatic tools are still far behind when comparing with bioinformatic tools for identification. In this work, QuiXot software, *v 1.2.81*, was used (Jorge *et al.* 2009).

With the introduction of systems biology which attempts to understand the workings of natural biological systems (Chuang *et al.* 2010) several bioinformatic tools have been developed which may be used to organize data and give some interpretation to these results by comparing and fitting them in their biological system. KEGG – Kyoto encyclopedia of genes and genome (Ogata *et al.* 1999), GOTM – Gene ontology tree machine, (Zhang *et al.* 2004), Ingenuity Pathway Analysis (Ingenuity® Systems, www.ingenuity.com) and Cystoscape (www.cytoscape.org) are some of the bioinformatic tools available to help organizing and interpreting data.

V.1.2. THE PROTEOMES OF HEPATITIS B VIRUS AND HEPATITIS C VIRUS INFECTED CELLS AND THE WAY TO HEPATOCELLULAR CARCINOMA

Hepatitis B virus

Hepatitis B virus (HBV) is a virus from the hepadnaviruses family that infects hepatocytes. HBV has a 32 Kb partially double-stranded circular DNA genome that encodes four overlapping reading frames: the *S* ORF, the *C* ORF, the *P* ORF and the *X* ORF. The *S* ORF codes for the viral envelope surface proteins, the *C* ORF codes for the viral nucleocapsid HBcAg and HBeAg whose function is not well known, the *P* ORF codes for the virus polymerase and the *X* ORF codes for HBxAg which has multiple

functions like signal transduction, transcriptional activation, DNA repair and inhibition of protein degradation.

When the virus enters the hepatocytes, its DNA is transported to the nucleus where the viral polymerase repairs the single stranded gap region in the virus DNA which is then circularized into a covalently closed circular molecule (cccDNA). The cccDNA serves as the template for the transcription of the subgenomic RNAs and the pregenomic RNAs (pgRNAs). In the cytoplasm, while subgenomic RNAs are translated into the virus proteins, the pgRNA is packaged into progeny capsids and reversed transcribed by the viral polymerase into relaxed circular DNA. The capsids containing mature DNA are either used for intracellular cccDNA amplification or for assembly with the viral envelope in the endoplamic reticulum, leading to the formation of viral particles that will be released from the cell (Liang 2009). Despite of the existence of an effective vaccine against HBV, about 2 billion people worldwide have been infected. Although 90% will recover, some will experience acute hepatitis with 0-1% developing fulminate hepatitis and the others will develop chronic hepatitis which eventually may lead to cirrhosis and/or hepatocellular carcinoma (HCC) (Benhenda *et al.* 2009).

Several proteomic studies have been made to determine which host proteins maybe be involved in HBV replication and pathogenesis. Tong *et al*, determined the protein expression changes in cells producing HBV and grouped the differentially expressed proteins into three major groups: proteins involved in retinol metabolism, calcium ion binding proteins and proteins associated with protein degradation pathways. The authors managed to establish a connection between the differentially expressed proteins and HBV leading to a better understanding of HBV biology (Tong *et al.* 2008). Huang et al, made a similar study in which a proteome analysis of HBV, in an hepatoblastoma cell line, and found that differentially expressed proteins were classified in functional categories like lipid metabolism, protein synthesis, protein folding and metabolism, cell proliferation, cytoskeleton, also establishing connections among these proteins and HBV machinery (Huang *et al.* 2009). Of notice, is that both studies found differentially expressed proteins that seem to be involved in the initiation or progression of HCC. Some of those proteins are the Acyl-coenzyme A dehydrogenase, Aldehyde dehydrogenase 1, Annexin V and apolipoprotein E.

Hepatitis C virus

Hepatitis C virus (HCV) is an RNA virus that belongs to the *Hepacivirus* genus of the Flaviviridae family. HCV has a positive sense single-stranded RNA genome of about 9.6 Kb, flanked by 5'- and 3'- untranslated regions (UTR) that are involved in both replication and translation. The genome has one single ORF that codes for a polyprotein of about 3000 a.a. which is then cleaved by cellular and viral proteases giving rise to the 10 viral proteins: the highly basic core (C) protein; glycoproteins E1 and E2; a small integral membrane protein, p7; and the nonstructural (NS) proteins NS2, NS3, NS4A, NS4B, NS5A and NS5B.

HCV infects preferentially hepatocytes and the viral life cycle starts with viral entry, uncoating and release of the viral genome into the cytoplasm where translation occurs using a mechanism dependent of an internal ribosomal entry site. Replication is then facilitated by the replication complex formation that induces membrane web synthesis which concentrates lipid-rich structures that also facilitate HCV assembly. Several host cell factors are involved in the virus life cycle. Among them, highly sulfated heparin sulfate, low density lipoprotein receptor, CD81, scavenger receptor BI, claudin-1 and occluding are involved in virus entry; internalization is performed via clathrin-dependent endocytosis; in translation, liver-specific microRNA 122 and in replication cyclophilin A (Georgel *et al.* 2010). Due to the high heterogeneity of the virus there is no vaccine against HCV.

HCV is a major cause of liver disease. According to the World Health Organization (WHO), 300 million people are HCV carriers and more than 170 million people, 3% of the world population, are chronically infected. Among the patients with chronic HCV, 10-20% will develop cirrhosis and 1-5% will develop hepatocellular carcinoma (10-40 years after infection). In order to understand better the mechanisms of infection several studies involving proteomics have been performed. These studies show that proteins involved in lipid metabolism, oxidative stress and carbohydrate metabolism are always found to be differentially expressed in HCV infected cells (Jacobs *et al.* 2005; Woodhouse *et al.* 2010). Components of host lipid metabolism are known to be involved in HCV replication, also, reactive oxygen species (ROS) are known to increase during HCV infection. A more detailed investigation of the identified differentially expressed proteins will surely give some answers in the understanding of the mechanisms involved in HCV replication and pathogenesis. Jacobs *et al*, also found,

by the proteome analysis of human liver biopsy tissue from HCV infected patients that several differentially expressed proteins were associated to HCV pathological processes like HCC (Jacobs *et al.* 2005). Some of these proteins are the Acyl-coenzyme A dehydrogenase, Aldehyde dehydrogenase 1, catalase and glutamate dehydrogenase. Some of these proteins are the same as the ones detected as markers for HBV induced HCC.

Hepatocellular Carcinoma

Hepatocellular carcinoma (HCC) is the seventh most common cancer worldwide and the third leading cause of cancer related deaths. The major risk factors related to HCC are HBV and HCV which are responsible for three-quarters of HCCs. Thus, HCC incidence is higher in countries with high prevalence of HBV and/or HCV. Other risk factors for HCC include alcoholic liver disease, nonalcoholic steatohepatitis (NASH) and aflatoxin B exposure.

Two major HBV-specific mechanisms mat lead to HCC: the integration of the viral genome in the host chromosome causing cis-effects, resulting in the loss of tumour suppresser gene functions, and/or activation of tumour promoting genes which occurs occasionally; and the expression of trans-activating factors derived from the HBV genome, which have the potential to influence intracellular signal transduction pathways and alter host gene expression (Chemin and Zoulim 2009).

As for HCV, three important features different from those of HBV, are relevant to the hepatocarcinogenesis. The first is that HCV increases by far the risks of chronic infection (10% of HBV cases versus 60-80% of HCV cases), probably because of the immune evasion of the HCV quasi-species generated from high rates of replication errors; the second is that HCV has a 10-20 fold higher propensity to promote cirrhosis than HBV does; and finally, HCV is an RNA virus without any DNA intermediates and it cannot integrate into the host genome thus HCC is mainly induced through indirect pathways like chronic inflammation, cell deaths and proliferation. Because of this, HCC is found almost exclusively in cirrhotic HCV patients but is sometimes found in HBV patients without liver cirrhosis (Castello *et al.* 2010).

Finally, although mechanisms are unknown, Hepatitis Delta Virus (HDV) in co-infection with HBV leads to more severe liver disease than chronic HBV monoinfection and is associated with an increase risk of hepatocellular carcinoma.

Proteomics has been giving a good contribution to determine mechanisms of HBV and HCV infection and also to determine the mechanisms that may lead to HCC related HBV and HCV. Studies showed that several differentially expressed proteins found while studying proteomes infected with HBV and HCV, were associated with mechanisms leading to HCC. Considering the severity of HCC it has become urgent to find biomarkers to detect the stages of the disease and that may be useful as potential therapeutic targets. Until now several groups have been using quantitative proteomics to address the question. In 2003, Kim *et al*, compared the proteomes of HBV and HCV associated HCC cells and came up with a list of differentially expressed proteins present in both cases (Kim *et al.* 2003). Later, in 2005, Lee *et al*, using the same approach performed another proteome analysis of HCC (Lee *et al.* 2005) and although some proteins differed from the previous work by Kim *et al*, one protein HSP70 seemed to be a common point among the two works. Another study by Lee *et al*, in 2009, using again the same approach, performed a proteome analysis of HBV associated HCC (Lee *et al.* 2009). Five proteins were identified like potential biomarkers and one of those proteins HSP27 had already been described by Lee *et al*, in 2005. Finally, also in 2009, another study made by Li *et al*, in which the proteome analysis of HCV associated HCC was performed. Again the differentially expressed proteins were different from the ones found in previous works.

Despite all the works performed in the area and the promising results, the discovery for HCC biomarkers is still away from the end. As described above, most HCCs result from chronic infections with HBV and HCV thus returning a great heterogeneity in results. Also the stages of the disease may also lead to differences in HCCs proteome. Further work is thus required to obtain more conclusive results.

V.1.3. HDV AND HOST CELLULAR PROTEINS

HDV, as described in chapter I, is a very simple virus which codes only for one protein that exists in two forms – the small form (SHDAg) and the large form (LHDAg). Due to its simplicity, it is clear that the recruitment of host cellular proteins is essential for HDV replication and pathogenesis. However, until now little is known about which host cellular factors are involved in HDV replication and pathogenesis. Throughout the years, researchers have tried to clarify the mechanisms of HDV

replication and pathogenesis and some host cellular factors have been discovered to interact with HDV components.

One of the first host cellular factors discovered to interact with HDV was DIPA, delta interacting protein A. DIPA was described to have a high homology to the delta antigen. They were both similar in size and the homology extended over the entire length of both proteins, including the distinctive proline and glycine rich region of the HDAg COOH terminus. Although its function is still unclear, DIPA may act as a nucleic acid binding protein or even as a transcription factor. DIPA was also shown to interact with HDAg in mammalian cells and when overexpressed DIPA markedly inhibited HDV replication (Brazas and Ganem 1996). In 2006, Du *et al*, demonstrated that DIPA acts as a repressor of gene transcription (Du *et al.* 2006).

The interaction between HDAg and nucleolin was also studied and the authors showed that the nucleolin binding activity of HDAg was critical for its nucleolar targeting and that nucleolin was involved in the modulation of HDV replication (Lee *et al.* 1998).

Both forms of the delta antigen, SHDAg and LHDAg, are phosphorylated. Casein kinase II (CKII) and protein kinase C (PKC) have been described to modulate HDV RNA replication and it seems that both proteins are involved in the phosphorylation of the delta antigens (Yeh *et al.* 1996). A study by Chen *et al*, reinforced the involvement of PKC in S-HDAg phosphorylation and the interaction between the two proteins (Chen *et al.* 2002).

B23 is a nucleolar phosphoprotein involved in different processes such as nuclear transport, cellular proliferation and ribosome biogenesis that can directly interact with the two forms of the delta antigen. The interaction domains of B23-HDAg reside within the fragment containing the nuclear localization signal of HDAg, suggesting that B23 acts as a shuttle protein for transport of HDAg into the nucleus. Additionally, while on one hand, the interaction of S-HDAg with B23 seems to regulate HDV RNA replication, on the other hand S-HDAg and B23 were found in a complex with nucleolin thus suggesting that association among these three proteins represents an important mechanism for HDV RNA replication (Huang *et al.* 2001).

Several approaches were used to determine which host RNA polymerase was used for the RNA-directed transcription of HDV RNA. Most assays agree that RNA Pol II is essential for HDV replication. Furthermore, Yamaguchi *et al* reported that HDAg binds directly to RNA Pol II and stimulates transcription by displacing NELF (negative

elongation factor) and promoting RNA Pol II elongation. Briefly, during transcription of cellular genes, NELF and DSIF (DRB-sensitivity inducing factor) block mRNA chain elongation through direct interaction with RNA Pol II. It was observed that NELF is composed by five polypeptides and one of them, NELF-A shows limited sequence similarity with HDAg. Thus, when both proteins are present they compete for the same binding location in RNA Pol II. When HDAg binds to RNA Pol II activates RNA Pol II elongation. Thus, HDAg stimulates transcription by two different mechanisms: It reverses the negative effect of DSFI/NELF by displacing NELF from RNA Pol II and directly stimulates transcription elongation (Yamaguchi *et al.* 2001; Yamaguchi *et al.* 2002). Moreover, another study by Lehmann *et al*, showed that the complex of transcription factor IIS (TFIIS) with RNA Pol II could cleave one HDV strand, create a reactive stem-loop and extend the new RNA 3' end (Lehmann *et al.* 2007). Other studies have shown that RNA pol I and RNA pol III also bind to HDV RNAs (Modahl and Lai 2000; Macnaughton and Lai 2002; Li *et al.* 2006; Tseng *et al.* 2008).

Adenosine deaminase (ADAR) is also an important host cellular protein for HDV life cycle. As described in chapter I, ADAR1 promotes the editing mechanism in the antigenomic RNA, from which results the LHDAg.

MOV10 is the homolog of *A. thaliana SDE3*, which encodes a putative RNA helicase and AGO4 is a translation factor also involved in RNA silencing. Haussecker *et al*, showed that by knocking down *MOV10* and AGO4, HDV replication was inhibited, showing that MOV10 and AGO4 may be involved in HDV replication (Haussecker *et al.* 2008).

YY1 (Yin Yang 1) is a ubiquitous zinc finger transcription factor that interacts with RNA PolII, B23 and nucleolin and modulates the transcription activity of promoters mainly through recruitment of different transcriptional regulatory partners. Huang *et al*, showed that YY1 interacts with both forms of HDAg and that SHDAg is cosedimented with YY1 in a high molecular mass nuclear complex that also contains the YY1-associated CBP (CREB-binding protein) and p300. Overexpression of the three factors can enhance HDV RNA replication (Huang *et al.* 2008).

Mota *et al*, using a proteomic approach, showed that HSP105 and EIF2S1 were differentially expressed in the presence of the LHDAg; hnRNP D and ZNF326 were differentially expressed in the presence of the S-HDAg and that vigilin and La ribonucleoprotein were differentially expressed in the presence of the genomic and antigenomic RNAs, respectively. The authors also showed, by using a HDV cDNA

stably transfected cell line, that ZNF326 and La ribonucleoprotein were differentially expressed, confirming the previous results, and that histone H1 binding protein was differentially expressed in the presence of HDV (Mota 2008; Mota *et al.* 2009). The fact that histone H1 binding protein appears differentially expressed in the previous assay is an interesting result since Lee et al, found that histone H1e, seems to directly interact with the SHDAg affecting HDV replication (Lee and Sheu 2008).

More recently, Cao *et al*, using a cell line carrying a functional FLAG-S-HDAg performed an immunoprecipitation assay and identified by MS more than 100 polypeptides associated with SHDAg. Using RNAi they confirmed that a significant portion of these factors have a measurable impact on HDV RNA accumulation. Among the identified proteins were nine out of twelve subunits of the RNA Pol II; PKR and a part of DSIF were also identified in this study; hnRNP D and ZNF326, already detected by Mota *et al* by 2DE as a result of transiently expression of SHDAg, were also identified as SHDAg interacting proteins. ILF2, ILF3, DDX1, DHX15 were found to interfere with HDV accumulation (Cao *et al.* 2009).

eEF1A1, p54, hnRNPD-L, GAPDH and ASF/SF2 were also found to interact with the right terminal stem loop domain of the genomic HDV RNA *in vitro* and with both polarities of HDV RNA within HeLa cells (Sikora *et al.* 2009).

SUMO (small ubiquitin-related modifier) has been identified as a reversible posttranslational protein modifier whose targets are cellular and viral proteins that function in the nucleus. Sumoylation has several outcomes such as changes in intracellular localization, protein-protein interaction, protein-DNA interaction and stability and activity of modified proteins. A very recent work by Tseng *et al*, showed that SHDAg is posttranscriptionally modified by the SUMO pathway, both *in vitro* and *in vivo*. Moreover, it seems that conjugation of SUMO to SHDAg selectively enhances HDV genomic RNA and mRNA synthesis, but not antigenomic RNA synthesis leading to the proposition that perhaps the cellular machinery involved in HDV antigenomic RNA synthesis differs from the machinery involved in HDV genomic RNA synthesis and mRNA transcription, requiring different modified forms of SHDAg (Tseng *et al.* 2010).

V.1.4. STUDY MODELS FOR HDV REPLICATION

Although 30 years have passed since HDV was discovered and some proteins have been linked to, or observed to affect, HDV antigens and/or HDV RNAs little is known about the mechanisms of replication and pathogenesis. The lack of a robust model to study HDV replication has became a drawback in this matter. The Huh7-D12 cell line has been previously used to study HDV replication and pathogenesis. This cell line was obtained by stably transfection of a human liver carcinoma cell line, Huh7, with three copies of the HDV genomic RNA. The cDNA was synthesized from total liver RNA obtained from an infected woodchuck inoculated with human serum containing HDV. Several HDV expressing clones were isolated and expanded and the characterization of the D12 clone showed that it constitutively expressed both delta antigens and replicated the virus RNA (Kuo *et al.* 1988). Furthermore, the molar ratio between HDAg and virus RNA in these clones was reported to be similar to that found in HDV particles released into the serum of experimentally infected woodchucks (Cheng *et al.* 1993; Cunha *et al.* 1998). Huh7-D12 showed however, that in culture, only 10% of cells expressed the delta antigens and HDV RNAs thus becoming difficult to normalize the results.

A few years ago, Chang *et al*, developed a new model to study HDV replication, the 293-δAg cell line. A line of human embryonic kidney cells, HEK 293, was stably transfected with a single copy of the cDNA encoding the SHDAg, with expression under tetracycline (TET) control thus conditionally expressing the SHDAg. HDV genome replication was then started in these cells by transfection with a mutated RNA unable to express HDAg. Replication of the RNA was thus under the control of TET-induced SHDAg. In the absence of TET there was a low production of SHDAg that was sufficient to allow HDV replication that could be maintained for at least one year. In the presence of TET, both SHDAg and genomic HDV RNA dramatically increased within 2 days leading to cell death in 6 days (Chang *et al.* 2005).

Other authors have developed their own models to try to understand HDV replication. Cao et al, developed a stable cell line carrying a functional FLAG-SHDAg to study interaction among SHDAg and other cellular proteins (Cao *et al.* 2009).

Another option is transient transfection of Huh7 cells with a vector coding for all the components of the virus, which has also been used by some authors (Tavanez *et al.* 2002).

Although none of the models is perfect, significant advances have been made in the study of HDV.

V.2. OBJECTIVES

The objective of this chapter is to determine any possible alterations in the proteome of a tetracycline inducible cell line expressing the small delta antigen, 293-δAg, and in 293-δAg-HDV cells in which HDV RNA accumulation occurs, in an attempt to clarify HDV replication mechanisms.

V.3. MATERIALS AND METHODS

V.3.1. CELL LINE AND PROTEIN EXTRACTION

Cells 293, cells 293-δAg (Chang *et al.* 2005) and cells 293-δAg transfected with HDV RNA, in presence and absence of tetracycline, used in this work were kindly provided by Dr. J.M. Taylor from Fox Chase Cancer Center, Philadelphia, USA.

Cells were seeded in 10 cm plates to a concentration of 5.10^7 cells per plate and incubated at 37ºC for 6 hours. After the incubation period cells were submitted to two different conditions – absence and presence (1 μg/ml) of tetracycline. Medium was removed and replaced by fresh medium supplemented with or without tetracycline, and incubated for 16 hours at 37ºC. Cells were then rinsed with ice cold PBS and scrapped in a total volume of 5 ml PBS which was divided in 1 ml aliquots. Samples were centrifuged at 1500 rpm for 5 minutes and cell pellets were maintained at -80ºC until used.

For protein extraction three cell pellet aliquots were mixed in order to obtain a larger concentration of protein. Cells were lysed using lysis buffer [1%Triton X100, 1mM EDTA, 10 μM PMSF in PBS] and incubated for 1 hour at 4ºC. Supernatants were recovered by centrifugation at 14000 g, at 4ºC, for 15 min and protein concentration was measured using the Pierce® BCA Protein Assay Kit (Pierce).

V.3.2. SDS PAGE

SDS PAGE was used with two different purposes in this work. It was used first as a focusing step allowing protein concentration in only one band, and second as a separation technique to perform Western blot analysis. In the former case, 200 μg of total protein of each sample, previously diluted in Laemmli sample buffer [0.0625 M Tris.HCl pH 6.8, 5% SDS, 12.5 mM DTT, 10% glycerol, 0.01% Bromophenol Blue] (Laemmli 1970), were loaded into a 1.5 mm gel with a 4% stacking gel [4% acrylamide; 0.125 M Tris-HCl, pH 6.8; 0.1% SDS; 0.05% APS; TEMED] casted over a 10% resolving gel [10% acrylamide; 0.375 M Tris-HCl, pH 8.8; 0.1% SDS; 0.05% APS; TEMED] and electrophoresis was performed at 40 V. When samples entered the resolving gel, electrophoresis was stopped and gels were stained with Coomassie Brilliant Blue R-250 (BioRad) [40% Methanol, 10% Acetic Acid, 0.1% Coomassie

Brilliant Blue R-250] for 15 min, at room temperature and gentle shaking. Destaining was performed using destaining solution [40% Methanol; 10% Acetic Acid] after which the gel was re-hydrated, in water, for 1.30 h. Bands, corresponding to each sample and containing the whole proteome (see chapter V.4.1., figure V.4.2.), were removed from the gel, sliced in similar pieces, rinsed twice with HPLC-water for 10 min, with gentle shaking and in gel digested. Five proteome comparisons were performed which corresponds to 10 proteomes and subsequently 10 bands.

As for the later, 10 μg of total protein of each sample, previously diluted in Laemmli sample buffer, were loaded into a 0.75 mm gel with a 4% stacking gel [4% acrylamide; 0.125 M Tris-HCl, pH 6.8; 0.1% SDS; 0.05% APS; TEMED] and casted over a 12% resolving gel [12% acrylamide; 0.375 M Tris-HCl, pH 8.8; 0.1 %SDS; 0.05% APS; TEMED]. Electrophoresis of proteins was performed at 60 V during protein focusing and at 100 V during protein separation.

V.3.3. *IN GEL* DIGESTION OF PROTEINS

For in gel digestion, the bands removed from the gel containing the proteomes, were initially dehydrated with 100% CH_3CN, for 10 min, at room temperature and with gentle shaking. Supernatant was removed and disulfide bonds were reduced with 10 mM dithiothreitol (DTT) in 25 mM ammonium bicarbonate (AB) pH 8.8 for 1 hour, with shaking. DTT was removed and the sulphydryl groups were blocked by alkylation with 54 mM IOA in 25 mM AB, pH 8.8 for 1 hour, in the dark, with shaking. Iodoacetamide (IOA) was removed and gel pieces were dehydrated with 100% CH_3CN for 10 min, with shaking to completely remove DTT and IOA. CH_3CN was removed and gel pieces were rehydrated with 250 μl AB 50 mM, pH 8.8 for 5 min with shaking. Without removing the supernantant, 250 μl 100% CH_3CN were added to the gel pieces which were incubated for another 15 min with shaking. Finally the supernantant was eliminated and gel pieces were dried in a speed-vac centrifuge. Meanwhile lyophilized trypsin (Sequencing Grade Modified Trypsin, Promega, Madison, WI, USA) was resuspended in digestion buffer (50 mM AB pH 8.8, 10% CH_3CN, 0.01% Cyclohexyl-pentyl-β-D-maltoside) to a final concentration of 80 ng/μl to perform digestion (Bonzon-Kulichenko *et al.* 2010).

Digestion was performed using a 1:5 (w/w) trypsin:total protein ratio. To each sample (200 μg of total protein) previously dried, 500 μl of trypsin were added and

samples were incubated for 1 h, on ice. Digestion buffer was added to the samples to reach a final trypsin concentration of 60 ng/μl and samples were then incubated over night (ON), at 37ºC, with gentle shaking. The supernatant containing the digested peptides was collected and in order to recover any possible tryptic peptides that may have stayed in the gel, gel pieces were incubated with 12 mM AB for 1 h, at RT, with shaking. Recovered peptides were then added to the peptides initially recovered. Finally, peptides were acidified using 25% trifluoroacetic acid (TFA) to stop the reaction and pH was checked to confirm pH 3. Samples containing tryptic peptides were desalted using Oasis HBL (hydrophilic-lipophylic balance) extraction cartridges (Waters). Oasis columns were washed with 1 ml 50% CH_3CN followed by 1 ml 100% CH_3CN and equilibrated with 3x1 ml 0.1% TFA. Samples were then loaded to the columns and washed with 1 ml 0.1% TFA. Finally, tryptic peptides were eluted with 2x200 μl of 0.1% TFA/50% CH_3CN. An aliquot of 1/10 of each sample was collected to determine the efficiency of digestion and the remaining sample was dried in the speed vac. Meanwhile aliquots were desalted using Zip-Tip C18 columns (Millipore, Billerica, MA, USA), accordingly to the manufacturer's instructions and analyzed in a linear ion trap mass spectrometer. Digestion efficiencies were determined by dividing the number of partial digested peptides by the total number of peptides.

V.3.4. ^{18}O LABELING OF PEPTIDES

^{18}O labeling was performed post-digestion using immobilized trypsin. Peptides were labeled with $H_2{}^{18}O$ (Isotech, Sigma-Aldrich, Miamisburg, OH, USA) in 100 mM ammonium acetate, pH 6, 20% CH_3CN in the presence of immobilized trypsin (Pierce, Rockford, IL, USA) at a ratio of 1:5 (v/w) immobilized trypsin:protein. As for non-labeled peptide samples, they were treated in the same way using $H_2{}^{16}O$ instead of $H_2{}^{18}O$. Samples' pH was checked to confirm pH 6 and samples were incubated at 37ºC, ON, with vigorous shaking.

Because the labeling reaction is reversible, immobilized trypsin was removed from peptides by filtration using Wizard® Minicolumns (Promega, Madison, WI, USA). The columns were first washed with 100 μl of 100% CH_3CN, the samples were then loaded and columns centrifuged for 15 min at 13000 g and 4ºC to allow maximum recovery of the samples. Although immobilized trypsin was removed, samples were also treated with N_α-Tosyl-L-lysine chloromethyl ketone hydrochloride (TLCK)

(BioChemika, Sigma-Aldrich, Miamisburg, OH, USA) in case some molecules of trypsin have cut loose from the beads. A stock solution of 0.135 M TLCK was first prepared in methanol and TLCK was added to the samples to a final concentration of 1 mM and incubated for 1 h at 37ºC. At this point another aliquot of 1/10 of each sample was collected in order to determine labeling efficiency. To each aliquot 1 M ammonium formiate pH 3 were added in order to lower CH_3CN concentration from 20% to 1.5% and reach a pH of 3. Aliquots were then desalted using Zip-Tip C18 columns following manufacturer's intructions and analyzed in a linear ion trap. Meanwhile the original samples were maintained at 37ºC until results were verified. Labeling efficiencies were determined using Quixot (see chapter V.3.8.).

Finally, labeled samples were added to the correspondent non-labeled samples and 1 M ammonium formiate pH 3 was added in order to lower CH_3CN concentration from 20% to 1.5% and reach a pH of 3. Samples were desalted using Oasis HBL as described previously and dried in the speed vac (Bonzon-Kulichenko *et al.* 2010).

V.3.5. ISOELECTRIC FOCUSING OF PEPTIDES

Due to the complexity of the sample, an initial separation step was performed. Peptides were separated by their isoelectric point using Isoelectric Focusing (IEF) performed in an Agilent 3100 OFFGEL Fractionator system. Previously dried samples were resuspended in focusing buffer [5% glycerol, 1:50 IPG buffer pH 3-10 (GE Healthcare)] and loaded in a Immobiline^{TM} DryStrip gel (IPG strips), which contains a pre-formed pH gradient immobilized in a homogeneous polyacrylamide gel, of 13 cm and pH 3-10 (GE Healthcare) previously rehydrated with focusing buffer in a 12-well manifold accordingly to the user's manual. IPG strips, frames and electrodes were assembled accordingly to the user's manual. IEF was carried out using the standard method for peptides recommended by the manufacturer. Samples were recovered in 12 fractions each corresponding to a determined pH and 1 M ammonium formiate pH 3 was added to all samples to lower CH_3CN concentration from 20% to 1.5%. Samples were then desalted using OMIX® Pipette Tips C18 (Varian, Inc.). Columns were initially washed twice with 50 μl of 50% CH_3CN followed by twice with 50 μl of 100% CH_3CN and equilibrated three times with 50 μl of 5 mM ammonium formiate pH3/3% CH3CN. Each fraction was loaded into a tip, washed 2x100 μl with 5 mM ammonium

formiate pH 3/3% CH_3CN and eluted with 50 µl of 5 mM ammonium formiate pH3/50% CH_3CN. Finally, samples were dried in a speed vac centrifuge.

V.3.6. LC-MS/MS ANALYSIS

All fractions were analyzed by LC-MS/MS using a Surveyor LC system coupled to a linear ion trap mass spectrometer (LTQ, Thermo-Finnigan, San Jose, CA, USA). Peptides were concentrated and desalted using a Reverse Phase (RP) column (0.32x30 mm, BioBasic C18, Thermo Electron) and eluted on line onto an analytical RP column (0.18x150 mm BioBasic C18, Thermo Electron) operating at 2 µl/min. Two gradients of 60 min and 90 min, from 0% to 40% solvent B, were used to elute peptides depending on the complexity of the sample (Solvent A: 0.1% Formic acid; Solvent B: 0.1% Formic acid, 80% CH_3CN). The LTQ was operated in a data dependent Zoom Scan and MS/MS switching mode. For each FullScan, from 400 to 1600 amu and using 3 µscans, 6 ZoomScan/(MS/MS) events of the 6 most intense precursor peaks were performed in order to quantify and identify most peptides (Jorge *et al.* 2007). ZoomScan mass windows were set to 6 Da on the right and 8 Da on the left to allow the monitoring of the entire $^{16}O/^{18}O$ isotopic envelope of peptides. ZoomScan settings were set to a maximum Injection Time (IT) of 100 ms and 10 µscans (Lopez-Ferrer *et al.* 2006). Single, doubly and triply charged peptides were allowed in the analysis. Normalized collision energy was set to 35% and dynamic exclusion was applied for 75 s so that LTQ was able to fragment the same ion twice. The window of exclusion was set to 2.60 Da both ways.

V.3.7. PROTEIN IDENTIFICATION

Protein identification was performed as described previously (Lopez-Ferrer *et al.* 2004). MS/MS raw files acquired on the mass spectrometer were searched against the human Swiss Prot database (release 15.6) using the SEQUEST algorithm (Bioworks *v3.2* package, Thermo Finnigan). The same collection of MS/MS spectra were searched against an inverted database constructed by inverting the aminoacid sequence of proteins present in the original database. Search parameters included a precursor mass tolerance of 2 Da and a fragment ion tolerance of 1.2 Da. Also allowed were fixed modifications in cysteine residues due to cysteine carboxamidomethylation (+57 Da)

and variable modifications in methionine residues (+16 Da) and lysine and arginine residues (+4 Da) due to methionine oxidation and the possible incorporation of two ^{18}O, respectively.

Statistical significance of peptide identification was evaluated by determining the False Discovery Rate (FDR). FDR is defined as the number of false positive identifications among a population of total identifications and can be estimated by using decoy databases constructed from the target databases (like inverted databases). FDR was determined by using the Probability Ratio method (pRatio) (Martinez-Bartolome *et al.* 2008).

V.3.8. PEPTIDE QUANTIFICATION AND STATISTICAL ANALYSIS

Protein quantification from ZoomScan spectra was performed using the QuiXoT software, *v 1.2.81* (Jorge *et al.* 2009) kindly provided by Dr. Jesús Vázquez. The software automatically opens peptide identification results and the respective raw files and selects the ZoomScan spectra correspondent to the identified peptide. Only ZoomScan spectra corresponding to peptide identifications with a false discovery rate lower than 5% were used for quantification.

Quantification was performed as previously described (Ramos-Fernandez *et al.* 2007). Briefly, ZoomScan spectra were fitted into a theoretical curve, a mixed Gaussian/double exponential distribution. The best fit parameters were then used to determine peptide concentration in the non-labeled (A) and labeled (B) samples, expressed in units of area, and labeling efficiency (f). Finally, using this values the proportion of non-labeled (B_0), mono-labeled (B_1) and di-labeled (B_2) peptides in the labeled sample ($B=B_0+B_1+B_2$) could be determined along with the ratio between the non-labeled and labeled samples (A/B). Also determined were σ and β. The best fit values for the parameters σ (a scale parameter which determines the half-width of the peak) and β (relative proportion of double exponential component) and the labeling efficiency were used to discard unreliable quantifications. So as a first filtering step for quantification, Zoom Scans with values of $f > 1.5$, $\sigma > 0.15$ and a $\beta > 0.15$ were considered unreliable and eliminated. After this filtering step, the fitting weight, variances and average means at the scan, peptide and protein level were calculated as described previously (Jorge *et al.* 2009).

When two scans (spectra) from the same experiment are used to quantify the same peptide, values obtained may be very different due to the quality of the scans. So the error during quantification depends of the quality of the spectra and it is not constant. The fitting weight, based on the mean square deviation between the experimental spectra and the theoretical curve, allows the correction of this error. Other errors like protein quantification from the respective peptides, variability in sample concentration and sample handling, so called systematic errors, occur during quantification. Because each protein is quantified using more than 1 peptide and peptides are quantified using more than one spectra, a grand mean – an estimation of the systematic errors – is determined for each value. The grand mean for each one of these values is determined by means of the average means associated to each scan, peptide and protein and respective statistical weight which in turn is determined by calculating the variances at the scan, peptide and protein level.

Outliers are values that deviate from an assumed normal distribution. By calculating variances one can determine if a value deviates from average, more than the expected, according to the assumed normal distribution. The probability that a value deviates from average may be calculated thus allowing to calculate the FDR at scan level (FDRs), at the peptide level (FDRp) and at the protein level (FDRq) (Jorge *et al.* 2009). Outliers at scan, peptide and protein level were determined. At the scan and peptide levels outliers generally result from bad fittings and/or peptides containing missed cleavage sites or oxidized methionines. At the protein level, however, outliers represent proteins differentially expressed. At a scan and peptide level each scan and peptide with and FDR, FDRs and FDRp respectively, lower than 5% were visually inspected and those who were badly quantified were removed. At the protein level, proteins with an FDRq lower than 0.1% were considered as differentially expressed and proteins with an FDRq lower than 1% with more than 1 peptide per protein and more than 1 scan per peptide were also considered as differentially expressed.

V.3.9. SYSTEMS BIOLOGY

GOTM - was used to facilitate data interpretation. GOTM – GO Tree Machine, now called Gene Set Analysis Toolkit V2 (http://bioinfo.vanderbilt.edu/webgestalt), is a gene ontology enrichment online tool which allows the comparison of a user-uploaded protein list with all GO categories to identify those with enriched number of user-

uploaded proteins. In this work, quantified proteins were divided into up-regulated and down-regulated proteins and then again divided by different FDRqs and compared with a reference list containing all quantified proteins in order to determine all enriched categories.

Pathway and network analysis was also performed by using Ingenuity Pathway Analysis (IPA) (Ingenuity® Systems, www.ingenuity.com). Differentially expressed proteins were submitted to IPA allowing to determine all possible relationships between them and determine which metabolic pathways may be triggered by these proteins. Several networks relating these proteins with proteins within IPA databases were also built.

V.3.10. WESTERN BLOT ANALYSIS

Western blot analysis was performed to validate results obtained by mass spectrometry using relative quantification.

After SDS-PAGE, proteins were transferred to nitrocellulose membranes (PROTRAN® Nitrocellulose Transfer Membrane, WHATMAN®, Whatman GmbH, Germany), blocked with 5% low fat milk powder in PBS and incubated ON, at 4ºC, with primary antibodies. Membranes were than washed with 2% low fat milk powder in PBS, supplemented with 0.05% Tween 20 and incubated 1 h with appropriate secondary antibodies conjugated with horseradish peroxidase (BioRad). Membranes were then washed with 2% low fat milk powder in PBS supplemented with 0.05% Tween 20 followed by washes with PBS. Membrane development was performed using ECL™ Western Blotting Detection Reagents (GE Healthcare, Buckinghamshire, UK). Finally, images were digitalized and analyzed using ImageJ.

Primary antibodies used in this work were as follows: Rabbit polyclonal antibody against Clathrin HC (Santa Cruz Biotechnology), mouse monoclonal antibody against HuR (Santa Cruz Biotechnology), mouse monoclonal antibody against p53 (Santa Cruz Biotechnology), mouse monoclonal antibody against karyopherin β2 (Santa Cruz Biotechnology), mouse monoclonal antibody against 14-3-3 σ (Santa Cruz Biotechnology) and mouse monoclonal antibody against Cyclin B1 (Santa Cruz Biotechnology).

V.4. RESULTS

V.4.1. HIGH THROUGHPUT IDENTIFICATION OF PROTEINS IN 293, 293-δAG AND 293-HDV CELLS BY LC-MS/MS ANALYSIS

293-δAg cell line results from the 293 cell line stably transfected with a single copy of cDNA encoding the small delta antigen (SHDAg), under the control of tetracycline. In the presence of tetracycline, 293-δAg cells thus express the small delta antigen. When 293-δAg cells are transfected with HDV RNA (293-HDV cells) they increase in large extent the production of HDV genomic RNA (Chang *et al.* 2005). In this work a high-throughput identification of the proteome of cells 293, 293-δAg and 293-HDV was performed followed by high-throughput quantification of proteins differentially expressed during HDV replication.

In order to determine differential expression changes induced during HDV replication, an ^{18}O-based quantitative proteomics analysis was performed in which 5 comparison assays were performed (figure V.4.1.). The first assay compared 293 cells in the presence (TET +) and absence (TET -) of tetracycline, and was used to ensure that tetracycline was not one of the causes of expression changes in cells proteome. Assays 2 and 3, in which 293 cells were compared with 293-δAg cells in absence of tetracycline, and 293-δAg were compared with 293-HDV cells in absence of tetracycline, respectively, were used as controls for cell manipulation (stable and transient transfections) and low level expression of SHDAg and HDV RNA accumulation. Finally, assays 4 and 5, allowed determination of expression changes occurring in cells expressing SHDAg and in cells replicating HDV, respectively, by comparing 293 cells with 293-δAg cells, and 293-δAg cells with 293-HDV cells, in presence of tetracycline.

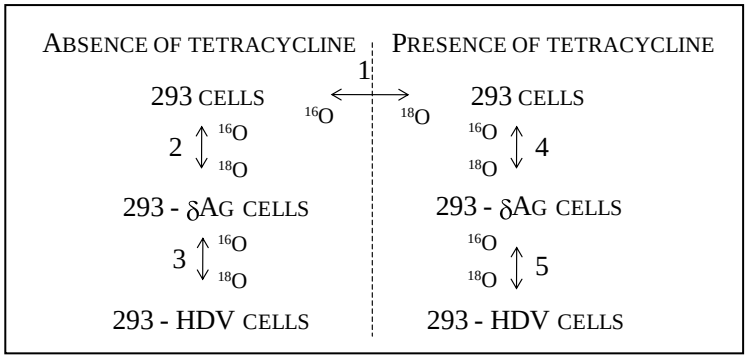

Figure V.4.1.: Experiment design. Cells 293 were compared with each other in the absence and presence of tetracycline (experiment 1). Cells 293 were compared with 293-δAg and cells 293-δAg were compared with cells 293-HDV in the absence of tetracycline (experiments 2 and 3, respectively). Finally the same comparisons were performed in the presence of tetracycline (experiments 4 and 5, respectively).

Protein extracts were prepared from cell pellets and protein concentration was measured as described previously. Two hundred μg of total protein of each sample were loaded into an SDS polyacrylamide gel and electrophoresis was stopped as soon as samples entered the resolving gel allowing for just one band containing all proteins (figure V.4.2.).

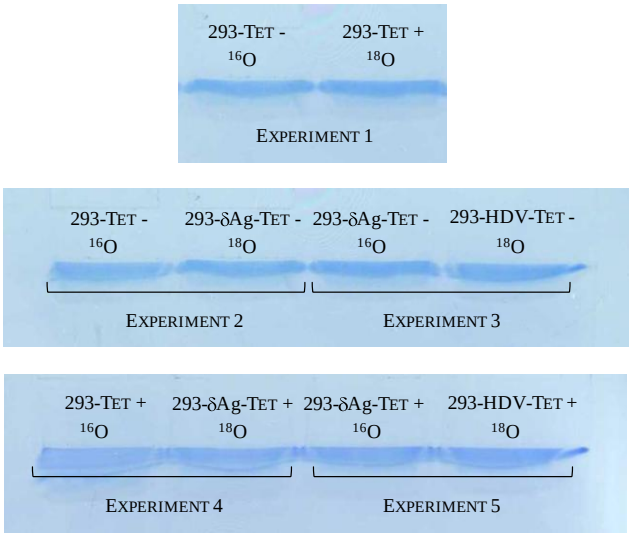

Figure V.4.2.: SDS PAGE. SDS PAGE was used as concentrating step allowing focusing of all cell proteome in one band.

Besides functioning as a concentrating step, SDS PAGE also functioned as a cleaning step since it allowed removing low molecular mass impurities, like detergents and buffer components, which in many cases are detrimental for mass spectrometry.

The bands were removed and digested with trypsin and for each sample an aliquot was collected and analyzed in a LTQ mass spectrometer to determine digestion efficiencies. Good digestion efficiencies are important, not only because good quantification depends on a good labeling efficiency which in turn depends on good digestion efficiency, but also because partially digested peptides do not accurately reflect the protein concentration in the samples. Digestion efficiencies were found to be among 80% and 100% for all samples.

After digestion with trypsin, samples were labeled with $H_2{}^{16}O/H_2{}^{18}O$ in the presence of trypsin covalently bound to cross-linked agarose beads. Because this labeling reaction is reversible, it must be stopped after all peptides are labeled and before the reversible reaction takes place. In order to stop the labeling reaction, immobilized trypsin was removed from samples. However, because some molecules of trypsin may have loosened from beads, samples were also treated with TLCK which inactivates serine proteases such as trypsin hence guaranteeing the end of the labeling reaction. After treatment with TLCK another aliquot of each sample was taken in order to determine labeling efficiency. All samples presented a good labeling efficiency of about 80% and labeled samples and non-labeled samples were mixed, desalted using Oasis columns, and separated by their isoelectric point using Isoelectric Focusing (IEF) performed in an Agilent 3100 OFFGEL Fractionator system. OFFGEL fractionation allowed peptide separation by their isoelectric point in twelve fractions diminishing the complexity of the sample and allowing a better identification and quantification of peptides during LC-MS/MS analysis. The distribution pattern of identified scans, peptides and proteins in Off Gel fractions was similar to all samples and accordingly to this distribution two different gradients were used. A compromise between the number of peptides in a sample and the gradient applied must be reached to all samples. An extensive gradient will generate wider and less intense chromatographic peaks. This means that, firstly the intensity of the ZoomScan spectras will be lower leading to a lower fitting weight (Vs) and hence a poorer quantification. Secondly, because the intensity of chromatographic peaks is lower, the ion trap will receive less analyte ions and the background will increase leading to worst identifications. On the other hand, if the gradient is too short, there will not be sufficient resolution of the chromatographic peaks which means that there will be a mixture of peptides. In this case, it is not possible to isolate peptides for quantification in ZoomScan spectras and fragmentation spectra will have too much information to give good identifications. In these

experiments, a gradient of 90 min was used for most samples. For samples 3, 9 and 10 a gradient of 60 min was used. Figure V.4.3. shows the distribution pattern of OFFGEL fractions, obtained with a 90 min gradient, showing that for fractions 3, 9 and 10 the number of identified peptides is much lower than in the remaining fractions. If the gradient is too long results will not be optimal. These results thus allowed to decrease the gradient for fractions with less peptides optimizing the results.

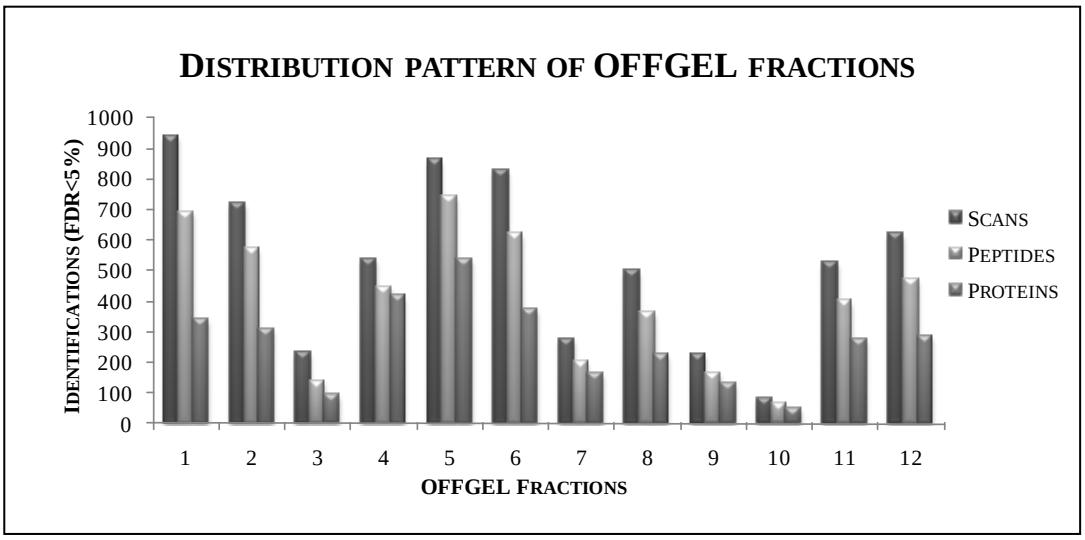

Figure V.4.3.: Distribution pattern of OFFGEL fractionation. After OFFGEL fractionation, fractions were analyzed by LC-MS/MS, submitted to Sequest for peptide identification and run through pRatio to determine peptides with an FDR<5% allowing to determine the distribution pattern of identifications of scans, peptides and proteins in OFFGEL fractions. This distribution pattern was the same for all samples

Each fraction was analyzed by LC-MS/MS as described previously and spectra from fractions corresponding to the same experiment were searched against the human Swiss Prot database (release 15.6) using the SEQUEST algorithm (Bioworks *v3.2* package, Thermo Finnigan) and then submitted to pRatio (Martinez-Bartolome *et al.* 2008) altogether in order to increase the statistical significance of the results. For each experiment and for a FDR<5%, the number of identifications was as follows:

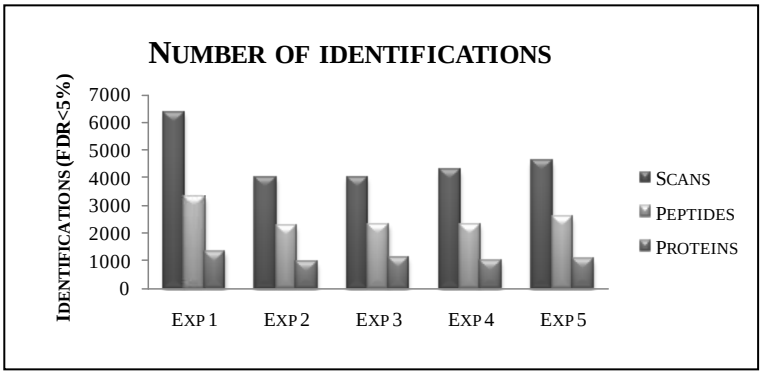

Figure V.4.4.: Number of total identifications at the scan level, peptide level and protein level for an FDR <5%.

V.4.2. HIGH THROUGHPUT QUANTIFICATION OF PROTEINS DIFFERENTIALLY EXPRESSED DURING HDV REPLICATION

After protein identification, quantification of peptides was performed using QuiXot (Jorge *et al.* 2009). Only ZoomScan spectra corresponding to peptide identifications with a false discovery rate lower than 5% were used for quantification. As described in Materials and Methods section, ZoomScan spectra were fitted into a theoretical curve allowing the determination of peptide concentration (in units of area) and labeling efficiency. Spectra with $f > 1.5$, $\sigma > 0.15$ and a $\beta > 0.15$, the best fit values to the adjustment of the curve, were considered unreliable and eliminated.

As mentioned earlier, partially digested peptides do not accurately reflect the protein concentration in the samples. On the other hand, oxidized methionines, which occur spontaneously during sample treatment, lead to an incorrect quantification of peptides since the proportion of oxidized and non-oxidized methionines in the labeled sample and non labeled sample may be different. Taken these into account, scans corresponding to peptides with one or more missed cleavages and oxidized methionine were also considered unreliable and eliminated. Scans corresponding to peptides of the C-terminus were also discarded as they are not tryptic peptides and hence do not incorporate ^{18}O during the enzymatic labeling reaction (Jorge *et al.* 2009).

In order to obtain a good quantification, a good labeling efficiency is necessary, so all steps in digestion and labeling were well controlled in order to achieve a good labeling efficiency. For these experiments, labeling efficiency was around 80% (figure V.4.5.). The distribution of ratio values ($^{16}O/^{18}O$) was analyzed using a base 2

logarithmic scale which is expected to produce a symmetric distribution tightly centered on zero.

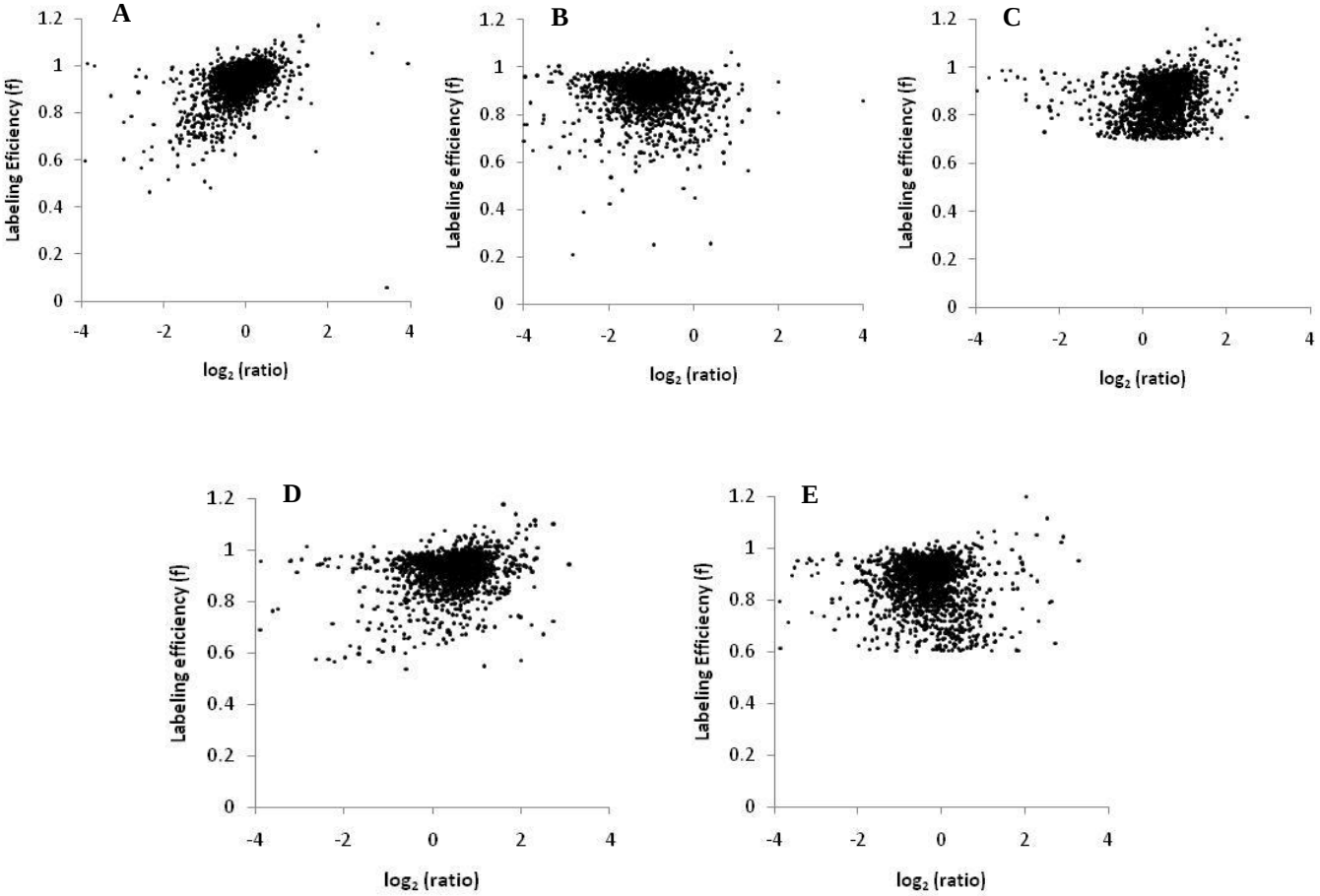

Figure V.4.5.: Distribution of labeling efficiencies as function of log2 ratios. A, B, C, D and E represent labeling efficiencies as function of log2 ratios for experiments 1, 2, 3, 4 and 5, respectively.

Several errors in quantification result from sample handling. One of those errors occurs due to the variability of the sample concentration. In figure 5B, regarding experiment 2, that kind of error is evident when analyzing the distribution of $\log_2(^{16}O/^{18}O)$ which deviates towards the left side meaning that the concentration of B is larger than the concentration of A. That kind of error is corrected by calculating the grand mean as described in materials and methods.

After eliminating unreliable data, variances at the scan level, peptide level and protein level were determined and used to calculate protein averages and the grand mean allowing the determination of outliers at scan, peptide and protein levels.

If a population of scans has the same statistical weight it behaves as a normal distribution. Outliers are values that deviate from that normal distribution. The presence

of outliers at the scan level was determined by looking for the presence of scans which have a deviation higher than the expected from the peptide average. The probability that a scan deviates from the peptide average was calculated allowing the determination of the corresponding false discovery rate at the scan level (FDRs). For FDRs lower than 5%, a more detailed inspection of the scans was made. For each experiment, at a scan level, no more than 4 outliers were found (figure V.4.6.):

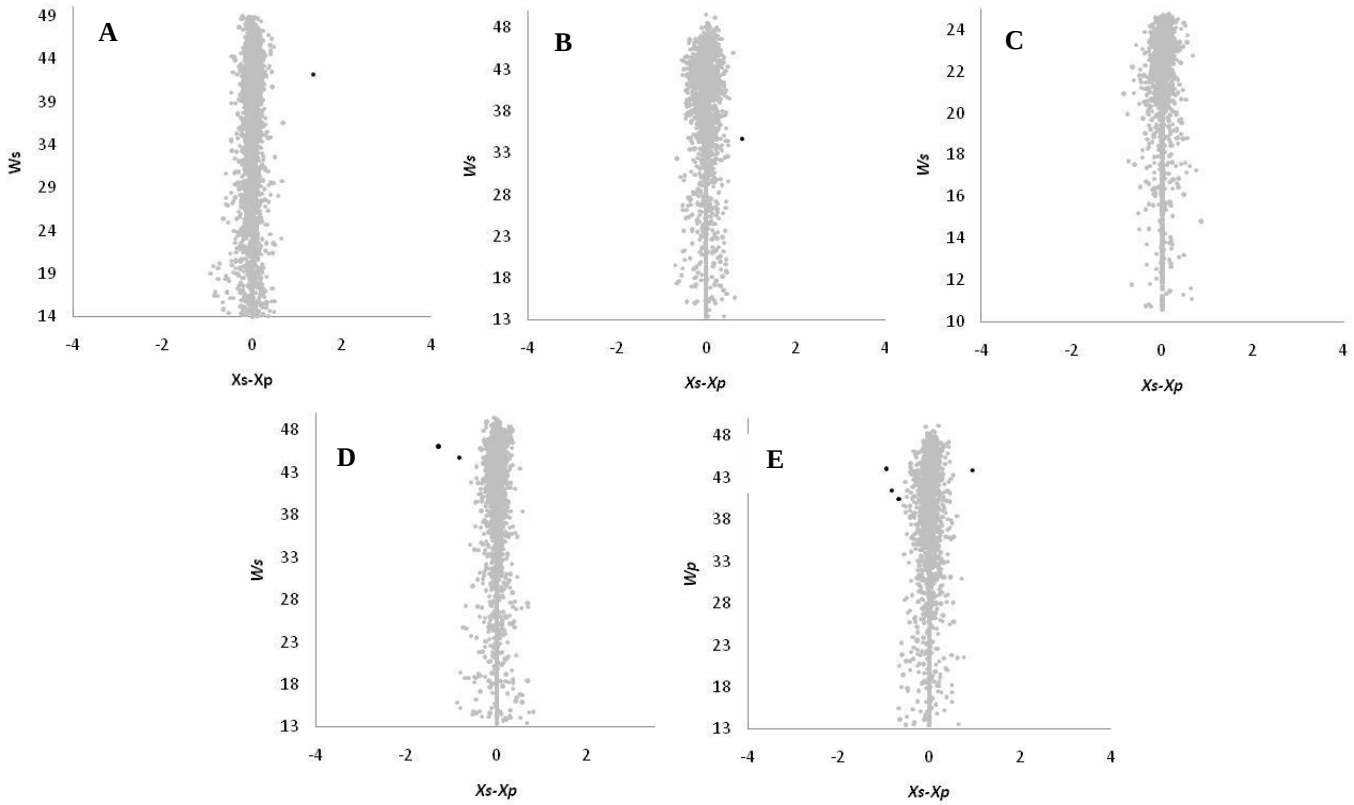

Figure V.4.6.: Outliers at the scan level. Dark points represent outliers at the scan level for an FDRs<5% and for experiments 1 (A), 2 (B), 3 (C), 4(D) and 5 (E).

The low number of outliers indicates that most scans that quantify for one peptide show the expected deviation towards the peptide average, meaning that most scans behave as part of a normal distribution with homogeneous and constant variances and thus may be used to perform a valid statistical analysis.

A similar analysis to determine peptide quantifications that significantly deviate from the corresponding protein averages – outliers at the peptide level – was also performed. The false discovery rate at the peptide level (FDRp) was determined and peptides with FDRp lower than 5% were subjected to a more detailed inspection. In experiment 1 (figure V.4.7.A) two outliers at the peptide level were detected, however

in all other experiments the number of outliers at the peptide level was significantly larger although not larger enough when comparing with the total number of quantified peptides (figure V.4.7.).

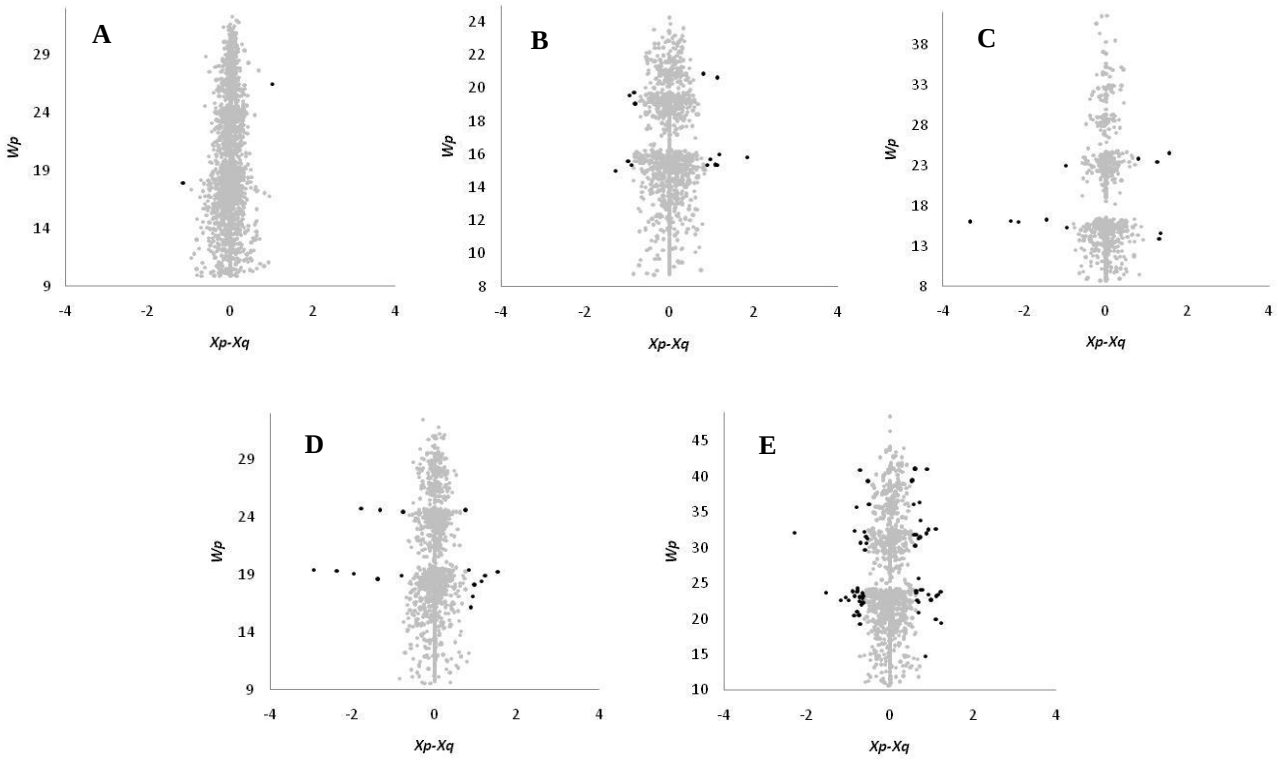

Figure V.4.7.: Outliers at the peptide level. Dark points represent outliers at the peptide level for an FDRp<5% for experiments 1 (A), 2 (B), 3 (C), 4(D) and 5 (E).

From a statistically point of view, an outlier at the protein level is a significant expression change. Outliers at the protein level are thus determined in the same way that outliers at the peptide and scan level were. False discovery rates at the protein level were determined and all proteins with an FDRq lower than 1 % were considered as differentially expressed (figure V.4.8.):

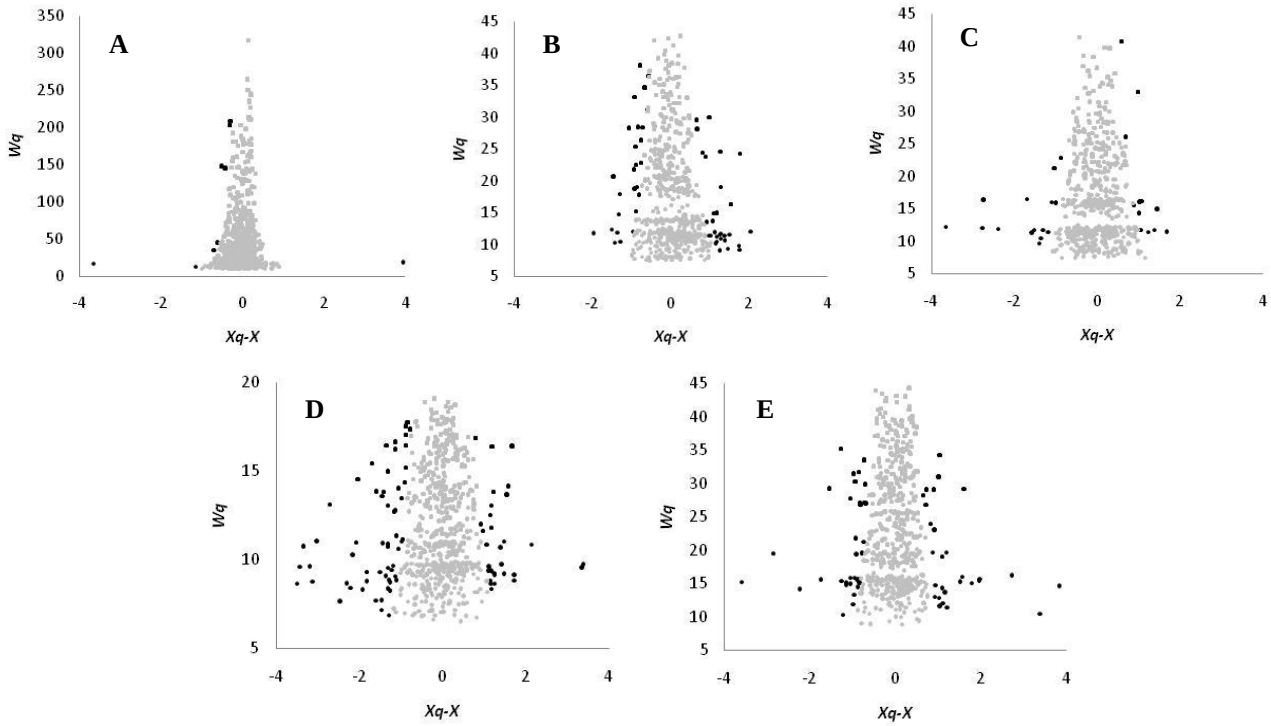

Figure V.4.8.: Differentially expressed proteins. Dark points represent outliers at the protein level (FDRq<1%) for experiments 1 (A), 2 (B), 3 (C), 4(D) and 5 (E) and correpond to significant expression changes.

As expected in experiment 1, the number of differentially expressed proteins was very low (7 outliers at the protein level). As for the remaining experiments the number of differentially expressed proteins was higher in experiments 4 and 5 than the number of differentially expressed proteins in experiments 2 and 3, also as expected, since experiments 2 and 3 functioned as controls for experiments 4 and 5 (see figure V.4.11. for values).

In order to give more consistency to the results, log2 ratios at the protein level (Xq) were converted to standard normal values (Zq), and plotted against each other. Zq values from experiments 2 and 3 were plotted against Zq values from experiments 4 and 5, respectively. As seen in figure IV.4.9., it seems to exist a correlation between samples 2 and 4 and 3 and 5.

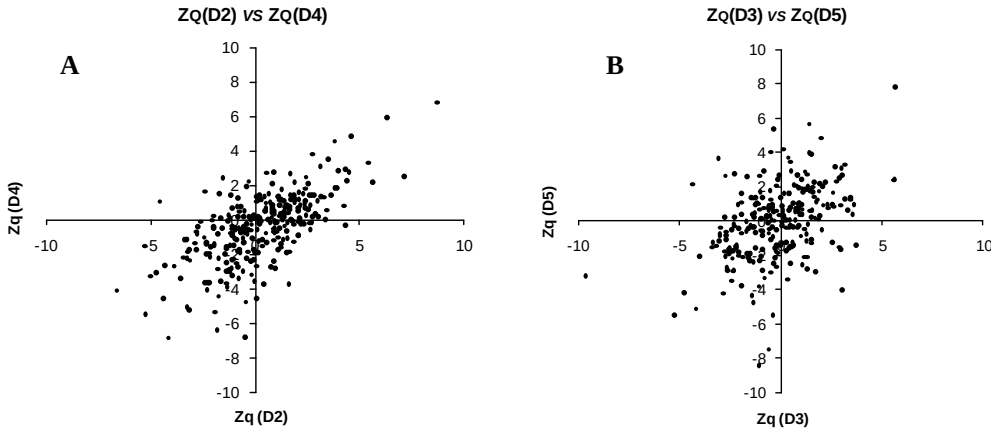

Figure V.4.9.: Correlation between assays 2 and 4 and 3 and 5. By plotting Zq values from assays 2 and 4 and 3 and 5 against each other a correlation between them exists showing the consistency of the results.

After statistical analysis the number of quantified scans, peptides and proteins was as follows:

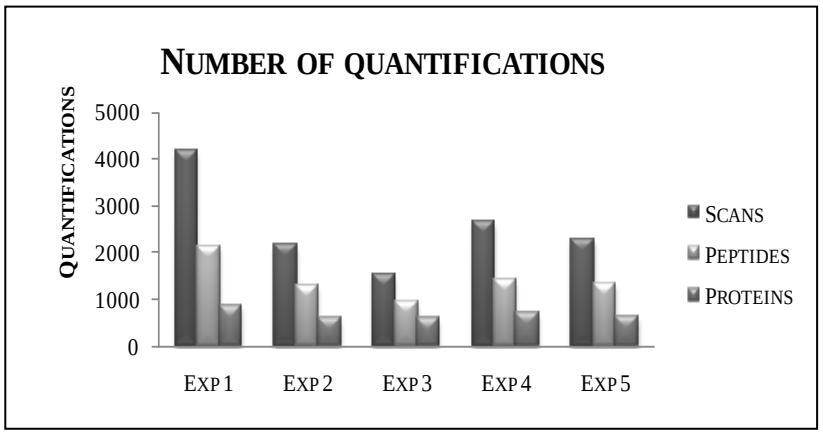

Figure V.4.10: Quantifications at the scan, peptide and protein levels.

Quantifications at a peptide or protein levels, are more reliable when they are calculated from two or more quantifications from scans or peptides, respectively. This means that the quantification of a protein using two or more peptides is more reliable than the quantification of a protein using only one peptide as well as the quantification of a peptide using two or more scans is more reliable than the quantification of a peptide using only one scan. However, that does not mean that proteins quantified with only one peptide and peptides quantified with only one scan are not reliable. Accuracy of quantification is measured by its associated variance. This variance depends on the number of peptides used to measure it and on the accuracy of each measure. So one

protein quantified by two peptide measurements with low accuracy may have a higher variance than one protein quantified by only one peptide with high accuracy. As described before proteins with FDRq <1% were considered differentially expressed. For FDRq <1%, only proteins quantified with more than one peptide and more than one scan were taken into account. For FDRq <0.1% proteins quantified with one peptide and one scan were also considered reliable (see Supplementary Information for differentially expressed proteins and statistical quantification parameters for all experiments). Figure V.4.11. shows the number of differentially expressed proteins per experiment.

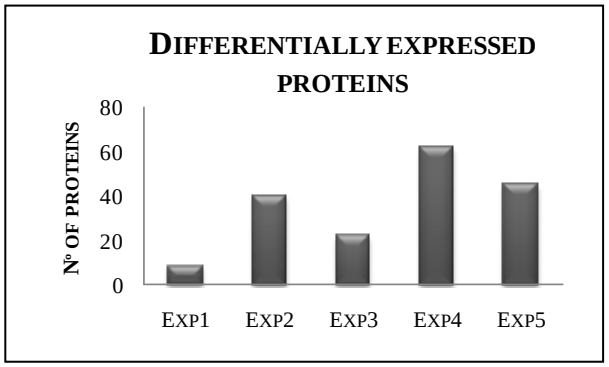

Figure V.4.11.: Differentially expressed proteins per experiment.

As described previously, experiments 1, 2 and 3 were used as controls for experiments 4 and 5, helping to discard all differential expression changes resulting from the presence of tetracycline, transfections and basal levels of SHDAg and HDV RNA. When discarding those false positives significant expression changes in cells expressing the delta antigen (experiment 4) and in cells replicating HDV (experiment 5) were as follows (table V.4.1.).

	PROTEIN NAME	GENE SYMBOL[a]	ACCESSION NUMBER	FOLD	FDRQ (%)[b]
Experiment 4	Cofilin-1	CFL1	P23528	51.1	0.00
	Dermcidin	DCD	P81605	43.9	0.00
	Obg-like ATPase 1	OLA1	Q9NTK5	24.5	0.00
	RNA-binding protein 8A	RBM8A	Q9Y5S9	10.2	0.00
	G-rich sequence factor 1	GRSF1	Q12849	10.8	0.00
	Eukaryotic translation initiation factor 3 subunit D	EIF3D	O15371	11.2	0.00
	Hornerin	HRNR	Q86YZ3	9.1	0.00
	ADP-ribosylation factor 1	ARF1	P84077	6.5	0.00
	Ras-related protein Rab-6A	RAB6	P20340	8.7	0.00

	Glucosidase 2 subunit beta	PRKCSH	P14314	-10.5	0.00
	Protein FAM136A	FAM136A	Q96C01	-37.7	0.00
	ATP synthase subunit e, mitochondrial	ATP5I	P56385	-4.4	0.00
	Signal recognition particle 19 kDa protein	SRP19	P09132	4.5	0.00
	DNA-binding protein A	CSDA	P16989	4.9	0.00
	Transcription intermediary factor 1-beta	TIF1β/TRIM28	Q13263	5.5	0.00
	Protein S100-A9	S100A9	P06702	4.6	0.00
	10 kDa heat shock protein, mitochondrial	HSPE1	P61604	-2.9	0.00
	Cytosolic non-specific dipeptidase	CNDP2	Q96KP4	3.8	0.00
	Leucyl-tRNA synthetase, cytoplasmic	LARS	Q9P2J5	3.5	0.00
	26S proteasome non-ATPase regulatory subunit 11	PSMD11	O00231	3.6	0.00
	Elongation factor 1-gamma	EEF1G	P26641	2.7	0.00
	Junction plakoglobin	JUP	P14923	-3.3	0.00
	L-lactate dehydrogenase A chain	LDHA	P00338	2.7	0.00
	Tight junction protein Z	TJP1	Q07157	-3.3	0.00
	Elongation factor 2	EEF2	P13639	2.5	0.00
	Oligosaccharyltransferase complex subunit OSTC	OSTC	Q9NRP0	-2.8	0.00
	Heterogeneous nuclear ribonucleoprotein D-like	HNRPDL	O14979	2.4	0.00
	Peptidyl-prolyl cis-trans isomerase A	PPIA	P62937	2.7	0.00
	Heat shock 70 kDa protein 4	HSPA4	P34932	2.5	0.00
	C-1-tetrahydrofolate synthase, cytoplasmic	MTHFD1	P11586	2.8	0.01
	L-lactate dehydrogenase B chain	LDHB	P07195	2.2	0.01
	Up-regulated during skeletal muscle growth protein 5	USMG5	Q96IX5	-2.6	0.01
	GPI-anchor transamidase	PIGK	Q92643	-2.8	0.01
	Squalene synthetase	FDFT1	P37268	-2.7	0.01
	Putative nucleoside diphosphate kinase	NME2P1	O60361	3.0	0.01
	Rab GDP dissociation inhibitor beta	GDI2	P50395	2.5	0.02
	Delta(3,5)-Delta(2,4)-dienoyl-CoA isomerase, mitochondrial	ECH1	Q13011	-2.3	0.03
	2-oxoglutarate dehydrogenase E1 component, mitochondrial	OGDH	Q02218	2.5	0.03
	Triosephosphate isomerase	TPI1	P60174	2.2	0.05
	Fascin	FSCN1	Q16658	2.8	0.06
	DNA-dependent protein kinase catalytic subunit	PRKDC	P78527	-2.2	0.06

	T-complex protein 1 subunit gamma	CCT3	P49368	2.2	0.07
	40S ribosomal protein S7	RPS7	P62081	2.5	0.07
	Cellular tumor antigen p53	TP53/P53	P04637	-2.3	0.07
	Heat shock protein HSP 90-alpha	HSP90AA	P07900	2.1	0.08
	Alpha-enolase	ENO1	P06733	1.8	0.26
	Ubiquitin-like modifier-activating enzyme 1	UBA1	P22314	1.8	0.35
	Splicing factor U2AF 65 kDa subunit	U2AF2	P26368	1.8	0.55
	Creatine kinase B-type	CKB	P12277	1.7	0.93
Experiment 5	2',3'-cyclic-nucleotide 3'-phosphodiesterase	CNP	P09543	-10.5	0.00
	Protein disulfide-isomerase A4	PDIA4	P13667	12.0	0.00
	ADP-ribosylation factor 1	ARF1	P84077	2.9	0.00
	60S ribosomal protein L6	RPL6	Q02878	-3.0	0.00
	BRI3-binding protein	BRI3BP	Q8WY22	33.7	0.00
	Transportin-1	TNPO1	Q92973	7.2	0.00
	Protein FAM136A	FAM136A	Q96C01	-14.3	0.00
	Nascent polypeptide-associated complex subunit alpha-2	NACA2	Q9H009	-6.6	0.00
	RNA-binding protein 8A	RBM8A	Q9Y5S9	4.7	0.00
	DNA-(apurinic or apyrimidinic site) lyase	APEX1	P27695	-3.9	0.00
	Alpha-actinin-4	ACTN4	O43707	2.4	0.00
	DNA topoisomerase 2-beta	TOP2B	Q02880	-3.5	0.00
	Cystatin-A	CSTA	P01040	3.3	0.00
	Erlin-1	ERLIN1	O75477	-3.0	0.00
	Neutral alpha-glucosidase AB	GANAB	Q14697	-2.1	0.00
	U4/U6.U5 tri-snRNP-associated protein 2	USP39	Q53GS9	-2.9	0.00
	ELAV-like protein 1	ELAVL1	Q15717	-2.0	0.00
	Alpha-actinin-1	ACTN1	P12814	2.0	0.00
	Peripherin	PRPH	P41219	-2.3	0.00
	Glutathione S-transferase omega-1	GSTO1	P78417	2.4	0.00
	Transcription intermediary factor 1-beta	TIF1β/TRIM28	Q13263	-1.9	0.00
	60S ribosomal protein L7	RPL7	P18124	-2.2	0.00
	60S ribosomal protein L7a	RPL7A	P62424	-2.2	0.00
	Peroxiredoxin-4	PRDX4	Q13162	1.8	0.00
	60S ribosomal protein L36	RPL36	Q9Y3U8	2.2	0.02
	Small nuclear ribonucleoprotein Sm D2	SNRPD2	P62316	2.2	0.02
	Basigin	BSG	P35613	-1.8	0.02
	60S ribosomal protein L22	RPL22	P35268	1.9	0.03

	Polypeptide N-acetylgalactosaminyltransferase 2	GALNT2	Q10471	-2.2	0.03
	Protein cornichon homolog 4	CNIH4	Q9P003	2.1	0.04
	Peroxiredoxin-1	PRDX1	Q06830	1.8	0.04
	Ubiquilin-1	UBQLN1	Q9UMX0	-2.2	0.05
	Alpha-adducin	ADD1	P35611	-2.3	0.07
	Cytochrome c oxidase subunit 4 isoform 1, mitochondrial	COX4I1	P13073	2.1	0.07
	Putative heat shock protein HSP 90-alpha A5	-	Q58FG0	1.9	0.08
	60S ribosomal protein L12	RPL12	P30050	-1.8	0.09
	L-lactate dehydrogenase A chain	LDHA	P00338	-1.7	0.10
	Ribosomal L1 domain-containing protein 1	RSL1D1	O76021	-1.6	0.27
	DNA topoisomerase 2-alpha	TOP2A	P11388	1.6	0.37

Table V.4.1: Differentially expressed proteins in the presence of the delta antigen (experiment 4) and during HDV replication (experiment 5). See Supplementary Information for differentially expressed proteins and statistical quantification parameters for all experiments.

a. gene symbol according to IPA.

b. False discovery rate at the protein level.

For experiment 4, from a total of 49 proteins differentially expressed, 36 proteins were up regulated while 13 were down regulated. As for experiment 5, from a total of 39 proteins differentially expressed, 18 proteins were up regulated and 21 proteins were down regulated (figure V.4.12.). Proteins RNA-binding protein 8A (RBM8A - Q9Y5S9), ADP-ribosylation factor 1 (ARF1 - P84077), Protein FAM136A (Q96C01), Transcription intermediary factor 1-beta (TIF1B - Q13263) and L-lactate dehydrogenase A chain (LDHA - P00338) were found to be differentially expressed in both experiments. Proteins ARF1, FAM136A and RBM8A were found to be up regulated in both experiments whereas proteins TIF1B and LDHA were found to be up-regulated in the presence of the delta antigen, experimenting down regulation during HDV replication. Of notice is the fact that protein LDHA is approximately 2x up-regulated in the presence of the delta antigen and approximately 2x down regulated during HDV genomic RNA accumulation. On the other hand, protein TIF1B is approximately 5x up-regulated in the presence of the delta antigen and approximately 2x down-regulated during HDV genomic RNA accumulation meaning that although there is a down-regulation during HDV genomic RNA accumulation this protein still finds itself up-regulated during HDV replication.

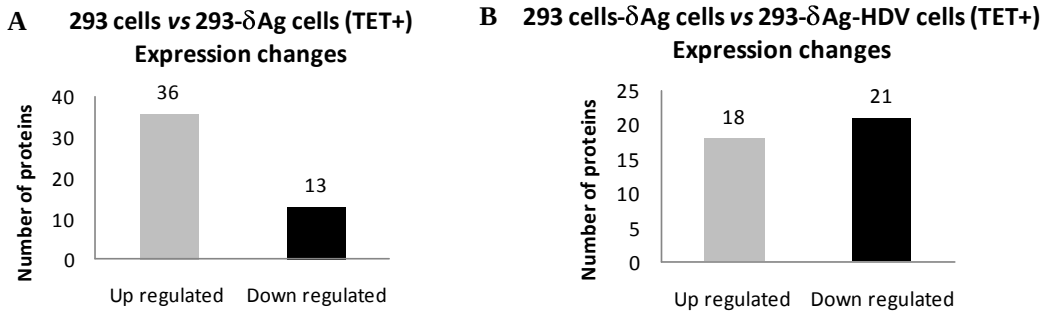

Figure V.4.12.: Significant expression changes. A shows the number of differentially expressed proteins in cells expressing the small delta antigen and B shows the number of differentially expressed proteins during HDV replication.

Proteins were then arranged by their biological function with the help of expasy (www.expasy.org) showing, for both experiments 4 and 5, that differentially expressed proteins are mainly involved in protein metabolism (experiments 4) and energy pathways (experiment 5; figure V.4.13.).

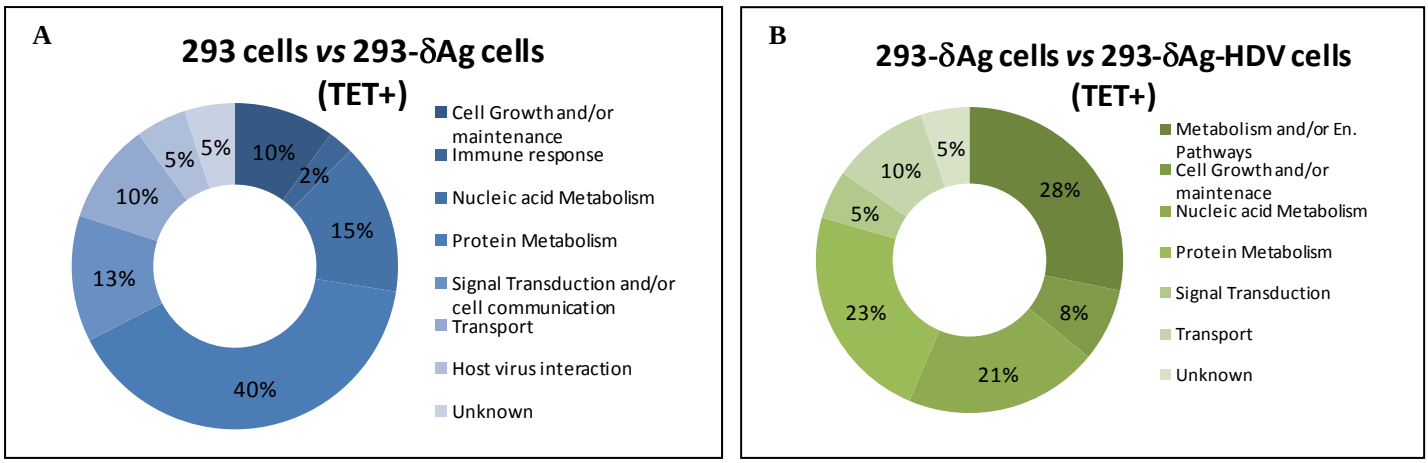

Figure V.4.13: Biological function of differentially expressed proteins. A shows the biological function of differentially expressed proteins in cells expressing the small delta antigen and B shows the biological function of differentially expressed proteins during HDV replication.

V.4.3. VALIDATION OF PROTEOMICS RESULTS

Relative quantification by western blot analysis was performed to validate results obtained by mass spectrometry. After determining differentially expressed proteins and using systems biology as an aiding tool to interpret data, three differentially expressed proteins of interest – Cellular tumor antigen p53, transportin-1 (or

karyopherin β2, or TNPO1) and ELAV-like protein 1 (ELAVL1 or HuR) – were chosen to validate proteomics results.

These proteins were chosen due to its possible relevance with HDV replication and pathogenesis. p53 is a tumor suppressor protein that regulates cell cycle and the expression of several proteins involved in many pathways like apoptosis, hypoxic stress and uncontrolled cell death. This protein may thus be relevant in HDV life cycle. TNPO1 is a nuclear transport receptor involved in nuclear protein import serving as a receptor for nuclear localization signals (NLS) in cargo substrates. Because both delta antigens have NLSs, TNPO1 may interact with both proteins. Finally, ELAVL1, besides interacting with TNPO1, which imports it to the nucleus, is also involved in c-myc stabilization. ELAVL1 may be relevant for HDV replication by interacting with the delta antigens or by inducing apoptosis and/or cell cycle deregulation.

For each protein an SDS-PAGE was loaded with 10 μg of total protein extracts from each sample (293, 293-dAg and 293-HDV in absence and presence of tetracycline) and after electrophoresis, proteins were electroblotted into a nitrocellulose membrane and incubated both with the specific primary antibody to detect the protein of interest and the primary antibody against clathrin, which acted as housekeeping to perform relative quantification. Using ImageJ, the areas of the bands corresponding to the gene of interest and clathrin were determined and results were normalized by dividing the area of the band of the gene of interest by the area of the band corresponding to clathrin allowing a relative quantification of the protein of interest in samples.

p53

Using ^{18}O-based quantitative proteomics, p53 (P04637) was found to be down regulated 2.25x in cells expressing the delta antigen (experiment 4). In experiment 5, in cells replicating HDV, no alteration in the expression of this protein was found. Because in experiment 5 a comparison between 293-δAg cells and 293-δAg-HDV is made and p53 was already down regulated in 293-δAg cells it was assumed that p53 was also down regulated in cells replicating HDV. These results were confirmed by western blot analysis, which showed a decrease in the expression of p53 of 70% in cells expressing the delta antigen and a decrease in 80% in cells replicating HDV RNA (figure V.4.14). Interestingly, in the absence of tetracycline results followed the same pattern although down-regulation of p53 in that case was not so high.

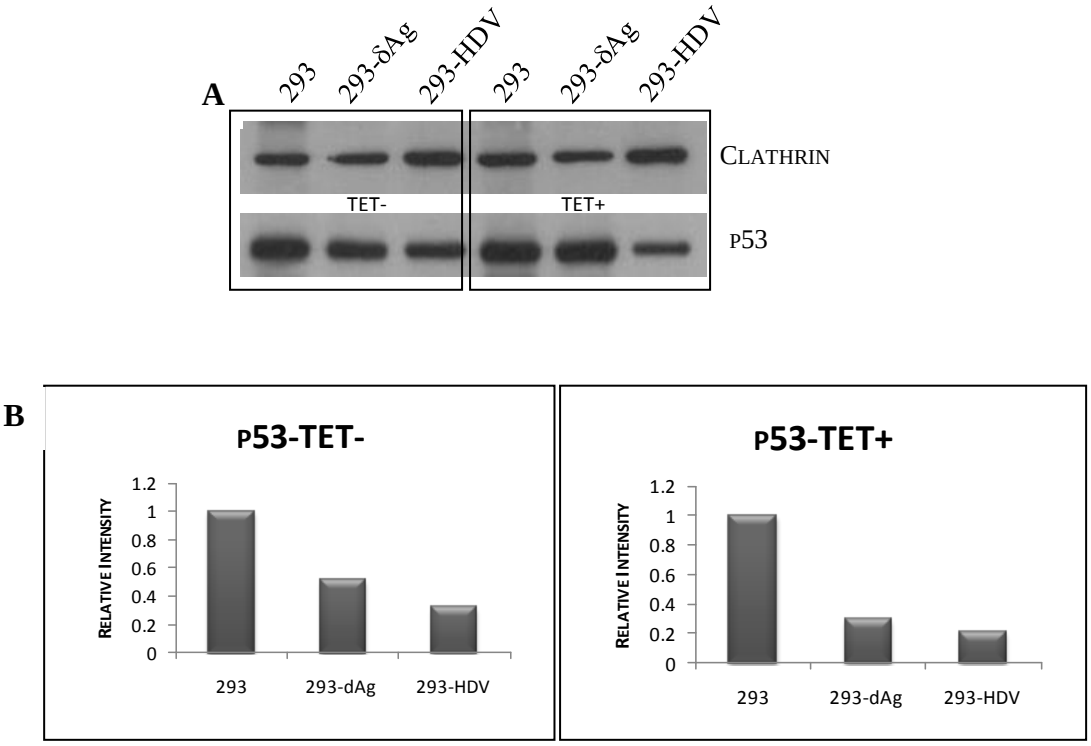

Figure V.4.14.: Western blot analysis of p53 and clathrin. 10 μg/lane of total protein extracts were loaded into a 12% SDS-PAGE and after electrophoresis, electroblotted into a nitrocellulose membrane. Membrane was incubated with both mouse monoclonal antibody against p53 (1:2500) and rabbit polyclonal antibody against Clathrin HC (1:1000) (A). Images were analyzed using ImageJ and relative quantification was performed by normalizing results obtained for p53 with the results obtained for clathrin (B).

Transportin-1

Using ^{18}O-based quantitative proteomics, Transportin-1 (Q92973) was found to be up-regulated 7.19x in cells replicating HDV (293-HDV cells in the presence of tetracycline) when comparing with cells expressing only the delta antigen (293-δAg) (experiment 5). Results were confirmed by western blot analysis showing an increase of approximately 80% of the expression of transportin-1 in cells replicating HDV (figure V.4.15.). In the absence of tetracycline results followed the same pattern although the increase of transportin-1 was lower in the absence of tetracycline.

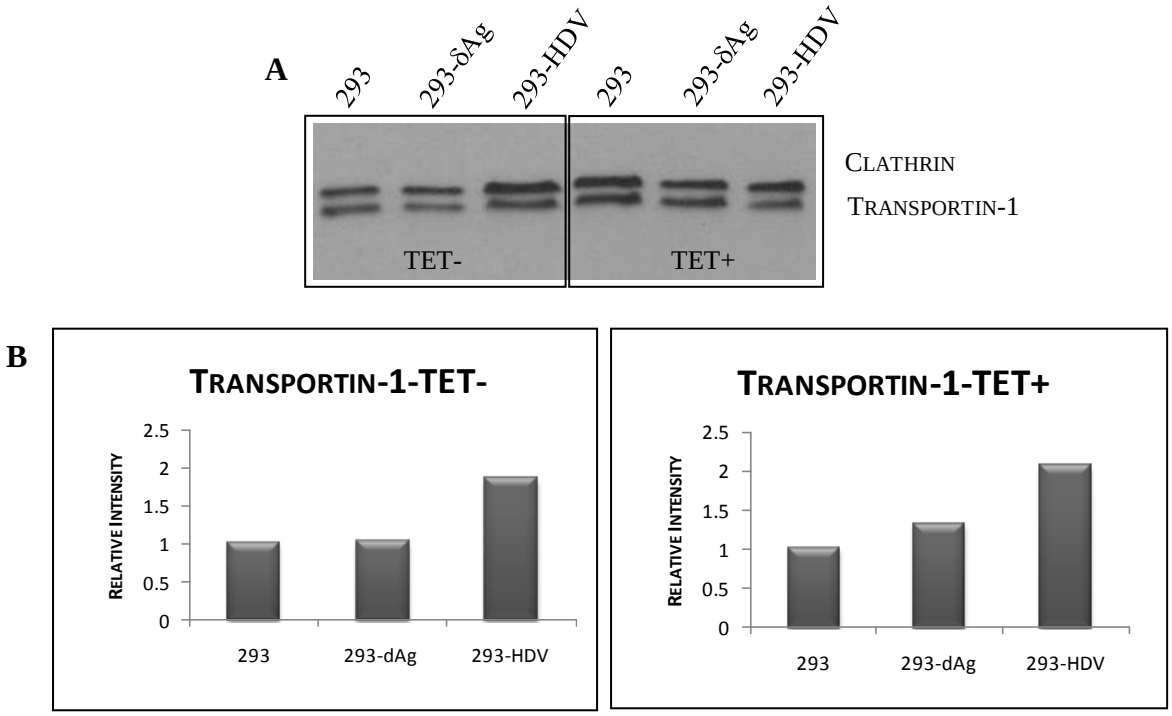

Figure V.4.15: Western blot analysis of transportin-1 and clathrin. 10 μg/lane of total protein extracts were loaded into a 12% SDS-PAGE and after electrophoresis, electroblotted into a nitrocellulose membrane. Membrane was incubated with both mouse monoclonal antibody against transportin-1 (1:2500) and rabbit polyclonal antibody against Clathrin HC (1:1000) (A). Images were analyzed using ImageJ and relative quantification was performed by normalizing results obtained for transportin-1 with the results obtained for clathrin (B).

ELAV-like protein 1

Using ^{18}O-based quantitative proteomics, ELAV-like protein 1 (Q15717) was found to be down-regulated 2 times in cells replicating HDV (293-HDV cells in the presence of tetracycline) when comparing with cells expressing only the delta antigen (293-δAg) (experiment 5). Results were confirmed by western blot analysis showing a decrease of approximately 80% of the expression of ELAV-like protein 1 in cells replicating HDV (figure V.4.16.). In the absence of tetracycline, ELAV-like protein 1 was also found down regulated but at a minor extent.

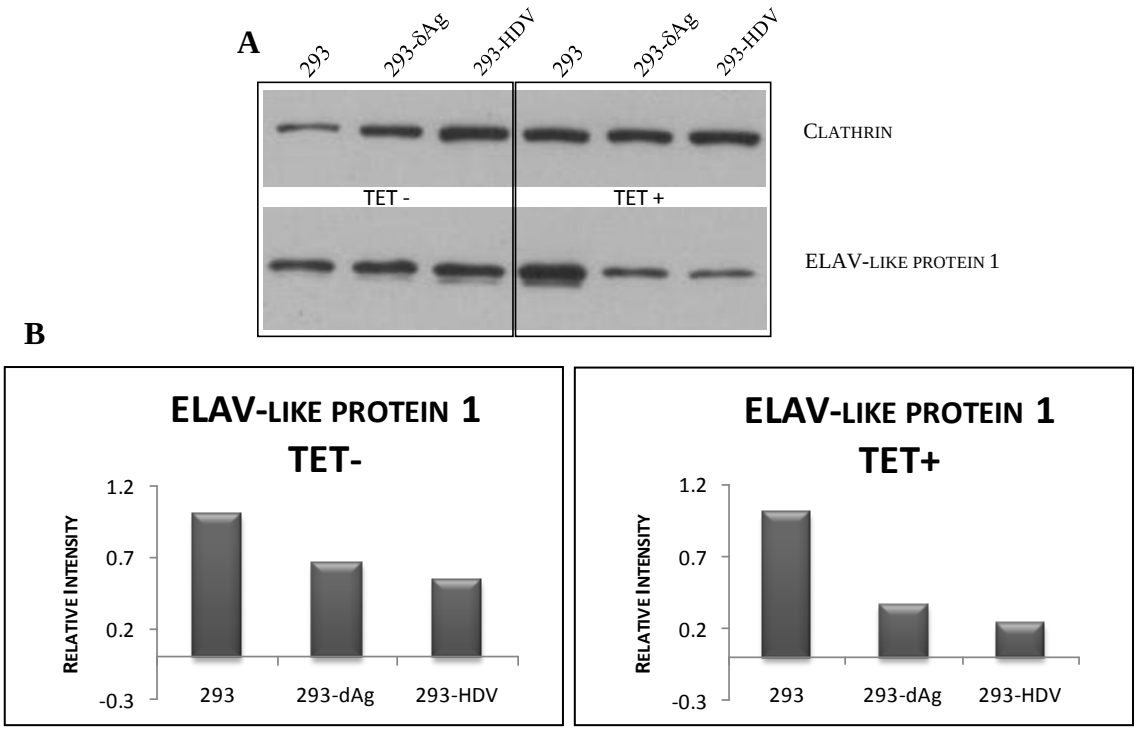

Figure V.4.16: Western blot analysis of ELAV-like protein 1 and clathrin. 10 µg/lane of total protein extracts were loaded into a 12% SDS-PAGE and after electrophoresis, electroblotted into a nitrocellulose membrane. Membrane was incubated with both mouse monoclonal antibody against ELAV-like protein 1 (1:1000) and rabbit polyclonal antibody against Clathrin HC (1:1000) (A). Images were analyzed using ImageJ and relative quantification was performed by normalizing results obtained for ELAV-like protein 1 with the results obtained for clathrin (B).

V.4.4. SYSTEMS BIOLOGY

High throughput identification generates a huge amount of data that becomes very difficult to interpret without the help of bioinformatic tools. In this work, although differentially expressed proteins were approximately 5% of identified proteins, about 60% (3000 proteins) were quantified. Statistically speaking, these proteins are not differentially expressed however they cannot be discarded since they may follow a tendency leading to some important results.

GOTM – GO Tree Machine, now called Gene Set Analysis Toolkit V2 (http://bioinfo.vanderbilt.edu/webgestalt) and Ingenuity Pathway Analysis (IPA) (Ingenuity® Systems, www.ingenuity.com) were used to facilitate data organization and thus interpretation.

With GOTM, an attempt was made to withdraw some more information of all these results. GOTM is a gene ontology enrichment online tool which allows the

comparison of a user-uploaded protein list with all Gene Ontology (GO) categories (reference list) to identify those with enriched number of user-uploaded proteins (target list). In other words, a target list containing proteins of interest will be compared with a reference list. If the number of proteins for one specific category in the target list is higher than the number of proteins for the same category in the reference list, than that category is said to be enriched.

As a reference list, a list with all quantified proteins from each experiment was used. As for the target list, quantified proteins of each experiment were first divided by Zq in up regulated (Zq<0) and down regulated (Zq>0) and then each group was divided by cutting by FDRq from 10% to 100%. For each experiment 12 target lists were obtained and compared with all quantified proteins of that experiment (reference list). By doing so, an observation was made that by increasing FDRq, and consequently the number of proteins of the target list, the number of enriched categories increases to a certain point, decreasing afterwards. This decrease occurs because at that point the number of proteins of the target list is so close to the number of proteins of the reference list that, statistically, one cannot say that a category is enriched. So the FDRq at which enriched categories reach the highest value is the *optimal* FDRq in which one can say that these enriched categories seem to follow a tendency to up or down regulate (figure V.4.17.).

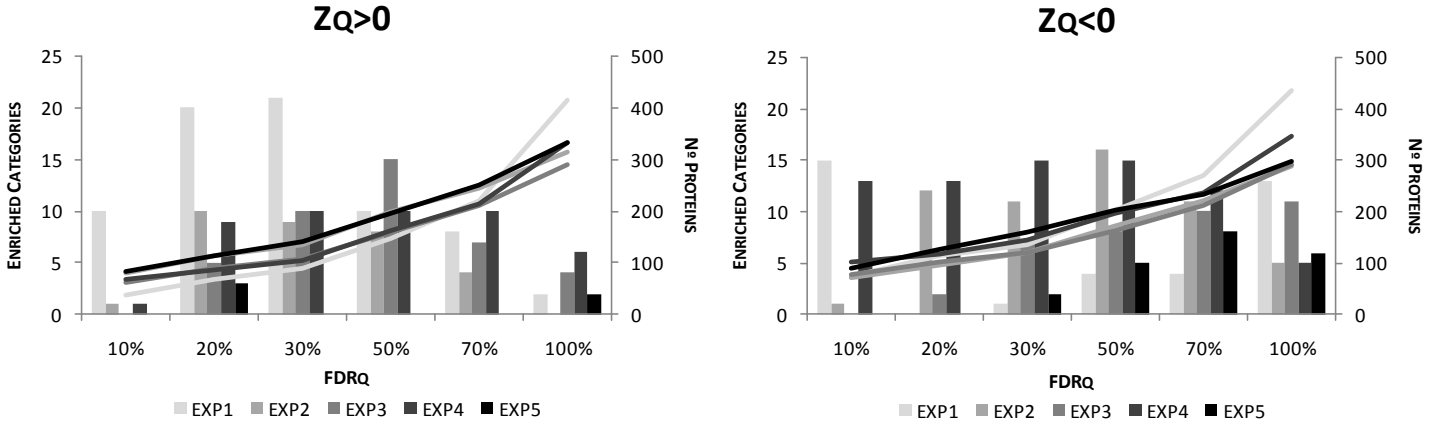

Figure V.4.17.: Variation of the number of enriched categories accordingly to FDRq. By increasing FDRq and consequently the number of proteins in the target list (represented by the lines), the number of enriched categories (represented by bars) increases until a certain FDRq after which it decreases. This FDRq is the *optimal* FDRq in which one can say that enriched categories seem to follow a tendency to up or down regulate.

Because quantified proteins resulting from experiments 1, 2 and 3 are a result of the presence of tetracycline and cell manipulation, only results regarding experiments 4 and 5 were submitted to analysis. For experiments 4 and 5 the *optimal* FDRq is given in table V.4.2 along with the nº of enriched categories and nº of proteins at that FDRq, accordingly to Zq.

EXPERIMENT	ZQ	Nº ENRICHED CATEGORIES	Nº PROTEINS	OPTIMAL FDRQ (%)
4	Positive	10	215	70
4	Negative	15	196	50
5	Positive	3	114	20
5	Negative	8	235	70

Table V.4.2: FDRq at which there is a reliable number of enriched categories that seem to follow a tendency to up (Zq<0) or down (Zq>0) regulate.

Enriched categories are named accordingly to Gene Ontology terms (http://www.geneontology.org/) and divided in 3 main domains: Biological Processes, Molecular Function and Cellular Components. Within each domain several categories exist that originate other categories and in two related enriched categories some proteins will coincide.

Enriched categories for experiments 4 and 5 were as follows:

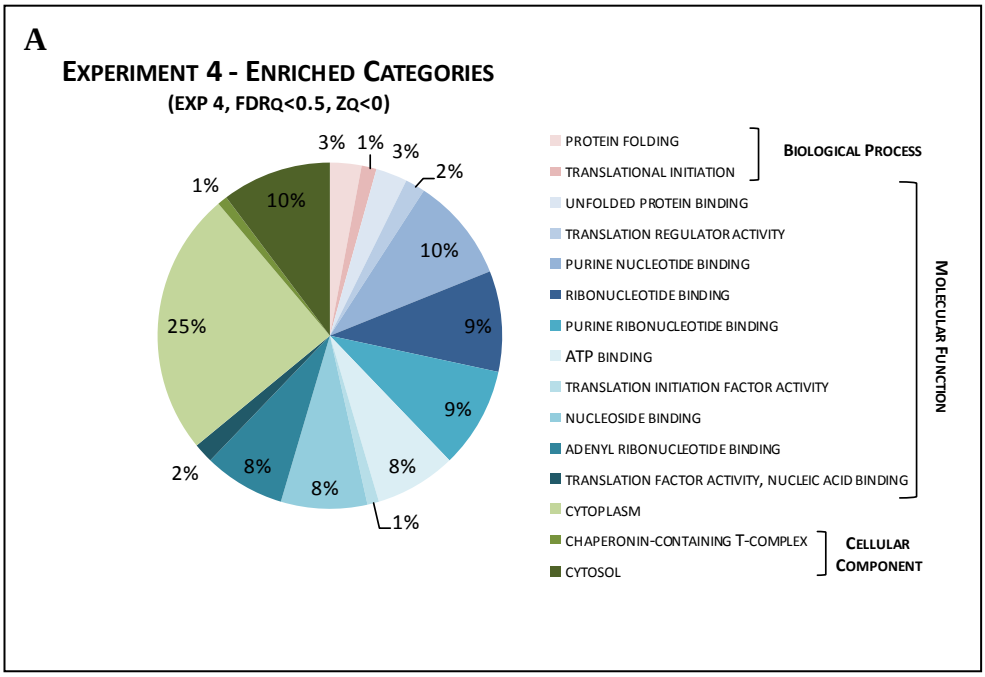

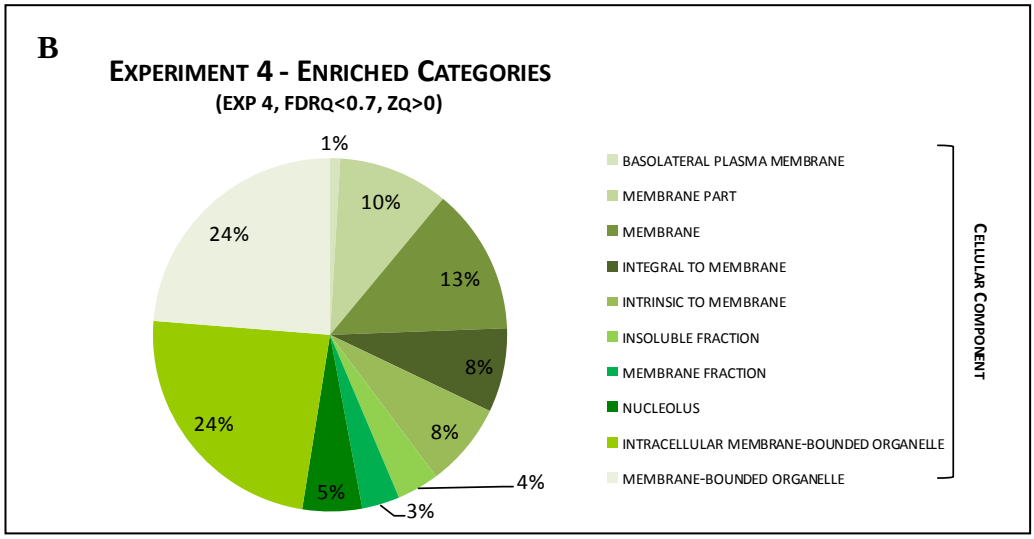

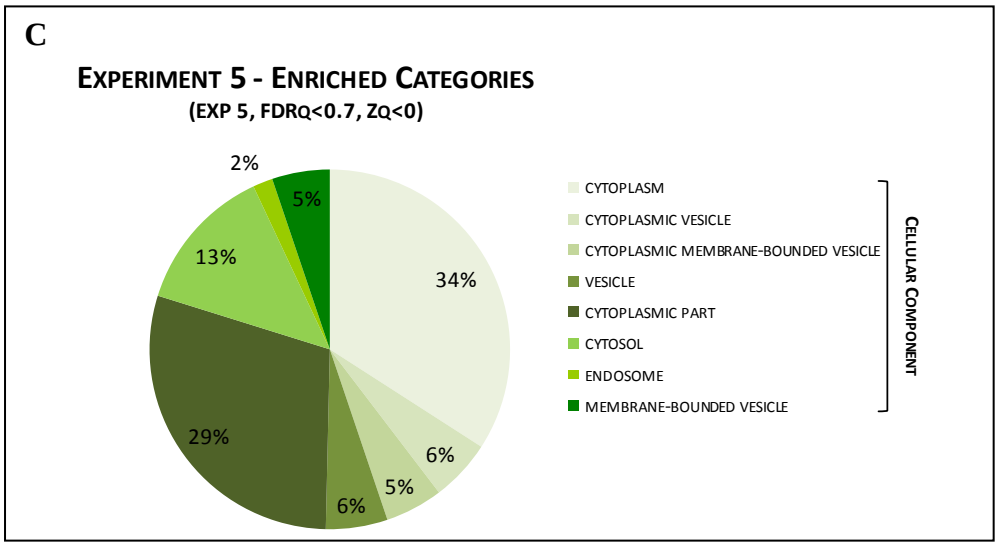

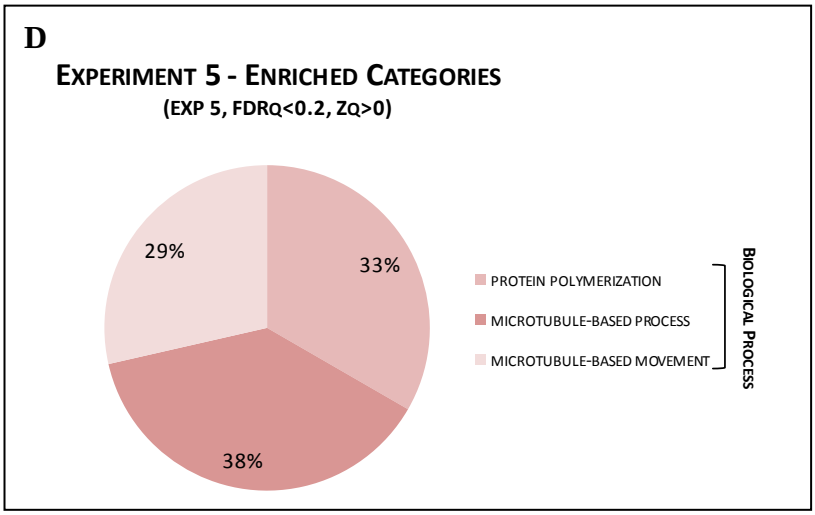

Figure V.4.18.: Enriched categories for experiments 4 (A, B) and 5 (C, D). Using GOTM, enriched categories for experiments 4 and 5 were determined accordingly to Zq and FDRq. In A are represented enriched categories for experiment 4, Zq<0 (up regulation) and an FDRq<50%; in B are represented enriched categories for experiment 4, Zq>0 (down regulation) and an FDRq<70%; in C are represented enriched categories for experiment 5, Zq<0 (up regulation) and an FDRq<70% and finally in D are represented enriched categories for experiment 5, Zq>0 (down regulation) and an FDRq<20%.

For experiment 4 and for proteins which have an increase in its expression (Zq<0) to an FDRq<50%, two categories – *protein folding and translational initiation* – belonging to *Biological Processes* were enriched. Regarding the *Molecular Function*, categories involved in *translational regulator activity and ribonucleotide binding* were also enriched. For proteins which have a decrease in its expression (Zq>0) to an FDRq<70%, enriched categories regarded only *Cellular Components* and one important enriched category was the *nucleolus*. As expected, some of the proteins involved in one enriched category may also be found in other category or in other categories.

For experiment 5, for proteins with a Zq<0 and an FDRq<70% enriched categories were only found in the *Cellular component* domain, with an highlight to *vesicles*. As for proteins with Zq>0 and an FDRq<20%, 3 categories – *Protein Polymerization, Microtubule-based process and Microtubule-based movement* – were enriched.

After an analysis of all the quantified proteins an analysis of the differentially expressed proteins was performed. IPA was used to identify possible signaling pathways involved in HDV replication and pathogenesis and perform network analysis in order to determine the relationship between the differentially expressed proteins obtain in experiments 4 and 5.

By using IPA databases, it was also possible to determine which metabolic and cell signaling pathways were most affected by differentially expressed proteins. For experiment 4, the three most affected canonical pathways were *Glycolysis/Gluconeogenesis*, *HIF1α signaling*, *Propanoate metabolism* and *Protein Ubiquitination Pathway* (figure V.4.19.).

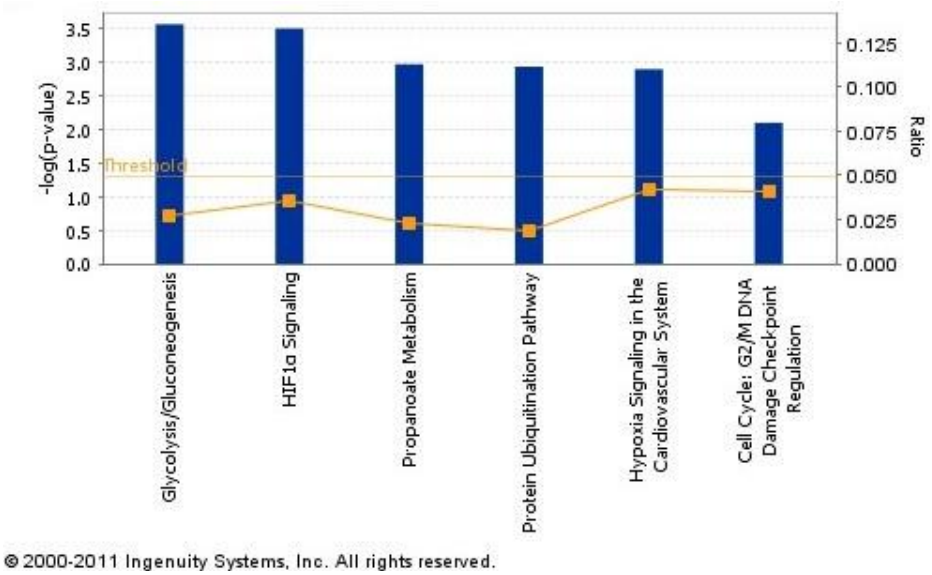

Figure V.4.19.: Significant affected canonical pathways by the expression of the delta antigen (experiment 4). Yellow points represent the ratio, calculated by dividing the number of genes in a giving pathway that follow cut-off criteria, by the total number of genes that make up that pathway. The ratio gives an idea of the percentage of genes in a pathway that were also found in our uploaded list. The yellow line corresponds to the threshold, or cut-off, which corresponds to the p value of 0.05. p values were calculated by IPA using Fisher's exact test.

For each pathway the associated proteins are listed in table V.4.3.

CANONICAL PATHWAY	ACCESS NUMBER	PROTEIN	FOLD
Glycolysis/Glucogenesis	P06733	Alpha-enolase	1.8
	P00338	L-lactate dehydrogenase A chain	2.7
	P07195	L-lactate dehydrogenase B chain	2.2
	P60174	Triosephosphate isomerase	2.2
HIF1α Signaling	P07900	Heat shock protein HSP 90-alpha	2.1
	P00338	L-lactate dehydrogenase A chain	2.7
	P07195	L-lactate dehydrogenase B chain	2.2
	P04637	Cellular tumor antigen p53	-2.3
Propanoate Metabolism	Q13011	Delta(3,5)-Delta(2,4)-dienoyl-CoA isomerase, mitochondrial	-2.5
	P00338	L-lactate dehydrogenase A chain	2.7
	P07195	L-lactate dehydrogenase B chain	2.2
Protein Ubiquitination Pathway	P07900	Heat shock protein HSP 90-alpha	2.1
	P34932	Heat shock 70 kDa protein 4	2.5
	P61604	10 kDa heat shock protein, mitochondrial	-3.0
	O00231	26S proteosome non-ATPase regulatory subunit 11	3.6

	P22314	Ubiquitin-like modifier-activating enzyme 1	1.8

Table V.4.3: Differentially expressed proteins associated to the most significant affected canonical pathways for experiment 4.

For differentially expressed proteins resulting from the expression of the small delta antigen (experiment 4), a network showing the relationship between these proteins was built (figure V.4.20.). Up regulated proteins were colored in green while down regulated proteins were colored in red. The lines represent interactions between proteins.

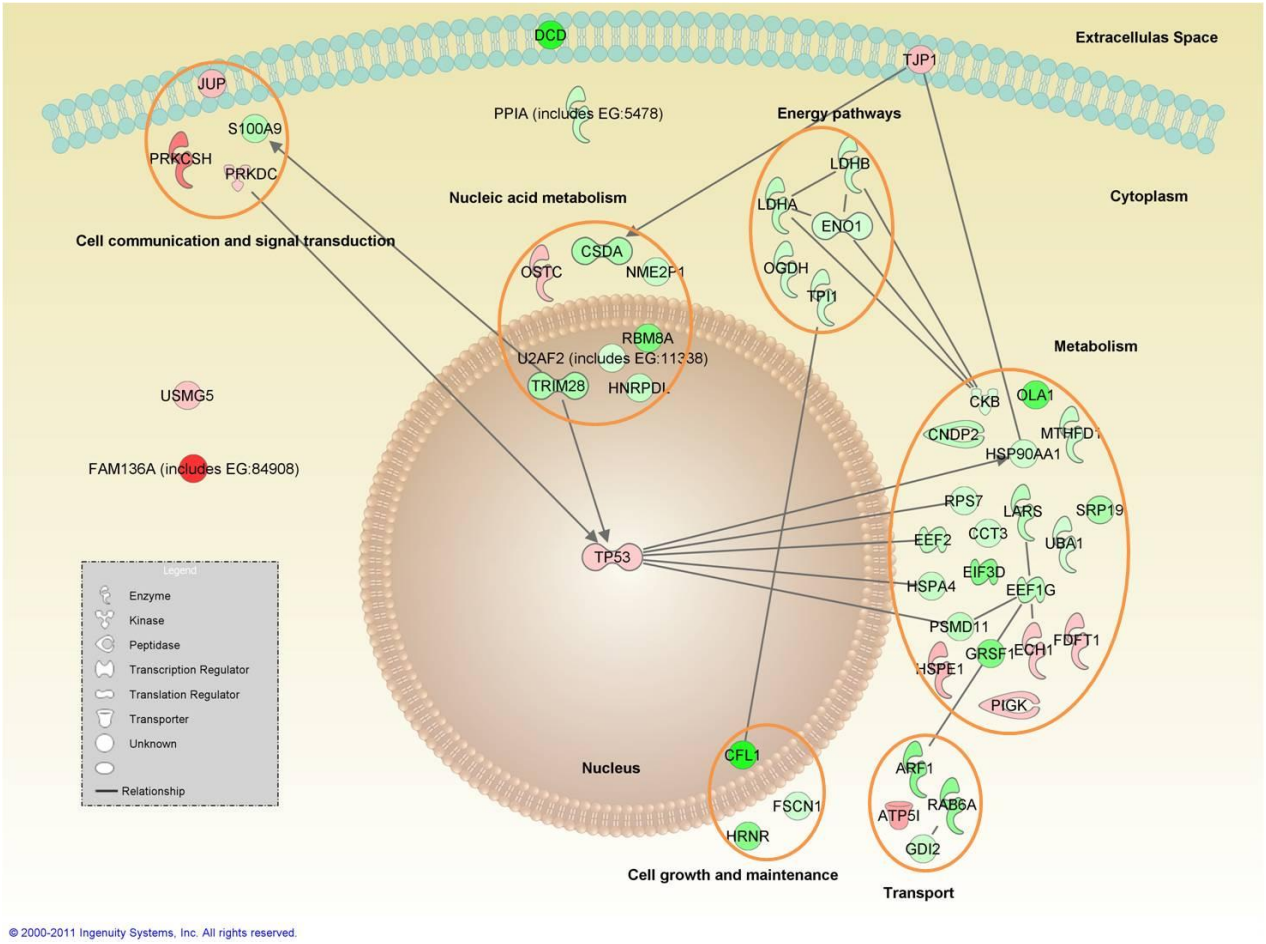

Figure V.4.20.: Interactions among differentially expressed proteins resulting from cells expressing the small delta antigen (experiment 4). Up regulated proteins are colored in green and down regulated proteins are colored in red. Lines represent protein interactions. Proteins were grouped by their function.

Finally, it was also possible to establish relevant relationships between these differentially expressed proteins and other proteins by creating networks which establish interrelationships between them. Among these, a network with associated functions

related with *Cell signaling, molecular transport and small molecule biochemistry* was established (figure V.4.21.).

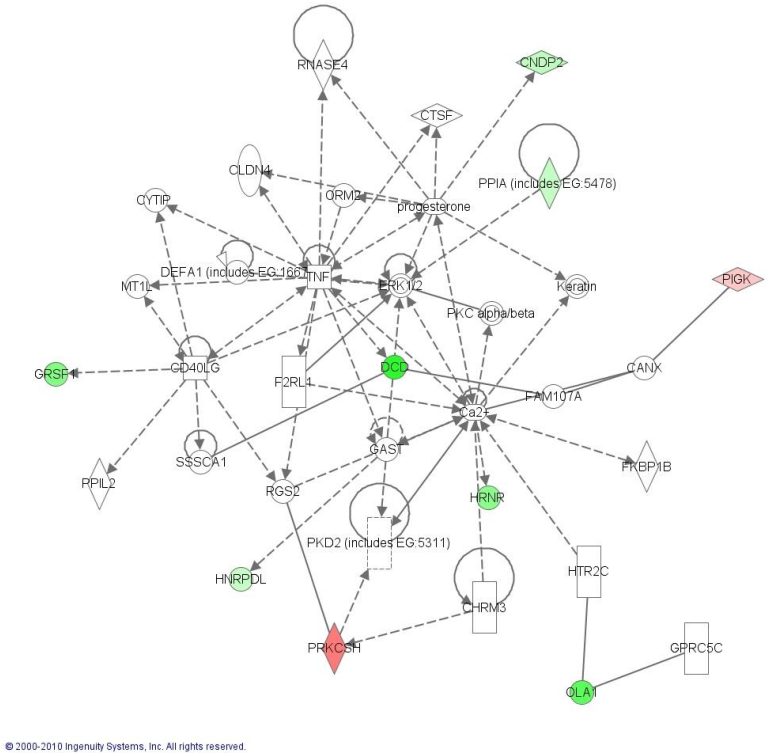

Figure V.4.21.: Relevant interactions between differentially expressed proteins resulting from the expression of the small delta antigen (experiment 4) and proteins in IPA database. Up regulated proteins are colored in green and down regulated proteins are colored in red. Lines represent protein interactions. In this figure is shown the associated network with function in *cell signaling, molecular transport and small molecule biochemistry.*

As for canonical pathways, the most relevant canonical pathways affected by differentially expressed proteins due to HDV replication were *VEGF signaling, cell cycle: G2/M DNA damage checkpoint regulation, integrin signaling* and *HIF1α signaling pathway* (figure V.4.22.) (See supplementary information for pathways illustrations).

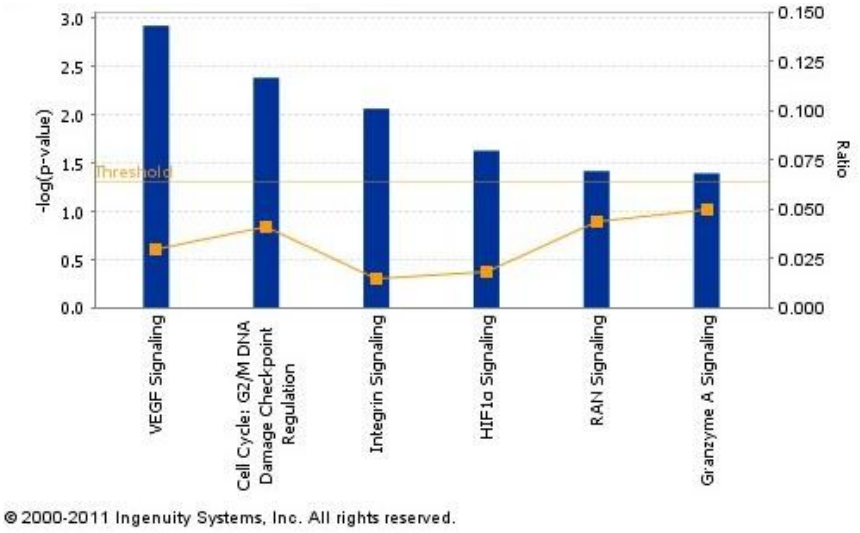

Figure V.4.22.: Significant affected canonical pathways by the accumulation of HDV RNA (experiment 5). Yellow points represent the ratio, calculated by dividing the number of genes in a giving pathway that follow cut-off criteria, by the total number of genes that make up that pathway. The ratio gives an idea of the percentage of genes in a pathway that were also found in our uploaded list. The yellow line corresponds to the threshold, or cut-off, which corresponds to the p value of 0.05. p values were calculated by IPA using Fisher's exact test.

Table V.4.4. shows the differentially expressed proteins in each pathway.

CANONICAL PATHWAY	ACCESS NUMBER	PROTEIN	FOLD
VEGF signaling	P12814	Alpha-actinin-1	2.0
	O43707	Alpha-actinin-4	2.4
	Q15717	ELAV-like protein 1	-2.0
Cell cycle: G2/M DNA damage check point regulation	P11338	DNA topoisomerase 2-alpha	1.6
	Q02880	DNA topoisomerase 2-beta	-3.5
Integrin signalling	P12814	Alpha-actinin-1	2.0
	O43707	Alpha-actinin-4	2.4
	P84077	ADP-ribosylation factor 1	2.9
HIF1a signaling pathway	P00338	L-lactate dehydrogenase A chain	-1.7
	P27695	DNA-(apurinic and apyrimidinic site) lyase	-3.9

Table V.4.4.: Differentially expressed proteins associated to the most significant canonical pathways for experiment 5.

As for experiment 5, in which differentially expressed proteins result from the replication of HDV, the same approach was used. Figure IV.4.23. represents a network in which all possible interactions of the differentially expressed proteins resulting from the expression of HDV are shown.

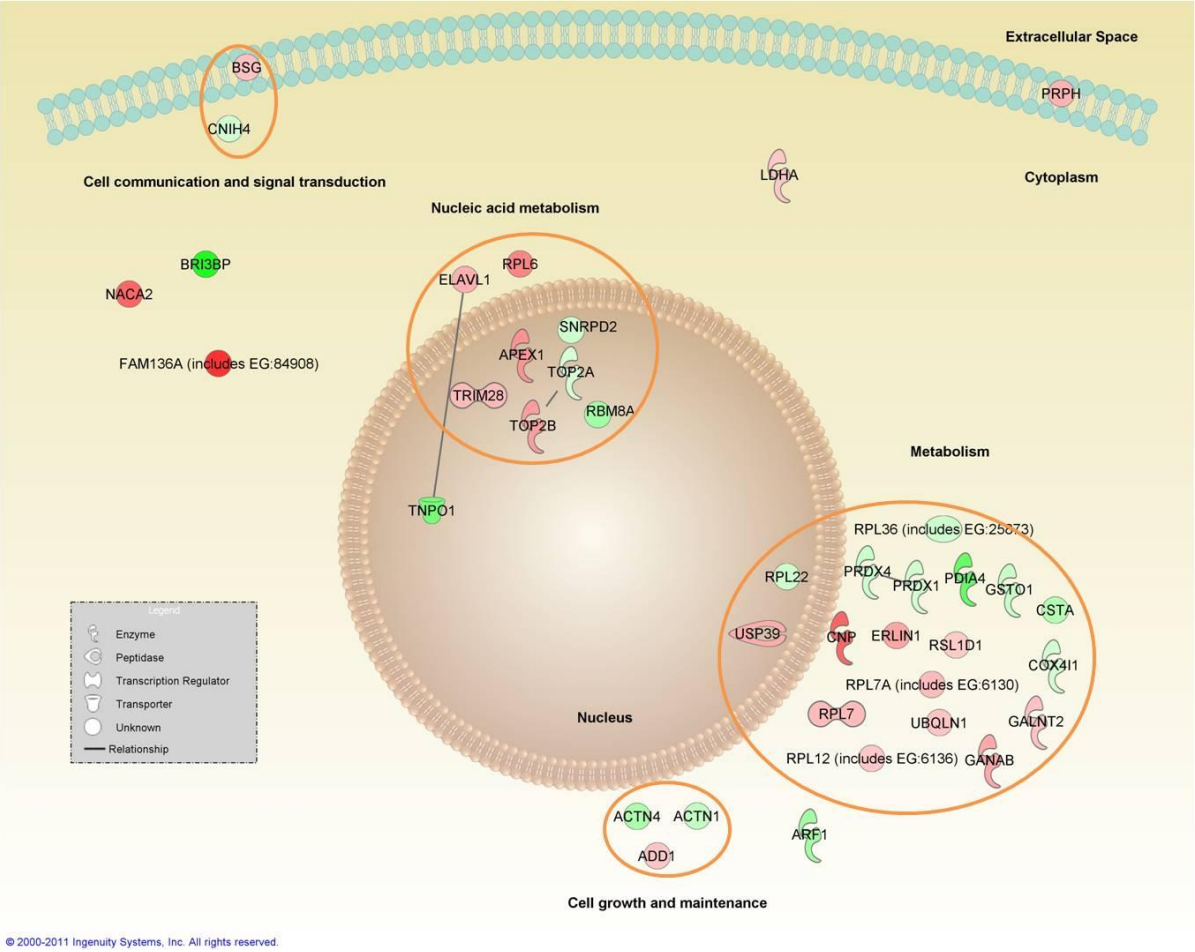

Figure V.4.23: Interactions among differentially expressed proteins resulting from HDV replication (experiment 5). Up regulated proteins are colored in green and down regulated proteins are colored in red. Lines represent protein interactions. Proteins were grouped by their function.

Networks establishing possible relationships between differentially expressed proteins resulting from HDV replication and other proteins were obtained. Among them, a network with associated functions related with *cellular assembly and organization, RNA post-transcriptional modification and cellular compromise* was established (figure V.4.24.) (See supplementary information for pathways illustrations).

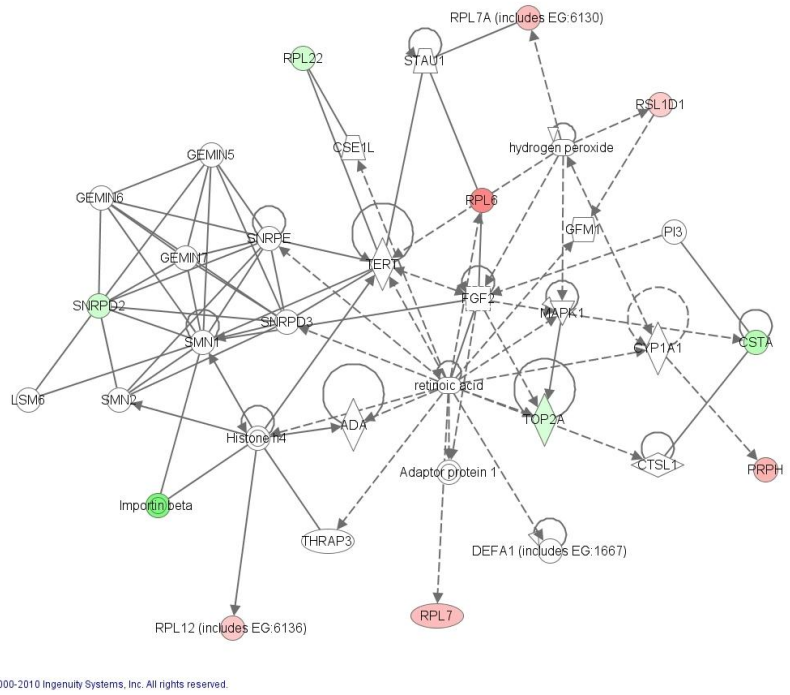

Figure V.4.24.: Relevant interactions between differentially expressed proteins resulting from the accumulation of HDV RNA (experiment 5) and proteins in IPA database. Up regulated proteins are colored in green and down regulated proteins are colored in red. Lines represent protein interactions. Figure V.4.24. shows the associated network with function in *cellular assembly and organization, RNA post-transcriptional modification and cellular compromise*.

In experiment 4, by comparing the proteome of 293 cells with the proteome of cells 293 expressing the small delta antigen, expression changes due to the expression of the small delta antigen were determined. In experiment 5 a comparison between 293 cells expressing the small delta antigen and 293 cells replicating HDV was made. Because HDV only replicates in the presence of the small delta antigen expression changes caused by virus replication are all expression changes resulting from both experiments 4 and 5.

When considering results from both experiments 4 and 5, the most relevant canonical pathways affected by HDV were *Cell cycle: G2/M DNA damage checkpoint regulation, HIF1α Signaling, protein ubiquitination pathway* and *glycolysis/gluconeogenesis* (figure V.4.25.) (See supplementary information for pathways illustrations).

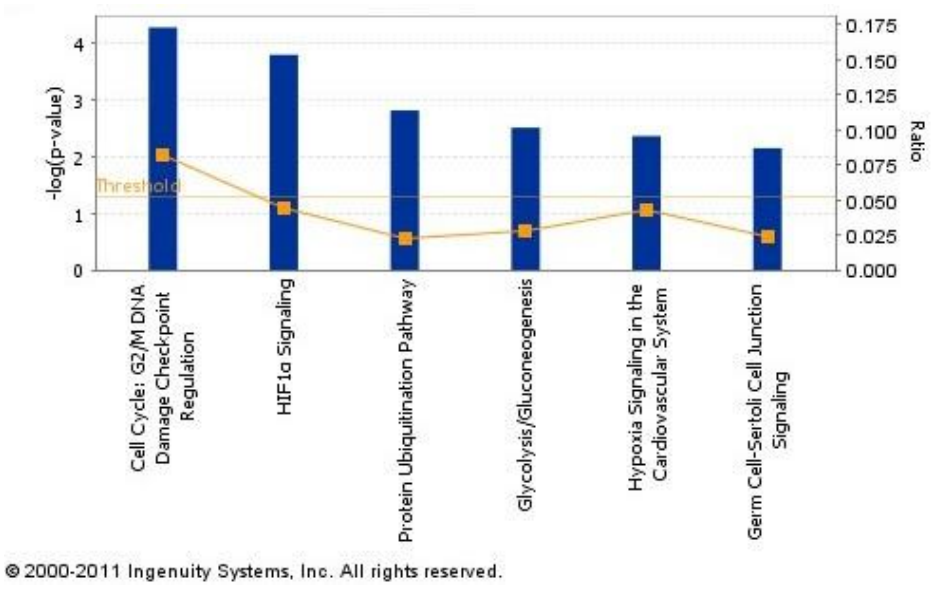

Figure V.4.25.: Significant canonical pathways affected by HDV replication. Yellow points represent the ratio, calculated by dividing the number of genes in a giving pathway that follow cut-off criteria, by the total number of genes that make up that pathway. The ratio gives an idea of the percentage of genes in a pathway that were also found in our uploaded list. The yellow line corresponds to the threshold, or cut-off, which corresponds to the p value of 0.05. p values were calculated by IPA using Fisher's exact test.

Table V.5.5. shows the differentially expressed proteins in each pathway.

CANONICAL PATHWAY	ACCESS NUMBER	PROTEIN	FOLD
Cell cycle: G2/M DNA damage check point regulation	P78527	DNA-dependent protein kinase catalytic subunit	-2.2
	P04637	Cellular tumor antigen p53	-2.3
	P11338	DNA topoisomerase 2-alpha	1.6
	Q02880	DNA topoisomerase 2-beta	-3.5
HIF1α Signaling	P07900	Heat shock protein HSP 90-alpha	2.1
	P00338	L-lactate dehydrogenase A chain	up-regulated[a]
	P07195	L-lactate dehydrogenase B chain	2.2
	P27695	DNA-(apurinic or apyrimidinic site) lyase	-3.9
	P04637	Cellular tumor antigen p53	-2.3
Protein ubiquitination pathway	P07900	Heat shock protein HSP 90-alpha	2.1
	P34932	Heat shock 70 kDa protein 4	2.5
	P61604	10 kDa heat shock protein, mitochondrial	-2.0
	O00231	26S proteasome non-ATPase regulatory subunit 11	3.6

	P22314	Ubiquitin-like modifier-activating enzyme 1	1.8
	Q53GS9	U4/U6.U5 tri-snRNP-associated protein 2	-2.9
Glycolysis/Gluconeogenesis	P06733	Alpha-enolase	1.8
	P00338	L-lactate dehydrogenase A chain	up-regulated[a]
	P07195	L-lactate dehydrogenase B chain	2.2
	P60174	Triosephosphate isomerase	2.2

Table V.4.5.: Differentially expressed proteins associated to the most significant canonical pathways for experiment 4 and 5 altogether.

a. The fold for protein LDHA is omitted because as described before LDHA is up-regulated in experiment 4 and down-regulated in experiment 5. The final fold is positive.

By combining all the results from experiment 4 and 5, the following network showing possible interactions among all differentially expressed proteins was obtained (figure V.4.26.).

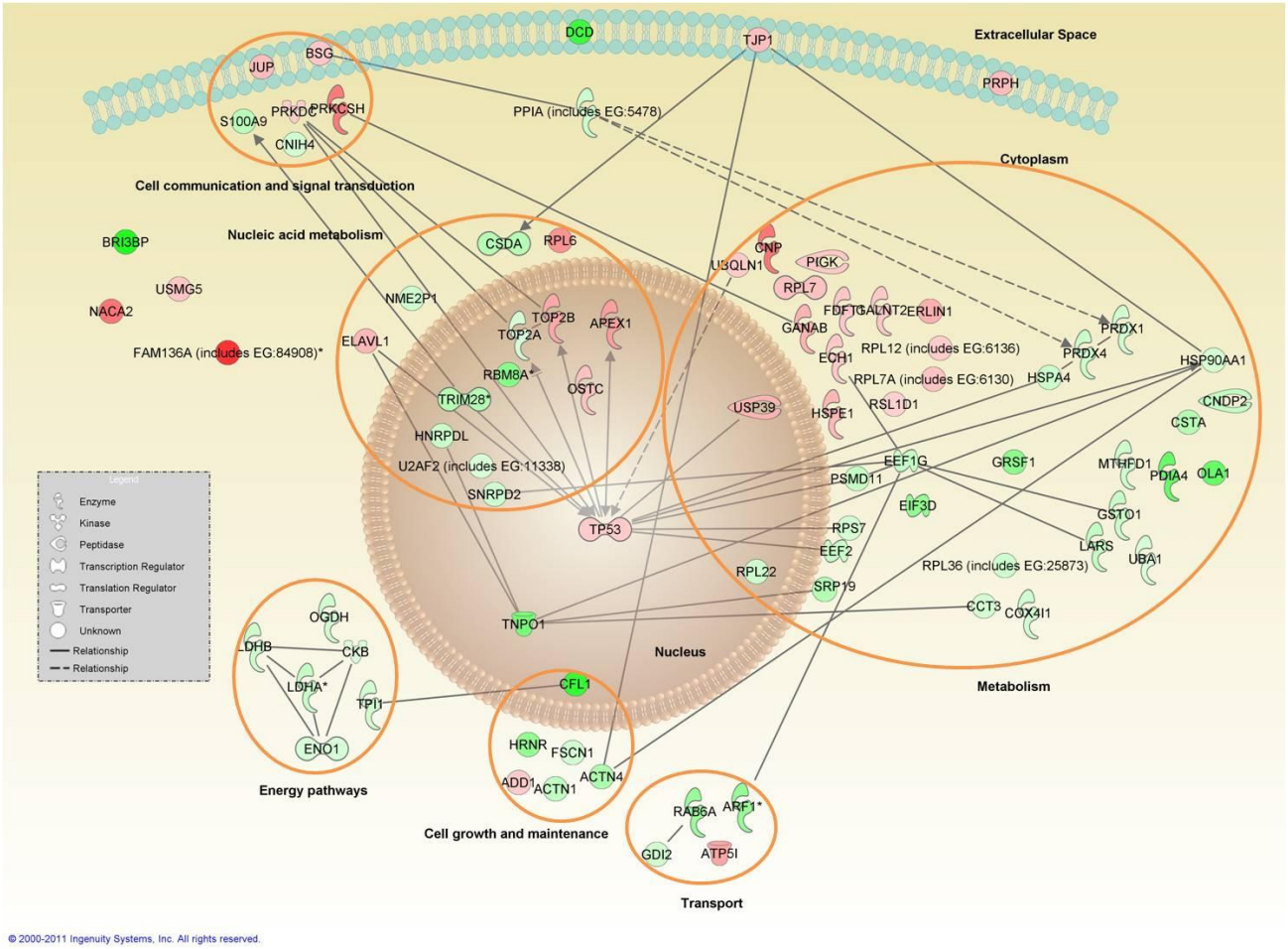

Figure V.4.26.: Interactions among differentially expressed proteins resulting from the expression of the delta antigen and HDV replication. Up regulated proteins are colored in green and down regulated proteins are colored in red. Lines represent protein interactions. Proteins were grouped by their function.

Networks establishing relationships among differentially expressed proteins resulting from the experiments 4 and 5 altogether and other proteins were built. Among them, a network with associated functions related with *Cellular Assembly and Organization, Lipid Metabolism, Molecular Transport* (figure V.4.27.).

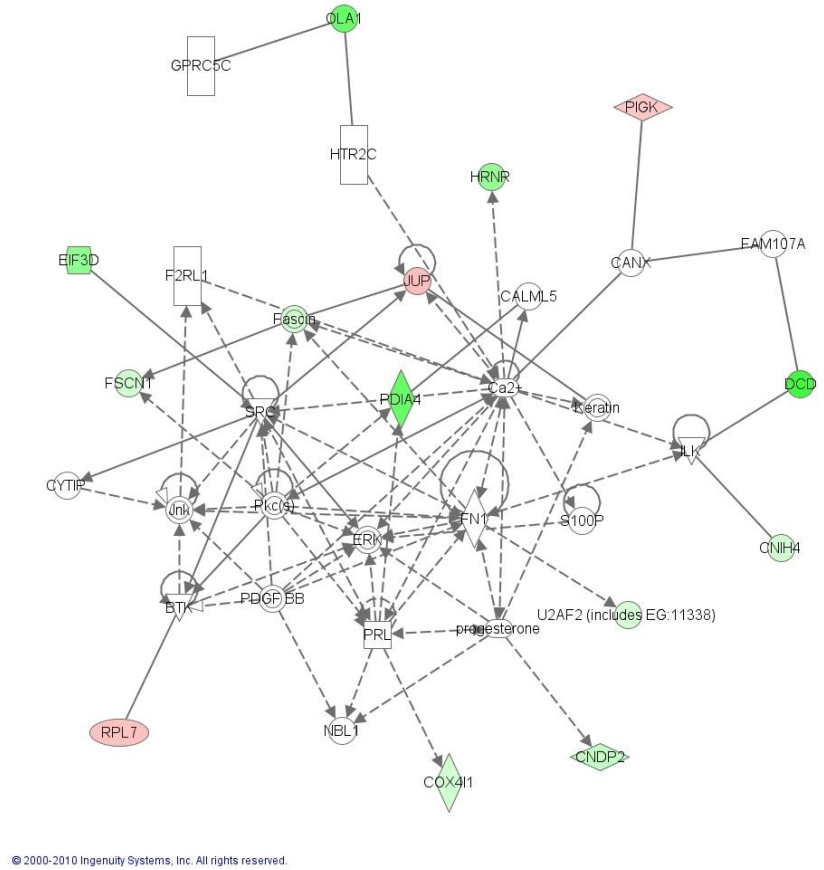

Figure V.4.27.: Relevant interactions between differentially expressed proteins resulting from experiments 4 and 5 altogether and proteins in IPA database. Up regulated proteins are colored in green and down regulated proteins are colored in red. Lines represent protein interactions. In this figure is shown the associated network with function in *Cellular Assembly and Organization, Lipid Metabolism, Molecular Transport*.

V.4.5. CELL CYCLE: G2/M DNA DAMAGE CHECKPOINT REGULATION PATHWAY

As described above, one of the pathways affected by HDV replication was the pathway related with *Cell cycle: G2/M DNA damage checkpoint regulation*. In this pathway, p53 regulates 14-3-3σ which binds to the phosphorylated CDK1-cyclin B complex exporting it from the nucleus avoiding dephosphorylation, avoiding the checkpoint and leading to uncontrolled cell division (figure IV.4.28.).

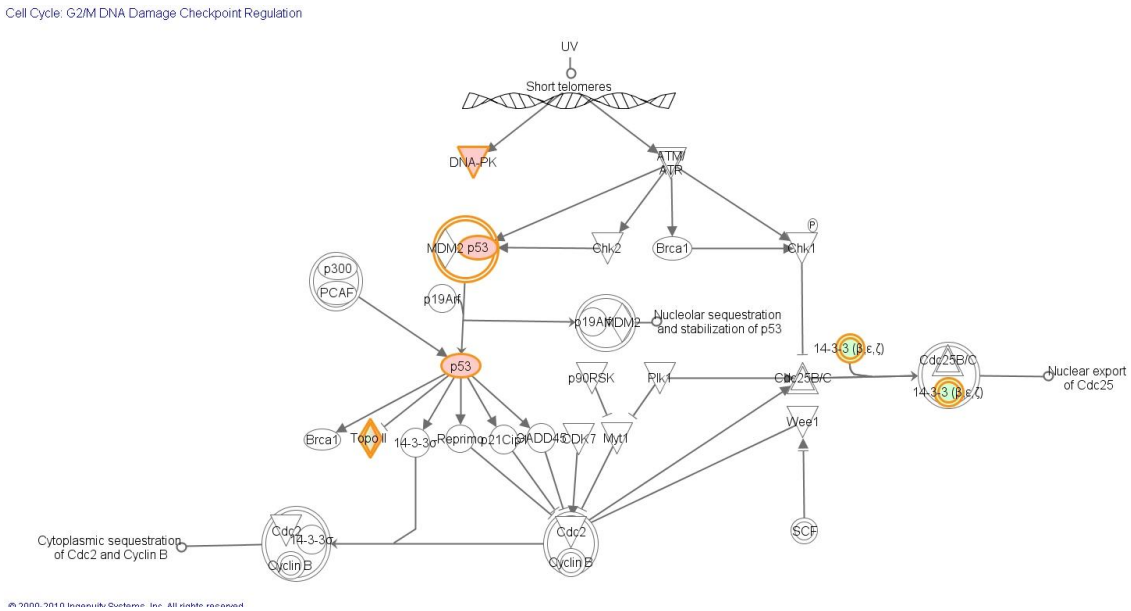

Figure V.4.28.: *Cell cycle: G2/M DNA damage checkpoint regulation* pathway.

If p53 is down regulated, then a down regulation of the 14-3-3 σ would also be expected. In order to consolidate even more the results western blot analysis was performed to determine if in fact these proteins were down regulated. For 14-3-3 σ results showed in fact a down regulation of this protein (figure IV.4.29).

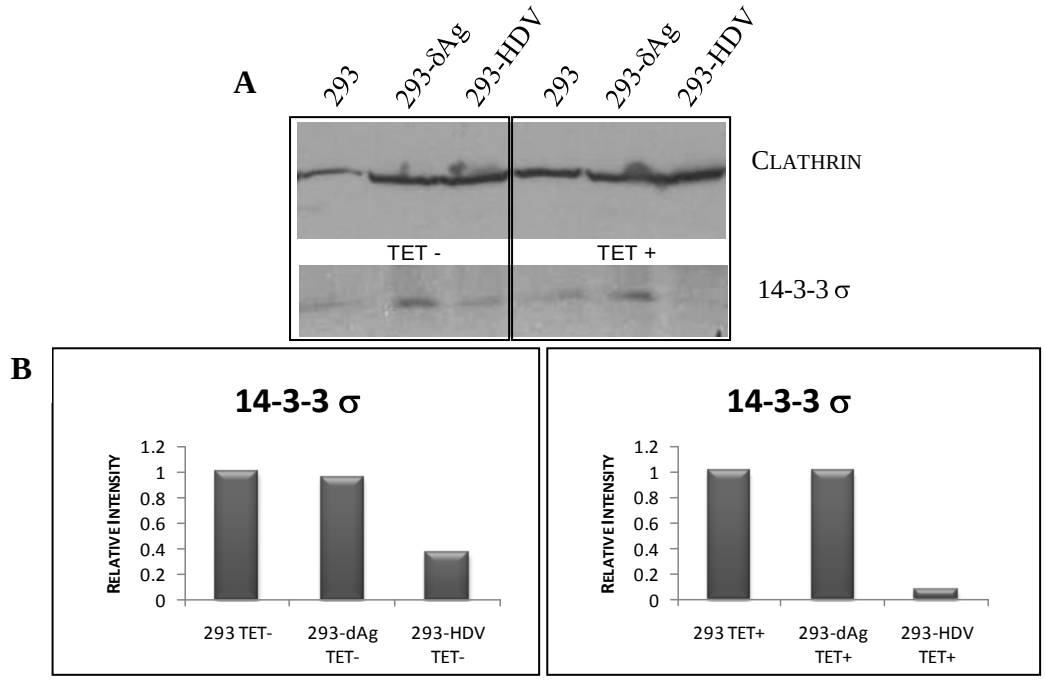

Figure V.4.29.: Western blot analysis of 14-3-3 σ and clathrin. 10 µg/lane of total protein extracts were loaded into a 12% SDS-PAGE and after electrophoresis, electroblotted into a nitrocellulose membrane. Membrane was incubated with both mouse monoclonal antibody against 14-3-3 σ (1:1000) and rabbit polyclonal antibody against Clathrin HC (1:1000) (A). Images were analyzed using ImageJ and relative quantification was performed by normalizing results obtained for 14-3-3σ with the results obtained for clathrin (B).

V.5. DISCUSSION

Hepatitis delta virus replication is highly dependent on host cellular proteins since it only codes for one protein, the delta antigen (HDAg). In order to clarify the mechanisms involved in HDV replication and pathogenesis, an MS-based quantitative proteomics approach consisting in $^{16}O/^{18}O$ enzymatic labeling was used to determine alterations in cells proteome during HDV replication. For that purpose, the 293-δAg cell line, that conditionally expresses SHDAg, and 293-δAg-HDV cells, that replicates HDV RNA, were used (Chang *et al.* 2005). Although HDV only infects hepatocytes, replication efficiently occurs in 293 cells, establishing that this cell line has all the necessary host factors for HDV replication.

Five experiments were performed to determine protein expression changes during HDV replication in 293 cell line. Three were used as controls to discard any expression changes resulting from the addition of tetracycline (experiment 1), cell manipulation (by stable and transient transfection) and/or basal expression levels of SHDAg and HDV RNA (experiments 2 and 3, respectively) and two were performed to determine alterations in cells expressing SHDAg and cells expressing HDV genomic RNA (experiments 4 and 5, respectively). When comparing 293 cells in the presence and absence of tetracycline (experiment 1), seven proteins were found differentially expressed. These results show that tetracycline, at the point of harvest, is not toxic to cells inducing insignificant expression changes. Furthermore, these proteins were involved in signal transduction and metabolism suggesting that tetracycline induces cell signaling to inform the cell of a possible stress. These proteins were discarded since these quantifications were just a control to determine if tetracycline induced significant changes at the point of harvest.

Cells 293 and 293-δAg and cells 293-δAg and 293-δAg-HDV were compared both in the absence (experiments 2 and 3) and presence (experiments 4 and 5) of tetracycline. As expected, results showed that the number of differentially expressed proteins is higher in the presence of tetracycline. Furthermore, when comparing 293 cells with 293-δAg cells in the absence and presence of tetracycline (experiment 2 and 4) some differentially expressed proteins were common between the experiments. These results were also expected and may be due to stable transfection of SHDAg under the control of tetracycline in 293-cells or to the low level expression of SHDAg in absence of tetracycline. By comparing 293-δAg cells and 293-δAg-HDV cells in the absence

and presence of tetracycline, proteins in common were also found between the experiments, in this case due to transitory transfection of HDV RNA and low level accumulation of HDV RNA in absence of tetracycline. Because in most cases it is impossible to determine the origin of such alterations, common proteins between experiments 2 and 4 and 3 and 5 were discarded from experiments 4 and 5, respectively. Clear examples of proteins differentially expressed due to cell line modification are adenovirus proteins ADE05_E1B and ADE02_E1, which were found differentially expressed in experiments 2 and 4 and are a result from the transformation of primary Human Embryonic Kidney cells with sheared fragments of adenovirus DNA leading to the 293 cell line. These results altogether confirm, on one hand the data of Chang *et al* showing that in fact SHDAg and HDV RNA accumulate in the absence of tetracycline. On the other hand results show the consistency of the model, since an increase of tetracycline leads to an increase of SHDAg expression and HDV RNA accumulation and thus to higher expression changes. Another interesting result is that, both in the absence and presence of tetracycline, SHDAg induces more changes in cells proteome than HDV RNA. These were already seen by our laboratory in a previous work, using another model (Mota *et al.* 2008). Being the only protein encoded by the virus, SHDAg is expected to induce the most significant changes on cells in order to induce HDV RNA replication.

Considering only quantified proteins resulting from SHDAg expression and HDV RNA accumulation, results were organized and analyzed using systems biology tools in an attempt to determine the behavior of these proteins. Using GOTM for $Zq<0$ and $Zq>0$, the optimal FDRq at which enriched categories are reliable was determined for both experiments 4 and 5. 10 categories were found enriched for proteins with $Zq>0$ in experiment 4. While most of the enriched down regulated categories were related with the *membrane* and *membrane bounded organelles*, interestingly one enriched category was the *nucleolus*. In mammals, the nucleolus is involved in ribosome biogenesis, viral replication, nuclear export pathways and is also thought to be a stress sensor. After exposure to stress, cells rapidly decrease the synthesis of ribosomal RNA. Furthermore, stress will lead to changes in gene expression patterns and reprogramming of protein synthesis (Mayer and Grummt 2005; Boulon *et al.* 2010). SHDAg, when cells are not replicating, is predominantly located in the nucleolus and it was seen to associate with two nucleolar proteins: nucleolin for targeting SHDAg to the nucleoli and B23 to modulate HDV replication. Besides nucleolin and B23, SHDAg may recruit

other nucleolar proteins forcing the decrease of ribosome synthesis and giving the cell time to adjust to a new phase of translation with the virus inducing translation of key proteins to its replication.

As for Zq<0, for the same experiment, 15 categories were found enriched. Most categories were related with *translational regulator activity and ribonucleotide binding*. With a decrease in the expression of the nucleolus proteins, and consequently of ribosome synthesis, proteins involved in translation regulation activity suffer an increase in its expression. It is possible that SHDAg expression modulates proteins involved in translation in order to allow virus replication. The up regulation of proteins involved in ribonucleotide binding is also interesting since HDV is an RNA virus and HDV RNA surely interacts with cellular proteins during its replication and pathogenesis.

Regarding experiment 5, for proteins with Zq<0, eight categories were found enriched. All the categories were inserted in the *Cellular Component* category and most categories were involved in *vesicles* category. Vesicles are small fluid-filled spherical organelles enclosed by membrane that carry cargo within the cell. They gather their cargo through a process called budding move through the cell with that cargo and finally deliver it by fusing with another membrane-enclosed compartment. Many viruses rely on host intracellular membranes and vesicle formation for replication and viral assembly. Recently, it was shown that the morphogenesis of HDV is mediated by a clathrin-mediated post-Golgi membrane trafficking and that clathrin heavy chain (CHC) is essential for the formation of HDV VLPs (virus like particles) by LHDAg, which has been identified as a clathrin-adaptor like protein (Huang *et al.* 2007; Huang *et al.* 2009). Nuclear LHDAg is transported to the *trans* Golgi network (TGN) where interacts with HBsAg and CHC for HDV morphogenesis. Subsequently, HDV particles are packaged into CCVs (clathrin coated vesicles) that leave the TGN and enter into the late endosome or secretory vesicle before release (Huang *et al.* 2009). The up-regulation of proteins that belong to the vesicles enriched category is in agreement with the processes previously described. Results suggest that during HDV replication proteins involved in vesicle formation increase their expression in order to provide all the conditions for viral assembly.

For a Zq>0 enriched categories were inserted in *Biological Process* category and involved in *microtubule-based movement*. In the presence of HDV, proteins involved in microtubule based movement tend to decrease their expression. Along with

the previously stated these results support the theory that HDV replication is performed with the help of trafficking vesicles.

After an analysis of all quantified proteins with GOTM, a deeper analysis of the differentially expressed proteins obtained in this work was performed. Differentially expressed proteins resulting from SHDAg expression and HDV RNA accumulation (experiments 4 and 5) were first grouped by their function showing that most proteins are involved in protein metabolism and energy pathways, respectively.

With IPA it was possible to determine which canonical pathways were most affected due to SHDAg expression and HDV RNA accumulation and thus HDV replication and to perform network analysis to determine the relationship among differentially expressed proteins resulting from SHDAg expression, HDV RNA accumulation and thus HDV replication. Finally, interactions among differentially expressed proteins and host cellular proteins were also established.

Significant canonical pathways affected by SHDAg expression were *glycolysis/gluconeogenesis*, *HIF1α signaling pathway*, *propanoate metabolism* and *protein ubiquitination pathway*. A briefly description of each pathway is given in the next paragraphs.

Glycolysis is the process by which cells degrade glucose, which enters in cells through glucose transporters, to pyruvate and ATP. From here, mammalian cells can obtain energy by two metabolic processes: oxidative phosphorylation or lactic fermentation. During oxidative phosphorylation, which can only occur in the presence of O_2, the pyruvate is converted to acetil-CoA, enters the tricarboxylic acid (TCA) cycle and undergoes a series of oxidative reactions (oxidative phosphorylation), yielding 36 ATP molecules per molecule of glucose. Alternatively, and in the absence of O_2, pyruvate is converted to lactate, which is excreted to the bloodstream, yielding two molecules of ATP per molecule of glucose. Oxidative phosphorylation has thus a much higher energy yield than lactic fermentation. Four proteins involved in *glycolysis/gluconeogenesis* and *lactic fermentation pathways*, ENO1, LDHA, LDHB and TPI1, were found to be up regulated in the presence of SHDAg.

Oxygen (O_2) is essential for life and an essential element that serves as a key substrate in cellular metabolism and bioenergetics. Aerobic organisms need O_2 to produce energy. In the absence or low O_2 conditions (a process named hypoxia) cells enter into a stress state and undergo a number of adaptative responses to match O_2

supply with metabolic, bioenergetic and redox demands. In mammals, the primary transcriptional response to hypoxic stress is mediated by hypoxic-inducible factors (HIFs). HIF1α is an inducible transcription factor whose activity depends on oxygen levels and cellular stress. Under normal O_2 conditions HIF1α is hydroxylated, targeting it for rapid degradation through the von Hippel-Lindau (VHL)/proteosome pathway. In hypoxia, reduced O_2 levels block VHL mediated degradation leading to HIF1α accumulation. HIF1α then translocates to the nucleus activating expression of HIF1α target genes (Bardos and Ashcroft 2005). For instance, almost all the enzymes of the glycolytic pathway are encoded by genes whose expression is under the control of HIF1α. Oxidative stress, leading to the accumulation of reactive oxygen species (ROS) in cells also leads to HIF1α accumulation. Non-hypoxia related factors have also been shown to contribute to the activation of HIF1. In response to hypoxia, p53, a tumor suppressor in many tumours, has been shown to induce apoptosis. HIF1α is stabilized in response to low O_2 levels and in response, p53 is also stabilized inducing apoptosis. However, apoptosis induced by hypoxia follows different mechanisms then apoptosis induced by DNA damage (Koumenis *et al.* 2001). Four proteins belonging to HIF1α signaling pathway were found differentially expressed in the presence of SHDAg. HSP90AA1, LDHA and LDHB were found up-regulated while interestingly, p53 was found down-regulated.

The metabolism of propionic acid, or propanoate metabolism, begins with the conversion of the propionic acid to propionyl coenzyme A (propionyl-CoA), which is the usual first step in the metabolism of carboxylic acids. Propionyl-CoA is then carboxylated to D-methylmalonyl-CoA, which is isomerized to L-methylmalonyl-CoA and finally a vitamin B12-dependent enzyme, called methylmalonyl CoA mutase catalyzes the rearrangement of L-methylmalonyl-CoA to succinyl-CoA which is an intermediate of the Kreb's Cycle. Three proteins belonging to propanoate metabolism, LDHA, LDHB and ECH1 were found differentially expressed. LDHA and LDHB were up-regulated and ECH1 was down-regulated due to the presence of SHDAg.

Ubiquitin is a 76 aa protein which is widely expressed in eukaryotes. It acts as a molecular tag that besides marking proteins for degradation by the proteosome also has an important role in several other processes in cells like DNA repair, transcription, endocytosis, membrane transport, protein localization and antigen processing. Ubiquitination is a post-translational modification process that comprises several steps

until ubiquitin, synthesized as an inactive precursor, becomes active and capable of substrate modification. Briefly, ubiquitin precursors are processed by deubiquitinating enzymes (DUBs) or ubiquitin-like specific proteases to expose a C-terminal glycine in the mature ubiquitin that becomes conjugation competent and can be activated with ATP by ubiquitin activating enzyme (E1). Once activated, the ubiquitin is then transferred to the ubiquitin-conjugating enzymes (E2). E3-ubiquitin ligases then recruit the ubiquitin-E2 complex, recognize specific substrates and finally mediate, or directly catalyze, the ubiquitin transfer to the substrates. One of the most extensively studied E3-ubiquitin ligase is the Mdm2. Ubiquitin contains seven acceptor lysines that could be utilized in the process of ubiquitin conjugation, resulting in ubiquitin chains of various lengths, types and functional consequences. Polyubiquitination mediated by Lys48 leads to substrate degradation via proteosome whereas the polyubiquitination mediated by Lys63 plays a role in DNA repair and signal transduction. Five proteins belonging to the protein ubiquitination pathway were found differentially expressed in the presence of SHDAg. Proteins HSP90AA1, HSPA4, PSMD11 and UBA1 were found up-regulated while HSPE1 was found down-regulated.

When cells are exposed to extra or intracellular stress they rapidly alter their metabolism to compensate for that stress. Since the activation of survival pathways to the initiation of cell death that eventually eliminates damaged cells, depending on the severity of the insult, cells will respond differently. Viral infection is a major cause of stress to cells since viruses interfere with host cell metabolism in many ways to enhance their own replication. One of the major pathways affected by viruses is the HIF1 signaling pathway, which has been implicated in the pathogenesis of several viruses. Epstein Barr virus (EBV) oncoprotein, latent membrane protein 1 (LMP1) activates HIF1α and subsequently activates expression of HIF1α-responsive genes in epithelial cells (Kondo *et al.* 2006). Upon HIV1 infection, HIF1 signaling pathway is also activated. HIV1 viral protein R (Vpr) induces ROS (reactive oxygen species) by increasing H_2O_2 production which contributes to HIF1α accumulation. Increased levels of HIF1α then up-regulate the HIV-1 promoter inducing HIV1 gene expression and deregulation of multiple host cellular pathways (Deshmane *et al.* 2009). Human papillomavirus (HPV) E7 protein also seems to enhance HIF1 transcriptional activity by inducing the dissociation of histone deacetylases (HDACs) from HIF1α. Furthermore HPV E6 seems to promote degradation of p53, blocking apoptosis, and allowing cell

proliferation (Bodily *et al.* 2010). HCV induces a state of oxidative stress by affecting mitochondrial-respiratory chain activity. HCV protein expression seems to activate HIF1 by stabilization of its α subunit. In consequence, expression of HIF controlled genes, including those for glycolytic enzymes are up-regulated (Ripoli *et al.* 2010). Long term HCV protein expression causes depression of mitochondrial oxidative phosphorylation. Cell survival is then preserved by enhancing lactic fermentation. This adaptative response to HCV-induced mitochondrial injury proved to be mediated by stabilization of HIF1α and in consequence, up-regulation of glycolytic enzymes (Ripoli *et al.* 2010). Finally, HBx, an HBV regulatory protein thought to play a central role in HBV replication and pathogenesis, has been shown to increase the transcriptional activity of HIF1. HBx stimulates HIF1 stability by blocking proteosomal degradation mediated by VHL and also increases its transcriptional activity (Moon *et al.* 2004).

Protein ubiquitination pathway is another pathway commonly affected by viruses, since viruses seem to target cell cycle regulator proteins for degradation. The HPV-16 and 18E6 proteins co-opt the cellular E3 ligase E6AP to mediate ubiquitin-dependent proteosomal degradation of p53. Adenovirus proteins E1B55K and E4orf6 also cause degradation of p53 inducing the assembly of the E3 ligase complex and targeting p53.

Differentially expressed proteins resulting from SHDAg expression, along with the previous findings, seem to show that SHDAg, just like HCV and other viruses, induces oxidative stress in cells leading to the accumulation of HIF1α and consequent up-regulation of glycolytic enzymes. Up-regulation of both LDHA and LDHB further indicates that SHDAg induces lactic fermentation. Indirectly, LDHA, LDHB and ECH1 interact with the propanoate metabolism confirming that SHDAg in fact induces stress in cells, altering their metabolism. Furthermore, SHDAg seems to be responsible for targeting proteins for degradation thus increasing the expression of the proteins involved in the protein ubiquitination pathway. These results also explain the down regulation of p53 in HIF1α signaling pathway. SHDAg seems to cause degradation of p53 by inducing the ubiquitination pathway. The down regulation of p53 was validated by western blot analysis giving further consistency to the results. An interesting result obtained during western blot validation is that when comparing results of p53 in the presence and absence of tetracycline, it is clear that the expression of the proteins follows the same pattern either in presence or absence of tetracycline. This result shows

taht there is in fact a basal expression of SHDAg and HDV RNA the absence of tetracycline.

After analysis of significant canonical pathways, differentially expressed proteins resultant from SHDAg expression (experiment 4) were used to built an interaction network. 23 proteins out of 49 interact with each other. GDI binds with RAB6A; TJP1 binds to HSP90AA and acts on CSDA; CFL1 binds to TPI1; EFF1G binds to ARF1, LARS, ECH1 and PSMD11; ENO1, LDHA, LDHB and CKB bind with each other; TIF1B binds to S100A9; PRKDC and TIF1B both act on P53 and finally, P53 binds with RPS7, HSPA4, EEF2, PSMD11 and HSP90AA1. Most of these interactions are physical interactions confirmed by yeast-to-hybrid and/or pull down assays and thus biologically, poorly understood. However, others are that are well biologically defined.

RAB6A is involved in protein transport and regulates membrane traffic from the Golgi to the ER. GDI2 regulates GDP/GTP exchanging reactions of most RAB proteins. Both proteins were found up-regulated. This result may be a confirmation of the use of vesicles by HDV.

LDHA, LDHB and ENO1 are all involved in glycolysis. LDHA and LDHB catalyze the reversible conversion of (S)-lactate and NAD^+ to pyruvate and NADH while ENO1 catalyzes the reversible conversion of 2-phospho-D-glycerate to phosphoenolpyruvate. Besides its catalytic activity, ENO1 also plays a part in growth control, hypoxia tolerance and allergic responses. Furthermore, ENO1 binds to the myc promoter and acts as a transcriptional repressor (Feo *et al.* 2000). All proteins were up-regulated indicating an up-regulation of glycolysis which may be a result of cellular stress induced by SHDAg.

TIF1B acts on p53. By interacting with MDM2, a major regulator of p53, TIF1B stimulates p53-HDAC1 complex formation and inhibits p53 acetylation contributing to its functional regulation (Wang *et al.* 2005). Results imply that TIF1B is up-regulated, inhibiting p53 acetylation and thus diminishing its transcriptional activity.

Finally, p53 also binds to RPS7. RPS7 besides being involved in rRNA maturation, is an MDM2 interacting partner. MDM2 oncogene is a major negative regulator of p53. MDM2 promotes p53 proteosomal degradation and negatively regulates p53 fuction. RPS7 binds to MDM2 modulating MDM2-p53 binding, resulting in p53 stabilization. An over expression of RPS7 increases p53 transactivational activity

inducing apoptosis and inhibiting cell proliferation (Chen *et al.* 2007). Interestingly, RPS7 is up regulated and p53 is down regulated. This result suggests that up-regulation of RPS7 is probably due the need of SHDAg to induce rRNA maturation and that down-regulation of p53 is induced by another pathway.

Networks involving differentially expressed proteins due to SHDAg expression and proteins involved in IPA database were also built. These networks may be useful to indicate interesting lines of research.

Significant canonical pathways altered due to the presence of HDV RNA were also determined. These pathways were: *VEGF signaling*, *Cell cycle: G2/M DNA damage checkpoint regulation*, *integrin signaling* and *HIF1α signaling*. A brief description of the pathways is given in the following paragraphs.

Vascular endothelial growth factors (VEGFs) regulate vascular development during embryogenesis (vasculogenesis) as well as blood-vessel formation (angiogenesis) in the adult. VEGFs act through ligand binding to their cognate VEGF receptors increasing vascular permeability and angiogenesis and inducing cellular processes like cell migration, survival and proliferation (Olsson *et al.* 2006). As described before, hypoxia stabilizes the HIFs which directly regulate a considerable amount of genes. Expression of VEGFA and VGFR are directly regulated by HIFs and this VEGF expression induced by hypoxia is considered to be an inducer of increased vascular supply to tumors allowing them to grow and metastasize. Three proteins involved in the VEGF pathway were found differentially expressed in the presence of HDV RNA. ACTN1 and ACTN4 were found both up regulated and ELAVL1 was found down-regulated.

In eukaryotic cells, the cell cycle is a highly regulated process controlled by *checkpoints* that monitor the successful completion of every cell cycle step facilitating DNA repair and promoting cell death in unrepaired cells. One of those checkpoints is G2/M checkpoint that monitors DNA damage that occurred in G2 phase and cells that have escaped G1 and S checkpoints. Briefly, during G2 phase, CDK1 (cdc2 in yeast)/Cyclin B complex is maintained inactive by phosphorylation of CDK1 by WEE1 and Mt1 kinases. When approaching mitosis, CDK1/Cyclin B are dephosphorylated by CDC25 phosphatase. CDK1/Cyclin B can then phosphorylate CDC25, inactivating it and efficiently driving cells to mitosis. If G2 is arrested, kinases DNA-PK, ATR and ATM are activated initiating parallel cascades that inactive CDK1/Cyclin B. On one

hand, ATR and ATM phosphorylate and activate serine kinases Chk1 and Chk2. Chk1 and Chk2 then can phosphorylate CDC25 inactivating it by creating a binding site for 14-3-3 protein family which lead CDC25 to the cytoplasm avoiding dephosphorylation of CDK1/Cyclin B. On the other hand, p53 is phosphorylated which dissociates it from MDM2 and activating its DNA binding activity. p53 is also acetylated by p300/PCAF which activates its transcriptional activity. One of the genes turned on by p53 is 14-3-3σ, which binds the phosphorylated CDK1/CyclinB exporting it from the nucleus and avoiding dephosphorylation. Another mechanism that involves G2 arrest not involving CDK1 is repression of topoisomerase II. In G2 phase, topoisomerase II helps to bring about the higher order compaction of chromatin to form highly condensed mitotic chromosomes. Inhibition of topoisomerase II is sufficient to arrest cells in G2 phase (Anderson and Roberge 1996). CDK1 is also commonly targeted by viral proteins which mediate host cell cycle machinery to benefit viral survival or replication. For instance, cell cycle G2/M arrest is induced by HIV-1 Vpr (Zhao and Elder 2005). In the presence of HDV RNA TOP2A and TOP2B were found differentially expressed. TOP2A was found up-regulated and TOP2B was found down regulated.

Integrins are cell surface receptors which mediate the adhesion to the extracellular matrix (ECM). Integrins can signal through the cell membrane in either direction: the extracellular binding activity of integrins is regulated from the inside of the cell (inside-out signaling), while the binding of the ECM elicits signals that are transmitted into the cell (outside-in signaling) (Desgrosellier and Cheresh 2010). Because many integrins recognize Arg-Gly-Asp (RGD) sequences, which are displayed on the exposed loops of many viral capsid proteins, integrins became an easy target to viral attachment and entry. Adenovirus, for instance, interacts with αv integrins via an RGD sequence which allows it to enter cells. Human cytomegalovirus (HCMV) and Kaposi's sarcoma-associated herpesvirus (KSHV) also bind to several integrins thus facilitating cell entry and infection. β3 integrins are also receptors for pathogenic strains of hantaviruses. Rotaviruses seem to utilize β1 integrins and finally Echovirus-1 (EV1) uses integrins as receptors during cell entry. (Stewart and Nemerow 2007). Integrins may also provide signals that may render macrophages more susceptible to HIV-1 infection (Ballana *et al.* 2011). Integrin signaling mediates cell migration, tumor metastasis and cell differentiation. Three proteins belonging to *integrin signaling* were found differentially expressed in the presence of HDV RNA. ACTN1, ACTN4 and

ARF1 were found up-regulated. In the presence of HDV RNA, just like in the presence of SHDAg, two proteins involved in *HIF1α signaling* were also found differentially expressed. Both APEX1 and LDHA were found down regulated.

Viral proteins mediate host cell cycle machinery to benefit viral survival or replication. Furthermore, some viruses seem to inhibit or activate some genes that may lead to uncontrolled cell proliferation and subsequently to cancer. Results obtained due to HDV RNA accumulation, showed it is possible that HDV RNA induces alterations in the host cell cycle in order to benefit its own replication. Moreover, since HDV increases the risk of development of HCC, HDV RNA also may interfere with genes involved in this pathway inducing cell proliferation by not allowing G2 arrest. As for HIF and VEGF signaling pathways, they seem to be connected since HIF seems to regulate the expression of VEGF proteins. HIF1α signaling pathway seems to be altered both in the presence of SHDAg and HDV RNA. As discussed above, HDV induces oxidative stress leading to the accumulation of HIF. Accumulation of HIF leads to the expression of VEGF signaling pathway genes. VEGF expression induced by hypoxia is considered to be an inducer of increased vascular supply to tumors allowing them to grow and metastasize. These results confirm that in fact HDV seems to increase the risk of development of cancer. As for integrins they are involved in viral attachment and entry due to their capacity to recognize RGD sequences in the viral capsid proteins. It is most unlikely that these alterations in this pathway may be due to viral entry, because there are no viral capsid proteins in the model used. However if HDV RNA replication can mimetize what happens in cells infected by HDV, then *integrin signaling* pathway may be altered because HDV provides signals to integrins which in turn increase susceptibility to HDV infection. Integrins also can regulate cell proliferation. This result once more confirms the remaining results that seem to point out to the capacity of HDV to increase cell proliferation.

A network with all differentially expressed proteins resulting from HDV accumulation was built. Thirty nine proteins were differentially expressed and only six proteins were found to interact with each other. Protein TNPO1 binds to protein ELAVL1, protein PRDX1 binds to PRDX4 and protein TOP2A binds to TOP2B.

TNPO1 is a nuclear transport receptor involved in nuclear protein import serving as a receptor for nuclear localization signals (NLS) in cargo substrates. It is thought to mediate docking of the importin/substrate complex to the nuclear pore complex (NPC) through binding to nucleoporin. Through an energy requiring RAN-dependent

mechanism, the complex is then translocated to the pore. In case of HIV-1 infection, TNPO1 binds to and mediates the nuclear import of HIV-1 Rev. ELAV-like protein 1 is a protein that binds and stabilizes AU- and U-rich elements (AREs)-containing mRNAs enconding proto-oncogenes, cell cycle regulators, cytokines and growth factors. ELAVL1 is involved in MYC stabilization. TNPO1 is up-regulated in the presence of HDV RNA while ELAVL1 is down regulated. ELAVL1 contains a bidirectional transport signal that mediated both its nuclear import and export. It was seen by Rebane *et al* that ELAV1 binds to TNPO1 and that most likely TNPO1 imports ELAVL1 (Rebane *et al.* 2004). Although these proteins interact with each other the relevance here is not so much that interaction but more the up-regulation of TNPO1 and the down regulation of ELAVL1. Because TNPO1 imports proteins with NLS it is possible that SHDAg, after translation, enters the nucleus via TNPO1 to form the ribonucleoproteins. As for ELAVL1, recently, it was shown by Kim *et al*. that c-myc was repressed by it (Kim *et al.* 2009). c-myc is a proto-oncogene that is stabilized by up-regulation and/or post-translational modifications. If ELAVL1 represses c-myc, then the down-regulation of ELAVL1 would increase the stabilization of c-myc. Since c-myc is an oncogene and HDV increases the risk to develop HCC, it is possible that HDV RNA down-regulates ELAVL1 in order to induce c-myc stabilization. Both the down-regulation of ELAVL1 and the up-regulation of TNPO1 were validated by western blot analysis. The same pattern obtained during p53 validation was also observed.

PRDX1 and PRDX4 are involved in redox regulation of the cell by, among other things, catalyzing peroxide reduction of H_2O_2. Recently, it was shown that H_2O_2 modulates cell signaling through oxidizing PRDX1 (Neumann *et al.* 2009). Both PRDX1 and PRDX4 were found up-regulated in the presence of HDV RNA. Until now, all the results point to oxidative stress induced by SHDAg. The up-regulation of both PRDX1 and PRDX4 seems to confirm even more those assumptions since an increase of peroxides should lead to an increase in PRDX in an attempt to the cells regulate their metabolism.

Type II DNA topoisomerases are ATP-dependent enzymes that catalyze topological changes in DNA. In mammalian cells two isoforms of type II DNA topoisomerases, encoded by different genes, exist: the TOP2A and TOP2B. These proteins have been seen to form heterodimers and seem to have differences in its expression during cell cycle. While TOP2A shows proliferation and cell cycle dependent expression, TOP2B is mainly expressed in stationary cells and at constant

level during all phases of cell cycle. TOP2A was found to be up-regulated while TOP2B was found to be downregulated, confirming that HDV RNA accumulation induces alterations in the host cell cycle.

Networks involving differentially expressed proteins due to HDV accumulation and proteins involved in IPA database were also built. Again these networks may be useful to indicate interesting lines of research.

In order to determine alterations in cells due to HDV replication, differentially expressed proteins obtained due to the expression of SHDAg and differentially expressed proteins obtained due to HDV RNA accumulation, were joined and analyzed altogether.

Using IPA it was possible to determine which pathways were found more significantly altered during HDV replication. Those pathways were: *Cell cycle: G2/M DNA damage checkpoint regulation*, *HIF1α Signaling*, *Protein ubiquitination pathway* and *Glycolysis/Gluconeogenesis*. Four proteins belonging to the *cell cycle: G2/M DNA damage checkpoint regulation pathway* were found differentially expressed. PRKDC, TOP2B and p53 were found down-regulated while TOP2A was found up-regulated. As for the *HIF1α Signaling pathway*, five proteins involved in this pathway were found differentially expressed. HSP90AA1, LDHA and LDHB were found up-regulated while APEX1 was found down-regulated. Six proteins belonging to the *Protein ubiquitination pathway* were found differentially expressed. HSP90AA1, HSPA4, PSMD11 and UBA1 were found up-regulated while HSPE1 and USP39 were found down-regulated. Finally, regarding *Glycolysis/Gluconeogenesis pathway*, ENO1, LDHA, LDHB and TPI1 were found up-regulated.

Both *HIF1α signaling* and *glycolysis/gluconeogenesis pathways* are directly connected since most genes encoding glycolysis proteins are under the control of HIF1α. As already described above, HCV seems to induce oxidative stress in cells. It is likely that HDV replication also leads to oxidative stress, leading to hypoxia and activation of HIF thus altering glycolysis. As for *cell cycle: G2/M DNA damage checkpoint regulation pathway* and *protein ubiquitination pathway* results suggest that SHDAg targets proteins for degradation thus increasing the expression of the proteins involved in the protein ubiquitination pathway. These results would also explain the down regulation of p53 both in *HIF1α signaling pathway* and in *cell cycle: G2/M DNA*

damage checkpoint regulation pathway and *protein ubiquitination pathway*. SHDAg would cause p53 degradation by inducing the ubiquitination pathway. If p53 is destroyed, G2 checkpoint will not be activated leading to uncontrolled cell proliferation. To further validate this result, by western blot analysis it was seen that protein 14-3-3σ is also found down-regulated during HDV replication. p53 regulates expression of 14-3-3σ which binds to the phosphorylated CDK1-cyclin B complex exporting it to the cytoplasm and preventing it from dephosphorylation thus inducing cell arrest. If SHDAg induces p53 degradation, 14-3-3σ will also be down-regulated avoiding CDK1/CyclinB export out of the nucleus and consequent dephosphorylation of the complex CDK1/CyclinB inducing mitosis and uncontrolled cell proliferation.

Finally, a network with all differentially expressed proteins was built. Besides the interactions already described above, it was also seen that APEX1 and ELAVL1 both act on p53. TNPO1 binds to CCT3, SRP19 and HSP90AA1. Furthermore, p53 binds to USP39, inhibits and acts on TOP2A and acts on TOP2B. Both TOP2A and TOP2B bind to PRKDC. BSG binds to PPIA, which indirectly interacts with both PRDX1 and PRDX4.

APEX1 is a multifunctional protein that plays a central role in the cellular response to oxidative stress. It is involved in DNA repair and also redox regulation of transcriptional factors. It was shown that APEX1 can stimulate p53 transactivation *in vivo* and silencing of APEX1 leads to a down-regulation of p53 levels and activity (Seemann and Hainaut 2005). Both APEX1 and p53 were found down-regulated showing a consistency of the results.

Both TOP2A and TOP2B were seen to interact with the c-terminal region of p53 (Cowell *et al.* 2000). The loss of wild type (wt) p53 or the decrease in p53 expression may lead to unregulated or inappropriate expression of TOP2A, resulting in cell proliferation, chromosomal rearrangements and/or gene amplifications seen in tumor cells. In the presence of HDV RNA p53 was found down-regulated as well as TOP2B and TOP2A was found up-regulated. Again these results seem to confirm the theory that HDV induces alterations in the cell cycle to increase cell proliferation.

Moreover, five proteins, RNA-binding protein 8A (RBM8A - Q9Y5S9), ADP-ribosylation factor 1 (ARF1 - P84077), Protein FAM136A (Q96C01), Transcription intermediary factor 1-beta (TIF1B - Q13263) and L-lactate dehydrogenase A chain (LDHA - P00338) were found differentially expressed both in experiments 4 and 5.

Proteins ARF1, FAM136A and RBM8A were found to be up regulated in both experiments showing that both SHDAg and HDV genomic RNA induce alterations in the expression of these proteins, whereas proteins TIF1B and LDHA were found to be up-regulated in the presence of the delta antigen, followed by down regulation during HDV genomic RNA accumulation.

RBM8A, also known as Y14, is part of the exon-exon junction complex (ECJ), a multiprotein complex that assembles on the exon-exon junctions of mRNAs produced by splicing enhancing their translation. In the nucleus, the ECJ complex stimulates the mRNA export which is probably mediated, at least in part, by the RNA binding protein Aly/REF, which binds the mRNA export factor TAP. Along with the mRNAs, the protein RBM8A is also exported to the cytoplasm. RBM8A remains associated with the mRNAs in the cytoplasm until they are translated and translation is required to remove RBM8A from mRNAs. Besides splicing, mRNA export and translation, ECJ is also involved in nonsense-mediated mRNA decay (NMD). RBM8A and TAP were found to accumulate within and around SC35 domains and functionally associate with RNA (Schmidt *et al.* 2006). In the presence of the delta antigen and HDV genomic RNA, RBM8A was found to be up regulated. Although HDV mRNA does not contain introns, such as many others viral transcripts also transcribed by RNA polymerase II, there must be a way to integrate these transcripts into cellular export pathways. Herpes simplex virus type 1 (HSV-1) and human cytomegalovirus (HCMV), for instance, express the multifunctional proteins ICP27 and UL69, respectively that bind to unspliced viral mRNAs and promote their export by interacting with mRNA export proteins Aly/Ref or UAP56 (Schneider and Wolff 2009). Since HDV only codes for one protein that contains an RNA binding motif and in presence of HDV RNA they accumulate in SC35 speckles just like RBM8A, it is possible that SHDAg recruits RBM8A promoting the export of the HDV mRNAs to the cytoplasm by interacting with the export receptor TAP.

The ADP ribosylation factor (Arf) family of proteins belongs to the Ras superfamily of small GTPases. Arf proteins were shown to regulate vesicular traffic and organelle structure by recruiting coat proteins, regulating phospholipid metabolism and modulating the structure of actin at membrane surfaces. Vesicular trafficking is mediated by transport vesicles that bud from a donor compartment to an acceptor compartment. The recruitment of “coat” proteins leads to local membrane deformation and is essential for the formation of transport vesicles during vesicle budding and cargo

selection. Along the secretory pathway, three types of coated carriers have already been well characterized: coat protein complex I (COPI)-coated vesicles that function in the early secretory pathway, COPII vesicles that that export proteins from the endoplasmic reticulum (ER) and Clathrin-coated vesicles (CCVs) that mediate transport in the late secretory pathway and the endocytic pathway transporting cargo that exists in the *trans*-Golgi network (TGN). Arf1, among other things, is involved in the recruitment of COPI allowing transport from the Golgi to the ER in the early secretory pathway and regulates the formation of CCVs on the TGN and endosomal membranes (D'Souza-Schorey and Chavrier 2006).

Plus-stranded RNA viruses replicate and assemble on modified intracellular membranes. Cells infected by these viruses undergo a dramatic remodeling of their intracellular membranes and RNA replication frequently takes place on the cytosolic leaflet of these remodeled membranes (Hsu *et al.* 2010). Hepatitis C virus (HCV) is one of those cases. In infected cells, HCV induces the formation of membrane alterations, so called, membranous webs, which are sites of RNA replication and viral particle assembly. Recently, Arf-1 was found to be implicated in the regulation of HCV RNA replication and the production of infectious particles (Matto *et al.* 2011).

It was recently shown that the morphogenesis of HDV is mediated by a clathrin-mediated post-Golgi membrane trafficking and that clathrin heavy chain (CHC) is essential for the formation of HDV VLPs by LHDAg, which has been identified as a clathrin-adaptor like protein (Huang *et al.* 2007; Huang *et al.* 2009). Nuclear LHDAg is transported to the TGN where interacts with HBsAg and CHC for HDV morphogenesis. Subsequently, HDV particles are packaged into CCVs that leave the TGN and enter into the late endosome or secretory vesicle before release (Huang *et al.* 2009).

Arf1 was found to be 6x up regulate in the presence of SHDAg and when HDV RNA was added to cells the expression of Arf1 increased approximately 40%. Until now, SHDAg was only described as essential for HDV accumulation. Although SHDAg apparently does not have a direct action in viral particle assembly and packaging, opposite to LHDAg which is essential for that matter, it is possible to speculate that SHDAg and HDV RNA cannot mimetize HDV infection and induce recruitment of clathrin adaptors that will regulate the formation of CCVs thus preparing cells for LHDAg which will induce viral particles assembly and packaging. Furthermore Arf1 belongs to the integrins signaling pathway which seems to increase susceptibility to

HDV infection. All these facts seem a good starting point to look further into this protein closely.

The KRAB domain, or Krüppel-associated box, is a conserved domain found in about one-third of genes encoding C_2H_2 zinc-finger proteins, being the largest single family of transcriptional regulators in the mammalian genome. Members of the KRAB-containing protein family bind DNA through their C_2H_2 zinc-finger domains whereas the KRAB domain, which is found in the amino-terminal region of proteins, behaves as a strong transcriptional repressor domain by binding corepressor proteins. Proteins from the KRAB-containing protein family seem to be involved in transcriptional repression of RNA polymerase I, II and III promoters and binding and splicing of RNA and control of nucleolus function (Urrutia 2003). Briefly, KRAB-containing proteins bind to their corresponding DNA sequence and trigger the recruitment of the corepressor protein transcriptional intermediary factor 1β (TIF1B, also known as KRAB-associating protein 1 (KAP1) and TRIM28). TIF1B acts as a scaffolding protein to recruit heterochromatin protein 1 isoforms (HP1α, HP1β and HP1γ), HDACs and Setdb1 and silences gene expression by forming a facultative heterochromatin environment on a target promoter (Schultz *et al.* 2002). By interacting with MDM2, a major regulator of the p53 tumor suppressor, TIF1B stimulates p53-HDAC1 complex formation and inhibits p53 acetylation contributing to p53 functional regulation (Wang *et al.* 2005). Several viruses seem to use the TIF1B pathway to silence genes. Karposi's sarcoma-associated herpesvirus (KSHV), an oncogenic γ-herpesvirus involved in the pathogenesis of Kaposi's sarcoma, undergoes both lytic and latent infections, with a strong tendency to the latter. TIF1B was found to be a regulator of viral latency in KSHV (Chang *et al.* 2009). TIF1B was also found to be involved in suppression of human papillomavirus (HPV) transcription and replication mediated by viral gene E8-E2C (Ammermann *et al.* 2008). In Epstein-Barr virus (EBV), TIF1B was found to be associated with the lytic replication origin (OriLyt). Until now, little is known about gene expression regulation during HDV infection. The delta antigens seem to interact with several host factors associated with transcription such as nucleolin, nucleophosmin, YY1 and DIPA (Lee *et al.* 1998; Du *et al.* 2006; Huang *et al.* 2008). Although the effects of these interactions on gene expression have not yet been demonstrated, there is a possibility that HDAgs, through these interactions, might have a role in genetic regulation. It has been shown that the RNA binding domain of SHDAg bears considerable homology to canonical

binding domains such as the one found in the eukaryotic SRY gene (Veretnik and Gribskov 1999). Furthermore, SHDAg contains a coiled-coil domain that allows protein-protein interaction and is essential for activator functions of SHDAg. In 2006, a model for SRY function was proposed in which SRY recruits the KRAB-TIF1B complex as a chromatin modulator which provides a molecular mechanism of SRY as a transcription factor (Oh and Lau 2006). In cells expressing the SHDAg, TIF1B was found to be 5x upregulated. All these observations taken together lead to the suggestion that SHDAg might be capable of direct interaction with cellular DNA promoters thus recruiting TIF1B and stimulating gene repression. In cells expressing HDV RNA, expression of TIF1B was not so high as in cells expressing only the SHDAg. These results suggest that HDV represses host gene expression facilitating its replication.

In order to generate ATP, cells convert glucose into pyruvate generating ATP using oxidative phosphorylation. In the absence of oxygen, cells go through lactic fermentation in which glucose is converted to pyruvate which is finally converted into lactate using L-lactate dehydrogenase A (LDHA), resulting in pronounced glucose consumption. Many rapidly growing cells, such as cancer cells, tend to convert all glucose to lactate regardless the presence of oxygen, which was called as the Warburg effect (Hsu and Sabatini 2008). The Warburg effect has been directly linked to the activation of oncogenes like the c-myc which thus results in the deregulated conversion of glucose to lactate (Vander Heiden *et al.* 2009). Furthermore, c-myc activation seems to inactivate the *ARF-Mdm2-p53 pathway* in vivo, canceling its protective checkpoint function and accelerating progression to malignancy (Dang *et al.* 2009).

In cells expressing the SHDAg results show that LDHA is 2x upregulated. When HDV RNA accumulated in cells, LDHA levels**,** although suffering a decrease in 40%, were still above its normal expression values. These results show that cells expressing SHDAg and HDV RNA utilize lactic fermentation. Since HDV highly increases the risk for the development of hepatocellular carcinoma it is possible that HDV activates c-myc leading first to the increase of LDHA favoring lactic fermentation and then inactivating p53, and consequently the *ARF-Mdm2-p53 pathway*, accelerating progression to malignancy.

Results obtained in this work give some important insights regarding host mechanisms used by HDV during its replication. Our results show that HDV replication affects mainly protein metabolism and energy pathways. One of the most altered energy

pathways induced by HDV replication is anaerobic glycolysis, which is seen by the up-regulation of the pathway and also of LDHA. The anabolism of the cell thus sees itself increased leading to oxidative stress which in turn activates the HIF1α signaling pathway to protect cells. Other interesting result is the up-regulation of the protein ubiquitination pathway. This result shows that HDV induces degradation of host proteins favoring the expression of the viral proteins. Vesicular trafficking is also affected by favoring the transport of viral particles, being Arf1 involved in this trafficking. Although all virus components are not present in this model, SHDAg and HDV RNAs, seem to induce vesicular trafficking preparing the cell to the formation of viral particles. In order to replicate and form viral particles HDV induces alteration in the cell cycle, by corrupting G2/M checkpoint regulation. p53 is down-regulated during HDV replication, maybe by being destroyed by the protein ubiquitination pathway, inducing down regulation of 14-3-3σ and uncontrolled cell division which may lead to neoplasia. Detachment of 293-HDV cells and death at day 6 after transfection and replication may be due to the fact that tetracycline may become toxic to the cells at a certain point leading to cell detachment and consequent cell death.

CHAPTER VI: FINAL CONCLUSIONS AND FUTURE PERSPECTIVES

Human hepatitis D virus is a very simple virus that directs host cell mechanisms to induce its own replication and pathogenesis, severely increasing the symptoms of patients previously infected with HBV and increasing the risk of HCC.

In the first part of this work, it was demonstrated that HSP105 and hnRNP H, found differentially expressed in the presence of HDV in a previous work (Mota 2008; Mota *et al*. 2009), affect HDV replication. Results showed that HSP105 may be involved in RNP transport and attachment to the ER or even in viral particle assembly. Furthermore, HSP105, as an anti-apoptotic, may be recruited by HDV enabling HDV replication. As for hnRNP H, it may be involved in HDV replication, probably by being recruited by the virus to regulate translation of the delta antigens and in the export of the RNPs to the cytoplasm. Furthermore, hnRNP H may also bind hnRNP H leading to the splicing of pre-mRNAs that will produce key proteins essential for viral replication and/or assembly.

In the second part of this work, using a model by Chang *et al* to study HDV replication, it was possible to determine some of the mechanisms used by the virus. Several metabolic pathways, like Glycolysis, HIF1a and G2/M checkpoint regulation and key proteins, like TNPO1, p53 and Arf1 were shown to be associated with HDV replication. An integration of all the data was possible giving a biological meaning to the results and showing some of the possible mechanisms of HDV replication at category level, pathway level and even at the protein level. Using western blot analysis the validation of the method was performed at the protein level and at the pathway level. The results obtained by proteomics gave some important insights regarding how HDV may replicate, however to deepen this results several assays may be performed. Using proteomics, cellular fractionation would be of great help to identify and quantify more proteins regarding a specific cellular component. Furthermore, PTM determination would also be of great importance for proteins of interest. As for functional assays, immunoprecipitation assays to determine interaction with the delta antigens; *in situ* hybridization to determine possible interaction with the HDV RNAs; immunofluorescence assays to determine co-localizations and RNAi to determine how the virus reacts to the silencing of proteins of interest, would be of great help. A nuclear import assay is being performed in our lab to determine involvement of TNPO1 in the transport of SHDAg into the nucleus. These assays will be of great help in unraveling HDV replication mechanisms.

SUPPLEMENTARY INFORMATION I: DIFFERENTIALLY EXPRESSED PROTEINS FOR EXPERIMENTS 1, 2, 3, 4 AND 5 AND SIGNIFICANT DATA ASSOCIATED

SI.1. DIFFERENTIALLY EXPRESSED PROTEINS IN EXPERIMENTS 1, 2, 3, 4 AND 5.

Table SI.1.: Differentially expressed proteins for experiments 1, 2, 3, 4 and 5.

	Protein name	Accession number	Symbol	Fold	FDRq (%)
Experiment 1	Mucolipin-2	Q8IZK6	MCOLN2	55.04	0.00
	ATP-citrate synthase	P53396	ACLY	12.80	0.00
	Nephrocystin-1	O15259	NPHP1	-15.33	0.00
	ATP-dependent RNA helicase A	Q08211	DHX9	1.43	0.00
	Fatty acid synthase	P49327	FASN	1.36	0.01
	Elongation factor 2	P13639	EEF2	1.24	0.16
	Poly [ADP-ribose] polymerase 1	P09874	PARP1	1.23	0.23
Experiment 2	ADE02 E1B protein, large T-antigen	P03244	E1B	-3.42	0.00
	60S ribosomal protein L12	P30050	RPL12	-4.14	0.00
	39S ribosomal protein L45, mitochondrial	Q9BRJ2	MRPL45	3.92	0.00
	Stress-induced-phosphoprotein 1	P31948	STIP1	2.75	0.00
	Histone H2A type 1-B/E	P04908	HIST1H2AB/E	-2.93	0.00
	ADE05 E1B protein, large T-antigen	P03243	E1B-55	-2.41	0.00
	14-3-3 protein epsilon	P62258	YWHAE	2.08	0.00
	DNA topoisomerase 2-beta	Q02880	TOP2B	-2.44	0.00
	Mitochondrial import inner membrane translocase subunit	Q3ZCQ8	TIMM50	-3.35	0.00
	Histone H2B type 1-B	P33778	HIST1H2BB	-1.98	0.00
	Plasminogen activator inhibitor 1 RNA-binding protein	Q8NC51	SERBP1	2.44	0.00
	Ras-related protein Rab-5C	P51148	RAB5C	-3.39	0.00
	Desmin	P17661	DES	2.83	0.00
	Pyruvate kinase isozymes M1/M2	P14618	PKM2	1.88	0.00
	Cytochrome b5 type B	O43169	CYB5B	-2.85	0.00
	Putative heat shock protein HSP 90-alpha A5	Q58FG0	HSP90AA5P	2.48	0.00
	Vimentin	P08670	VIM	1.71	0.01
	Transgelin-2	P37802	TAGLN2	2.55	0.01
	Lin-7 homolog A	O14910	LIN7A	-2.60	0.01
	Histone H4	P62805	HIST4H4	-2.28	0.01
	Oxysterol-binding protein-related protein 8	Q9BZF1	OSBPL8	-2.63	0.01
	Lamin-A/C	P02545	LMNA	2.68	0.01
	Signal recognition particle 14 kDa protein	P37108	SRP14	-2.78	0.02
	Nascent polypeptide-associated complex subunit alpha	Q13765	NACA	1.86	0.02
	Glyceraldehyde-3-phosphate dehydrogenase	P04406	GAPDH	1.77	0.03
	Glycerol kinase 2	Q14410	GK2	-2.43	0.03
	Succinate dehydrogenase [ubiquinone] flavoprotein subunit	P31040	SDHA	-1.86	0.03
	Heat shock 70 kDa protein 1	P08107	HSPA1B	1.90	0.03
	Small nuclear ribonucleoprotein-associated proteins B and	P14678	SNRPB	-2.40	0.03
	Neutral amino acid transporter B(0)	Q15758	SLC1A5	-2.16	0.03
	Pescadillo homolog	O00541	PES1	-2.43	0.04
	Elongation factor 1-alpha 2	Q05639	EEF1A2	2.43	0.06
	14-3-3 protein beta/alpha	P31946	YWHAB	1.83	0.06
	ATP-dependent RNA helicase DDX18	Q9NVP1	DDX18	-1.77	0.08

	Heat shock 70 kDa protein 1L	P34931	HSPA1L	1.58	0.15
	40S ribosomal protein S4, X isoform	P62701	RPS4X	1.69	0.16
	Dolichyl-diphosphooligosaccharide--protein glycosyltransfe	P04843	RPN1	-1.59	0.33
	Putative heat shock protein HSP 90-beta 2	Q58FF8	HSP90AB2P	1.68	0.41
	Elongation factor 1-alpha 1	P68104	EEF1A1	1.47	0.82
Experiment 3	Ras-related protein Rab-6A	P20340	RAB6A	35.63	0.00
	Uncharacterized protein C15orf42	Q7Z2Z1	TICRR	44.29	0.00
	Cofilin-1	P23528	CFL1	21.78	0.00
	Signal recognition particle 19 kDa protein	P09132	SRP19	12.64	0.00
	SWI/SNF-related matrix-associated actin-dependent regulat	O60264	SMARCA5	6.72	0.00
	Heterogeneous nuclear ribonucleoprotein D-like	O14979	HNRPDL	6.84	0.00
	Isocitrate dehydrogenase [NAD] subunit beta, mitochondri	O43837	IDH3B	5.24	0.00
	Protein S100-A9	P06702	S100A9	3.24	0.00
	Heat shock 70 kDa protein 1	P08107	HSPA1B	-1.97	0.00
	Squalene synthetase	P37268	FDFT1	-3.19	0.00
	Eukaryotic initiation factor 4A-I	P60842	EIF4A1	-2.71	0.00
	Elongation factor 1-beta	P24534	EEF1B2	2.99	0.00
	NADH-cytochrome b5 reductase 3	P00387	CYB5R3	2.88	0.00
	Histone H4	P62805	HIST4H4	2.05	0.01
	DNA replication licensing factor MCM2	P49736	MCM2	-2.61	0.01
	Stomatin-like protein 2	Q9UJZ1	STOML2	2.48	0.03
	rRNA 2'-O-methyltransferase fibrillarin	P22087	FBL	2.57	0.04
	Programmed cell death protein 6	O75340	PDCD6	2.63	0.04
	Calnexin	P27824	CANX	2.14	0.04
	Electron transfer flavoprotein subunit alpha, mitochondri	P13804	ETFA	-2.10	0.05
	Histone H3.1t	Q16695	HIST3H3	1.83	0.08
	Vacuolar protein sorting-associated protein 35	Q96QK1	VPS35	-2.36	0.08
Experiment 4	Cofilin-1	P23528	CFL1	51.10	0.00
	Dermcidin	P81605	DCD	43.87	0.00
	Obg-like ATPase 1	Q9NTK5	OLA1	24.51	0.00
	RNA-binding protein 8A	Q9Y5S9	RBM8A	10.18	0.00
	G-rich sequence factor 1	Q12849	GRSF1	10.75	0.00
	Eukaryotic translation initiation factor 3 subunit D	O15371	EIF3D	11.24	0.00
	Hornerin	Q86YZ3	HRNR	9.11	0.00
	ADP-ribosylation factor 1	P84077	ARF1	6.52	0.00
	Ras-related protein Rab-6A	P20340	RAB6A	8.71	0.00
	Glucosidase 2 subunit beta	P14314	PRHCSH	-10.45	0.00
	Protein FAM136A	Q96C01	FAM136A	-37.72	0.00
	ATP synthase subunit e, mitochondrial	P56385	ATP5I	-4.43	0.00
	Signal recognition particle 19 kDa protein	P09132	SRP19	4.48	0.00
	DNA-binding protein A	P16989	CSDA	4.94	0.00
	Transcription intermediary factor 1-beta	Q13263	TRIM28	5.51	0.00
	Protein S100-A9	P06702	S100A9	4.64	0.00
	10 kDa heat shock protein, mitochondrial	P61604	HSPE1	-2.92	0.00
	Cytosolic non-specific dipeptidase	Q96KP4	CNDP2	3.80	0.00
	Leucyl-tRNA synthetase, cytoplasmic	Q9P2J5	LARS	3.52	0.00
	26S proteasome non-ATPase regulatory subunit 11	O00231	PSMD11	3.55	0.00
	Elongation factor 1-gamma	P26641	EEF1G	2.74	0.00
	Junction plakoglobin	P14923	JUP	-3.30	0.00
	L-lactate dehydrogenase A chain	P00338	LDHA	2.65	0.00

	Tight junction protein Z	Q07157	TJP1	-3.31	0.00
	Elongation factor 2	P13639	EEF2	2.47	0.00
	Oligosaccharyltransferase complex subunit OSTC	Q9NRP0	OSTC	-2.80	0.00
	Heterogeneous nuclear ribonucleoprotein D-like	O14979	HNRPDL	2.37	0.00
	Peptidyl-prolyl cis-trans isomerase A	P62937	PPIA	2.72	0.00
	Heat shock 70 kDa protein 4	P34932	HSPA4	2.47	0.00
	C-1-tetrahydrofolate synthase, cytoplasmic	P11586	MTHFD1	2.83	0.01
	L-lactate dehydrogenase B chain	P07195	LDHB	2.19	0.01
	Up-regulated during skeletal muscle growth protein 5	Q96IX5	USMG5	-2.62	0.01
	GPI-anchor transamidase	Q92643	PIGK	-2.78	0.01
	Squalene synthetase	P37268	FDFT1	-2.68	0.01
	Putative nucleoside diphosphate kinase	O60361	NME2P1	3.03	0.01
	Rab GDP dissociation inhibitor beta	P50395	GDI2	2.47	0.02
	Delta(3,5)-Delta(2,4)-dienoyl-CoA isomerase, mitochondrial	Q13011	ECH1	-2.27	0.03
	2-oxoglutarate dehydrogenase E1 component, mitochondrial	Q02218	OGDH	2.47	0.03
	Triosephosphate isomerase	P60174	TPI1	2.23	0.05
	Fascin	Q16658	FSCN1	2.76	0.06
	DNA-dependent protein kinase catalytic subunit	P78527	PRKDC	-2.21	0.06
	T-complex protein 1 subunit gamma	P49368	CCT3	2.19	0.07
	40S ribosomal protein S7	P62081	RPS7	2.47	0.07
	Cellular tumor antigen p53	P04637	TP53	-2.25	0.07
	Heat shock protein HSP 90-alpha	P07900	HSP90AA1	2.09	0.08
	Alpha-enolase	P06733	ENO1	1.83	0.26
	Ubiquitin-like modifier-activating enzyme 1	P22314	UBA1	1.84	0.35
	Splicing factor U2AF 65 kDa subunit	P26368	U2AF2	1.84	0.55
	Creatine kinase B-type	P12277	CKB	1.71	0.93
Experiment 5	2',3'-cyclic-nucleotide 3'-phosphodiesterase	P09543	CNP	-10.45	0.00
	Protein disulfide-isomerase A4	P13667	PDIA4	12.03	0.00
	ADP-ribosylation factor 1	P84077	ARF1	2.91	0.00
	60S ribosomal protein L6	Q02878	RPL6	-3.04	0.00
	BRI3-binding protein	Q8WY22	BRI3BP	33.74	0.00
	Transportin-1	Q92973	TNPO1	7.19	0.00
	Protein FAM136A	Q96C01	FAM136A	-14.33	0.00
	Nascent polypeptide-associated complex subunit alpha-2	Q9H009	NACA2	-6.61	0.00
	RNA-binding protein 8A	Q9Y5S9	RBM8A	4.72	0.00
	DNA-(apurinic or apyrimidinic site) lyase	P27695	APEX1	-3.90	0.00
	Alpha-actinin-4	O43707	ACTN4	2.40	0.00
	DNA topoisomerase 2-beta	Q02880	TOP2B	-3.45	0.00
	Cystatin-A	P01040	CSTA	3.34	0.00
	Erlin-1	O75477	ERLIN1	-2.97	0.00
	Neutral alpha-glucosidase AB	Q14697	GANAB	-2.05	0.00
	U4/U6.U5 tri-snRNP-associated protein 2	Q53GS9	USP39	-2.87	0.00
	ELAV-like protein 1	Q15717	ELAVL1	-2.02	0.00
	Alpha-actinin-1	P12814	ACTN1	1.97	0.00
	Peripherin	P41219	PRPH	-2.30	0.00
	Glutathione S-transferase omega-1	P78417	GSTO1	2.40	0.00
	Transcription intermediary factor 1-beta	Q13263	TRIM28	-1.86	0.00
	60S ribosomal protein L7	P18124	RPL7	-2.15	0.00
	60S ribosomal protein L7a	P62424	RPL7A	-2.15	0.00

	Peroxiredoxin-4	Q13162	PRDX4	1.80	0.00
	60S ribosomal protein L36	Q9Y3U8	RPL36	2.22	0.02
	Small nuclear ribonucleoprotein Sm D2	P62316	SNRPD2	2.22	0.02
	Basigin	P35613	BSG	-1.89	0.02
	60S ribosomal protein L22	P35268	RPL22	1.91	0.03
	Polypeptide N-acetylgalactosaminyltransferase 2	Q10471	GALNT2	-2.24	0.03
	Protein cornichon homolog 4	Q9P003	CNIH4	2.08	0.04
	Peroxiredoxin-1	Q06830	PRDX1	1.76	0.04
	Ubiquilin-1	Q9UMX0	UBQLN1	-2.15	0.05
	Alpha-adducin	P35611	ADD1	-2.31	0.07
	Cytochrome c oxidase subunit 4 isoform 1, mitochondrial	P13073	COX4I1	2.08	0.07
	Putative heat shock protein HSP 90-alpha A5	Q58FG0	HSP90AA5P	1.89	0.08
	60S ribosomal protein L12	P30050	RPL12	-1.77	0.09
	L-lactate dehydrogenase A chain	P00338	LDHA	-1.66	0.10
	Ribosomal L1 domain-containing protein 1	O76021	RSL1D1	-1.64	0.27
	DNA topoisomerase 2-alpha	P11388	TOP2A	1.62	0.37

SI.2. DIFFERENTIALLY EXPRESSED PROTEINS IN EXPERIMENTS 1, 2, 3, 4 AND 5 AND RELEVANT STATISTICAL PARAMETERS FOR QUANTIFICATION

Abbreviation of statistical parameters

q_A	peptide concentration in the non-labeled sample
q_SD_A	standard deviation of peptide concentration in the non-labeled sample
q_B	peptide concentration in the labeled sample
q_SD_B	standard deviation of peptide concentration in the labeled sample
q_log2ratio	base 2 logarithm of the ratio of A over B
q_alpha	kinetic constant
q_SD_alpha	standard deviation of the kinetic constant
q_sigma	scale parameter which determines the half-width of the peak
q_SD_sigma	standard deviation of scale parameter which determines the half-width of the peak
Vs	fitting weight
Xs	grand mean at the scan level
SD_Xs	standard deviation of the grand mean at the scan level
Ws	statistical weight at the scan level
FDRs	false discovery rate at the scan level
Xp	grand mean at the peptide level
SD_Xp	standard deviation of the grand mean at the peptide level
Wp	statistical weight at the peptide level
FDRp	false discovery rate at the peptide level
Xq	grand mean at the protein level
SD_Xq	standard deviation of the grand mean at the protein level
Zq	standardized variable
Wq	statistical weight at the protein level
FDRq	false discovery rate at the protein level
Scan/peptide	number of scans per identified peptide
Peptide/protein	number of peptides per identified protein

Table SI.2: Differentially expressed proteins for experiments 1, 2, 3, 4 and 5 and respective access numbers, peptide sequences and statistical parameters relevant for quantification. The table is composed by 3 tables SI.2.1., SI2.2. and SI2.3.

Table SI.2.1. Differentially expressed proteins for experiments 1, 2, 3, 4 and 5 and respective access numbers, peptide sequence, pI and A and B quantities.

Experiment	Protein	Accession (UniProt)	Gene	Sequence	pI	q_A	q_SD_A	q_B	q_SD_B
1	HUMAN Mucolipin-2	Q8IZK6	MCLN2	K.FYFM*SPCEK#.Y	5.99	2.3488	1.2495	129.2784	1.9101
1	HUMAN ATP-citrate synthase	P53396	ACLY	R.FGGALDAAAK#.M	5.84	116.9438	26.1102	1496.5340	43.2060
1	HUMAN Nephrocystin-1	O15259	NPHP1	R.QILGDVLLK.D	5.84	2180.5135	33.8581	142.2712	31.7037
1	HUMAN ATP-dependent RNA helicase A	Q08211	DHX9	K.LAQFEPSQR@.Q	6.00	1239.3923	25.6592	1783.3299	35.1979
1	HUMAN Fatty acid synthase	P49327	FAS	K.FDLSQNHPLGM*AIFLK#.N	6.88	806.7326	18.2863	1041.9473	21.3064
1	HUMAN Elongation factor 2	P13639	EF2	K.AYLPVNESFGFTADLR@.S	4.37	1023.8623	35.5393	1307.1319	42.0090
1	HUMAN Poly [ADP-ribose] polymerase 1	P09874	PARP1	K.AEPVEVVAPR.G	4.53	3649.7724	106.9220	4452.0961	139.6069
2	ADE02 E1B protein, large T-antigen	P03244	E1BL	K.VNLNGVFDM*TM*K.I	5.84	2531.3059	69.9527	1596.3211	75.7642
2	HUMAN 60S ribosomal protein L12	P30050	RL12	R.QAQIEVVPSASALIIK.A	6.00	1767.7148	37.7271	847.4172	40.4983
2	HUMAN 39S ribosomal protein L45, mitochondrial	Q9BRJ2	RM45	R.LM*YGQEDVPK#.D	4.37	34.8651	3.6566	271.5911	5.9094
2	HUMAN Stress-induced-phosphoprotein 1	P31948	STIP1	K.DPQALSEHLK#.N	5.44	104.9236	7.7111	619.8908	12.6788
2	HUMAN Histone H2A type 1-B/E	P04908	H2A1B	R.VTIAQGGVLPNIQAVLLPK.K	9.00	26206.0332	700.0159	24035.2152	768.9144
2	ADE05 E1B protein, large T-antigen	P03243	E1BL	R.HRPECITFQQIK.D	8.11	822.4260	22.9415	663.9606	25.2691

2	HUMAN 14-3-3 protein epsilon	P62258	1433E	K.AASDIAM*TELPPTHPIR@.L	5.44	454.8299	34.2891	1830.2017	46.1615
2	HUMAN DNA topoisomerase 2-beta	Q02880	TOP2B	K.HLTYNDFINK.E	6.88	550.8700	11.8553	797.4959	15.7946
2	HUMAN Mitochondrial import inner membrane translocase subunit	Q3ZCQ8	TIM50	K.QNLFLGSLTSR.L	10.25	1158.4933	93.8874	686.7008	105.5787
2	HUMAN Histone H2B type 1-B	P33778	H2B1B	K.AM*GIM*NSFVNDIFER.I	4.37	1666.8071	35.8645	1442.8819	38.6244
2	HUMAN Plasminogen activator inhibitor 1 RNA-binding protein	Q8NC51	PAIRB	K.SEEAHAEDSVM*DHHFR@.K	4.88	111.0199	6.9712	553.1255	9.6407
2	HUMAN Ras-related protein Rab-5C	P51148	RAB5C	R.QASPNIVIALAGNK.A	9.00	1227.4989	53.1110	719.5558	58.4887
2	HUMAN Desmin	P17661	DESM	K.VELQELNDR@.F	4.14	117.8548	4.4144	663.0341	7.0404
2	HUMAN Pyruvate kinase isozymes M1/M2	P14618	KPYM	K.GDYPLEAVR@.M	4.37	521.5740	19.2115	1640.9371	30.5641
2	HUMAN Cytochrome b5 type B	O43169	CYB5B	K.ELWLVIHGR.V	6.88	1014.9223	27.5370	707.9652	31.3920
2	HUMAN Putative heat shock protein HSP 90-alpha A5	Q58FG0	HS905	K.HIYYITGETK#.D	6.88	155.8360	15.9414	827.8322	23.9151
2	HUMAN Vimentin	P08670	VIME	K.FADLSEAANR@.N	4.37	997.4218	59.9564	3511.2755	86.3522
2	HUMAN Transgelin-2	P37802	TAGL2	K.NVIGLQM*GTNR@.G	10.25	73.0978	5.8018	370.8459	8.9392
2	HUMAN Lin-7 homolog A	O14910	LIN7A	R.EVYQYMHETITVNGCPEFR.A	4.77	235.0455	5.7919	179.7127	5.7260
2	HUMAN Histone H4	P62805	H4	K.VFLENVIR.D	6.00	22365.9690	618.2352	18119.4691	732.2031
2	HUMAN Oxysterol-binding protein-related protein 8	Q9BZF1	OSBL8	K.VVLPTFILEPR.S	6.00	819.5707	20.5636	619.9757	23.1336
2	HUMAN Lamin-A/C	P02545	LMNA	R.VAVEEVDEEGK#.F	3.91	15.2547	2.0120	81.1207	3.2599
2	HUMAN Signal recognition particle 14 kDa protein	P37108	SRP14	K.FQM*AYSNLLR@.A	8.65	1033.1088	35.2184	738.1366	38.7749
2	HUMAN Nascent polypeptide-associated complex subunit alpha	Q13765	NACA	K.DIELVM*SQANVSR@.A	4.37	189.0986	17.8361	698.9181	26.8615

2	HUMAN Glyceraldehyde-3-phosphate dehydrogenase	P04406	G3P	K.IISNASCTTNCLAPLAK#.V	7.91	621.0173	37.7345	1666.0595	49.8576
2	HUMAN Glycerol kinase 2	Q14410	GLPK2	K.TGLPLSTYFSAVK.L	8.61	1157.7029	28.3771	944.5079	32.4278
2	HUMAN Succinate dehydrogenase [ubiquinone] flavoprotein subunit	P31040	DHSA	K.EPIPVLPTVHYNM*GGIPTNYK.G	6.88	1226.3963	43.2406	1385.4938	45.5204
2	HUMAN Heat shock 70 kDa protein 1	P08107	HSP71	K.NQVALNPQNTVFDAK#.R	5.84	4212.6762	350.2848	18666.0758	471.0089
2	HUMAN Small nuclear ribonucleoprotein-associated proteins B and	P14678	RSMB	K.M*LQHIDYR.M	6.88	349.4851	8.4092	288.7298	9.6891
2	HUMAN Neutral amino acid transporter B(0)	Q15758	AAAT	R.NIFPSNLVSAAFR.S	10.25	2100.8793	64.8794	1898.3757	76.0565
2	HUMAN Pescadillo homolog	O00541	PESC	R.FLLHEPIVNK.F	6.88	396.2264	12.1036	323.7192	13.6599
2	HUMAN Elongation factor 1-alpha 2	Q05639	EF1A2	K.YYITIIDAPGHR@.D	6.87	146.7899	18.2758	708.7707	27.9278
2	HUMAN 14-3-3 protein beta/alpha	P31946	1433B	K.DSTLIM*QLLR@.D	5.84	461.6091	18.8172	2076.3777	29.5031
2	HUMAN ATP-dependent RNA helicase DDX18	Q9NVP1	DDX18	K.ELM*THHVHTYGLIM*GGSNR@.S	7.17	284.7381	11.4408	308.4930	12.3499
2	HUMAN Heat shock 70 kDa protein 1L	P34931	HS71L	K.AFYPEEISSM*VLTK#.L	4.53	2857.0315	153.5196	8809.7798	206.5626
2	HUMAN 40S ribosomal protein S4, X isoform	P62701	RS4X	K.GIPHLVTHDAR@.T	7.06	324.6896	20.3472	1285.3651	30.6151
2	HUMAN Dolichyl-diphosphooligosaccharide--protein glycosyltransfe	P04843	RPN1	K.NLVEQHIQDIVVHYTFNK#.V	6.23	728.2187	20.1752	1064.6027	21.8540
2	HUMAN Putative heat shock protein HSP 90-beta 2	Q58FF8	H90B2	K.ADLINNLGTIAK#.F	5.84	502.8388	27.0551	1938.5505	40.0699
2	HUMAN Elongation factor 1-alpha 1	P68104	EF1A1	K.STTTGHLIYK#.C	8.62	288.5158	26.9244	1282.8408	41.6481
3	HUMAN Ras-related protein Rab-6A	P20340	RAB6A	R.GSDVIIM*LVGNK#.T	5.84	67.9329	26.1692	1728.9695	41.7791
3	HUMAN Uncharacterized protein C15orf42	Q7Z2Z1	CO042	K.PEPTYVSPPCPR@.L	5.99	11.3915	7.7702	360.4124	11.6080

3	HUMAN Cofilin-1	P23528	COF1	K.NIILEEGK#.E	4.53	39.7353	4.6805	618.3468	8.1134
3	HUMAN Signal recognition particle 19 kDa protein	P09132	SRP19	R.FICIYPAYLNNK#.K	8.05	193.2168	18.9178	1744.5551	28.1057
3	HUMAN SWI/SNF-related matrix-associated actin-dependent regulator of chromatin subfamily A member 5	O60264	SMCA5	K.TLQTISLLGYM*K#.H	8.61	940.7589	42.9811	4026.2341	64.9893
3	HUMAN Heterogeneous nuclear ribonucleoprotein D-like	O14979	HNRDL	K.VFVGGLSPDTSEEQIK#.E	4.14	531.4753	40.0587	2595.9444	58.4649
3	HUMAN Isocitrate dehydrogenase [NAD] subunit beta, mitochondrial	O43837	IDH3B	K.IHTPM*EYK#.G	6.88	20.1824	1.0508	75.6074	1.6421
3	HUMAN Protein S100-A9	P06702	S10A9	R.NIETIINTFHQYSVK#.L	6.88	263.5531	5.0848	614.6625	6.8502
3	HUMAN Heat shock 70 kDa protein 1	P08107	HSP71	K.HWPFQVINDGDKPK.V	6.88	3536.7207	105.5514	1639.8243	109.4529
3	HUMAN Squalene synthetase OS	P37268	FDFT	R.M*GIGM*AEFLDK.H	4.37	991.2533	21.6410	222.1745	19.2025
3	HUMAN Eukaryotic initiation factor 4A-I	P60842	IF4A1	R.VFDM*LNR.R	5.84	1800.0782	57.0010	522.9371	58.8957
3	HUMAN Elongation factor 1-beta	P24534	EF1B	K.SPAGLQVLNDYLADK#.S	4.21	560.0049	30.7110	1197.3660	41.0070
3	HUMAN NADH-cytochrome b5 reductase 3	P00387	NB5R3	K.DILLRPELEELR@.N	4.41	1084.6335	40.1749	2234.4104	55.3732
3	HUMAN Histone H4	P62805	H4	K.VFLENVIR@.D	6.00	5349.2118	122.6915	8474.5264	169.6414
3	HUMAN DNA replication licensing factor MCM2	P49736	MCM2	R.GLALALFGGEPK.N	6.00	362.7967	8.1349	99.3255	8.0244
3	HUMAN Stomatin-like protein 2	Q9UJZ1	STML2	R.ILEPGLNILIPVLDR.I	4.37	750.2167	30.7970	1328.3929	37.8828
3	HUMAN rRNA 2'-O-methyltransferase fibrillarin	P22087	FBRL	K.NVM*VEPHR@.H	6.88	13.7403	0.5908	25.1975	0.8321
3	HUMAN Programmed cell death protein 6	O75340	PDCD6	K.AGVNFSEFTGVWK#.Y	6.00	256.2968	16.7497	482.1515	23.2129
3	HUMAN Calnexin	P27824	CALX	K.TPELNLDQFHDK#.T	4.55	1667.9226	52.0482	2901.8880	66.9650

3	HUMAN Electron transfer flavoprotein subunit alpha, mitochondrial	P13804	ETFA	K.QFNYTHICAGASAFGK.N	8.09	639.7554	14.1477	183.0712	13.7720
3	HUMAN Histone H3.1t	Q16695	H31T	K.STELLIR.K	6.00	829.3617	32.9818	898.0725	42.6232
3	HUMAN Vacuolar protein sorting-associated protein 35	Q96QK1	VPS35	K.HASNM*LGELR.T	6.88	147.7740	4.4754	44.8147	4.6332
4	HUMAN Cofilin-1	P23528	COF1	K.NIILEEGK#.E	4.53	16.7767	2.4176	572.6917	4.0505
4	HUMAN Dermcidin	P81605	DCD	K.ENAGEDPGLAR@.Q	4.14	24.1463	5.8059	869.5387	9.9341
4	HUMAN Obg-like ATPase 1	Q9NTK5	OLA1	R.VPVPDER@.F	4.37	17.1060	3.2819	280.2265	5.6596
4	HUMAN RNA-binding protein 8A	Q9Y5S9	RBM8A	K.FAEYGEIK#.N	4.53	71.7662	7.3868	557.7205	12.4526
4	HUMAN G-rich sequence factor 1	Q12849	GRSF1	R.YIELFLNSCPK#.G	5.99	326.3151	32.2473	2344.9601	47.0887
4	HUMAN Eukaryotic translation initiation factor 3 subunit D	O15371	EIF3D	K.EEM*DFPQLM*K#.M	4.14	43.4096	7.5114	326.1927	11.8779
4	HUMAN Hornerin	Q86YZ3	HORN	R.GPYESGSGHSSGLGHR@.E	7.06	12.7030	1.0856	77.3212	1.6202
4	HUMAN ADP-ribosylation factor 1	P84077	ARF1	R.DAVLLVFANK#.Q	5.84	420.9557	13.2231	1336.8220	20.4003
4	HUMAN Ras-related protein Rab-6A	P20340	RAB6A	R.GSDVIIM*LVGNK#.T	5.84	150.5837	22.4787	876.6369	35.0491
4	HUMAN Glucosidase 2 subunit beta	P14314	GLU2B	K.SLEDQVEMLR.T	4.14	1399.7047	19.2991	89.5224	18.9761
4	HUMAN Protein FAM136A	Q96C01	F136A	R.VQEAVESM*VK.S	4.53	606.3866	7.9127	10.7438	7.0170
4	HUMAN ATP synthase subunit e, mitochondrial	P56385	ATP5I	R.YSALFLGVAYGATR.Y	8.49	774.0903	21.0516	116.8970	21.0888
4	HUMAN Signal recognition particle 19 kDa protein	P09132	SRP19	R.FICIYPAYLNNK#.K	8.05	114.7083	10.5939	343.3790	14.3468
4	HUMAN DNA-binding protein A	P16989	DBPA	K.EDVFVHQTAIK#.K	5.44	107.1508	8.4707	354.0544	13.1877
4	HUMAN Transcription intermediary factor 1-beta	Q13263	TIF1B	K.DIVENYFM*R.D	4.37	219.3998	32.0150	808.2475	49.5420

4	HUMAN Protein S100-A9	P06702	S10A9	R.NIETIINTFHQYSVK#.L	6.88	23.8937	2.3315	74.1588	3.2013
4	HUMAN 10 kDa heat shock protein, mitochondrial	P61604	CH10	K.FLPLFDR.V	5.84	3885.7679	39.4911	924.2518	38.7594
4	HUMAN Cytosolic non-specific dipeptidase	Q96KP4	CNDP2	R.YPSLSLHGIEGAFSGSGAK#.T	6.88	69.3584	5.2081	176.2356	7.0505
4	HUMAN Leucyl-tRNA synthetase, cytoplasmic	Q9P2J5	SYLC	K.VIASELGSM*PELK#.K	4.53	123.3231	12.9132	317.5690	18.5336
4	HUMAN 26S proteasome non-ATPase regulatory subunit 11	O00231	PSD11	R.YQEALHLGSQLLR@.E	6.88	265.4105	20.1346	629.1895	26.6403
4	HUMAN Elongation factor 1-gamma	P26641	EF1G	K.DPFAHLPK#.S	6.88	184.2167	4.8839	430.3547	7.2794
4	HUMAN Junction plakoglobin	P14923	PLAK	R.NLALCPANHAPLQEAAVIPR.L	6.86	234.3807	7.0141	47.4445	6.8220
4	HUMAN L-lactate dehydrogenase A chain	P00338	LDHA	K.DQLIYNLLK#.E	5.84	508.7572	21.6043	747.4455	29.5227
4	HUMAN Tight junction protein ZO-1	Q07157	ZO1	R.EAGFLRPVTIFGPIADVAR.E	6.07	301.6968	9.1422	61.0006	7.9535
4	HUMAN Elongation factor 2	P13639	EF2	K.AYLPVNESFGFTADLR@.S	4.37	1076.3943	50.4619	2016.8874	65.1965
4	HUMAN Oligosaccharyltransferase complex subunit OSTC	Q9NRP0	OSTC	R.VPFLVLECPNLK.L	5.99	2426.1855	31.1076	589.6446	29.1571
4	HUMAN Heterogeneous nuclear ribonucleoprotein D-like	O14979	HNRDL	K.DLTEYLSR.F	4.37	1291.9045	20.3146	874.4923	22.7975
4	HUMAN Peptidyl-prolyl cis-trans isomerase A	P62937	PPIA	K.FEDENFILK#.H	4.14	2240.3754	50.9799	4034.8565	70.9165
4	HUMAN Heat shock 70 kDa protein 4	P34932	HSP74	K.SNLAYDIVQLPTGLTGIK#.V	5.84	747.7425	22.2668	1098.9188	26.8754
4	HUMAN C-1-tetrahydrofolate synthase, cytoplasmic	P11586	C1TC	R.AAQAPSSFQLLYDLK#.L	5.84	421.7513	16.9712	797.0585	22.3768
4	HUMAN L-lactate dehydrogenase B chain	P07195	LDHB	K.GEM*M*DLQHGSLFLQTPK#.I	5.44	306.9574	8.2778	468.4723	9.9265
4	HUMAN Up-regulated during skeletal muscle growth protein 5	Q96IX5	USMG5	K.YFNSYTLTGR.M	8.49	785.3709	19.3527	200.0895	19.0748
4	HUMAN GPI-anchor transamidase	Q92643	GPI8	K.NVLITDFFGSVR.K	5.84	483.3730	14.0748	116.2553	13.3193

4	HUMAN Squalene synthetase	P37268	FDFT	R.M*GIGM*AEFLDK.H	4.37	1009.3908	14.5471	251.8514	12.8608
4	HUMAN Putative nucleoside diphosphate kinase	O60361	NDK8	R.GDFCIQVGR@.N	5.82	528.5472	29.5441	1070.0087	41.6505
4	HUMAN Rab GDP dissociation inhibitor beta	P50395	GDIB	K.FVSISDLLVPK#.D	5.84	1052.7982	21.4809	1525.2963	28.1194
4	HUMAN Delta(3,5)-Delta(2,4)-dienoyl-CoA isomerase, mitochondrial	Q13011	ECH1	K.VIGNQSLVNELAFTAR.K	6.00	2001.5437	31.5163	646.0254	30.3405
4	HUMAN 2-oxoglutarate dehydrogenase E1 component, mitochondrial	Q02218	ODO1	K.VFHLPTTTFIGGQESALPLR@.E	6.88	119.9952	4.3507	201.1768	5.0492
4	HUMAN Triosephosphate isomerase	P60174	TPIS	K.VAHALAEGLGVIACIGEK#.L	5.52	917.9860	52.8166	1410.1258	61.5007
4	HUMAN Fascin	Q16658	FSCN1	R.LVARPEPATGYTLEFR@.S	6.14	290.3715	20.9136	535.2416	26.7566
4	HUMAN DNA-dependent protein kinase catalytic subunit	P78527	PRKDC	K.AALSALESFLK.Q	6.00	444.6633	9.3529	165.4539	9.2599
4	HUMAN T-complex protein 1 subunit gamma	P49368	TCPG	K.GISDLAQHYLM*R.A	6.88	773.3842	21.5902	928.0209	26.3509
4	HUMAN 40S ribosomal protein S7	P62081	RS7	K.VETFSGVYK#.K	6.00	257.0519	8.0456	424.8341	11.3401
4	HUMAN Cellular tumor antigen p53	P04637	P53	R.RPILTIITLEDSSGNLLGR.N	6.07	832.2483	16.6293	270.8995	16.9906
4	HUMAN Heat shock protein HSP 90-alpha	P07900	HS90A	K.SLTNDWEDHLAVK#.H	4.55	3234.1320	87.4017	3530.9317	104.0435
4	HUMAN Alpha-enolase	P06733	ENOA	K.LAM*QEFM*ILPVGAANFR@.E	6.00	684.5964	12.3157	752.0596	13.5105
4	HUMAN Ubiquitin-like modifier-activating enzyme 1	P22314	UBA1	K.SLVASLAEPDFVVTDFAK#.F	4.03	797.2182	16.9200	1052.4919	20.2662
4	HUMAN Splicing factor U2AF 65 kDa subunit	P26368	U2AF2	K.ELLTSFGPLK.A	6.00	2154.1741	30.1661	2809.2333	39.4721
4	HUMAN Creatine kinase B-type	P12277	KCRB	K.LLIEM*EQR@.L	4.53	1232.6357	24.0773	1272.6945	29.9166
5	HUMAN BRI3-binding protein	Q8WY22	BRI3B	R.SSPSGPSNPSNPSVEEK#.L	4.53	3.3187	1.0770	134.3588	1.6519
5	HUMAN Protein disulfide-isomerase A4	P13667	PDIA4	R.SHM*M*DVQGSTQDSAIK#.D	5.33	15.5681	4.5058	224.7296	6.0545

5	HUMAN Transportin-1	Q92973	TNPO1	R.DELLPHILPLLK#.E	5.44	31.3516	3.2001	294.7330	5.0509
5	HUMAN RNA-binding protein 8A	Q9Y5S9	RBM8A	K.FAEYGEIK#.N	4.53	93.7111	8.3509	531.1992	13.8368
5	HUMAN ADP-ribosylation factor 1	P84077	ARF1	R.DAVLLVFANK#.Q	5.84	440.1032	16.2911	1649.1174	25.1274
5	HUMAN 60S ribosomal protein L6	Q02878	RL6	K.AIPQLQGYLR.S	8.65	1907.2742	64.6140	1144.6441	71.6361
5	HUMAN 2',3'-cyclic-nucleotide 3'-phosphodiesterase	P09543	CN37	K.M*DLVTYFGK.R	5.84	748.3549	47.8209	85.9286	37.0028
5	HUMAN Nascent polypeptide-associated complex subunit alpha-2	Q9H009	NACA2	K.LVM*SQANVSR.A	10.25	92.7736	1.1259	16.8470	1.1073
5	HUMAN Protein FAM136A	Q96C01	F136A	R.VQEAVESM*VK.S	4.53	253.5647	5.7771	21.2295	4.7324
5	HUMAN DNA-(apurinic or apyrimidinic site) lyase	P27695	APEX1	R.QGFGELLQAVPLADSFR.H	4.37	454.1632	10.0326	139.8711	9.4676
5	HUMAN Alpha-actinin-4	O43707	ACTN4	K.GISQEQM*QEFR@.A	4.53	376.8351	13.7069	1185.0134	20.0731
5	HUMAN DNA topoisomerase 2-beta	Q02880	TOP2B	R.HVDYVVDQVVGK.L	5.33	597.2611	13.7314	207.6537	14.0612
5	HUMAN Cystatin-A	P01040	CYTA	K.TQVVAGTNYYIK#.V	8.47	36.2150	2.3271	144.9420	3.6325
5	HUMAN Erlin-1	O75477	ERLN1	R.ISEIEDAAFLAR.E	4.14	1815.8544	27.0785	733.9694	27.1685
5	HUMAN Neutral alpha-glucosidase AB	Q14697	GANAB	K.HHGPQTLYLPVTLSSIPVFQR.G	8.68	137.3868	3.6873	130.7352	3.8201
5	HUMAN U4/U6.U5 tri-snRNP-associated protein 2	Q53GS9	SNUT2	K.NPTIVNFPITNVDLR.E	5.84	963.2000	21.6120	402.9985	21.5983
5	HUMAN ELAV-like protein 1	Q15717	ELAV1	K.DANLYISGLPR.T	5.84	1511.7879	26.3388	1255.8724	30.5055
5	HUMAN Alpha-actinin-1	P12814	ACTN1	K.AIM*TYVSSFYHAFSGAQK#.A	8.48	715.9661	22.2167	1368.0236	26.3906
5	HUMAN Peripherin	P41219	PERI	K.NLQEAEEWYK.S	4.25	2865.0173	33.9722	1563.4159	35.4819
5	HUMAN Glutathione S-transferase omega-1	P78417	GSTO1	R.HEVININLK#.N	6.88	148.8577	8.0471	428.2464	11.9957

5	HUMAN Transcription intermediary factor 1-beta	Q13263	TIF1B	K.DIVENYFM*R.D	4.37	1111.8967	36.0325	568.6690	39.0641
5	HUMAN 60S ribosomal protein L7	P18124	RL7	R.IVEPYIAWGYPNLK.S	6.00	3672.6358	73.3296	1985.2462	75.6779
5	HUMAN 60S ribosomal protein L7a	P62424	RL7A	K.NFGIGQDIQPK.R	5.84	2242.5718	39.2394	1391.2965	44.3886
5	HUMAN Peroxiredoxin-4	Q13162	PRDX4	R.IPLLSDLTHQISK#.D	6.88	1674.2617	36.1135	2380.4262	45.9238
5	HUMAN 60S ribosomal protein L36	Q9Y3U8	RL36	R.YPM*AVGLNK#.G	8.61	170.8821	7.3211	454.2470	11.3042
5	HUMAN Small nuclear ribonucleoprotein Sm D2	P62316	SMD2	K.SEM*TPEELQK#.R	4.25	37.4033	1.9281	99.7005	2.8938
5	HUMAN Basigin	P35613	BASI	K.SESVPPVTDWAWYK.I	4.37	1918.0595	38.6125	872.3463	38.0847
5	HUMAN 60S ribosomal protein L22	P35268	RL22	K.AGNLGGGVVTIER@.S	6.00	451.0024	21.4270	911.7098	31.0502
5	HUMAN Polypeptide N-acetylgalactosaminyltransferase 2	Q10471	GALT2	K.HM*DLCLTVVDR.A	5.33	322.2547	21.7461	172.8523	21.3983
5	HUMAN Protein cornichon homolog 4	Q9P003	CNIH4	R.YIM*VPSGNM*GVFDPTEIHNR@.G	5.44	1311.7292	58.2622	3274.5551	65.0544
5	HUMAN Peroxiredoxin-1	Q06830	PRDX1	K.ATAVM*PDGQFK#.D	5.84	224.8664	18.5809	614.6187	27.4526
5	HUMAN Ubiquilin-1	Q9UMX0	UBQL1	R.NPEISHM*LNNPDIM*R.Q	5.44	1224.7458	28.5248	682.7862	28.6699
5	HUMAN Alpha-adducin	P35611	ADDA	R.M*LDNLGYR.T	5.84	222.9876	11.2249	115.8305	12.5011
5	HUMAN Cytochrome c oxidase subunit 4 isoform 1, mitochondrial	P13073	COX41	R.DHPLPEVAHVK#.H	6.23	93.6394	3.8645	233.5495	5.7111
5	HUMAN Putative heat shock protein HSP 90-alpha A5	Q58FG0	HS905	K.HIYYITGETK#.D	6.88	807.2832	26.4079	1942.5816	38.6606
5	HUMAN 60S ribosomal protein L12	P30050	RL12	K.IGPLGLSPK.K	9.00	1267.2991	16.8250	1148.0613	20.6679
5	HUMAN L-lactate dehydrogenase A chain	P00338	LDHA	K.DQLIYNLLK.E	5.84	1605.1589	42.9804	930.7605	48.7806
5	HUMAN Ribosomal L1 domain-containing protein 1	O76021	RL1D1	K.TVSQIISLQTLK.K	9.00	423.7950	16.3030	216.1216	16.8205

5	HUMAN DNA topoisomerase 2-alpha	P11388	TOP2A	K.IM*IM*TDQDQDGSHIK#.G	4.42	204.6550	7.5848	355.0821	9.5393

Table SI.2.2. Differentially expressed proteins for experiments 1, 2, 3, 4 and 5 and respective labeling efficiencies and statistical parameters relevant for quantification.

Experiment	Accession (UniProt)	q_log2Ratio	q_f	q_SD_f	q_Alpha	q_SD_Alpha	q_Sigma	q_SD_Sigma	Vs	Xs	SD_Xs	Ws	FDRs
1	Q8IZK6	-5.7824	0.9864	0.0051	0.1798	0.0581	0.0606	0.0009	70.7560	-5.7824	0.2308	44.9210	1.0002
1	P53396	-3.6777	0.9982	0.0088	0.1197	0.1204	0.0535	0.0014	17.9279	-3.6777	0.2448	34.5726	1.0002
1	O15259	3.9380	1.0107	0.0865	0.3084	0.0677	0.0620	0.0011	60.1021	3.9380	0.2317	44.1265	1.0002
1	Q08211	-0.5249	0.9464	0.0065	0.1614	0.0662	0.0602	0.0010	50.1765	-0.5249	0.2328	43.1244	1.5325
1	P49327	-0.3691	0.9650	0.0091	0.2606	0.0659	0.0696	0.0011	33.6757	-0.3691	0.2361	40.4021	1.0002
1	P13639	-0.3524	0.9728	0.0129	0.0006	0.1150	0.0620	0.0015	14.9736	-0.3524	0.2484	32.5887	1.7252
1	P09874	-0.2867	0.9367	0.0106	0.0824	0.1013	0.0644	0.0015	18.9431	-0.2867	0.2438	35.1539	1.4533
2	P03244	0.6651	0.7855	0.0225	0.8320	0.0908	0.0933	0.0024	37.2069	0.6651	0.2908	40.7016	1.0005
2	P30050	16.4937	0.8858	0.0214	0.3415	0.0892	0.1101	0.0022	64.1826	1.0607	0.2875	44.1527	1.0005
2	Q9BRJ2	1.0607	0.9282	0.0070	0.0003	0.0942	0.0646	0.0013	37.5815	-2.9616	0.2907	40.7772	1.0005
2	P31948	-2.9616	0.9193	0.0064	0.0043	0.1994	0.0721	0.0014	48.7770	-2.5627	0.2889	42.5799	1.0005
2	P04908	-2.5627	0.7868	0.0159	0.4662	0.0793	0.1000	0.0019	46.0397	0.1247	0.2893	42.2075	1.0005
2	P03243	0.1247	0.9283	0.0155	0.2554	0.1053	0.0686	0.0017	24.4953	0.3088	0.2949	37.1194	0.7679
2	P62258	0.3088	0.9595	0.0101	0.4211	0.0913	0.0608	0.0015	31.1820	-2.0086	0.2923	39.2898	1.0005
2	Q02880	-2.0086	0.9601	0.0068	0.2239	0.0666	0.0683	0.0011	41.4006	-0.5338	0.2900	41.4831	1.0005

2	Q3ZCQ8	-0.5338	0.7194	0.0692	0.0030	0.9678	0.0629	0.0044	7.9949	0.7545	0.3182	24.2345	1.0005
2	P33778	0.7545	0.8005	0.0131	0.6831	0.0655	0.0821	0.0014	74.5990	0.2081	0.2868	44.8856	1.0005
2	Q8NC51	0.2081	0.9416	0.0069	0.2869	0.0663	0.0578	0.0010	66.4255	-2.3168	0.2873	44.3277	1.6128
2	P51148	-2.3168	0.7844	0.0352	0.0003	0.1707	0.0630	0.0024	6.0577	0.7705	0.3287	20.8058	1.0005
2	P17661	0.7705	0.9584	0.0034	0.0006	0.0420	0.0936	0.0009	218.2078	-2.4921	0.2842	48.1253	1.4906
2	P14618	-2.4921	0.9521	0.0058	0.2998	0.0726	0.0624	0.0011	45.3231	-1.6536	0.2894	42.1038	1.0005
2	O43169	-1.6536	0.8439	0.0170	0.3943	0.1049	0.0752	0.0020	25.8955	0.5196	0.2942	37.6437	1.0005
2	Q58FG0	0.5196	0.9758	0.0098	0.0163	0.1126	0.0949	0.0024	34.9079	-2.4093	0.2913	40.2092	1.0005
2	P08670	-2.4093	0.9562	0.0086	1.3334	0.0898	0.1002	0.0025	43.2468	-1.8157	0.2897	41.7869	1.6040
2	P37802	-1.8157	0.9577	0.0080	0.0011	0.1008	0.0754	0.0017	45.0443	-2.3429	0.2894	42.0627	1.0005
2	O14910	-2.3429	0.9277	0.0165	0.0009	0.8715	0.0703	0.0013	22.2989	0.3872	0.2960	36.2008	1.0005
2	P62805	0.3872	0.8481	0.0148	0.4919	0.1036	0.0842	0.0023	24.9931	0.3038	0.2946	37.3108	1.0005
2	Q9BZF1	0.3038	0.7585	0.0161	0.1095	0.0947	0.0690	0.0014	12.6431	0.4027	0.3057	29.8989	1.6053
2	P02545	0.4027	0.8870	0.0129	0.0007	0.1631	0.0543	0.0021	10.2925	-2.4108	0.3107	27.3846	1.4733
2	P37108	-2.4108	0.9348	0.0205	0.0134	0.1354	0.0685	0.0021	6.2603	0.4850	0.3273	21.2066	1.0005
2	Q13765	0.4850	0.8907	0.0135	0.6110	0.1429	0.0739	0.0030	18.0204	-1.8860	0.2991	33.9746	1.4733
2	P04406	-1.8860	0.9102	0.0123	0.5640	0.1093	0.0846	0.0025	38.2469	-1.4237	0.2906	40.9085	1.5442
2	Q14410	-1.4237	0.9539	0.0133	0.6102	0.0851	0.0867	0.0021	34.7168	0.2936	0.2914	40.1659	1.0005
2	P31040	0.2936	0.9254	0.0172	0.2870	0.1083	0.0773	0.0017	23.4086	-0.1760	0.2954	36.6807	1.0005

2	P08107	-0.1760	0.9524	0.0099	0.7010	0.0997	0.1067	0.0027	52.7167	-2.1476	0.2885	43.0574	1.0005
2	P14678	-2.1476	0.8601	0.0127	0.0000	38.7680	0.0645	0.0013	27.4136	0.2755	0.2936	38.1660	1.6270
2	Q15758	0.2755	0.8686	0.0163	0.1946	0.1109	0.0980	0.0025	25.1631	0.1462	0.2945	37.3749	1.0005
2	O00541	0.1462	0.9731	0.0156	0.0001	0.4096	0.0718	0.0019	15.2107	0.2916	0.3020	32.0756	1.5732
2	Q05639	0.2916	0.9145	0.0135	0.0212	0.1564	0.0667	0.0025	11.2112	-2.2716	0.3085	28.4386	1.0005
2	P31946	-2.2716	0.8726	0.0048	0.1529	0.0561	0.0762	0.0011	134.2764	-2.1693	0.2851	47.0233	1.0005
2	Q9NVP1	-2.1693	0.9960	0.0197	0.4674	0.1295	0.0743	0.0021	12.3983	-0.1156	0.3061	29.6635	1.6470
2	P34931	-0.1156	0.9468	0.0092	0.4255	0.0877	0.0945	0.0021	59.2172	-1.6246	0.2879	43.7239	1.0005
2	P62701	-1.6246	0.9232	0.0081	0.0032	0.0934	0.0977	0.0021	41.7945	-1.9850	0.2899	41.5498	1.2502
2	P04843	-1.9850	0.9252	0.0104	0.3182	0.1100	0.0933	0.0017	61.3836	-0.5479	0.2877	43.9185	1.6004
2	Q58FF8	-0.5479	0.9441	0.0071	0.4573	0.0761	0.0949	0.0019	53.5156	-1.9468	0.2884	43.1469	1.6326
2	P68104	-1.9468	0.9794	0.0105	0.0003	0.1304	0.0886	0.0025	26.9196	-2.1526	0.2938	38.0010	1.6114
3	P20340	-4.6697	0.9793	0.0079	0.1770	0.1011	0.0720	0.0016	45.2295	-4.6697	0.2894	22.8526	1.0006
3	Q7Z2Z1	-4.9836	1.0003	0.0112	0.0215	0.1302	0.0496	0.0014	11.0060	-4.9836	0.3089	18.0355	1.0006
3	P23528	-3.9599	0.9023	0.0039	0.0001	8.2948	0.0821	0.0010	116.2009	-3.9599	0.2854	24.1179	1.5765
3	P09132	-3.1746	0.9862	0.0057	0.0010	0.6741	0.0777	0.0011	90.4936	-3.1746	0.2861	23.8786	1.0006
3	O60264	-2.0975	0.9747	0.0055	0.1779	0.0657	0.0723	0.0011	76.4119	-2.0975	0.2867	23.6828	2.7426
3	O14979	-2.2882	0.9312	0.0082	0.4992	0.0836	0.0844	0.0019	57.3682	-2.2882	0.2880	23.2757	1.0006
3	O43837	-1.9054	0.9050	0.0071	0.1918	0.0825	0.0600	0.0013	39.7453	-1.9054	0.2903	22.5850	1.5717

3	P06702	-1.2217	0.9209	0.0043	0.1844	0.0405	0.0714	0.0007	218.4308	-1.2217	0.2842	24.5229	1.6628
3	P08107	1.1089	0.8040	0.0316	0.2232	0.1108	0.0605	0.0016	22.5550	1.1089	0.2959	21.0362	3.0548
3	P37268	2.1576	1.0342	0.0365	0.1951	0.1006	0.0637	0.0014	23.4400	2.1576	0.2954	21.1629	1.0006
3	P60842	1.7834	0.7911	0.0466	0.2452	0.1361	0.0600	0.0019	14.8794	1.7834	0.3024	19.4457	2.3725
3	P24534	-1.0964	0.7216	0.0147	0.2449	0.1173	0.0674	0.0020	20.2579	-1.0964	0.2973	20.6647	1.0006
3	P00387	-1.0427	0.7824	0.0097	0.1684	0.0924	0.0774	0.0017	32.6049	-1.0427	0.2919	22.1171	1.0006
3	P62805	-0.6638	0.7446	0.0075	0.5148	0.0646	0.0745	0.0013	60.1208	-0.6638	0.2878	23.3494	2.2865
3	P49736	1.8689	0.9788	0.0318	0.0817	0.0975	0.0678	0.0016	33.3750	1.8689	0.2917	22.1761	1.5717
3	Q9UJZ1	-0.8243	0.8867	0.0123	0.5007	0.1071	0.1131	0.0027	33.2724	-0.8243	0.2917	22.1684	1.0006
3	P22087	-0.8749	0.9746	0.0108	0.0007	0.1285	0.0527	0.0014	10.7545	-0.8749	0.3095	17.9188	1.0006
3	O75340	-0.9117	0.8934	0.0173	0.0735	0.1781	0.0649	0.0027	7.2663	-0.9117	0.3216	15.7739	1.5252
3	P27824	-0.7989	0.7973	0.0098	0.4468	0.0821	0.0733	0.0014	42.8032	-0.7989	0.2898	22.7419	2.6828
3	P13804	1.8051	0.8956	0.0357	0.2306	0.0870	0.0602	0.0013	40.2253	1.8051	0.2902	22.6110	3.0116
3	Q16695	-0.1148	0.7379	0.0179	0.2981	0.1415	0.0792	0.0027	12.6849	-0.1148	0.3056	18.7260	1.0006
3	Q96QK1	1.7213	0.8050	0.0440	0.1366	0.1242	0.0619	0.0019	21.9752	1.7213	0.2962	20.9486	1.0006
4	P23528	-5.0932	0.9639	0.0021	0.0328	0.0294	0.0823	0.0005	425.3253	-5.0932	0.3169	49.0203	1.4420
4	P81605	-5.1704	0.9310	0.0035	0.3781	0.0458	0.0704	0.0008	194.7038	-5.1704	0.3176	47.9085	1.4837
4	Q9NTK5	-4.0340	0.9399	0.0060	0.0472	0.0845	0.0542	0.0010	18.9015	-4.0340	0.3301	34.4899	1.0004
4	Q9Y5S9	-2.9582	0.9647	0.0067	0.4317	0.0864	0.0707	0.0016	44.4129	-2.9582	0.3222	41.9679	2.2833

4	Q12849	-2.8452	1.0134	0.0071	0.0098	0.0774	0.0677	0.0012	43.4529	-2.8452	0.3224	41.8195	1.0004
4	O15371	-2.9096	0.9382	0.0122	0.0101	0.1637	0.0582	0.0019	11.0209	-2.9096	0.3397	28.2285	1.0004
4	Q86YZ3	-2.6057	0.9443	0.0073	0.4090	0.0803	0.0583	0.0012	46.7437	-2.6057	0.3219	42.3068	1.0004
4	P84077	-1.6671	0.9481	0.0049	0.4992	0.0563	0.0848	0.0013	106.0747	-1.6671	0.3188	46.2906	1.0004
4	P20340	-2.5414	0.9722	0.0132	0.0000	35.7118	0.0632	0.0022	12.0396	-2.5414	0.3378	29.3082	1.0004
4	P14314	3.9667	0.8091	0.0934	0.1784	0.0587	0.0684	0.0010	73.0734	3.9667	0.3199	44.7900	1.0004
4	Q96C01	5.8187	1.0740	0.2689	0.1942	0.0617	0.0672	0.0009	83.4995	5.8187	0.3194	45.3804	1.4342
4	P56385	2.7273	0.7254	0.0905	0.2819	0.1031	0.0933	0.0024	40.0389	2.7273	0.3229	41.2441	1.0004
4	P09132	-1.5818	0.9779	0.0160	0.6577	0.1534	0.0933	0.0038	11.9329	-1.5818	0.3380	29.2002	1.4280
4	P16989	-1.7243	0.9281	0.0121	0.0367	0.1549	0.0595	0.0020	11.3478	-1.7243	0.3391	28.5870	1.0004
4	Q13263	-1.8812	0.8065	0.0218	0.0003	0.2515	0.0615	0.0034	5.6085	-1.8812	0.3610	19.8763	1.0004
4	P06702	-1.6340	0.9621	0.0164	0.0004	3.8016	0.0603	0.0024	9.0782	-1.6340	0.3446	25.8224	1.0004
4	P61604	2.0718	0.9835	0.0159	0.0837	0.0461	0.0644	0.0007	137.1725	2.0718	0.3182	47.0825	1.0004
4	Q96KP4	-1.3454	0.9713	0.0152	0.0005	3.2194	0.0501	0.0017	8.4831	-1.3454	0.3465	24.9751	1.0004
4	Q9P2J5	-1.3646	0.9419	0.0204	0.0005	4.9785	0.0726	0.0037	6.9792	-1.3646	0.3526	22.5438	2.1495
4	O00231	-1.2453	0.9200	0.0165	0.2507	0.1660	0.0733	0.0027	12.6496	-1.2453	0.3368	29.9051	1.0004
4	P26641	-1.2241	0.9589	0.0054	0.0013	0.5009	0.0528	0.0008	34.9700	-1.2241	0.3238	40.2232	1.0004
4	P14923	2.3045	0.8564	0.0771	0.3284	0.1243	0.0759	0.0020	18.9672	2.3045	0.3301	34.5270	1.0004
4	P00338	-0.5550	0.8836	0.0133	0.3128	0.1371	0.0701	0.0024	12.1835	-0.5550	0.3376	29.4522	2.1362

4	Q07157	2.3062	1.1164	0.0617	0.0111	0.1306	0.0573	0.0018	13.0671	2.3062	0.3362	30.2941	1.0004
4	P13639	-0.9059	0.9214	0.0127	0.1696	0.1154	0.0696	0.0020	20.1737	-0.9059	0.3293	35.1781	1.0004
4	Q9NRP0	2.0408	0.9990	0.0212	0.1034	0.0537	0.0648	0.0009	197.9926	2.0408	0.3176	47.9418	1.6490
4	O14979	0.5630	0.9274	0.0093	0.4162	0.0612	0.0764	0.0012	60.8617	0.5630	0.3206	43.8727	1.0004
4	P62937	-0.8488	0.9653	0.0058	0.3313	0.0619	0.0703	0.0011	71.6467	-0.8488	0.3200	44.6972	1.5333
4	P34932	-0.5555	0.9869	0.0100	0.3672	0.0804	0.0886	0.0018	43.0196	-0.5555	0.3224	41.7507	1.0004
4	P11586	-0.9183	0.7946	0.0115	0.2477	0.0958	0.0746	0.0018	23.8308	-0.9183	0.3273	36.8546	1.0004
4	P07195	-0.6099	0.9548	0.0090	0.0342	0.0782	0.0650	0.0011	40.3145	-0.6099	0.3228	41.2936	2.1893
4	Q96IX5	1.9727	0.9288	0.0380	0.2746	0.0997	0.0639	0.0017	25.1237	1.9727	0.3268	37.3601	1.0004
4	Q92643	2.0558	0.9408	0.0472	0.1571	0.1327	0.0671	0.0020	20.0643	2.0558	0.3294	35.1213	1.0004
4	P37268	2.0028	1.0694	0.0216	0.0240	0.0690	0.0646	0.0009	69.2020	2.0028	0.3201	44.5304	1.0004
4	O60361	-1.0175	0.9652	0.0130	0.1939	0.1353	0.0636	0.0022	5.6624	-1.0175	0.3606	19.9911	1.0004
4	P50395	-0.5349	0.9515	0.0067	0.4700	0.0591	0.0934	0.0014	74.5937	-0.5349	0.3198	44.8853	2.3239
4	Q13011	1.6315	0.8308	0.0220	0.2534	0.0632	0.0687	0.0010	139.9001	1.6315	0.3181	47.1361	1.8007
4	Q02218	-0.7455	0.9282	0.0117	0.2820	0.0903	0.0709	0.0014	27.1473	-0.7455	0.3260	38.0777	1.5926
4	P60174	-0.6193	0.9286	0.0203	0.4074	0.1775	0.0802	0.0028	10.3047	-0.6193	0.3413	27.3992	1.0004
4	Q16658	-0.8823	0.9470	0.0198	0.3059	0.1725	0.0556	0.0024	5.8094	-0.8823	0.3595	20.2992	1.4080
4	P78527	1.4263	0.9751	0.0216	0.1860	0.0938	0.0742	0.0016	52.1659	1.4263	0.3213	42.9944	1.0004
4	P49368	-0.2630	0.9246	0.0108	0.0678	0.0921	0.0658	0.0014	25.6655	-0.2630	0.3265	37.5606	1.0004

4	P62081	-0.7248	0.9151	0.0087	0.0000	64.0207	0.0644	0.0014	35.0723	-0.7248	0.3238	40.2461	1.0004
4	P04637	1.6193	0.9186	0.0308	0.2757	0.0940	0.0800	0.0015	62.3257	1.6193	0.3205	43.9994	2.1869
4	P07900	-0.1267	0.9541	0.0112	0.0011	0.8319	0.0636	0.0014	21.4144	-0.1267	0.3285	35.7928	1.8148
4	P06733	-0.1356	0.8725	0.0085	0.2318	0.0526	0.0745	0.0010	75.7458	-0.1356	0.3198	44.9552	1.6429
4	P22314	-0.4008	0.9522	0.0079	0.3517	0.0627	0.0861	0.0014	71.8640	-0.4008	0.3199	44.7116	2.1555
4	P26368	-0.3830	0.9706	0.0048	0.4126	0.0444	0.0734	0.0009	103.6555	-0.3830	0.3188	46.2106	1.4524
4	P12277	-0.0461	0.9354	0.0083	0.1537	0.0701	0.0624	0.0011	30.3323	-0.0461	0.3250	39.0555	1.6879
5	Q8WY22	-5.3393	0.9354	0.0043	0.1240	0.0482	0.0638	0.0008	166.1767	-5.3393	0.2470	47.5669	1.0004
5	P13667	-3.8515	0.9266	0.0111	0.2104	0.1150	0.0694	0.0017	31.2276	-3.8515	0.2558	39.3021	1.5533
5	Q92973	-3.2328	0.9427	0.0057	0.1294	0.0701	0.0642	0.0011	65.7469	-3.2328	0.2502	44.2759	2.1645
5	Q9Y5S9	-2.5030	0.9731	0.0079	0.3507	0.1013	0.0639	0.0016	16.4495	-2.5030	0.2652	32.9656	1.0004
5	P84077	-1.9058	0.9481	0.0050	0.4670	0.0564	0.0872	0.0013	120.2617	-1.9058	0.2478	46.6993	1.0004
5	Q02878	0.7366	0.8082	0.0253	0.0013	1.0531	0.0604	0.0018	25.9258	0.7366	0.2580	37.6546	2.0797
5	P09543	3.1225	1.3663	0.2122	0.0355	0.3138	0.0565	0.0036	4.7768	3.1225	0.3092	17.9892	1.0004
5	Q9H009	2.4612	0.7629	0.0294	0.2420	0.0517	0.0582	0.0007	113.3113	2.4612	0.2480	46.5110	1.0004
5	Q96C01	3.5782	1.2193	0.0989	0.0011	1.0350	0.0595	0.0014	20.7689	3.5782	0.2611	35.4795	1.0004
5	P27695	1.6991	0.8624	0.0320	0.0051	0.1875	0.0673	0.0013	37.3984	1.6991	0.2541	40.7404	1.0004
5	O43707	-1.6529	0.9000	0.0060	0.0862	0.0638	0.0631	0.0010	78.6134	-1.6529	0.2493	45.1213	1.0004
5	Q02880	1.5242	0.9044	0.0277	0.0003	0.0944	0.0590	0.0014	26.2808	1.5242	0.2578	37.7806	1.0004

5	P01040	-2.0008	0.9220	0.0083	0.2116	0.1016	0.0770	0.0018	42.1870	-2.0008	0.2530	41.6152	1.0004
5	O75477	1.3069	0.9008	0.0149	0.1916	0.0646	0.0687	0.0010	68.9184	1.3069	0.2499	44.5103	1.0004
5	Q14697	0.0716	0.7785	0.0165	0.3723	0.0789	0.0764	0.0012	46.5700	0.0716	0.2523	42.2825	1.3692
5	Q53GS9	1.2571	0.7836	0.0258	0.2986	0.0847	0.0800	0.0017	32.9254	1.2571	0.2553	39.7406	1.0004
5	Q15717	0.2676	0.8878	0.0090	0.3269	0.0670	0.0749	0.0012	53.8372	0.2676	0.2513	43.1822	1.5540
5	P12814	-0.9341	0.9466	0.0088	0.3569	0.0672	0.0667	0.0011	45.9697	-0.9341	0.2524	42.1975	2.1213
5	P41219	0.8738	0.9352	0.0088	0.1695	0.0511	0.0677	0.0008	120.2336	0.8738	0.2478	46.6986	1.9636
5	P78417	-1.5245	0.9531	0.0092	0.0017	0.6124	0.0930	0.0023	33.2018	-1.5245	0.2552	39.8086	1.0004
5	Q13263	0.9674	0.8334	0.0286	0.0471	0.1242	0.0571	0.0018	9.9642	0.9674	0.2776	26.9825	1.5250
5	P18124	0.8875	0.9006	0.0169	0.6562	0.0746	0.0867	0.0017	40.9554	0.8875	0.2533	41.4064	1.8015
5	P62424	0.6887	0.7823	0.0133	0.0645	0.0661	0.0703	0.0011	48.5788	0.6887	0.2520	42.5542	2.2485
5	Q13162	-0.5077	0.9532	0.0071	0.1861	0.0669	0.0544	0.0008	47.8336	-0.5077	0.2521	42.4557	1.6348
5	Q9Y3U8	-1.4105	0.9132	0.0080	0.2592	0.0984	0.0609	0.0014	29.0885	-1.4105	0.2566	38.6934	1.0004
5	P62316	-1.4144	0.9079	0.0098	0.0604	0.1150	0.0601	0.0015	22.7733	-1.4144	0.2597	36.4101	1.0004
5	P35613	1.1367	0.9374	0.0188	0.2327	0.0804	0.0702	0.0014	41.2603	1.1367	0.2532	41.4590	1.0004
5	P35268	-1.0154	0.8152	0.0120	0.3798	0.1227	0.0800	0.0025	15.8882	-1.0154	0.2659	32.5735	1.0004
5	Q10471	0.8987	0.9994	0.0508	0.0154	0.2982	0.0550	0.0034	13.3524	0.8987	0.2697	30.5513	1.0004
5	Q9P003	-1.3198	0.9084	0.0104	0.4118	0.0894	0.0810	0.0014	59.4294	-1.3198	0.2507	43.7435	1.0004
5	Q06830	-1.4506	0.9763	0.0148	0.2140	0.1748	0.0621	0.0025	4.7715	-1.4506	0.3092	17.9765	1.0004

5	Q9UMX0	0.8430	0.7877	0.0215	0.2021	0.0790	0.0579	0.0011	17.8884	0.8430	0.2636	33.8945	1.0004
5	P35611	0.9449	0.7648	0.0455	0.0021	0.9678	0.0610	0.0028	6.2506	0.9449	0.2953	21.1876	1.0004
5	P13073	-1.3185	0.9402	0.0082	0.2734	0.0890	0.0539	0.0012	25.4819	-1.3185	0.2582	37.4933	1.0004
5	Q58FG0	-1.2668	0.9461	0.0066	0.3183	0.0728	0.0686	0.0013	59.6727	-1.2668	0.2507	43.7658	2.0606
5	P30050	0.1426	0.8711	0.0063	0.0743	0.0506	0.0576	0.0007	59.6615	0.1426	0.2507	43.7648	1.0004
5	P00338	0.7862	0.9654	0.0201	0.9217	0.1087	0.1075	0.0031	27.1205	0.7862	0.2574	38.0687	1.7020
5	O76021	0.9715	1.0415	0.0303	0.0162	0.1609	0.0595	0.0023	4.8360	0.9715	0.3085	18.1315	2.2073
5	P11388	-0.7950	0.9313	0.0109	0.0982	0.0933	0.0515	0.0012	21.7361	-0.7950	0.2604	35.9440	1.6476

Table SI.2.3. Differentially expressed proteins for experiments 1, 2, 3, 4 and 5 and respective statistical parameters relevant for quantification, scans per peptide quantified, peptides per protein quantified and fold.

Experiment	Accession (UniProt)	Xp	SD_Xp	Wp	FDRp	Xq	SD_Xq	Zq	Wq	FDRq	Scan/peptide	Pep/protein	Fold
1	Q8IZK6	-5.7824	0.2308	19.1346	1.0005	-5.7824	0.2308	-24.9726	18.7754	0.0000	1	1	55.04
1	P53396	-3.6777	0.2448	16.9708	1.0005	-3.6777	0.2448	-14.9457	16.6876	0.0000	1	1	12.80
1	O15259	3.9380	0.2317	18.9890	1.0005	3.9380	0.2317	17.0820	18.6351	0.0000	1	1	-15.33
1	Q08211	-0.5050	0.2087	23.4964	1.3096	-0.5343	0.0823	-6.2614	147.7329	0.0000	2	8	1.43
1	P49327	-0.3691	0.2361	18.2644	1.4012	-0.4457	0.0831	-5.1368	144.9700	0.0001	1	9	1.36
1	P13639	-0.3957	0.1978	26.2170	1.4318	-0.3249	0.0703	-4.3506	202.4767	0.0016	3	12	1.24
1	P09874	-0.3000	0.2116	22.8449	1.2946	-0.3159	0.0694	-4.2788	207.8923	0.0023	2	12	1.23
2	P03244	0.6651	0.2908	15.4873	1.1500	0.7829	0.2028	8.7438	24.3209	0.0000	1	3	-3.42
2	P30050	16.4937	0.2925	15.2561	1.0008	16.4937	0.2925	59.7768	11.6894	0.0000	1	1	-183298.16
2	Q9BRJ2	1.0607	0.2875	15.9620	1.0008	1.0607	0.2875	7.1337	12.0994	0.0000	1	1	-4.14
2	P31948	-2.9616	0.2907	15.4982	1.0008	-2.9616	0.2907	-6.7812	11.8310	0.0000	1	1	3.92
2	P04908	-2.5627	0.2889	15.7517	1.1499	-2.4506	0.2198	-6.6444	20.6984	0.0000	1	2	2.75
2	P03243	0.5604	0.2474	24.2699	1.0008	0.5604	0.2474	6.2675	16.3390	0.0000	19	1	-2.93
2	P62258	0.3088	0.2949	14.9387	1.3292	0.2812	0.2018	6.3001	24.5606	0.0000	1	3	-2.41
2	Q02880	-2.0086	0.2923	15.2784	1.3044	-2.0499	0.1878	-5.6434	28.3529	0.0000	1	4	2.08

2	Q3ZCQ8	-0.5338	0.2900	15.5991	0.0728	0.2985	0.2288	5.6310	19.0970	0.0000	1	2	-2.44
2	P33778	0.7545	0.3182	12.3056	1.0008	0.7545	0.3182	5.4824	9.8752	0.0000	1	1	-3.35
2	Q8NC51	0.0675	0.2544	22.3734	1.2117	-0.0010	0.1825	5.4204	30.0314	0.0000	5	4	-1.98
2	P51148	-2.3168	0.2873	15.9848	1.3071	-2.2785	0.2363	-5.4523	17.9069	0.0000	1	2	2.44
2	P17661	0.7705	0.3287	11.3554	1.0008	0.7705	0.3287	5.3559	9.2538	0.0000	1	1	-3.39
2	P14618	-2.4921	0.2842	16.4530	1.0008	-2.4921	0.2842	-5.2846	12.3794	0.0000	1	1	2.83
2	O43169	-1.6536	0.2894	15.6861	0.9048	-1.9044	0.1735	-5.2694	33.2158	0.0000	1	6	1.88
2	Q58FG0	0.5196	0.2942	15.0229	1.0008	0.5196	0.2942	5.1313	11.5520	0.0000	1	1	-2.85
2	P08670	-2.3012	0.2604	20.9214	1.0008	-2.3012	0.2604	-5.0352	14.7497	0.0000	3	1	2.48
2	P37802	-1.8157	0.2897	15.6419	1.2860	-1.7613	0.1619	-4.7631	38.1495	0.0001	1	9	1.71
2	O14910	-2.3429	0.2894	15.6804	1.0008	-2.3429	0.2894	-4.6740	11.9369	0.0001	1	1	2.55
2	P62805	0.3872	0.2960	14.7877	1.0008	0.3872	0.2960	4.6530	11.4124	0.0001	1	1	-2.60
2	Q9BZF1	0.1968	0.2582	21.4225	1.0008	0.1968	0.2582	4.5963	14.9970	0.0001	4	1	-2.28
2	P02545	0.4027	0.3057	13.6154	1.0008	0.4027	0.3057	4.5561	10.7014	0.0001	1	1	-2.63
2	P37108	-2.4108	0.3107	13.0690	1.0008	-2.4108	0.3107	-4.5730	10.3609	0.0001	1	1	2.68
2	Q13765	0.4850	0.3273	11.4738	1.0008	0.4850	0.3273	4.5063	9.3323	0.0002	1	1	-2.78
2	P04406	-1.8860	0.2991	14.4022	1.3659	-1.8854	0.1985	-4.5114	25.3898	0.0002	1	3	1.86
2	Q14410	-1.4237	0.2906	15.5172	0.6707	-1.8116	0.1874	-4.3842	28.4833	0.0003	1	4	1.77
2	P31040	0.2936	0.2914	15.4091	1.0008	0.2936	0.2914	4.4058	11.7790	0.0003	1	1	-2.43

2	P08107	-0.1760	0.2954	14.8672	1.2171	-0.0915	0.2048	4.3879	23.8430	0.0003	1	3	-1.86
2	P14678	-2.0154	0.2670	19.5034	1.1572	-1.9195	0.2139	-4.3444	21.8490	0.0003	2	2	1.90
2	Q15758	0.2755	0.2936	15.1054	1.0008	0.2755	0.2936	4.3107	11.6008	0.0003	1	1	-2.40
2	O00541	0.1242	0.2588	21.2847	1.0008	0.1242	0.2588	4.3054	14.9294	0.0003	4	1	-2.16
2	Q05639	0.2916	0.3020	14.0496	1.0008	0.2916	0.3020	4.2446	10.9678	0.0004	1	1	-2.43
2	P31946	-2.2716	0.3085	13.3043	1.0008	-2.2716	0.3085	-4.1541	10.5082	0.0006	1	1	2.43
2	Q9NVP1	-2.1020	0.2657	19.7634	0.8724	-1.8623	0.2106	-4.1410	22.5401	0.0006	2	2	1.83
2	P34931	-0.1156	0.3061	13.5664	1.2968	-0.1682	0.2022	4.0642	24.4498	0.0008	1	3	-1.77
2	P62701	-1.3776	0.2681	19.2853	0.8126	-1.6513	0.1697	-3.8952	34.7060	0.0015	2	6	1.58
2	P04843	-1.9568	0.2686	19.1703	0.9571	-1.7440	0.1944	-3.8773	26.4487	0.0016	2	3	1.69
2	Q58FF8	-0.5979	0.2672	19.4516	0.8056	-0.3186	0.1839	3.6521	29.5817	0.0033	2	4	-1.59
2	P68104	-1.8544	0.2540	22.4569	1.1245	-1.7414	0.2093	-3.5893	22.8254	0.0041	5	2	1.68
3	P20340	-4.6697	0.2894	15.6842	1.0011	-4.6697	0.2894	-17.8118	11.9391	0.0000	1	1	35.63
3	Q7Z2Z1	-4.9836	0.3089	13.2545	1.0011	-4.9836	0.3089	-17.7019	10.4771	0.0000	1	1	44.29
3	P23528	-3.9599	0.2854	16.2700	1.7375	-3.9599	0.2854	-15.5744	12.2755	0.0000	1	1	21.78
3	P09132	-3.1746	0.2861	16.1607	1.0011	-3.1746	0.2861	-12.7902	12.2132	0.0000	1	1	12.64
3	O60264	-2.2643	0.2470	24.3934	1.0011	-2.2643	0.2470	-11.1330	16.3949	0.0000	2	1	6.72
3	O14979	-2.2882	0.2880	15.8823	1.0011	-2.2882	0.2880	-9.6289	12.0535	0.0000	1	1	6.84
3	O43837	-1.9054	0.2903	15.5576	1.0011	-1.9054	0.2903	-8.2351	11.8656	0.0000	1	1	5.24

3	P06702	-1.2124	0.2460	24.6777	1.0011	-1.2124	0.2460	-6.9007	16.5228	0.0000	2	1	3.24
3	P08107	1.3824	0.2364	27.8838	1.7302	1.4655	0.1741	5.6292	32.9766	0.0000	3	4	-1.97
3	P37268	2.1576	0.2954	14.8693	1.0011	2.1576	0.2954	5.6614	11.4610	0.0000	1	1	-3.19
3	P60842	1.9237	0.2583	21.3963	1.7375	1.9237	0.2583	5.5682	14.9842	0.0000	2	1	-2.71
3	P24534	-1.0964	0.2973	14.6216	1.0011	-1.0964	0.2973	-5.3198	11.3133	0.0000	1	1	2.99
3	P00387	-1.0427	0.2919	15.3341	1.0011	-1.0427	0.2919	-5.2343	11.7352	0.0000	1	1	2.88
3	P62805	-0.5520	0.2170	36.9024	1.0011	-0.5520	0.2170	-4.7796	21.2321	0.0001	6	1	2.05
3	P49736	1.8689	0.2917	15.3625	1.0011	1.8689	0.2917	4.7433	11.7518	0.0001	1	1	-2.61
3	Q9UJZ1	-0.8243	0.2917	15.3588	1.0011	-0.8243	0.2917	-4.4889	11.7496	0.0003	1	1	2.48
3	P22087	-0.8749	0.3095	13.1913	1.0011	-0.8749	0.3095	-4.3942	10.4376	0.0004	1	1	2.57
3	O75340	-0.9117	0.3216	11.9910	1.0011	-0.9117	0.3216	-4.3444	9.6716	0.0004	1	1	2.63
3	P27824	-0.6095	0.2503	23.4379	1.0011	-0.6095	0.2503	-4.3734	15.9576	0.0004	2	1	2.14
3	P13804	1.5589	0.2492	23.7583	1.0011	1.5589	0.2492	4.3087	16.1055	0.0005	2	1	-2.10
3	Q16695	-0.1148	0.3056	13.6236	1.4804	-0.3897	0.2094	-4.1778	22.7966	0.0008	1	2	1.83
3	Q96QK1	1.7213	0.2962	14.7632	1.0011	1.7213	0.2962	4.1731	11.3978	0.0008	1	1	-2.36
4	P23528	-5.0939	0.3003	24.8896	1.0007	-5.0939	0.3003	-18.8964	11.0892	0.0000	2	1	51.10
4	P81605	-4.8738	0.3008	24.7181	1.0007	-4.8738	0.3008	-18.1355	11.0551	0.0000	2	1	43.87
4	Q9NTK5	-4.0340	0.3301	16.9509	1.0007	-4.0340	0.3301	-13.9776	9.1748	0.0000	1	1	24.51
4	Q9Y5S9	-2.7670	0.3048	23.3186	1.4058	-2.7670	0.3048	-10.9841	10.7661	0.0000	2	1	10.18

4	Q12849	-2.8452	0.3224	18.5486	1.0007	-2.8452	0.3224	-10.6275	9.6235	0.0000	1	1	10.75
4	O15371	-2.9096	0.3397	15.2846	1.0007	-2.9096	0.3397	-10.2731	8.6636	0.0000	1	1	11.24
4	Q86YZ3	-2.6057	0.3219	18.6439	1.0007	-2.6057	0.3219	-9.8975	9.6491	0.0000	1	1	9.11
4	P84077	-1.6671	0.3188	19.3789	0.7560	-2.1237	0.2759	-9.8008	13.1346	0.0000	1	2	6.52
4	P20340	-2.5414	0.3378	15.5957	1.0007	-2.5414	0.3378	-9.2417	8.7627	0.0000	1	1	8.71
4	P14314	3.9667	0.3199	19.1108	1.0007	3.9667	0.3199	10.5855	9.7726	0.0000	1	1	-10.45
4	Q96C01	5.8187	0.3194	19.2175	1.0007	5.8187	0.3194	16.3982	9.8005	0.0000	1	1	-37.72
4	P56385	2.7273	0.3035	23.7400	1.0007	2.7273	0.3035	7.0727	10.8551	0.0000	2	1	-4.43
4	P09132	-1.5818	0.3116	21.2210	1.4016	-1.5818	0.3116	-6.9387	10.2962	0.0000	2	1	4.48
4	P16989	-1.7243	0.3391	15.3891	1.0007	-1.7243	0.3391	-6.7974	8.6971	0.0000	1	1	4.94
4	Q13263	-1.8812	0.3610	12.4516	1.0007	-1.8812	0.3610	-6.8197	7.6739	0.0000	1	1	5.51
4	P06702	-1.6340	0.3446	14.5505	1.0007	-1.6340	0.3446	-6.4271	8.4227	0.0000	1	1	4.64
4	P61604	2.0718	0.3182	19.5163	1.4156	2.1262	0.2702	5.7193	13.6926	0.0000	1	2	-2.92
4	Q96KP4	-1.3454	0.3465	14.2776	1.4016	-1.3454	0.3465	-5.5588	8.3306	0.0000	1	1	3.80
4	Q9P2J5	-1.2322	0.3279	17.3847	1.0007	-1.2322	0.3279	-5.5285	9.3004	0.0000	2	1	3.52
4	O00231	-1.2453	0.3368	15.7631	1.0007	-1.2453	0.3368	-5.4211	8.8153	0.0000	1	1	3.55
4	P26641	-1.2241	0.3238	18.2278	0.9830	-0.8729	0.2711	-5.3618	13.6072	0.0000	1	2	2.74
4	P14923	2.3045	0.3301	16.9598	1.0007	2.3045	0.3301	5.2226	9.1774	0.0000	1	1	-3.30
4	P00338	-0.8476	0.2964	26.4106	1.4129	-0.8266	0.2687	-5.2370	13.8505	0.0000	4	2	2.65

4	Q07157	2.3062	0.3362	15.8706	1.0007	2.3062	0.3362	5.1332	8.8488	0.0000	1	1	-3.31
4	P13639	-0.9059	0.3293	17.1154	1.3937	-0.7258	0.2582	-5.0587	14.9941	0.0000	1	3	2.47
4	Q9NRP0	2.0685	0.3007	24.7388	1.0007	2.0685	0.3007	4.9481	11.0592	0.0000	2	1	-2.80
4	O14979	0.5630	0.3206	18.9418	0.0000	-0.6606	0.2571	-4.8277	15.1294	0.0000	1	2	2.37
4	P62937	-0.8619	0.3022	24.1950	1.3932	-0.8619	0.3022	-4.7731	10.9492	0.0000	2	1	2.72
4	P34932	-0.5555	0.3224	18.5351	1.3733	-0.7221	0.2768	-4.7059	13.0503	0.0000	1	2	2.47
4	P11586	-0.9183	0.3273	17.5028	1.3932	-0.9183	0.3273	-4.5793	9.3341	0.0001	1	1	2.83
4	P07195	-0.7171	0.2962	26.5054	1.3519	-0.5471	0.2481	-4.5455	16.2468	0.0001	3	4	2.19
4	Q96IX5	1.9727	0.3056	23.0504	1.0007	1.9727	0.3056	4.5557	10.7086	0.0001	2	1	-2.62
4	Q92643	2.0558	0.3294	17.1020	1.0007	2.0558	0.3294	4.4793	9.2189	0.0001	1	1	-2.78
4	P37268	2.0028	0.3201	19.0634	1.0007	2.0028	0.3201	4.4433	9.7602	0.0001	1	1	-2.68
4	O60361	-1.0175	0.3606	12.4965	1.0007	-1.0175	0.3606	-4.4320	7.6910	0.0001	1	1	3.03
4	P50395	-0.7239	0.3029	23.9488	1.0007	-0.7239	0.3029	-4.3065	10.8985	0.0002	2	1	2.47
4	Q13011	1.6806	0.3010	24.6361	1.4102	1.7640	0.2766	4.2786	13.0711	0.0003	2	2	-2.27
4	Q02218	-0.7215	0.3053	23.1386	1.3932	-0.7215	0.3053	-4.2648	10.7276	0.0003	2	1	2.47
4	P60174	-0.6193	0.3413	15.0382	1.4053	-0.5757	0.2803	-4.1258	12.7319	0.0005	1	2	2.23
4	Q16658	-0.8823	0.3595	12.6162	1.0007	-0.8823	0.3595	-4.0688	7.7362	0.0006	1	1	2.76
4	P78527	1.4263	0.3213	18.7762	1.1386	1.7265	0.2826	4.0543	12.5178	0.0006	1	2	-2.21
4	P49368	-0.2630	0.3265	17.6605	1.1469	-0.5501	0.2796	-4.0437	12.7901	0.0007	1	2	2.19

4	P62081	-0.7248	0.3238	18.2325	1.0007	-0.7248	0.3238	-4.0316	9.5377	0.0007	1	1	2.47
4	P04637	1.7528	0.2909	28.8874	1.0007	1.7528	0.2909	4.0299	11.8179	0.0007	5	1	-2.25
4	P07900	-0.0688	0.3074	22.4683	0.7927	-0.4803	0.2669	-3.9755	14.0431	0.0008	2	2	2.09
4	P06733	-0.1085	0.2929	27.9578	1.2840	-0.2899	0.2386	-3.6475	17.5584	0.0026	4	6	1.83
4	P22314	-0.3043	0.3086	22.1136	1.4050	-0.2982	0.2464	-3.5666	16.4723	0.0035	2	4	1.84
4	P26368	-0.3800	0.3014	24.4844	1.4138	-0.2959	0.2566	-3.4163	15.1910	0.0055	2	3	1.84
4	P12277	-0.0857	0.3051	23.2218	1.3990	-0.1929	0.2398	-3.2251	17.3837	0.0093	2	6	1.71
5	Q8WY22	-5.3393	0.2470	24.3766	1.0008	-5.3393	0.2470	-20.5494	16.3873	0.0000	1	1	33.74
5	P13667	-3.8515	0.2558	22.0052	1.0008	-3.8515	0.2558	-14.0274	15.2803	0.0000	1	1	12.03
5	Q92973	-3.1083	0.2260	32.1674	1.0008	-3.1083	0.2260	-12.5884	19.5743	0.0000	2	1	7.19
5	Q9Y5S9	-2.5030	0.2652	19.8670	1.0008	-2.5030	0.2652	-8.4459	14.2177	0.0000	1	1	4.72
5	P84077	-1.9058	0.2478	24.1467	1.1494	-1.8032	0.1848	-8.3325	29.2688	0.0000	1	3	2.91
5	Q02878	0.6326	0.2293	30.6826	0.0043	1.3426	0.1851	8.6762	29.1968	0.0000	2	2	-3.04
5	P09543	3.1225	0.3092	13.2295	1.3789	3.1225	0.3092	10.9503	10.4615	0.0000	1	1	-10.45
5	Q9H009	2.4612	0.2480	24.0962	1.0008	2.4612	0.2480	10.9853	16.2601	0.0000	1	1	-6.61
5	Q96C01	3.5782	0.2611	20.7532	1.0008	3.5782	0.2611	14.7105	14.6659	0.0000	1	1	-14.33
5	P27695	1.6991	0.2541	22.4489	1.0008	1.6991	0.2541	7.7232	15.4929	0.0000	1	1	-3.90
5	O43707	-1.6529	0.2493	23.7178	1.0791	-1.5268	0.1685	-7.4994	35.2146	0.0000	1	5	2.40
5	Q02880	1.5242	0.2578	21.5199	1.3760	1.5242	0.2578	6.9322	15.0447	0.0000	1	1	-3.45

5	P01040	-2.0008	0.2530	22.7120	1.0008	-2.0008	0.2530	-6.8676	15.6178	0.0000	1	1	3.34
5	O75477	1.3069	0.2499	23.5479	1.0008	1.3069	0.2499	6.2813	16.0085	0.0000	1	1	-2.97
5	Q14697	0.3657	0.2271	31.6606	0.1912	0.7719	0.1708	6.0584	34.2692	0.0000	2	4	-2.05
5	Q53GS9	1.2571	0.2553	22.1419	1.0008	1.2571	0.2553	5.9549	15.3461	0.0000	1	1	-2.87
5	Q15717	0.2678	0.2401	26.5544	0.1472	0.7507	0.1796	5.6461	31.0181	0.0000	2	3	-2.02
5	P12814	-0.7480	0.2280	31.2486	0.0829	-1.2444	0.1781	-5.5104	31.5307	0.0000	2	3	1.97
5	P41219	0.9411	0.2252	32.5513	1.0008	0.9411	0.2252	5.3469	19.7158	0.0000	2	1	-2.30
5	P78417	-1.5245	0.2552	22.1630	1.0008	-1.5245	0.2552	-4.9433	15.3562	0.0000	1	1	2.40
5	Q13263	0.9674	0.2776	17.5251	0.5738	0.6351	0.1852	4.8487	29.1478	0.0000	1	3	-1.86
5	P18124	0.8434	0.2291	30.7693	1.0008	0.8434	0.2291	4.8289	19.0477	0.0000	2	1	-2.15
5	P62424	0.8387	0.2294	30.6492	1.0008	0.8387	0.2294	4.8028	19.0016	0.0000	2	1	-2.15
5	Q13162	-0.5300	0.2185	36.0694	0.0175	-1.1082	0.1775	-4.7614	31.7420	0.0000	3	3	1.80
5	Q9Y3U8	-1.4105	0.2566	21.8130	1.0008	-1.4105	0.2566	-4.4717	15.1874	0.0002	1	1	2.22
5	P62316	-1.4144	0.2597	21.0682	1.0008	-1.4144	0.2597	-4.4329	14.8225	0.0002	1	1	2.22
5	P35613	1.1367	0.2532	22.6654	0.1881	0.6527	0.2080	4.4017	23.1041	0.0002	1	2	-1.89
5	P35268	-1.0154	0.2659	19.7240	0.9739	-1.1935	0.2141	-4.3451	21.8074	0.0003	1	2	1.91
5	Q10471	0.8987	0.2697	18.9639	1.0008	0.8987	0.2697	4.3076	13.7491	0.0003	1	1	-2.24
5	Q9P003	-1.3198	0.2507	23.3315	1.0008	-1.3198	0.2507	-4.2150	15.9082	0.0004	1	1	2.08
5	Q06830	-1.4506	0.3092	13.2226	0.5979	-1.0782	0.1929	-4.2251	26.8671	0.0004	1	3	1.76

5	Q9UMX0	0.8430	0.2636	20.2007	1.3633	0.8430	0.2636	4.1953	14.3878	0.0005	1	1	-2.15
5	P35611	0.9449	0.2953	14.8815	1.0008	0.9449	0.2953	4.0908	11.4682	0.0007	1	1	-2.31
5	P13073	-1.3185	0.2582	21.4264	1.0008	-1.3185	0.2582	-4.0878	14.9989	0.0007	1	1	2.08
5	Q58FG0	-1.1793	0.2267	31.8371	1.0008	-1.1793	0.2267	-4.0409	19.4515	0.0008	2	1	1.89
5	P30050	0.1426	0.2507	23.3375	0.2726	0.5596	0.2044	4.0242	23.9315	0.0009	1	2	-1.77
5	P00338	0.7501	0.2318	29.6306	0.5109	0.4722	0.1853	3.9669	29.1128	0.0010	2	3	-1.66
5	O76021	0.7578	0.2545	22.3413	0.5378	0.4497	0.1930	3.6940	26.8597	0.0027	2	2	-1.64
5	P11388	-0.8204	0.2349	28.4334	1.0063	-0.9552	0.1923	-3.5998	27.0509	0.0037	2	2	1.62

SUPPLEMENTARY INFORMATION II: SIGNALING PATHWAYS AFFECTED BY SHDAG AND HDV RNA REPLICATION

GLYCOLYSIS/GLUCONEOGENESIS PATHWAY

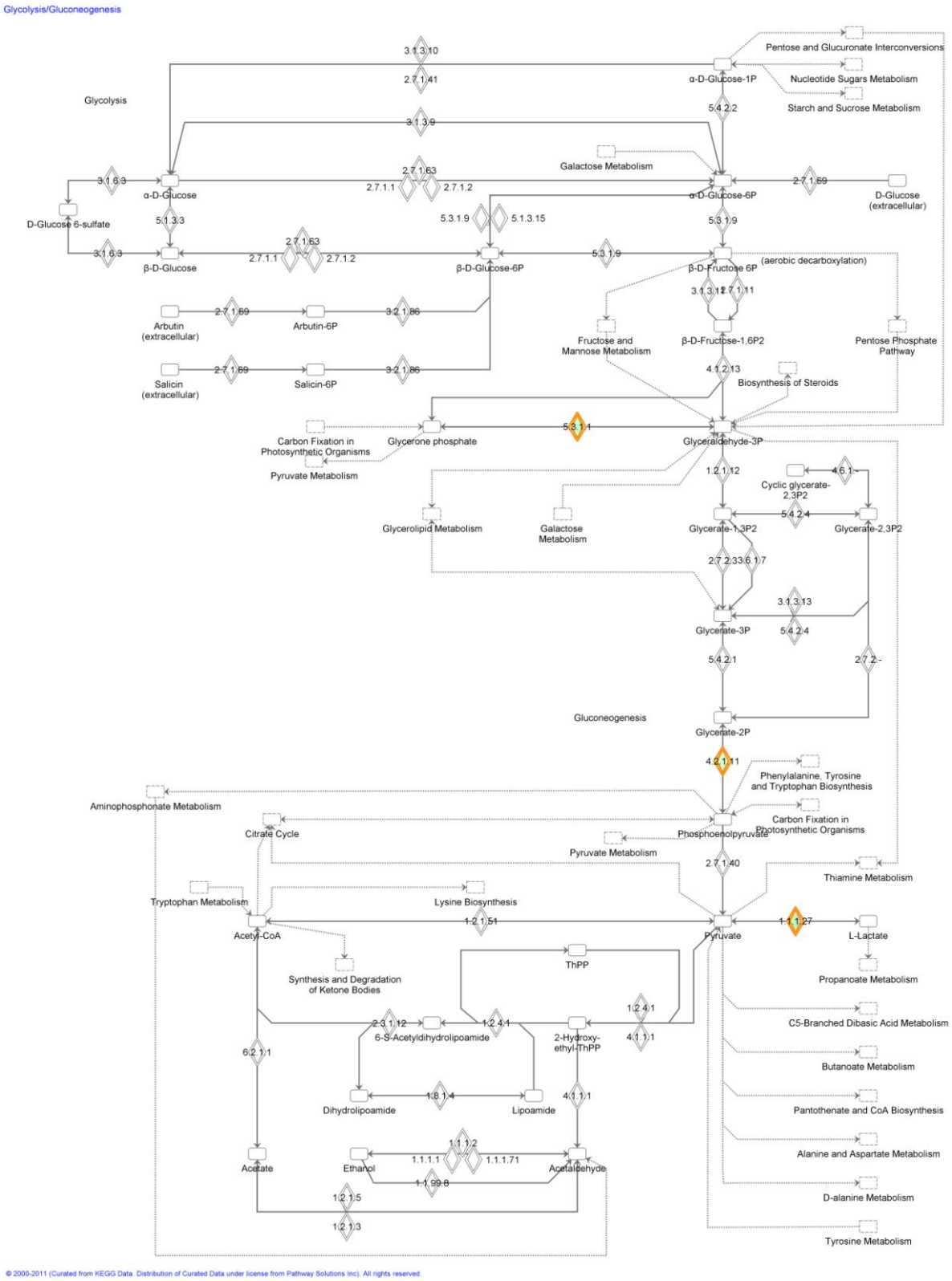

Figure SII.1: Glycolysis/Gluconeogenesis pathway.

HIF1α SIGNALING

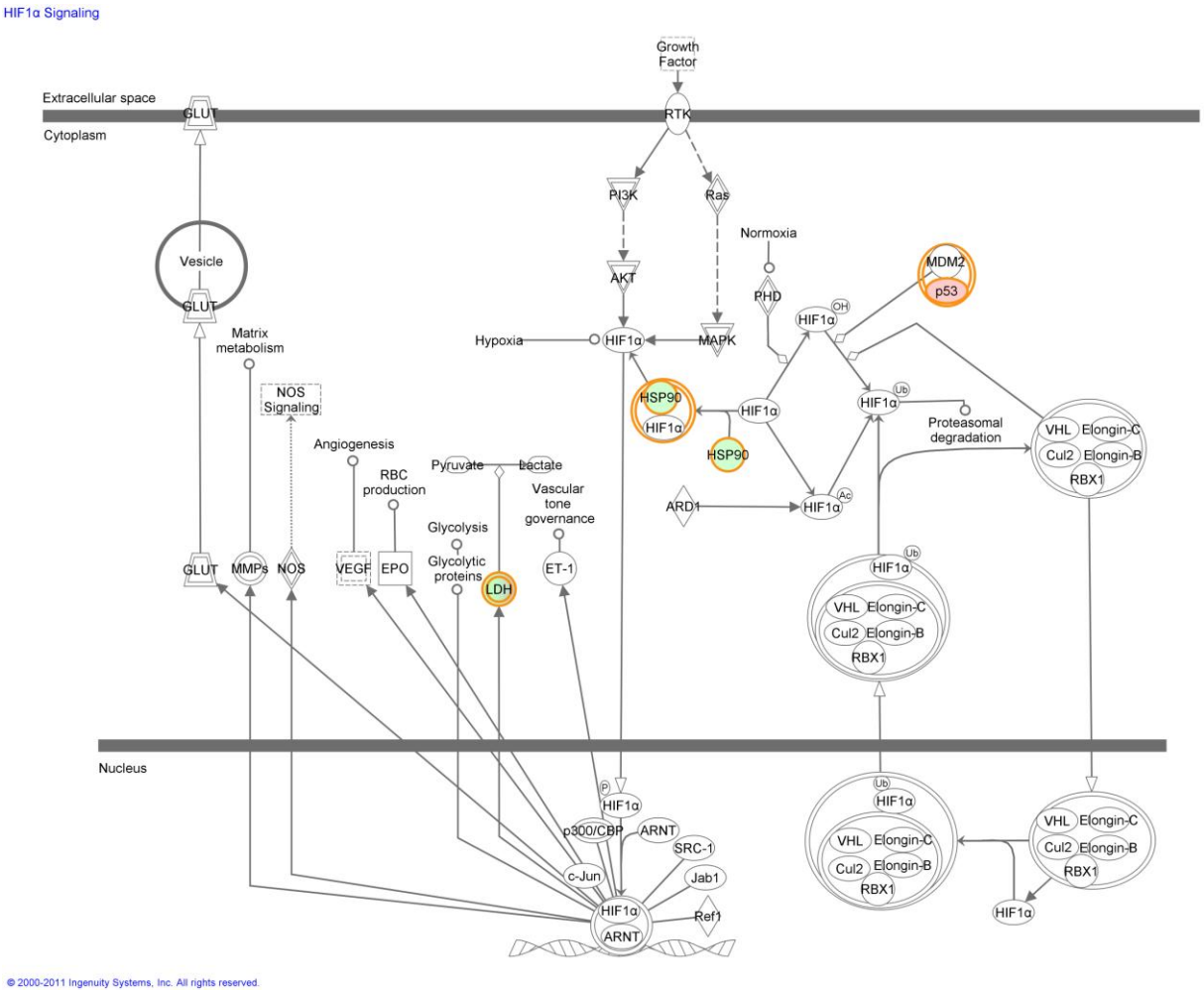

Figure SII.2: HIF1α signaling pathway.

PROPANOATE METABOLISM PATHWAY

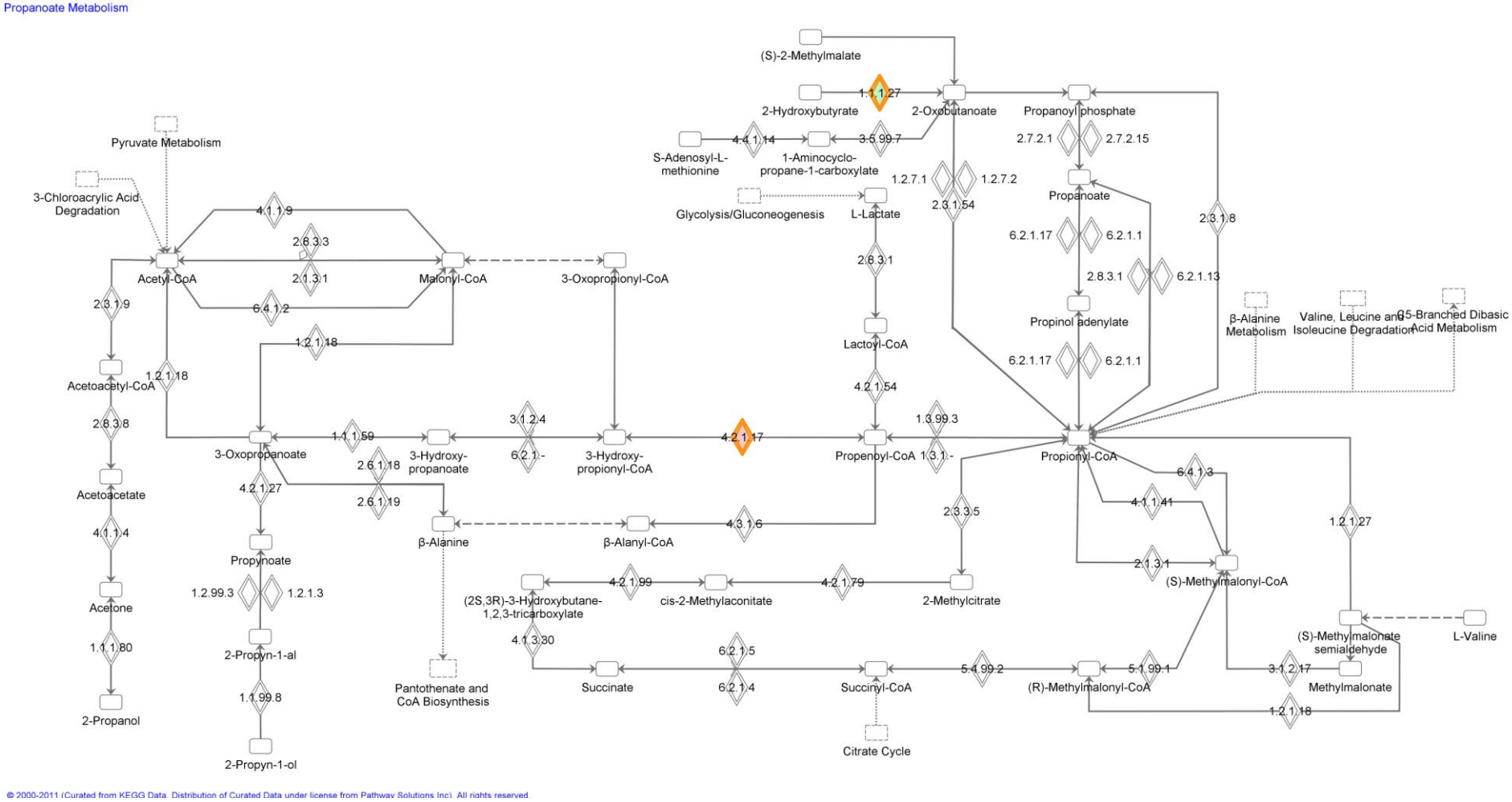

Figure SII.3: Propanoate metabolism pathway.

PROTEIN UBIQUITINATION PATHWAY

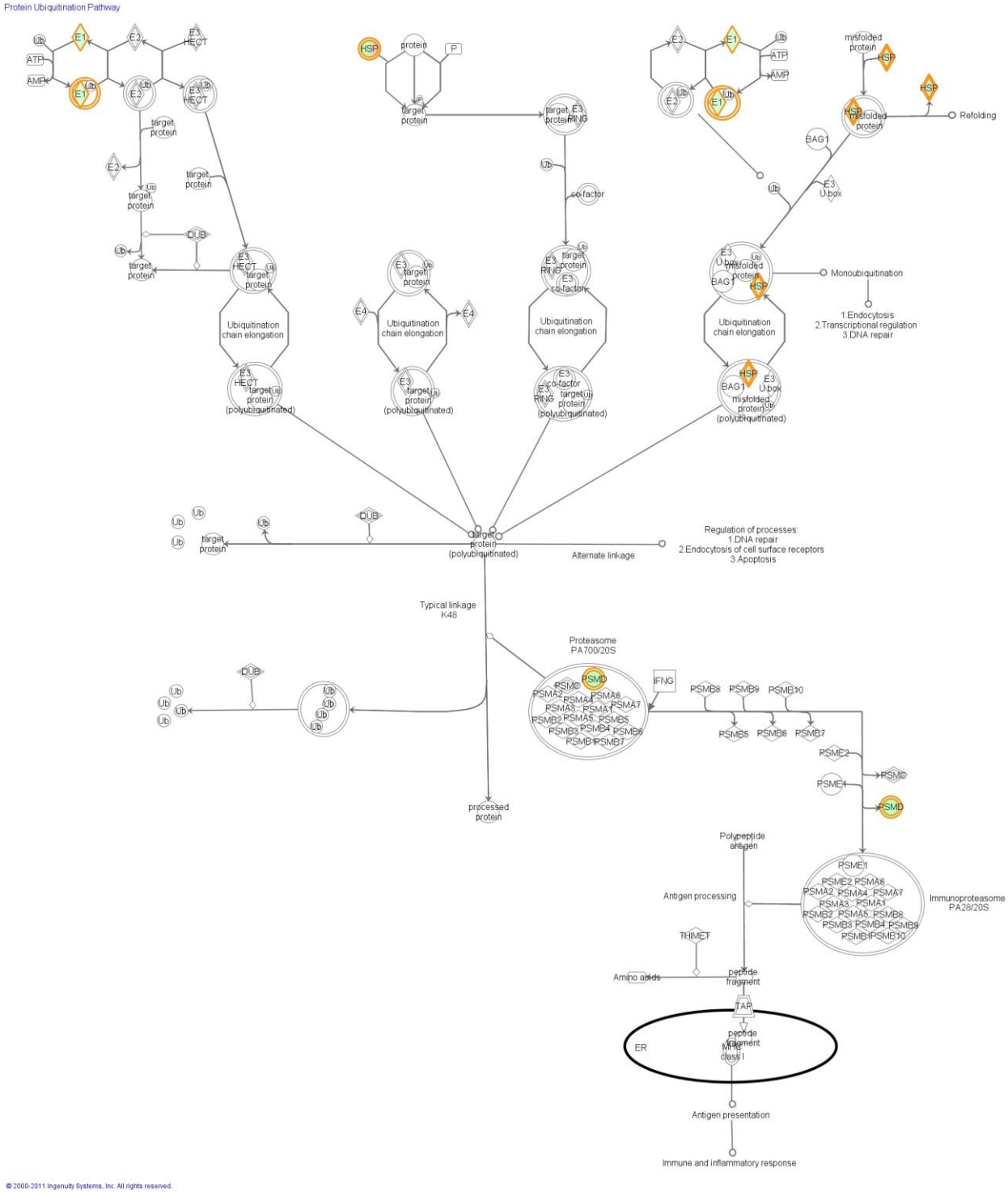

Figure SII.4: Protein ubiquitination pathway.

VEGF SIGNALING PATHWAY

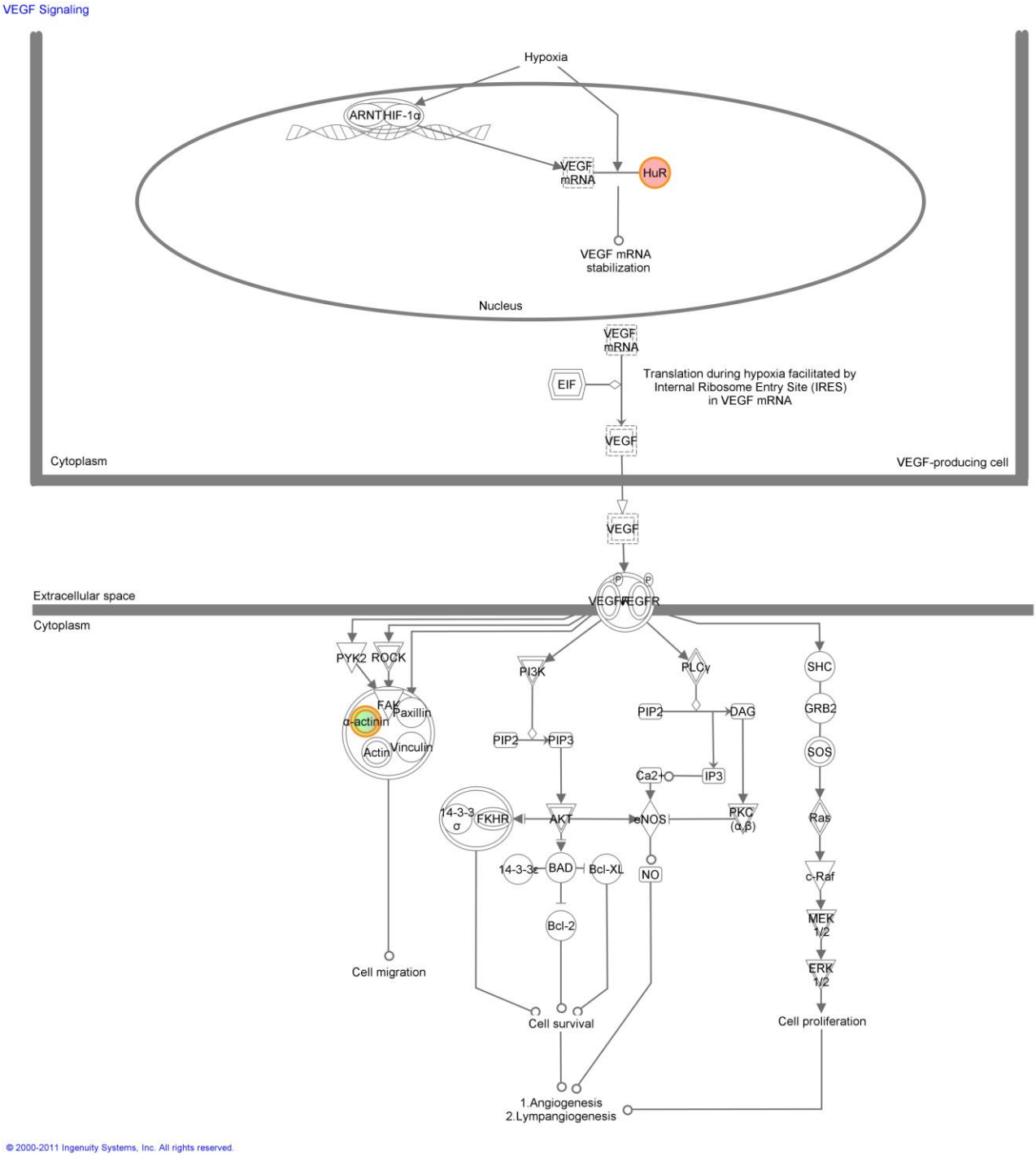

Figure SII.5: VEGF pathway.

INTEGRIN SIGNALING PATHWAY

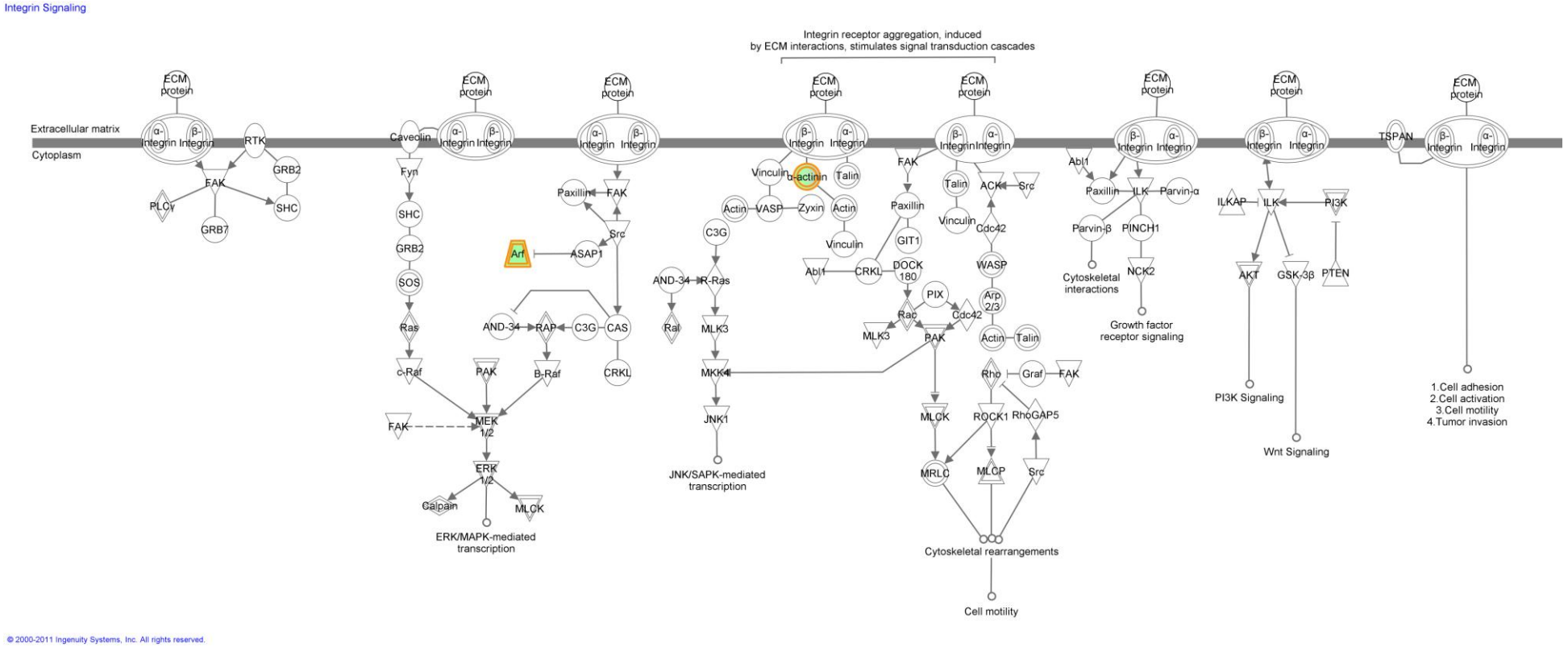

Figure SII.6: Integrin signaling pathway.

REFERENCES

Abe, T., T. Konishi, T. Hirano, H. Kasai, K. Shimizu, M. Kashimura and K. Higashi (1995). "Possible correlation between DNA damage induced by hydrogen peroxide and translocation of heat shock 70 protein into the nucleus." Biochem Biophys Res Commun **206**(2): 548-555.

Alves, C., N. Freitas and C. Cunha (2008). "Characterization of the nuclear localization signal of the hepatitis delta virus antigen." Virology **370**(1): 12-21.

Amarzguioui, M. and H. Prydz (2004). "An algorithm for selection of functional siRNA sequences." Biochem Biophys Res Commun **316**(4): 1050-1058.

Ammermann, I., M. Bruckner, F. Matthes, T. Iftner and F. Stubenrauch (2008). "Inhibition of transcription and DNA replication by the papillomavirus E8-E2C protein is mediated by interaction with corepressor molecules." J Virol **82**(11): 5127-5136.

Anderson, H. and M. Roberge (1996). "Topoisomerase II inhibitors affect entry into mitosis and chromosome condensation in BHK cells." Cell Growth Differ **7**(1): 83-90.

Arhin, G. K., M. Boots, P. S. Bagga, C. Milcarek and J. Wilusz (2002). "Downstream sequence elements with different affinities for the hnRNP H/H' protein influence the processing efficiency of mammalian polyadenylation signals." Nucleic Acids Res **30**(8): 1842-1850.

Bajenova, O., E. Stolper, S. Gapon, N. Sundina, R. Zimmer and P. Thomas (2003). "Surface expression of heterogeneous nuclear RNA binding protein M4 on Kupffer cell relates to its function as a carcinoembryonic antigen receptor." Exp Cell Res **291**(1): 228-241.

Ballana, E., E. Pauls, B. Clotet, F. Perron-Sierra, G. C. Tucker and J. A. Este (2011). "beta5 integrin is the major contributor to the alphaVintegrin-mediated blockade of HIV-1 replication." J Immunol **186**(1): 464-470.

Bantscheff, M., M. Schirle, G. Sweetman, J. Rick and B. Kuster (2007). "Quantitative mass spectrometry in proteomics: a critical review." Anal Bioanal Chem **389**(4): 1017-1031.

Bardos, J. I. and M. Ashcroft (2005). "Negative and positive regulation of HIF-1: a complex network." Biochim Biophys Acta **1755**(2): 107-120.

Barrera, A., B. Guerra, L. Notvall and R. E. Lanford (2005). "Mapping of the hepatitis B virus pre-S1 domain involved in receptor recognition." J Virol **79**(15): 9786-9798.

Benhenda, S., D. Cougot, M. A. Buendia and C. Neuveut (2009). "Hepatitis B virus X protein molecular functions and its role in virus life cycle and pathogenesis." Adv Cancer Res **103**: 75-109.

Bichko, V., S. Barik and J. Taylor (1997). "Phosphorylation of the hepatitis delta virus antigens." J Virol **71**(1): 512-518.

Bichko, V. V. and J. M. Taylor (1996). "Redistribution of the delta antigens in cells replicating the genome of hepatitis delta virus." J Virol **70**(11): 8064-8070.

Blais, D. R., M. Brulotte, Y. Qian, S. Belanger, S. Q. Yao and J. P. Pezacki (2010). "Activity-based proteome profiling of hepatoma cells during hepatitis C virus replication using protease substrate probes." J Proteome Res **9**(2): 912-923.

Bloomfield, V. A., Crothers, D. M., Tinoco Jr, I. (2000). Nucleic Acids: Structures, properties and functions.

Bodily, J. M., K. P. Mehta and L. A. Laimins (2010). "Human Papillomavirus E7 Enhances Hypoxia-Inducible Factor 1 Mediated Transcription by Inhibiting Binding of Histone Deacetylases." Cancer Res.

Bonzon-Kulichenko, E., D. Perez-Hernandez, E. Nunez, P. Martinez-Acedo, P. Navarro, M. Trevisan-Herraz, M. D. Ramos, S. Sierra, S. Martinez-Martinez, M. Ruiz-Meana, E. Miro-Casas, D. Garcia-Dorado, J. M. Redondo, J. S. Burgos and J. Vazquez (2010). "A robust method for quantitative high-throughputanalysis of proteomes by 18O labeling." Mol Cell Proteomics.

Boulon, S., B. J. Westman, S. Hutten, F. M. Boisvert and A. I. Lamond (2010). "The nucleolus under stress." Mol Cell **40**(2): 216-227.

Bradford, M. M. (1976). "A rapid and sensitive method for the quantitation of microgram quantities of protein utilizing the principle of protein-dye binding." Anal Biochem **72**: 248-254.

Branch, A. D. and H. D. Robertson (1984). "A replication cycle for viroids and other small infectious RNA's." Science **223**(4635): 450-455.

Brazas, R. and D. Ganem (1996). "A cellular homolog of hepatitis delta antigen: implications for viral replication and evolution." Science **274**(5284): 90-94.

Brewer, G. (1991). "An A + U-rich element RNA-binding factor regulates c-myc mRNA stability in vitro." Mol Cell Biol **11**(5): 2460-2466.

Brummelkamp, T. R., R. Bernards and R. Agami (2002). "A system for stable expression of short interfering RNAs in mammalian cells." Science **296**(5567): 550-553.

Brunner, J. E., K. J. Ertel, J. M. Rozovics and B. L. Semler (2010). "Delayed kinetics of poliovirus RNA synthesis in a human cell line with reduced levels of hnRNP C proteins." Virology **400**(2): 240-247.

Bukau, B. and A. L. Horwich (1998). "The Hsp70 and Hsp60 chaperone machines." Cell **92**(3): 351-366.

Bukau, B., J. Weissman and A. Horwich (2006). "Molecular chaperones and protein quality control." Cell **125**(3): 443-451.

Cao, D., D. Haussecker, Y. Huang and M. A. Kay (2009). "Combined proteomic-RNAi screen for host factors involved in human hepatitis delta virus replication." RNA **15**(11): 1971-1979.

Caputi, M. and A. M. Zahler (2002). "SR proteins and hnRNP H regulate the splicing of the HIV-1 tev-specific exon 6D." EMBO J **21**(4): 845-855.

Casey, J., P. J. Cote, I. A. Toshkov, C. K. Chu, J. L. Gerin, W. E. Hornbuckle, B. C. Tennant and B. E. Korba (2005). "Clevudine inhibits hepatitis delta virus viremia: a pilot study of chronically infected woodchucks." Antimicrob Agents Chemother **49**(10): 4396-4399.

Casey, J. L. (2006). Hepatitis delta virus. Berlin, Springer.

Castello, G., S. Scala, G. Palmieri, S. A. Curley and F. Izzo (2010). "HCV-related hepatocellular carcinoma: From chronic inflammation to cancer." Clin Immunol **134**(3): 237-250.

Chang, J., S. O. Gudima, C. Tarn, X. Nie and J. M. Taylor (2005). "Development of a novel system to study hepatitis delta virus genome replication." J Virol **79**(13): 8182-8188.

Chang, J., X. Nie, H. E. Chang, Z. Han and J. Taylor (2008). "Transcription of hepatitis delta virus RNA by RNA polymerase II." J Virol **82**(3): 1118-1127.

Chang, J., X. Nie, S. Gudima and J. Taylor (2006). "Action of inhibitors on accumulation of processed hepatitis delta virus RNAs." J Virol **80**(7): 3205-3214.

Chang, M. F., S. C. Baker, L. H. Soe, T. Kamahora, J. G. Keck, S. Makino, S. Govindarajan and M. M. Lai (1988). "Human hepatitis delta antigen is a nuclear phosphoprotein with RNA-binding activity." J Virol **62**(7): 2403-2410.

Chang, M. F., C. Y. Sun, C. J. Chen and S. C. Chang (1993). "Functional motifs of delta antigen essential for RNA binding and replication of hepatitis delta virus." J Virol **67**(5): 2529-2536.

Chang, P. C., L. D. Fitzgerald, A. Van Geelen, Y. Izumiya, T. J. Ellison, D. H. Wang, D. K. Ann, P. A. Luciw and H. J. Kung (2009). "Kruppel-associated box domain-associated protein-1 as a latency regulator for Kaposi's sarcoma-associated herpesvirus and its modulation by the viral protein kinase." Cancer Res **69**(14): 5681-5689.

Chao, M., S. Y. Hsieh and J. Taylor (1990). "Role of two forms of hepatitis delta virus antigen: evidence for a mechanism of self-limiting genome replication." J Virol **64**(10): 5066-5069.

Chaudhury, A., P. Chander and P. H. Howe (2010). "Heterogeneous nuclear ribonucleoproteins (hnRNPs) in cellular processes: Focus on hnRNP E1's multifunctional regulatory roles." RNA **16**(8): 1449-1462.

Chelius, D. and P. V. Bondarenko (2002). "Quantitative profiling of proteins in complex mixtures using liquid chromatography and mass spectrometry." J Proteome Res **1**(4): 317-323.

Chemin, I. and F. Zoulim (2009). "Hepatitis B virus induced hepatocellular carcinoma." Cancer Lett **286**(1): 52-59.

Chen, C. D., R. Kobayashi and D. M. Helfman (1999). "Binding of hnRNP H to an exonic splicing silencer is involved in the regulation of alternative splicing of the rat beta-tropomyosin gene." Genes Dev **13**(5): 593-606.

Chen, C. W., Y. G. Tsay, H. L. Wu, C. H. Lee, D. S. Chen and P. J. Chen (2002). "The double-stranded RNA-activated kinase, PKR, can phosphorylate hepatitis D virus small delta antigen at functional serine and threonine residues." J Biol Chem **277**(36): 33058-33067.

Chen, D., Z. Zhang, M. Li, W. Wang, Y. Li, E. R. Rayburn, D. L. Hill, H. Wang and R. Zhang (2007). "Ribosomal protein S7 as a novel modulator of p53-MDM2 interaction: binding to MDM2, stabilization of p53 protein, and activation of p53 function." Oncogene **26**(35): 5029-5037.

Chen, L. C., H. P. Liu, H. P. Li, C. Hsueh, J. S. Yu, C. L. Liang and Y. S. Chang (2009). "Thymidine phosphorylase mRNA stability and protein levels are increased through ERK-mediated cytoplasmic accumulation of hnRNP K in nasopharyngeal carcinoma cells." Oncogene **28**(17): 1904-1915.

Cheng, D., A. Yang, H. Thomas and J. Monjardino (1993). "Characterization of stable hepatitis delta expressing hepatoma cell lines: effect of HDAg on cell growth." Prog Clin Biol Res **382**: 149-153.

Cheng, Q., G. C. Jayan and J. L. Casey (2003). "Differential inhibition of RNA editing in hepatitis delta virus genotype III by the short and long forms of hepatitis delta antigen." J Virol **77**(14): 7786-7795.

Cheunim, T., J. Zhang, S. G. Milligan, M. G. McPhillips and S. V. Graham (2008). "The alternative splicing factor hnRNP A1 is up-regulated during virus-infected epithelial cell differentiation and binds the human papillomavirus type 16 late regulatory element." Virus Res **131**(2): 189-198.

Chkheidze, A. N. and S. A. Liebhaber (2003). "A novel set of nuclear localization signals determine distributions of the alphaCP RNA-binding proteins." Mol Cell Biol **23**(23): 8405-8415.

Choi, S. H., K. J. Park and S. B. Hwang (2002). "Large hepatitis delta antigen is phosphorylated at multiple sites and phosphorylation is associated with protein conformational change." Intervirology **45**(3): 142-149.

Chou, M. Y., N. Rooke, C. W. Turck and D. L. Black (1999). "hnRNP H is a component of a splicing enhancer complex that activates a c-src alternative exon in neuronal cells." Mol Cell Biol **19**(1): 69-77.

Choudhary, C. and M. Mann (2010). "Decoding signalling networks by mass spectrometry-based proteomics." Nat Rev Mol Cell Biol **11**(6): 427-439.

Chuang, H. Y., M. Hofree and T. Ideker (2010). "A decade of systems biology." Annu Rev Cell Dev Biol **26**: 721-744.

Cowell, I. G., A. L. Okorokov, S. A. Cutts, K. Padget, M. Bell, J. Milner and C. A. Austin (2000). "Human topoisomerase IIalpha and IIbeta interact with the C-terminal region of p53." Exp Cell Res **255**(1): 86-94.

Craig, E. A., J. S. Weissman and A. L. Horwich (1994). "Heat shock proteins and molecular chaperones: mediators of protein conformation and turnover in the cell." Cell **78**(3): 365-372.

Cunha, C., N. Freitas and S. Mota (2003). "Developments in hepatitis delta research " The Internet Journal of Tropical Medicine **1**(2).

Cunha, C., J. Monjardino, D. Cheng, S. Krause and M. Carmo-Fonseca (1998). "Localization of hepatitis delta virus RNA in the nucleus of human cells." RNA **4**(6): 680-693.

D'Souza-Schorey, C. and P. Chavrier (2006). "ARF proteins: roles in membrane traffic and beyond." Nat Rev Mol Cell Biol **7**(5): 347-358.

Dang, C. V., A. Le and P. Gao (2009). "MYC-induced cancer cell energy metabolism and therapeutic opportunities." Clin Cancer Res **15**(21): 6479-6483.

Desgrosellier, J. S. and D. A. Cheresh (2010). "Integrins in cancer: biological implications and therapeutic opportunities." Nat Rev Cancer **10**(1): 9-22.

Deshmane, S. L., R. Mukerjee, S. Fan, L. Del Valle, C. Michiels, T. Sweet, I. Rom, K. Khalili, J. Rappaport, S. Amini and B. E. Sawaya (2009). "Activation of the oxidative stress pathway by HIV-1 Vpr leads to induction of hypoxia-inducible factor 1alpha expression." J Biol Chem **284**(17): 11364-11373.

Dreyfuss, G., V. N. Kim and N. Kataoka (2002). "Messenger-RNA-binding proteins and the messages they carry." Nat Rev Mol Cell Biol **3**(3): 195-205.

Dreyfuss, G., M. J. Matunis, S. Pinol-Roma and C. G. Burd (1993). "hnRNP proteins and the biogenesis of mRNA." Annu Rev Biochem **62**: 289-321.

Du, X., Q. Wang, Y. Hirohashi and M. I. Greene (2006). "DIPA, which can localize to the centrosome, associates with p78/MCRS1/MSP58 and acts as a repressor of gene transcription." Exp Mol Pathol **81**(3): 184-190.

Elbashir, S. M., W. Lendeckel and T. Tuschl (2001). "RNA interference is mediated by 21- and 22-nucleotide RNAs." Genes Dev **15**(2): 188-200.

Elliott, M. H., D. S. Smith, C. E. Parker and C. Borchers (2009). "Current trends in quantitative proteomics." J Mass Spectrom **44**(12): 1637-1660.

Eversole, A. and N. Maizels (2000). "In vitro properties of the conserved mammalian protein hnRNP D suggest a role in telomere maintenance." Mol Cell Biol **20**(15): 5425-5432.

Expert-Bezancon, A., J. P. Le Caer and J. Marie (2002). "Heterogeneous nuclear ribonucleoprotein (hnRNP) K is a component of an intronic splicing enhancer complex that activates the splicing of the alternative exon 6A from chicken beta-tropomyosin pre-mRNA." J Biol Chem **277**(19): 16614-16623.

Farci, P., T. Roskams, L. Chessa, G. Peddis, A. P. Mazzoleni, R. Scioscia, G. Serra, M. E. Lai, M. Loy, L. Caruso, V. Desmet, R. H. Purcell and A. Balestrieri (2004). "Long-term benefit of interferon alpha therapy of chronic hepatitis D: regression of advanced hepatic fibrosis." Gastroenterology **126**(7): 1740-1749.

Fenn, J. B., M. Mann, C. K. Meng, S. F. Wong and C. M. Whitehouse (1989). "Electrospray ionization for mass spectrometry of large biomolecules." Science **246**(4926): 64-71.

Feo, S., D. Arcuri, E. Piddini, R. Passantino and A. Giallongo (2000). "ENO1 gene product binds to the c-myc promoter and acts as a transcriptional repressor: relationship with Myc promoter-binding protein 1 (MBP-1)." FEBS Lett **473**(1): 47-52.

Ferre-D'Amare, A. R., K. Zhou and J. A. Doudna (1998). "Crystal structure of a hepatitis delta virus ribozyme." Nature **395**(6702): 567-574.

Fogel, B. L. and M. T. McNally (2000). "A cellular protein, hnRNP H, binds to the negative regulator of splicing element from Rous sarcoma virus." J Biol Chem **275**(41): 32371-32378.

Ford, L. P., W. E. Wright and J. W. Shay (2002). "A model for heterogeneous nuclear ribonucleoproteins in telomere and telomerase regulation." Oncogene **21**(4): 580-583.

Gaeta, G. B., T. Stroffolini, M. Chiaramonte, T. Ascione, G. Stornaiuolo, S. Lobello, E. Sagnelli, M. R. Brunetto and M. Rizzetto (2000). "Chronic hepatitis D: a vanishing Disease? An Italian multicenter study." Hepatology **32**(4 Pt 1): 824-827.

Garneau, D., T. Revil, J. F. Fisette and B. Chabot (2005). "Heterogeneous nuclear ribonucleoprotein F/H proteins modulate the alternative splicing of the apoptotic mediator Bcl-x." J Biol Chem **280**(24): 22641-22650.

Georgel, P., C. Schuster, M. B. Zeisel, F. Stoll-Keller, T. Berg, S. Bahram and T. F. Baumert (2010). "Virus-host interactions in hepatitis C virus infection: implications for molecular pathogenesis and antiviral strategies." Trends Mol Med **16**(6): 277-286.

Gerber, S. A., J. Rush, O. Stemman, M. W. Kirschner and S. P. Gygi (2003). "Absolute quantification of proteins and phosphoproteins from cell lysates by tandem MS." Proc Natl Acad Sci U S A **100**(12): 6940-6945.

Glenn, J. S., J. A. Watson, C. M. Havel and J. M. White (1992). "Identification of a prenylation site in delta virus large antigen." Science **256**(5061): 1331-1333.

Greco-Stewart, V. S., E. Schissel and M. Pelchat (2009). "The hepatitis delta virus RNA genome interacts with the human RNA polymerases I and III." Virology **386**(1): 12-15.

Grosset, C., C. Y. Chen, N. Xu, N. Sonenberg, H. Jacquemin-Sablon and A. B. Shyu (2000). "A mechanism for translationally coupled mRNA turnover: interaction between the poly(A) tail and a c-fos RNA coding determinant via a protein complex." Cell **103**(1): 29-40.

Gudima, S., K. Dingle, T. T. Wu, G. Moraleda and J. Taylor (1999). "Characterization of the 5' ends for polyadenylated RNAs synthesized during the replication of hepatitis delta virus." J Virol **73**(8): 6533-6539.

Gudima, S., S. Y. Wu, C. M. Chiang, G. Moraleda and J. Taylor (2000). "Origin of hepatitis delta virus mRNA." J Virol **74**(16): 7204-7210.

Gudima, S. O., J. Chang and J. M. Taylor (2004). "Features affecting the ability of hepatitis delta virus RNAs to initiate RNA-directed RNA synthesis." J Virol **78**(11): 5737-5744.

Gudima, S. O., J. Chang and J. M. Taylor (2005). "Reconstitution in cultured cells of replicating HDV RNA from pairs of less than full-length RNAs." RNA **11**(1): 90-98.

Gui, H., C. W. Lu, S. Adams, V. Stollar and M. L. Li (2010). "hnRNP A1 interacts with the genomic and subgenomic RNA promoters of Sindbis virus and is required for the synthesis of G and SG RNA." J Biomed Sci **17**: 59.

Gygi, S. P., B. Rist, S. A. Gerber, F. Turecek, M. H. Gelb and R. Aebersold (1999). "Quantitative analysis of complex protein mixtures using isotope-coded affinity tags." Nat Biotechnol **17**(10): 994-999.

Han, Z., C. Alves, S. Gudima and J. Taylor (2009). "Intracellular localization of hepatitis delta virus proteins in the presence and absence of viral RNA accumulation." J Virol **83**(13): 6457-6463.

Hatayama, T., K. Honda and M. Yukioka (1986). "HeLa cells synthesize a specific heat shock protein upon exposure to heat shock at 42 degrees C but not at 45 degrees C." Biochem Biophys Res Commun **137**(3): 957-963.

Hatayama, T. and K. Yasuda (1998). "Association of HSP105 with HSC70 in high molecular mass complexes in mouse FM3A cells." Biochem Biophys Res Commun **248**(2): 395-401.

Haussecker, D., D. Cao, Y. Huang, P. Parameswaran, A. Z. Fire and M. A. Kay (2008). "Capped small RNAs and MOV10 in human hepatitis delta virus replication." Nat Struct Mol Biol **15**(7): 714-721.

Hendrick, J. P. and F. U. Hartl (1993). "Molecular chaperone functions of heat-shock proteins." Annu Rev Biochem **62**: 349-384.

Hernaez, B., J. M. Escribano and C. Alonso (2008). "African swine fever virus protein p30 interaction with heterogeneous nuclear ribonucleoprotein K (hnRNP-K) during infection." FEBS Lett **582**(23-24): 3275-3280.

Honda, K., T. Hatayama and M. Yukioka (1988). "Characterization of a 42 degrees C-specific heat shock protein of mammalian cells." J Biochem **103**(1): 81-85.

Hosaka, S., T. Nakatsura, H. Tsukamoto, T. Hatayama, H. Baba and Y. Nishimura (2006). "Synthetic small interfering RNA targeting heat shock protein 105 induces apoptosis of various cancer cells both in vitro and in vivo." Cancer Sci **97**(7): 623-632.

Hsu, N. Y., O. Ilnytska, G. Belov, M. Santiana, Y. H. Chen, P. M. Takvorian, C. Pau, H. van der Schaar, N. Kaushik-Basu, T. Balla, C. E. Cameron, E. Ehrenfeld, F. J. van Kuppeveld and N. Altan-Bonnet (2010). "Viral reorganization of the secretory pathway generates distinct organelles for RNA replication." Cell **141**(5): 799-811.

Hsu, P. P. and D. M. Sabatini (2008). "Cancer cell metabolism: Warburg and beyond." Cell **134**(5): 703-707.

Hu, Q., R. J. Noll, H. Li, A. Makarov, M. Hardman and R. Graham Cooks (2005). "The Orbitrap: a new mass spectrometer." J Mass Spectrom **40**(4): 430-443.

Huang, C., S. C. Chang, H. C. Yang, C. L. Chien and M. F. Chang (2009). "Clathrin-mediated post-Golgi membrane trafficking in the morphogenesis of hepatitis delta virus." J Virol **83**(23): 12314-12324.

Huang, C., S. C. Chang, I. C. Yu, Y. G. Tsay and M. F. Chang (2007). "Large hepatitis delta antigen is a novel clathrin adaptor-like protein." J Virol **81**(11): 5985-5994.

Huang, Q., L. Wang, S. Bai, W. Lin, W. Chen, J. Lin and X. Lin (2009). "Global proteome analysis of hepatitis B virus expressing human hepatoblastoma cell line HepG2." J Med Virol **81**(9): 1539-1550.

Huang, W. H., R. T. Mai and Y. H. Lee (2008). "Transcription factor YY1 and its associated acetyltransferases CBP and p300 interact with hepatitis delta antigens and modulate hepatitis delta virus RNA replication." J Virol **82**(15): 7313-7324.

Huang, W. H., B. Y. Yung, W. J. Syu and Y. H. Lee (2001). "The nucleolar phosphoprotein B23 interacts with hepatitis delta antigens and modulates the hepatitis delta virus RNA replication." J Biol Chem **276**(27): 25166-25175.

Huang, Y. H., M. H. Tao, C. P. Hu, W. J. Syu and J. C. Wu (2004). "Identification of novel HLA-A*0201-restricted CD8+ T-cell epitopes on hepatitis delta virus." J Gen Virol **85**(Pt 10): 3089-3098.

Huang, Z. S. and H. N. Wu (1998). "Identification and characterization of the RNA chaperone activity of hepatitis delta antigen peptides." J Biol Chem **273**(41): 26455-26461.

Hwang, S. B. and M. M. Lai (1993). "Isoprenylation mediates direct protein-protein interactions between hepatitis large delta antigen and hepatitis B virus surface antigen." J Virol **67**(12): 7659-7662.

Hwang, S. B. and M. M. Lai (1994). "Isoprenylation masks a conformational epitope and enhances trans-dominant inhibitory function of the large hepatitis delta antigen." J Virol **68**(5): 2958-2964.

Hwang, S. B., C. Z. Lee and M. M. Lai (1992). "Hepatitis delta antigen expressed by recombinant baculoviruses: comparison of biochemical properties and post-translational modifications between the large and small forms." Virology **190**(1): 413-422.

Ishihara, K., N. Yamagishi and T. Hatayama (2003). "Protein kinase CK2 phosphorylates Hsp105 alpha at Ser509 and modulates its function." Biochem J **371**(Pt 3): 917-925.

Ishihara, K., K. Yasuda and T. Hatayama (1999). "Molecular cloning, expression and localization of human 105 kDa heat shock protein, hsp105." Biochim Biophys Acta **1444**(1): 138-142.

Jacobs, J. M., D. L. Diamond, E. Y. Chan, M. A. Gritsenko, W. Qian, M. Stastna, T. Baas, D. G. Camp, 2nd, R. L. Carithers, Jr., R. D. Smith and M. G. Katze (2005). "Proteome analysis of liver cells expressing a full-length hepatitis C virus (HCV) replicon and biopsy specimens of posttransplantation liver from HCV-infected patients." J Virol **79**(12): 7558-7569.

Jacquenet, S., A. Mereau, P. S. Bilodeau, L. Damier, C. M. Stoltzfus and C. Branlant (2001). "A second exon splicing silencer within human immunodeficiency virus type 1 tat exon 2

represses splicing of Tat mRNA and binds protein hnRNP H." J Biol Chem **276**(44): 40464-40475.

Jardi, R., F. Rodriguez, M. Buti, X. Costa, M. Cotrina, R. Galimany, R. Esteban and J. Guardia (2001). "Role of hepatitis B, C, and D viruses in dual and triple infection: influence of viral genotypes and hepatitis B precore and basal core promoter mutations on viral replicative interference." Hepatology **34**(2): 404-410.

Jeng, K. S., P. Y. Su and M. M. Lai (1996). "Hepatitis delta antigens enhance the ribozyme activities of hepatitis delta virus RNA in vivo." J Virol **70**(7): 4205-4209.

Jorge, I., E. M. Casas, M. Villar, I. Ortega-Perez, D. Lopez-Ferrer, A. Martinez-Ruiz, M. Carrera, A. Marina, P. Martinez, H. Serrano, B. Canas, F. Were, J. M. Gallardo, S. Lamas, J. M. Redondo, D. Garcia-Dorado and J. Vazquez (2007). "High-sensitivity analysis of specific peptides in complex samples by selected MS/MS ion monitoring and linear ion trap mass spectrometry: application to biological studies." J Mass Spectrom **42**(11): 1391-1403.

Jorge, I., P. Navarro, P. Martinez-Acedo, E. Nunez, H. Serrano, A. Alfranca, J. M. Redondo and J. Vazquez (2009). "Statistical model to analyze quantitative proteomics data obtained by 18O/16O labeling and linear ion trap mass spectrometry: application to the study of vascular endothelial growth factor-induced angiogenesis in endothelial cells." Mol Cell Proteomics **8**(5): 1130-1149.

Kim, C. S., S. K. Seol, O. K. Song, J. H. Park and S. K. Jang (2007). "An RNA-binding protein, hnRNP A1, and a scaffold protein, septin 6, facilitate hepatitis C virus replication." J Virol **81**(8): 3852-3865.

Kim, H. H., Y. Kuwano, S. Srikantan, E. K. Lee, J. L. Martindale and M. Gorospe (2009). "HuR recruits let-7/RISC to repress c-Myc expression." Genes Dev **23**(15): 1743-1748.

Kim, W., S. Oe Lim, J. S. Kim, Y. H. Ryu, J. Y. Byeon, H. J. Kim, Y. I. Kim, J. S. Heo, Y. M. Park and G. Jung (2003). "Comparison of proteome between hepatitis B virus- and hepatitis C virus-associated hepatocellular carcinoma." Clin Cancer Res **9**(15): 5493-5500.

Kondo, S., S. Y. Seo, T. Yoshizaki, N. Wakisaka, M. Furukawa, I. Joab, K. L. Jang and J. S. Pagano (2006). "EBV latent membrane protein 1 up-regulates hypoxia-inducible factor 1alpha through Siah1-mediated down-regulation of prolyl hydroxylases 1 and 3 in nasopharyngeal epithelial cells." Cancer Res **66**(20): 9870-9877.

Koumenis, C., R. Alarcon, E. Hammond, P. Sutphin, W. Hoffman, M. Murphy, J. Derr, Y. Taya, S. W. Lowe, M. Kastan and A. Giaccia (2001). "Regulation of p53 by hypoxia: dissociation of transcriptional repression and apoptosis from p53-dependent transactivation." Mol Cell Biol **21**(4): 1297-1310.

Krijgsveld, J., R. F. Ketting, T. Mahmoudi, J. Johansen, M. Artal-Sanz, C. P. Verrijzer, R. H. Plasterk and A. J. Heck (2003). "Metabolic labeling of C. elegans and D. melanogaster for quantitative proteomics." Nat Biotechnol **21**(8): 927-931.

Kuo, M. Y., J. Goldberg, L. Coates, W. Mason, J. Gerin and J. Taylor (1988). "Molecular cloning of hepatitis delta virus RNA from an infected woodchuck liver: sequence, structure, and applications." J Virol **62**(6): 1855-1861.

Laemmli, U. K. (1970). "Cleavage of structural proteins during the assembly of the head of bacteriophage T4." Nature **227**(5259): 680-685.

Laroia, G., R. Cuesta, G. Brewer and R. J. Schneider (1999). "Control of mRNA decay by heat shock-ubiquitin-proteasome pathway." Science **284**(5413): 499-502.

Lau, D. T., D. E. Kleiner, Y. Park, A. M. Di Bisceglie and J. H. Hoofnagle (1999). "Resolution of chronic delta hepatitis after 12 years of interferon alfa therapy." Gastroenterology **117**(5): 1229-1233.

Lazinski, D. W. and J. M. Taylor (1993). "Relating structure to function in the hepatitis delta virus antigen." J Virol **67**(5): 2672-2680.

Lazinski, D. W. and J. M. Taylor (1994). "Expression of hepatitis delta virus RNA deletions: cis and trans requirements for self-cleavage, ligation, and RNA packaging." J Virol **68**(5): 2879-2888.

Lee, C. H., S. C. Chang, C. J. Chen and M. F. Chang (1998). "The nucleolin binding activity of hepatitis delta antigen is associated with nucleolus targeting." J Biol Chem **273**(13): 7650-7656.

Lee, C. H., S. C. Chang, C. H. Wu and M. F. Chang (2001). "A novel chromosome region maintenance 1-independent nuclear export signal of the large form of hepatitis delta antigen that is required for the viral assembly." J Biol Chem **276**(11): 8142-8148.

Lee, C. Z., J. H. Lin, M. Chao, K. McKnight and M. M. Lai (1993). "RNA-binding activity of hepatitis delta antigen involves two arginine-rich motifs and is required for hepatitis delta virus RNA replication." J Virol **67**(4): 2221-2227.

Lee, C. Z. and J. C. Sheu (2008). "Histone H1e interacts with small hepatitis delta antigen and affects hepatitis delta virus replication." Virology **375**(1): 197-204.

Lee, I. N., C. H. Chen, J. C. Sheu, H. S. Lee, G. T. Huang, C. Y. Yu, F. J. Lu and L. P. Chow (2005). "Identification of human hepatocellular carcinoma-related biomarkers by two-dimensional difference gel electrophoresis and mass spectrometry." J Proteome Res **4**(6): 2062-2069.

Lee, J. H., S. H. Kim, P. N. Pascua, M. S. Song, Y. H. Baek, X. Jin, J. K. Choi, C. J. Kim, H. Kim and Y. K. Choi (2010). "Direct interaction of cellular hnRNP-F and NS1 of influenza A virus accelerates viral replication by modulation of viral transcriptional activity and host gene expression." Virology **397**(1): 89-99.

Lee, N. P., L. Chen, M. C. Lin, F. H. Tsang, C. Yeung, R. T. Poon, J. Peng, X. Leng, L. Beretta, S. Sun, P. J. Day and J. M. Luk (2009). "Proteomic expression signature distinguishes cancerous and nonmalignant tissues in hepatocellular carcinoma." J Proteome Res **8**(3): 1293-1303.

Lehmann, E., F. Brueckner and P. Cramer (2007). "Molecular basis of RNA-dependent RNA polymerase II activity." Nature **450**(7168): 445-449.

Li, Y. J., T. Macnaughton, L. Gao and M. M. Lai (2006). "RNA-templated replication of hepatitis delta virus: genomic and antigenomic RNAs associate with different nuclear bodies." J Virol **80**(13): 6478-6486.

Li, Y. J., M. R. Stallcup and M. M. Lai (2004). "Hepatitis delta virus antigen is methylated at arginine residues, and methylation regulates subcellular localization and RNA replication." J Virol **78**(23): 13325-13334.

Liang, T. J. (2009). "Hepatitis B: the virus and disease." Hepatology **49**(5 Suppl): S13-21.

Lin, J. H., M. F. Chang, S. C. Baker, S. Govindarajan and M. M. Lai (1990). "Characterization of hepatitis delta antigen: specific binding to hepatitis delta virus RNA." J Virol **64**(9): 4051-4058.

Liu, H., R. G. Sadygov and J. R. Yates, 3rd (2004). "A model for random sampling and estimation of relative protein abundance in shotgun proteomics." Anal Chem **76**(14): 4193-4201.

Livak, K. J. and T. D. Schmittgen (2001). "Analysis of relative gene expression data using real-time quantitative PCR and the 2(-Delta Delta C(T)) Method." Methods **25**(4): 402-408.

Long, M., S. J. de Souza and W. Gilbert (1997). "Delta-interacting protein A and the origin of hepatitis delta antigen." Science **276**(5313): 824-825.

Lopez-Ferrer, D., S. Martinez-Bartolome, M. Villar, M. Campillos, F. Martin-Maroto and J. Vazquez (2004). "Statistical model for large-scale peptide identification in databases from tandem mass spectra using SEQUEST." Anal Chem **76**(23): 6853-6860.

Lopez-Ferrer, D., A. Ramos-Fernandez, S. Martinez-Bartolome, P. Garcia-Ruiz and J. Vazquez (2006). "Quantitative proteomics using 16O/18O labeling and linear ion trap mass spectrometry." Proteomics **6 Suppl 1**: S4-11.

Lu, J. Y., N. Bergman, N. Sadri and R. J. Schneider (2006). "Assembly of AUF1 with eIF4G-poly(A) binding protein complex suggests a translation function in AU-rich mRNA decay." RNA **12**(5): 883-893.

Macnaughton, T. B. and M. M. Lai (2002). "Large hepatitis delta antigen is not a suppressor of hepatitis delta virus RNA synthesis once RNA replication is established." J Virol **76**(19): 9910-9919.

Mallick, P. and B. Kuster (2010). "Proteomics: a pragmatic perspective." Nat Biotechnol **28**(7): 695-709.

Manns, M. P., H. Wedemeyer and M. Cornberg (2006). "Treating viral hepatitis C: efficacy, side effects, and complications." Gut **55**(9): 1350-1359.

Martinez-Bartolome, S., P. Navarro, F. Martin-Maroto, D. Lopez-Ferrer, A. Ramos-Fernandez, M. Villar, J. P. Garcia-Ruiz and J. Vazquez (2008). "Properties of average score distributions of SEQUEST: the probability ratio method." Mol Cell Proteomics **7**(6): 1135-1145.

Matter, N., M. Marx, S. Weg-Remers, H. Ponta, P. Herrlich and H. Konig (2000). "Heterogeneous ribonucleoprotein A1 is part of an exon-specific splice-silencing complex controlled by oncogenic signaling pathways." J Biol Chem **275**(45): 35353-35360.

Matto, M., E. H. Sklan, N. David, N. Melamed-Book, J. E. Casanova, J. S. Glenn and B. Aroeti (2011). "Role for ADP ribosylation factor 1 in the regulation of hepatitis C virus replication." J Virol **85**(2): 946-956.

Mayeda, A. and A. R. Krainer (1992). "Regulation of alternative pre-mRNA splicing by hnRNP A1 and splicing factor SF2." Cell **68**(2): 365-375.

Mayer, C. and I. Grummt (2005). "Cellular stress and nucleolar function." Cell Cycle **4**(8): 1036-1038.

McCullough, A. J. and S. M. Berget (1997). "G triplets located throughout a class of small vertebrate introns enforce intron borders and regulate splice site selection." Mol Cell Biol **17**(8): 4562-4571.

Mendes, M. (2003). Clonagem do cDNA do δAg-S num vector de baculovirus e produção da proteína viral em células de insecto. Molecular Biology. Lisboa, Universidade Nova de Lisboa e Universidade Técnica de Lisboa. **Licenciatura**.

Michael, W. M., P. S. Eder and G. Dreyfuss (1997). "The K nuclear shuttling domain: a novel signal for nuclear import and nuclear export in the hnRNP K protein." EMBO J **16**(12): 3587-3598.

Michelotti, E. F., G. A. Michelotti, A. I. Aronsohn and D. Levens (1996). "Heterogeneous nuclear ribonucleoprotein K is a transcription factor." Mol Cell Biol **16**(5): 2350-2360.

Mizutani, A., M. Fukuda, K. Ibata, Y. Shiraishi and K. Mikoshiba (2000). "SYNCRIP, a cytoplasmic counterpart of heterogeneous nuclear ribonucleoprotein R, interacts with ubiquitous synaptotagmin isoforms." J Biol Chem **275**(13): 9823-9831.

Modahl, L. E. and M. M. Lai (2000). "The large delta antigen of hepatitis delta virus potently inhibits genomic but not antigenomic RNA synthesis: a mechanism enabling initiation of viral replication." J Virol **74**(16): 7375-7380.

Moon, E. J., C. H. Jeong, J. W. Jeong, K. R. Kim, D. Y. Yu, S. Murakami, C. W. Kim and K. W. Kim (2004). "Hepatitis B virus X protein induces angiogenesis by stabilizing hypoxia-inducible factor-1alpha." FASEB J **18**(2): 382-384.

Moraleda, G. and J. Taylor (2001). "Host RNA polymerase requirements for transcription of the human hepatitis delta virus genome." J Virol **75**(21): 10161-10169.

Morozov, A., J. Subjeck and P. Raychaudhuri (1995). "HPV16 E7 oncoprotein induces expression of a 110 kDa heat shock protein." FEBS Lett **371**(3): 214-218.

Mota, S. (2008). Estudo da influência dos siRNAs na replicação do vírus da hepatite delta e análise da expressão genética em células infectadas. Molecular Biology. Lisbon, Universidade Nova de Lisboa. **PhD**.

Mota, S., M. Mendes, N. Freitas, D. Penque, A. V. Coelho and C. Cunha (2009). "Proteome analysis of a human liver carcinoma cell line stably expressing hepatitis delta virus ribonucleoproteins." J Proteomics **72**(4): 616-627.

Mota, S., M. Mendes, D. Penque, A. V. Coelho and C. Cunha (2008). "Changes in the proteome of Huh7 cells induced by transient expression of hepatitis D virus RNA and antigens." J Proteomics **71**(1): 71-79.

Mu, J. J., Y. G. Tsay, L. J. Juan, T. F. Fu, W. H. Huang, D. S. Chen and P. J. Chen (2004). "The small delta antigen of hepatitis delta virus is an acetylated protein and acetylation of lysine 72 may influence its cellular localization and viral RNA synthesis." Virology **319**(1): 60-70.

Mu, J. J., H. L. Wu, B. L. Chiang, R. P. Chang, D. S. Chen and P. J. Chen (1999). "Characterization of the phosphorylated forms and the phosphorylated residues of hepatitis delta virus delta antigens." J Virol **73**(12): 10540-10545.

Nelson, C. J., E. L. Huttlin, A. D. Hegeman, A. C. Harms and M. R. Sussman (2007). "Implications of 15N-metabolic labeling for automated peptide identification in Arabidopsis thaliana." Proteomics **7**(8): 1279-1292.

Neumann, C. A., J. Cao and Y. Manevich (2009). "Peroxiredoxin 1 and its role in cell signaling." Cell Cycle **8**(24): 4072-4078.

Neurath, A. R., S. B. Kent, N. Strick and K. Parker (1986). "Identification and chemical synthesis of a host cell receptor binding site on hepatitis B virus." Cell **46**(3): 429-436.

Nie, X., J. Chang and J. M. Taylor (2004). "Alternative processing of hepatitis delta virus antigenomic RNA transcripts." J Virol **78**(9): 4517-4524.

Niro, G. A., F. Rosina and M. Rizzetto (2005). "Treatment of hepatitis D." J Viral Hepat **12**(1): 2-9.

Nisini, R., M. Paroli, D. Accapezzato, F. Bonino, F. Rosina, T. Santantonio, F. Sallusto, A. Amoroso, M. Houghton and V. Barnaba (1997). "Human CD4+ T-cell response to hepatitis delta virus: identification of multiple epitopes and characterization of T-helper cytokine profiles." J Virol **71**(3): 2241-2251.

Noisakran, S., S. Sengsai, V. Thongboonkerd, R. Kanlaya, S. Sinchaikul, S. T. Chen, C. Puttikhunt, W. Kasinrerk, T. Limjindaporn, W. Wongwiwat, P. Malasit and P. T. Yenchitsomanus (2008). "Identification of human hnRNP C1/C2 as a dengue virus NS1-interacting protein." Biochem Biophys Res Commun **372**(1): 67-72.

Oda, Y., K. Huang, F. R. Cross, D. Cowburn and B. T. Chait (1999). "Accurate quantitation of protein expression and site-specific phosphorylation." Proc Natl Acad Sci U S A **96**(12): 6591-6596.

Ogata, H., S. Goto, K. Sato, W. Fujibuchi, H. Bono and M. Kanehisa (1999). "KEGG: Kyoto Encyclopedia of Genes and Genomes." Nucleic Acids Res **27**(1): 29-34.

Oh, H. J. and Y. F. Lau (2006). "KRAB: a partner for SRY action on chromatin." Mol Cell Endocrinol **247**(1-2): 47-52.

Olsson, A. K., A. Dimberg, J. Kreuger and L. Claesson-Welsh (2006). "VEGF receptor signalling - in control of vascular function." Nat Rev Mol Cell Biol **7**(5): 359-371.

Ong, S. E., B. Blagoev, I. Kratchmarova, D. B. Kristensen, H. Steen, A. Pandey and M. Mann (2002). "Stable isotope labeling by amino acids in cell culture, SILAC, as a simple and accurate approach to expression proteomics." Mol Cell Proteomics **1**(5): 376-386.

Otto, J. C. and P. J. Casey (1996). "The hepatitis delta virus large antigen is farnesylated both in vitro and in animal cells." J Biol Chem **271**(9): 4569-4572.

Paddison, P. J., A. A. Caudy, E. Bernstein, G. J. Hannon and D. S. Conklin (2002). "Short hairpin RNAs (shRNAs) induce sequence-specific silencing in mammalian cells." Genes Dev **16**(8): 948-958.

Paek, K. Y., C. S. Kim, S. M. Park, J. H. Kim and S. K. Jang (2008). "RNA-binding protein hnRNP D modulates internal ribosome entry site-dependent translation of hepatitis C virus RNA." J Virol **82**(24): 12082-12093.

Paul, C. P., P. D. Good, I. Winer and D. R. Engelke (2002). "Effective expression of small interfering RNA in human cells." Nat Biotechnol **20**(5): 505-508.

Pinol-Roma, S. and G. Dreyfuss (1992). "Shuttling of pre-mRNA binding proteins between nucleus and cytoplasm." Nature **355**(6362): 730-732.

Radjef, N., E. Gordien, V. Ivaniushina, E. Gault, P. Anais, T. Drugan, J. C. Trinchet, D. Roulot, M. Tamby, M. C. Milinkovitch and P. Deny (2004). "Molecular phylogenetic analyses indicate a wide and ancient radiation of African hepatitis delta virus, suggesting a deltavirus genus of at least seven major clades." J Virol **78**(5): 2537-2544.

Ramos-Fernandez, A., D. Lopez-Ferrer and J. Vazquez (2007). "Improved method for differential expression proteomics using trypsin-catalyzed 18O labeling with a correction for labeling efficiency." Mol Cell Proteomics **6**(7): 1274-1286.

Rebane, A., A. Aab and J. A. Steitz (2004). "Transportins 1 and 2 are redundant nuclear import factors for hnRNP A1 and HuR." RNA **10**(4): 590-599.

Reid, C. E. and D. W. Lazinski (2000). "A host-specific function is required for ligation of a wide variety of ribozyme-processed RNAs." Proc Natl Acad Sci U S A **97**(1): 424-429.

Ripoli, M., A. D'Aprile, G. Quarato, M. Sarasin-Filipowicz, J. Gouttenoire, R. Scrima, O. Cela, D. Boffoli, M. H. Heim, D. Moradpour, N. Capitanio and C. Piccoli (2010). "Hepatitis C virus-linked mitochondrial dysfunction promotes hypoxia-inducible factor 1 alpha-mediated glycolytic adaptation." J Virol **84**(1): 647-660.

Rizzetto, M., M. G. Canese, S. Arico, O. Crivelli, C. Trepo, F. Bonino and G. Verme (1977). "Immunofluorescence detection of new antigen-antibody system (delta/anti-delta) associated to hepatitis B virus in liver and in serum of HBsAg carriers." Gut **18**(12): 997-1003.

Rizzetto, M., M. G. Canese, J. L. Gerin, W. T. London, D. L. Sly and R. H. Purcell (1980). "Transmission of the hepatitis B virus-associated delta antigen to chimpanzees." J Infect Dis **141**(5): 590-602.

Rizzetto, M., F. Rosina, G. Saracco, P. C. Bellando, G. C. Actis, F. Bonino, A. Smedile, P. Trinchero, F. Sansalvadore, C. Pintus and et al. (1986). "Treatment of chronic delta hepatitis with alpha-2 recombinant interferon." J Hepatol **3 Suppl 2**: S229-233.

Ross, P. L., Y. N. Huang, J. N. Marchese, B. Williamson, K. Parker, S. Hattan, N. Khainovski, S. Pillai, S. Dey, S. Daniels, S. Purkayastha, P. Juhasz, S. Martin, M. Bartlet-Jones, F. He, A. Jacobson and D. J. Pappin (2004). "Multiplexed protein quantitation in Saccharomyces cerevisiae using amine-reactive isobaric tagging reagents." Mol Cell Proteomics **3**(12): 1154-1169.

Saito, Y., N. Yamagishi and T. Hatayama (2007). "Different localization of Hsp105 family proteins in mammalian cells." Exp Cell Res **313**(17): 3707-3717.

Saldanha, J., E. Homer, R. Goldin, H. C. Thomas and J. Monjardino (1990). "Cloning and expression of an immunodominant region of the hepatitis delta antigen." J Gen Virol **71 (Pt 2)**: 471-475.

Sambrook, J., E. F. Fritsch and T. Maniatis (1989). Molecular Cloning, a laboratory manual, Cold Spring Harbor Laboratory Press

Sato, S., C. Cornillez-Ty and D. W. Lazinski (2004). "By inhibiting replication, the large hepatitis delta antigen can indirectly regulate amber/W editing and its own expression." J Virol **78**(15): 8120-8134.

Schaub, M. C., S. R. Lopez and M. Caputi (2007). "Members of the heterogeneous nuclear ribonucleoprotein H family activate splicing of an HIV-1 splicing substrate by promoting formation of ATP-dependent spliceosomal complexes." J Biol Chem **282**(18): 13617-13626.

Schmidt, U., K. Richter, A. B. Berger and P. Lichter (2006). "In vivo BiFC analysis of Y14 and NXF1 mRNA export complexes: preferential localization within and around SC35 domains." J Cell Biol **172**(3): 373-381.

Schneider, J. and T. Wolff (2009). "Nuclear functions of the influenza A and B viruses NS1 proteins: do they play a role in viral mRNA export?" Vaccine **27**(45): 6312-6316.

Schultz, D. C., K. Ayyanathan, D. Negorev, G. G. Maul and F. J. Rauscher, 3rd (2002). "SETDB1: a novel KAP-1-associated histone H3, lysine 9-specific methyltransferase that contributes to HP1-mediated silencing of euchromatic genes by KRAB zinc-finger proteins." Genes Dev **16**(8): 919-932.

Seemann, S. and P. Hainaut (2005). "Roles of thioredoxin reductase 1 and APE/Ref-1 in the control of basal p53 stability and activity." Oncogene **24**(24): 3853-3863.

Shaner, L. and K. A. Morano (2007). "All in the family: atypical Hsp70 chaperones are conserved modulators of Hsp70 activity." Cell Stress Chaperones **12**(1): 1-8.

Sharmeen, L., M. Y. Kuo, G. Dinter-Gottlieb and J. Taylor (1988). "Antigenomic RNA of human hepatitis delta virus can undergo self-cleavage." J Virol **62**(8): 2674-2679.

Sheldon, J., B. Ramos, C. Toro, P. Rios, J. Martinez-Alarcon, M. Bottecchia, M. Romero, J. Garcia-Samaniego and V. Soriano (2008). "Does treatment of hepatitis B virus (HBV) infection reduce hepatitis delta virus (HDV) replication in HIV-HBV-HDV-coinfected patients?" Antivir Ther **13**(1): 97-102.

Shi, S. T., P. Huang, H. P. Li and M. M. Lai (2000). "Heterogeneous nuclear ribonucleoprotein A1 regulates RNA synthesis of a cytoplasmic virus." EMBO J **19**(17): 4701-4711.

Sikora, D., V. S. Greco-Stewart, P. Miron and M. Pelchat (2009). "The hepatitis delta virus RNA genome interacts with eEF1A1, p54(nrb), hnRNP-L, GAPDH and ASF/SF2." Virology **390**(1): 71-78.

Siomi, H. and G. Dreyfuss (1995). "A nuclear localization domain in the hnRNP A1 protein." J Cell Biol **129**(3): 551-560.

Stewart, P. L. and G. R. Nemerow (2007). "Cell integrins: commonly used receptors for diverse viral pathogens." Trends Microbiol **15**(11): 500-507.

Sureau, C., C. Fournier-Wirth and P. Maurel (2003). "Role of N glycosylation of hepatitis B virus envelope proteins in morphogenesis and infectivity of hepatitis delta virus." J Virol **77**(9): 5519-5523.

Sureau, C., A. M. Moriarty, G. B. Thornton and R. E. Lanford (1992). "Production of infectious hepatitis delta virus in vitro and neutralization with antibodies directed against hepatitis B virus pre-S antigens." J Virol **66**(2): 1241-1245.

Swanson, M. S. and G. Dreyfuss (1988). "Classification and purification of proteins of heterogeneous nuclear ribonucleoprotein particles by RNA-binding specificities." Mol Cell Biol **8**(5): 2237-2241.

Tavanez, J. P., C. Cunha, M. C. Silva, E. David, J. Monjardino and M. Carmo-Fonseca (2002). "Hepatitis delta virus ribonucleoproteins shuttle between the nucleus and the cytoplasm." RNA **8**(5): 637-646.

Taylor, J., W. Mason, J. Summers, J. Goldberg, C. Aldrich, L. Coates, J. Gerin and E. Gowans (1987). "Replication of human hepatitis delta virus in primary cultures of woodchuck hepatocytes." J Virol **61**(9): 2891-2895.

Taylor, J. and M. Pelchat (2010). "Origin of hepatitis delta virus." Future Microbiol **5**(3): 393-402.

Taylor, J. M. (2009). "Chapter 3. Replication of the hepatitis delta virus RNA genome." Adv Virus Res **74**: 103-121.

Teixeira, A., A. Tahiri-Alaoui, S. West, B. Thomas, A. Ramadass, I. Martianov, M. Dye, W. James, N. J. Proudfoot and A. Akoulitchev (2004). "Autocatalytic RNA cleavage in the human beta-globin pre-mRNA promotes transcription termination." Nature **432**(7016): 526-530.

Tong, A., L. Wu, Q. Lin, Q. C. Lau, X. Zhao, J. Li, P. Chen, L. Chen, H. Tang, C. Huang and Y. Q. Wei (2008). "Proteomic analysis of cellular protein alterations using a hepatitis B virus-producing cellular model." Proteomics **8**(10): 2012-2023.

Tseng, C. H., T. S. Cheng, C. Y. Shu, K. S. Jeng and M. M. Lai (2010). "Modification of small hepatitis delta virus antigen by SUMO protein." J Virol **84**(2): 918-927.

Tseng, C. H., K. S. Jeng and M. M. Lai (2008). "Transcription of subgenomic mRNA of hepatitis delta virus requires a modified hepatitis delta antigen that is distinct from antigenomic RNA synthesis." J Virol **82**(19): 9409-9416.

Urrutia, R. (2003). "KRAB-containing zinc-finger repressor proteins." Genome Biol **4**(10): 231.

Vander Heiden, M. G., L. C. Cantley and C. B. Thompson (2009). "Understanding the Warburg effect: the metabolic requirements of cell proliferation." Science **324**(5930): 1029-1033.

Veretnik, S. and M. Gribskov (1999). "RNA binding domain of HDV antigen is homologous to the HMG box of SRY." Arch Virol **144**(6): 1139-1158.

Wakatsuki, T. and T. Hatayama (1998). "Characteristic expression of 105-kDa heat shock protein (HSP105) in various tissues of nonstressed and heat-stressed rats." Biol Pharm Bull **21**(9): 905-910.

Wang, C., A. Ivanov, L. Chen, W. J. Fredericks, E. Seto, F. J. Rauscher, 3rd and J. Chen (2005). "MDM2 interaction with nuclear corepressor KAP1 contributes to p53 inactivation." EMBO J **24**(18): 3279-3290.

Wang, D., J. Pearlberg, Y. T. Liu and D. Ganem (2001). "Deleterious effects of hepatitis delta virus replication on host cell proliferation." J Virol **75**(8): 3600-3604.

Wang, T. C. and M. Chao (2005). "RNA recombination of hepatitis delta virus in natural mixed-genotype infection and transfected cultured cells." J Virol **79**(4): 2221-2229.

Wang, Z., M. E. Rolish, G. Yeo, V. Tung, M. Mawson and C. B. Burge (2004). "Systematic identification and analysis of exonic splicing silencers." Cell **119**(6): 831-845.

Wedemeyer, H., B. Heidrich and M. P. Manns (2007). "Hepatitis D virus infection--not a vanishing disease in Europe!" Hepatology **45**(5): 1331-1332; author reply 1332-1333.

Wedemeyer, H. and M. P. Manns (2010). "Epidemiology, pathogenesis and management of hepatitis D: update and challenges ahead." Nat Rev Gastroenterol Hepatol **7**(1): 31-40.

Wei, C. C., S. L. Zhang, Y. W. Chen, D. F. Guo, J. R. Ingelfinger, K. Bomsztyk and J. S. Chan (2006). "Heterogeneous nuclear ribonucleoprotein K modulates angiotensinogen gene expression in kidney cells." J Biol Chem **281**(35): 25344-25355.

Welch, W. J. and L. A. Mizzen (1988). "Characterization of the thermotolerant cell. II. Effects on the intracellular distribution of heat-shock protein 70, intermediate filaments, and small nuclear ribonucleoprotein complexes." J Cell Biol **106**(4): 1117-1130.

Wong, S. K. and D. W. Lazinski (2002). "Replicating hepatitis delta virus RNA is edited in the nucleus by the small form of ADAR1." Proc Natl Acad Sci U S A **99**(23): 15118-15123.

Woodhouse, S. D., R. Narayan, S. Latham, S. Lee, R. Antrobus, B. Gangadharan, S. Luo, G. P. Schroth, P. Klenerman and N. Zitzmann (2010). "Transcriptome sequencing, microarray, and proteomic analyses reveal cellular and metabolic impact of hepatitis C virus infection in vitro." Hepatology **52**(2): 443-453.

Wu, J. C., T. Y. Chiang, W. K. Shiue, S. Y. Wang, I. J. Sheen, Y. H. Huang and W. J. Syu (1999). "Recombination of hepatitis D virus RNA sequences and its implications." Mol Biol Evol **16**(11): 1622-1632.

Xia, Y. P., C. T. Yeh, J. H. Ou and M. M. Lai (1992). "Characterization of nuclear targeting signal of hepatitis delta antigen: nuclear transport as a protein complex." J Virol **66**(2): 914-921.

Yamagishi, N., K. Ishihara, Y. Saito and T. Hatayama (2003). "Hsp105 but not Hsp70 family proteins suppress the aggregation of heat-denatured protein in the presence of ADP." FEBS Lett **555**(2): 390-396.

Yamagishi, N., K. Ishihara, Y. Saito and T. Hatayama (2006). "Hsp105 family proteins suppress staurosporine-induced apoptosis by inhibiting the translocation of Bax to mitochondria in HeLa cells." Exp Cell Res **312**(17): 3215-3223.

Yamagishi, N., H. Nishihori, K. Ishihara, K. Ohtsuka and T. Hatayama (2000). "Modulation of the chaperone activities of Hsc70/Hsp40 by Hsp105alpha and Hsp105beta." Biochem Biophys Res Commun **272**(3): 850-855.

Yamaguchi, Y., S. Delehouzee and H. Handa (2002). "HIV and hepatitis delta virus: evolution takes different paths to relieve blocks in transcriptional elongation." Microbes Infect **4**(11): 1169-1175.

Yamaguchi, Y., J. Filipovska, K. Yano, A. Furuya, N. Inukai, T. Narita, T. Wada, S. Sugimoto, M. M. Konarska and H. Handa (2001). "Stimulation of RNA polymerase II elongation by hepatitis delta antigen." Science **293**(5527): 124-127.

Yao, X., C. Afonso and C. Fenselau (2003). "Dissection of proteolytic 18O labeling: endoprotease-catalyzed 16O-to-18O exchange of truncated peptide substrates." J Proteome Res **2**(2): 147-152.

Yao, X., A. Freas, J. Ramirez, P. A. Demirev and C. Fenselau (2001). "Proteolytic 18O labeling for comparative proteomics: model studies with two serotypes of adenovirus." Anal Chem **73**(13): 2836-2842.

Yeh, T. S., S. J. Lo, P. J. Chen and Y. H. Lee (1996). "Casein kinase II and protein kinase C modulate hepatitis delta virus RNA replication but not empty viral particle assembly." J Virol **70**(9): 6190-6198.

Yu, J. Y., S. L. DeRuiter and D. L. Turner (2002). "RNA interference by expression of short-interfering RNAs and hairpin RNAs in mammalian cells." Proc Natl Acad Sci U S A **99**(9): 6047-6052.

Zachou, K., C. Yurdaydin, U. Drebber, G. N. Dalekos, A. Erhardt, Y. Cakaloglu, H. Degertekin, S. Gurel, S. Zeuzem, H. Bozkaya, V. Schlaphoff, H. P. Dienes, T. C. Bock, M. P. Manns and H. Wedemeyer (2010). "Quantitative HBsAg and HDV-RNA levels in chronic delta hepatitis." Liver Int **30**(3): 430-437.

Zarudnaya, M. I., I. M. Kolomiets, A. L. Potyahaylo and D. M. Hovorun (2003). "Downstream elements of mammalian pre-mRNA polyadenylation signals: primary, secondary and higher-order structures." Nucleic Acids Res **31**(5): 1375-1386.

Zhang, B., D. Schmoyer, S. Kirov and J. Snoddy (2004). "GOTree Machine (GOTM): a web-based platform for interpreting sets of interesting genes using Gene Ontology hierarchies." BMC Bioinformatics **5**: 16.

Zhao, R. Y. and R. T. Elder (2005). "Viral infections and cell cycle G2/M regulation." Cell Res **15**(3): 143-149.

Zhao, X., M. Rush and S. Schwartz (2004). "Identification of an hnRNP A1-dependent splicing silencer in the human papillomavirus type 16 L1 coding region that prevents premature expression of the late L1 gene." J Virol **78**(20): 10888-10905.

Zhu, W., J. W. Smith and C. M. Huang (2010). "Mass spectrometry-based label-free quantitative proteomics." J Biomed Biotechnol **2010**: 840518.


FCT
Fundação para a Ciência e a Tecnologia
MINISTÉRIO DA CIÊNCIA, TECNOLOGIA E ENSINO SUPERIOR


UNIÃO EUROPEIA
FEDER